

Richard Liew, J.Y.; Shanmugam, N.W. and Yu, C.H. "Structural Analysis"  
*Structural Engineering Handbook*  
Ed. Chen Wai-Fah  
Boca Raton: CRC Press LLC, 1999

# Structural Analysis

---

J.Y. Richard Liew,  
N.E. Shanmugam, and  
C.H. Yu  
*Department of Civil Engineering  
The National University of  
Singapore, Singapore*

- 2.1 Fundamental Principles
- 2.2 Flexural Members
- 2.3 Trusses
- 2.4 Frames
- 2.5 Plates
- 2.6 Shell
- 2.7 Influence Lines
- 2.8 Energy Methods in Structural Analysis
- 2.9 Matrix Methods
- 2.10 The Finite Element Method
- 2.11 Inelastic Analysis
- 2.12 Frame Stability
- 2.13 Structural Dynamic
- 2.14 Defining Terms
- References
- Further Reading

## 2.1 Fundamental Principles

---

*Structural analysis* is the determination of forces and deformations of the structure due to applied loads. *Structural design* involves the arrangement and proportioning of structures and their components in such a way that the assembled structure is capable of supporting the designed loads within the allowable limit states. An analytical model is an idealization of the actual structure. The structural model should relate the actual behavior to material properties, structural details, and loading and boundary conditions as accurately as is practicable.

All structures that occur in practice are three-dimensional. For building structures that have regular layout and are rectangular in shape, it is possible to idealize them into two-dimensional frames arranged in orthogonal directions. *Joints* in a structure are those points where two or more **members** are connected. A **truss** is a structural system consisting of members that are designed to resist only axial forces. Axially loaded members are assumed to be pin-connected at their ends. A structural system in which joints are capable of transferring end moments is called a *frame*. Members in this system are assumed to be capable of resisting bending moment axial force and shear force. A structure is said to be two dimensional or planar if all the members lie in the same plane. **Beams** are those members that are subjected to bending or flexure. They are usually thought of as being in horizontal positions and loaded with vertical loads. *Ties* are members that are subjected to axial tension only, while struts (columns or posts) are members subjected to axial compression only.

### 2.1.1 Boundary Conditions

A *hinge* represents a pin connection to a structural assembly and it does not allow translational movements (Figure 2.1a). It is assumed to be frictionless and to allow rotation of a *member* with

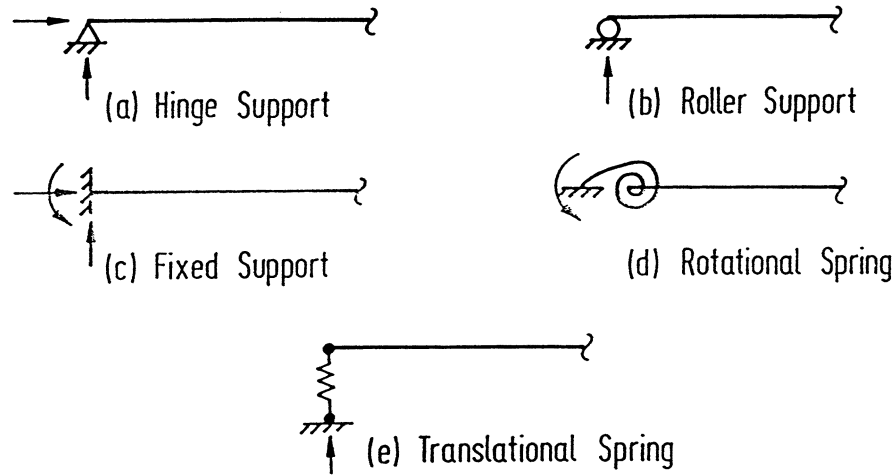


FIGURE 2.1: Various boundary conditions.

respect to the others. A *roller* represents a kind of support that permits the attached structural part to rotate freely with respect to the foundation and to translate freely in the direction parallel to the foundation surface (Figure 2.1b). No translational movement in any other direction is allowed. A *fixed support* (Figure 2.1c) does not allow rotation or translation in any direction. A *rotational spring* represents a support that provides some rotational restraint but does not provide any translational restraint (Figure 2.1d). A *translational spring* can provide partial restraints along the direction of deformation (Figure 2.1e).

### 2.1.2 Loads and Reactions

Loads may be broadly classified as *permanent loads* that are of constant magnitude and remain in one position and *variable loads* that may change in position and magnitude. Permanent loads are also referred to as *dead loads* which may include the self weight of the structure and other loads such as walls, floors, roof, plumbing, and fixtures that are permanently attached to the structure. Variable loads are commonly referred to as live or imposed loads which may include those caused by construction operations, wind, rain, earthquakes, snow, blasts, and temperature changes in addition to those that are movable, such as furniture and warehouse materials.

*Ponding* load is due to water or snow on a flat roof which accumulates faster than it runs off. *Wind loads* act as pressures on windward surfaces and pressures or suctions on leeward surfaces. *Impact loads* are caused by suddenly applied loads or by the vibration of moving or movable loads. They are usually taken as a fraction of the live loads. *Earthquake loads* are those forces caused by the acceleration of the ground surface during an earthquake.

A structure that is initially at rest and remains at rest when acted upon by applied loads is said to be in a state of *equilibrium*. The resultant of the external loads on the body and the supporting forces or *reactions* is zero. If a structure or part thereof is to be in equilibrium under the action of a system

of loads, it must satisfy the six static equilibrium equations, such as

$$\begin{aligned} \sum F_x = 0, \quad \sum F_y = 0, \quad \sum F_z = 0 \\ \sum M_x = 0, \quad \sum M_y = 0, \quad \sum M_z = 0 \end{aligned} \quad (2.1)$$

The summation in these equations is for all the components of the forces ( $F$ ) and of the moments ( $M$ ) about each of the three axes  $x$ ,  $y$ , and  $z$ . If a structure is subjected to forces that lie in one plane, say  $x$ - $y$ , the above equations are reduced to:

$$\sum F_x = 0, \quad \sum F_y = 0, \quad \sum M_z = 0 \quad (2.2)$$

Consider, for example, a beam shown in Figure 2.2a under the action of the loads shown. The

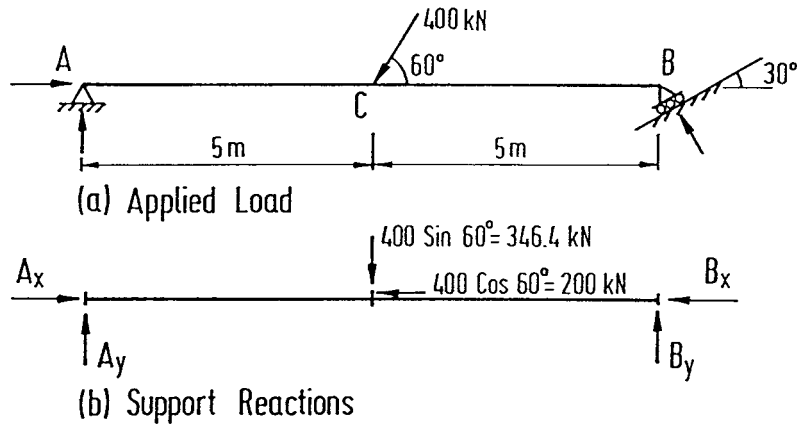


FIGURE 2.2: Beam in equilibrium.

*reaction* at support  $B$  must act perpendicular to the surface on which the rollers are constrained to roll upon. The support reactions and the applied loads, which are resolved in vertical and horizontal directions, are shown in Figure 2.2b.

From geometry, it can be calculated that  $B_y = \sqrt{3}B_x$ . Equation 2.2 can be used to determine the magnitude of the support reactions. Taking moment about  $B$  gives

$$10A_y - 346.4 \times 5 = 0$$

from which

$$A_y = 173.2 \text{ kN.}$$

Equating the sum of vertical forces,  $\sum F_y$  to zero gives

$$173.2 + B_y - 346.4 = 0$$

and, hence, we get

$$B_y = 173.2 \text{ kN.}$$

Therefore,

$$B_x = B_y / \sqrt{3} = 100 \text{ kN.}$$

Equilibrium in the horizontal direction,  $\sum F_x = 0$  gives,

$$A_x - 200 - 100 = 0$$

and, hence,

$$A_x = 300 \text{ kN.}$$

There are three unknown reaction components at a fixed end, two at a hinge, and one at a roller. If, for a particular structure, the total number of unknown reaction components equals the number of equations available, the unknowns may be calculated from the equilibrium equations, and the structure is then said to be *statically determinate externally*. Should the number of unknowns be greater than the number of equations available, the structure is *statically indeterminate externally*; if less, it is *unstable externally*. The ability of a structure to support adequately the loads applied to it is dependent not only on the number of reaction components but also on the arrangement of those components. It is possible for a structure to have as many or more reaction components than there are equations available and yet be unstable. This condition is referred to as *geometric instability*.

### 2.1.3 Principle of Superposition

The principle states that if the structural behavior is linearly elastic, the forces acting on a structure may be separated or divided into any convenient fashion and the structure analyzed for the separate cases. Then the final results can be obtained by adding up the individual results. This is applicable to the computation of structural responses such as moment, shear, [deflection](#), etc.

However, there are two situations where the principle of superposition cannot be applied. The first case is associated with instances where the geometry of the structure is appreciably altered under load. The second case is in situations where the structure is composed of a material in which the stress is not linearly related to the strain.

### 2.1.4 Idealized Models

Any complex structure can be considered to be built up of simpler components called *members* or [elements](#). Engineering judgement must be used to define an idealized structure such that it represents the actual structural behavior as accurately as is practically possible.

Structures can be broadly classified into three categories:

1. *Skeletal structures* consist of line elements such as a bar, beam, or column for which the length is much larger than the breadth and depth. A variety of skeletal structures can be obtained by connecting line elements together using hinged, rigid, or semi-rigid joints. Depending on whether the axes of these members lie in one plane or in different planes, these structures are termed as *plane structures* or *spatial structures*. The line elements in these structures under load may be subjected to one type of force such as axial force or a combination of forces such as shear, moment, torsion, and axial force. In the first case the structures are referred to as the truss-type and in the latter as frame-type.
2. *Plated structures* consist of elements that have length and breadth of the same order but are much larger than the thickness. These elements may be plane or curved in plane, in which case they are called plates or shells, respectively. These elements are generally used in combination with beams and bars. Reinforced concrete slabs supported on beams, box-girders, plate-girders, cylindrical shells, or water tanks are typical examples of plate and shell structures.
3. Three-dimensional solid structures have all three dimensions, namely, length, breadth, and depth, of the same order. Thick-walled hollow spheres, massive raft foundation, and dams are typical examples of solid structures.

Recent advancement in finite element methods of structural analysis and the advent of more powerful computers have enabled the economic analysis of skeletal, plated, and solid structures.

## 2.2 Flexural Members

One of the most common structural elements is a *beam*; it bends when subjected to loads acting transversely to its centroidal axis or sometimes by loads acting both transversely and parallel to this axis. The discussions given in the following subsections are limited to straight beams in which the centroidal axis is a straight line with shear center coinciding with the centroid of the cross-section. It is also assumed that all the loads and reactions lie in a simple plane that also contains the centroidal axis of the flexural member and the principal axis of every cross-section. If these conditions are satisfied, the beam will simply bend in the plane of loading without twisting.

### 2.2.1 Axial Force, Shear Force, and Bending Moment

*Axial force* at any transverse cross-section of a straight beam is the algebraic sum of the components acting parallel to the axis of the beam of all loads and reactions applied to the portion of the beam on either side of that cross-section. *Shear force* at any transverse cross-section of a straight beam is the algebraic sum of the components acting transverse to the axis of the beam of all the loads and reactions applied to the portion of the beam on either side of the cross-section. *Bending moment* at any transverse cross-section of a straight beam is the algebraic sum of the moments, taken about an axis passing through the centroid of the cross-section. The axis about which the moments are taken is, of course, normal to the plane of loading.

### 2.2.2 Relation Between Load, Shear, and Bending Moment

When a beam is subjected to transverse loads, there exist certain relationships between load, shear, and bending moment. Let us consider, for example, the beam shown in Figure 2.3 subjected to some arbitrary loading,  $p$ .

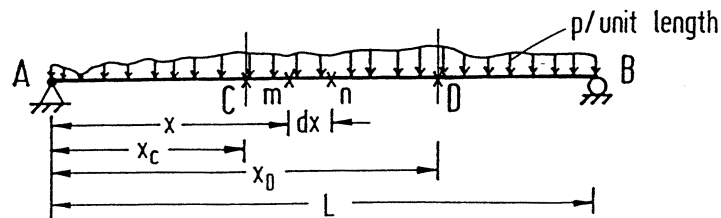


FIGURE 2.3: A beam under arbitrary loading.

Let  $S$  and  $M$  be the shear and bending moment, respectively, for any point ' $m$ ' at a distance  $x$ , which is measured from  $A$ , being positive when measured to the right. Corresponding values of shear and bending moment at point ' $n$ ' at a differential distance  $dx$  to the right of  $m$  are  $S + dS$  and  $M + dM$ , respectively. It can be shown, neglecting the second order quantities, that

$$p = \frac{dS}{dx} \quad (2.3)$$

and

$$S = \frac{dM}{dx} \quad (2.4)$$

Equation 2.3 shows that the rate of change of shear at any point is equal to the intensity of load applied to the beam at that point. Therefore, the difference in shear at two cross-sections C and D is

$$S_D - S_C = \int_{x_C}^{x_D} p dx \quad (2.5)$$

We can write in the same way for moment as

$$M_D - M_C = \int_{x_C}^{x_D} S dx \quad (2.6)$$

### 2.2.3 Shear and Bending Moment Diagrams

In order to plot the shear force and bending moment diagrams it is necessary to adopt a sign convention for these responses. A shear force is considered to be positive if it produces a clockwise moment about a point in the free body on which it acts. A negative shear force produces a counterclockwise moment about the point. The bending moment is taken as positive if it causes compression in the upper fibers of the beam and tension in the lower fiber. In other words, **sagging moment** is positive and **hogging moment** is negative. The construction of these diagrams is explained with an example given in Figure 2.4.

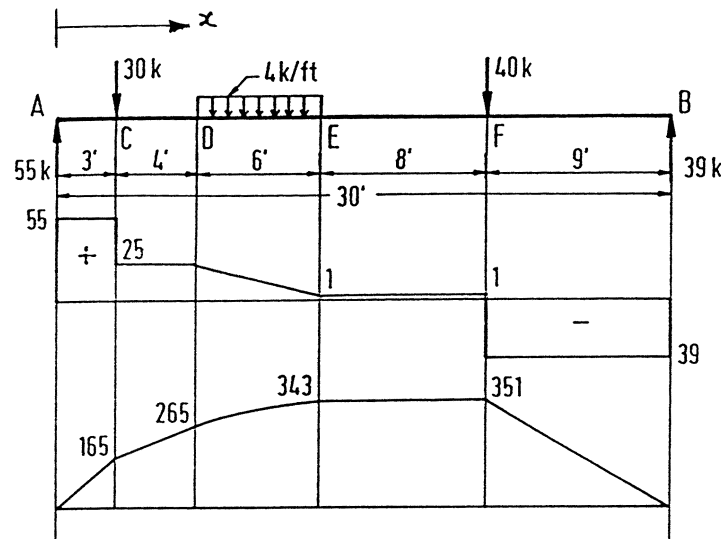


FIGURE 2.4: Bending moment and shear force diagrams.

The section at E of the beam is in equilibrium under the action of applied loads and internal forces acting at E as shown in Figure 2.5. There must be an internal vertical force and internal bending moment to maintain equilibrium at Section E. The vertical force or the moment can be obtained as the algebraic sum of all forces or the algebraic sum of the moment of all forces that lie on either side of Section E.



FIGURE 2.5: Internal forces.

The shear on a cross-section an infinitesimal distance to the right of point A is +55 k and, therefore, the shear diagram rises abruptly from 0 to +55 at this point. In the portion AC, since there is no additional load, the shear remains +55 on any cross-section throughout this interval, and the diagram is a horizontal as shown in Figure 2.4. An infinitesimal distance to the left of C the shear is +55, but an infinitesimal distance to the right of this point the 30 k load has caused the shear to be reduced to +25. Therefore, at point C there is an abrupt change in the shear force from +55 to +25. In the same manner, the shear force diagram for the portion CD of the beam remains a rectangle. In the portion DE, the shear on any cross-section a distance  $x$  from point D is

$$S = 55 - 30 - 4x = 25 - 4x$$

which indicates that the shear diagram in this portion is a straight line decreasing from an ordinate of +25 at D to +1 at E. The remainder of the shear force diagram can easily be verified in the same way. It should be noted that, in effect, a concentrated load is assumed to be applied at a point and, hence, at such a point the ordinate to the shear diagram changes abruptly by an amount equal to the load.

In the portion AC, the bending moment at a cross-section a distance  $x$  from point A is  $M = 55x$ . Therefore, the bending moment diagram starts at 0 at A and increases along a straight line to an ordinate of +165 k-ft at point C. In the portion CD, the bending moment at any point a distance  $x$  from C is  $M = 55(x + 3) - 30x$ . Hence, the bending moment diagram in this portion is a straight line increasing from 165 at C to 265 at D. In the portion DE, the bending moment at any point a distance  $x$  from D is  $M = 55(x + 7) - 30(x + 4) - 4x^2/2$ . Hence, the bending moment diagram in this portion is a curve with an ordinate of 265 at D and 343 at E. In an analogous manner, the remainder of the bending moment diagram can be easily constructed.

Bending moment and shear force diagrams for beams with simple boundary conditions and subject to some simple loading are given in Figure 2.6.

### 2.2.4 Fix-Ended Beams

When the ends of a beam are held so firmly that they are not free to rotate under the action of applied loads, the beam is known as a built-in or fix-ended beam and it is statically indeterminate. The bending moment diagram for such a beam can be considered to consist of two parts, namely the free bending moment diagram obtained by treating the beam as if the ends are simply supported and the fixing moment diagram resulting from the restraints imposed at the ends of the beam. The solution of a fixed beam is greatly simplified by considering Mohr's principles which state that:

1. the area of the fixing bending moment diagram is equal to that of the free bending moment diagram
2. the centers of gravity of the two diagrams lie in the same vertical line, i.e., are equidistant from a given end of the beam

The construction of bending moment diagram for a fixed beam is explained with an example shown in Figure 2.7. P Q U T is the free bending moment diagram,  $M_s$ , and P Q R S is the fixing

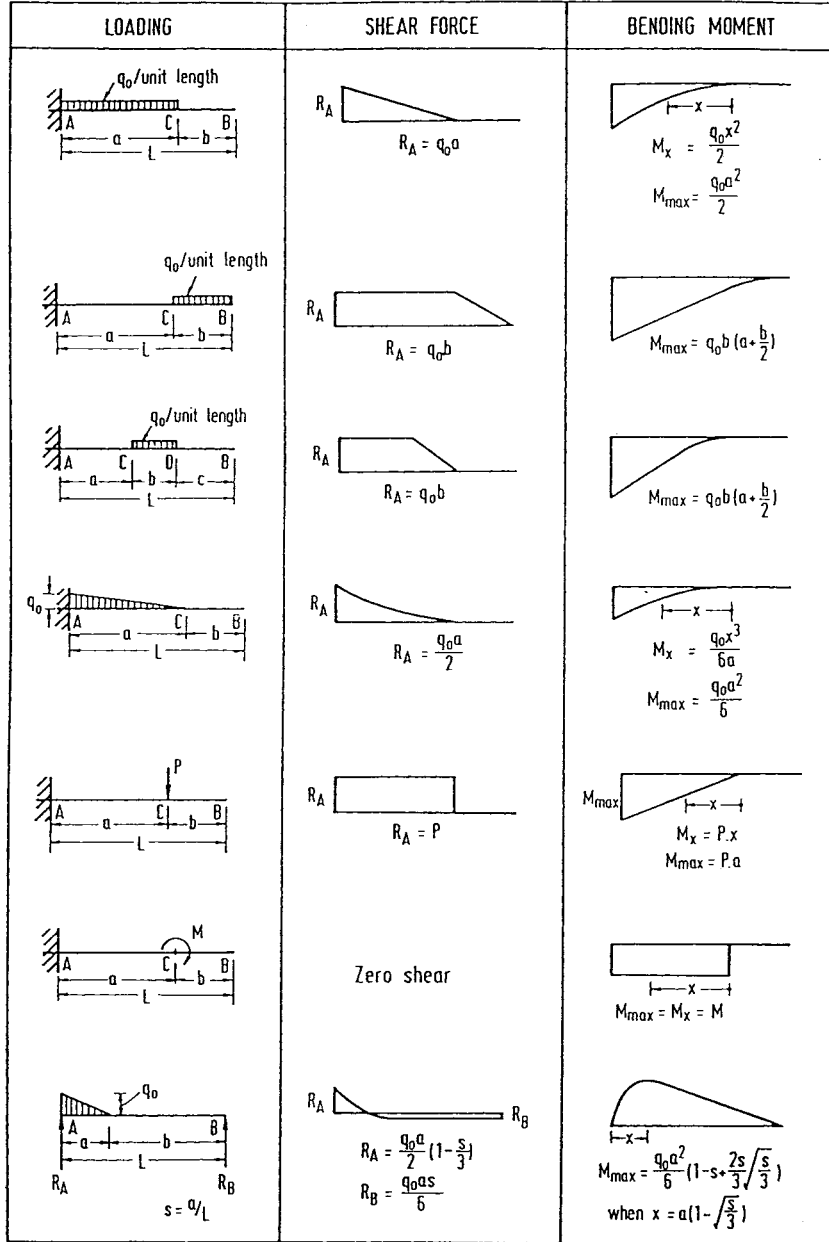


FIGURE 2.6: Shear force and bending moment diagrams for beams with simple boundary conditions subjected to selected loading cases.

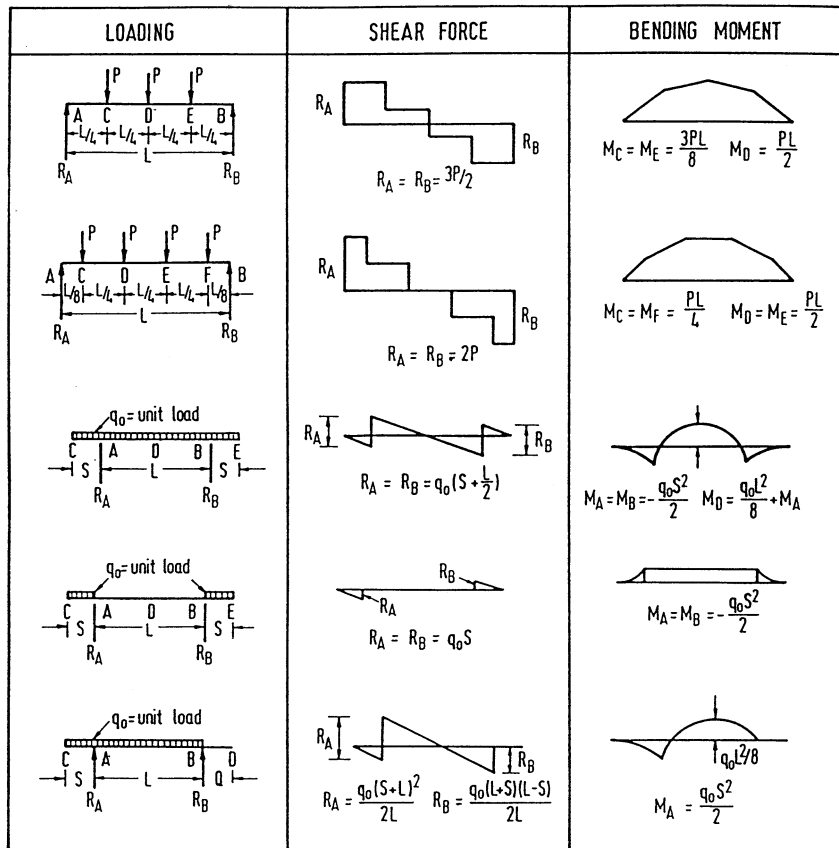


FIGURE 2.6: (Continued) Shear force and bending moment diagrams for beams with simple boundary conditions subjected to selected loading cases.

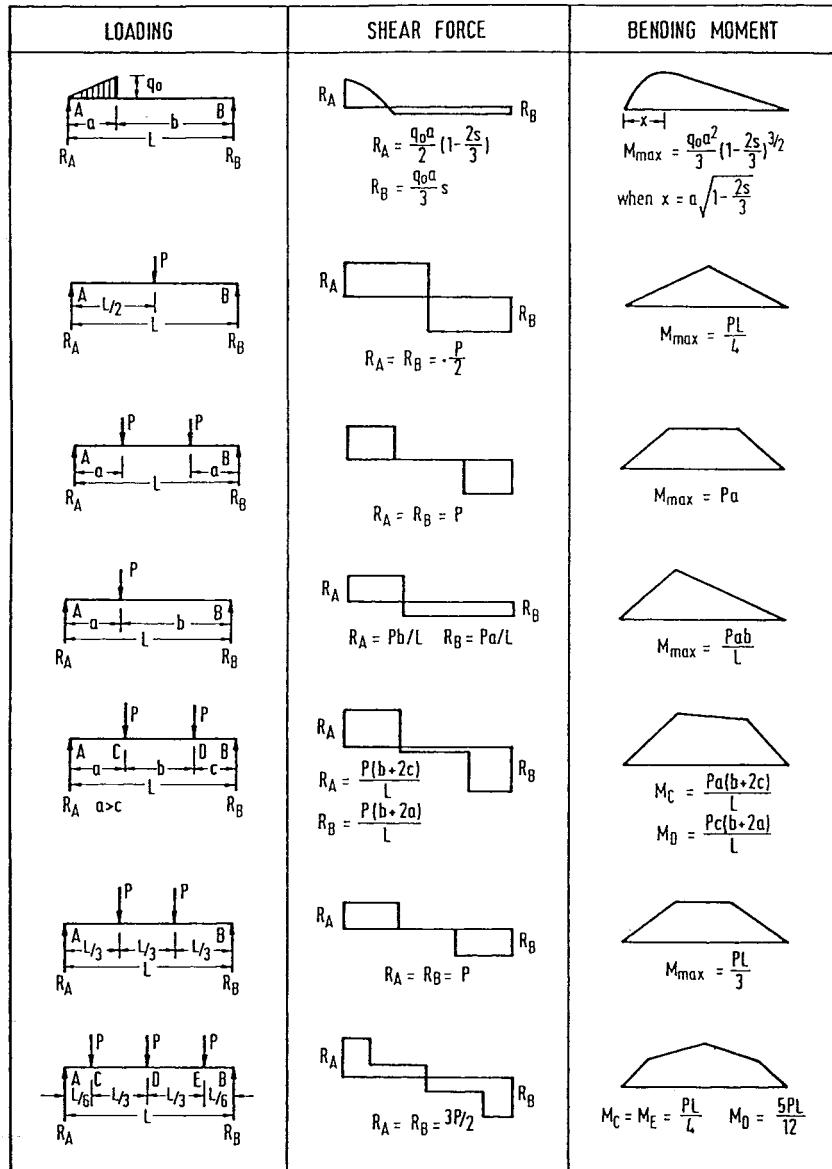


FIGURE 2.6: (Continued) Shear force and bending moment diagrams for beams with simple boundary conditions subjected to selected loading cases.

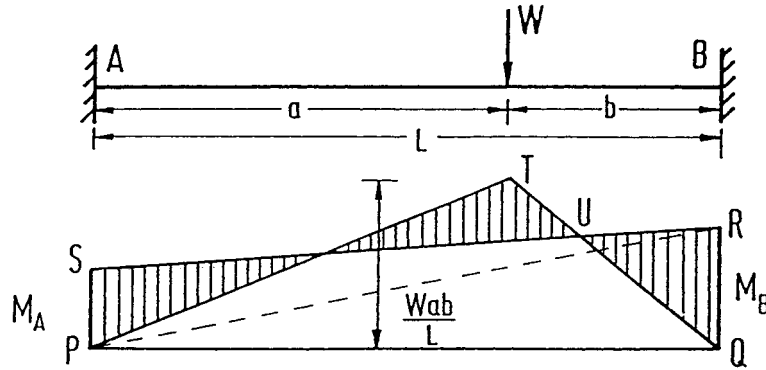


FIGURE 2.7: Fixed-ended beam.

moment diagram,  $M_i$ . The net bending moment diagram,  $M$ , is shown shaded. If  $A_s$  is the area of the free bending moment diagram and  $A_i$  the area of the fixing moment diagram, then from the first Mohr's principle we have  $A_s = A_i$  and

$$\begin{aligned} \frac{1}{2} \times \frac{Wab}{L} \times L &= \frac{1}{2} (M_A + M_B) \times L \\ M_A + M_B &= \frac{Wab}{L} \end{aligned} \quad (2.7)$$

From the second principle, equating the moment about A of  $A_s$  and  $A_i$ , we have,

$$M_A + 2M_B = \frac{Wab}{L^3} (2a^2 + 3ab + b^2) \quad (2.8)$$

Solving Equations 2.7 and 2.8 for  $M_A$  and  $M_B$ , we get

$$\begin{aligned} M_A &= \frac{Wab^2}{L^2} \\ M_B &= \frac{Wa^2b}{L^2} \end{aligned}$$

Shear force can be determined once the bending moment is known. The shear force at the ends of the beam, i.e., at A and B are

$$\begin{aligned} S_A &= \frac{M_A - M_B}{L} + \frac{Wb}{L} \\ S_B &= \frac{M_B - M_A}{L} + \frac{Wa}{L} \end{aligned}$$

Bending moment and shear force diagrams for some typical loading cases are shown in Figure 2.8.

### 2.2.5 Continuous Beams

Continuous beams, like fix-ended beams, are statically indeterminate. Bending moments in these beams are functions of the geometry, moments of inertia and modulus of elasticity of individual members besides the load and span. They may be determined by Clapeyron's Theorem of three moments, moment distribution method, or slope deflection method.

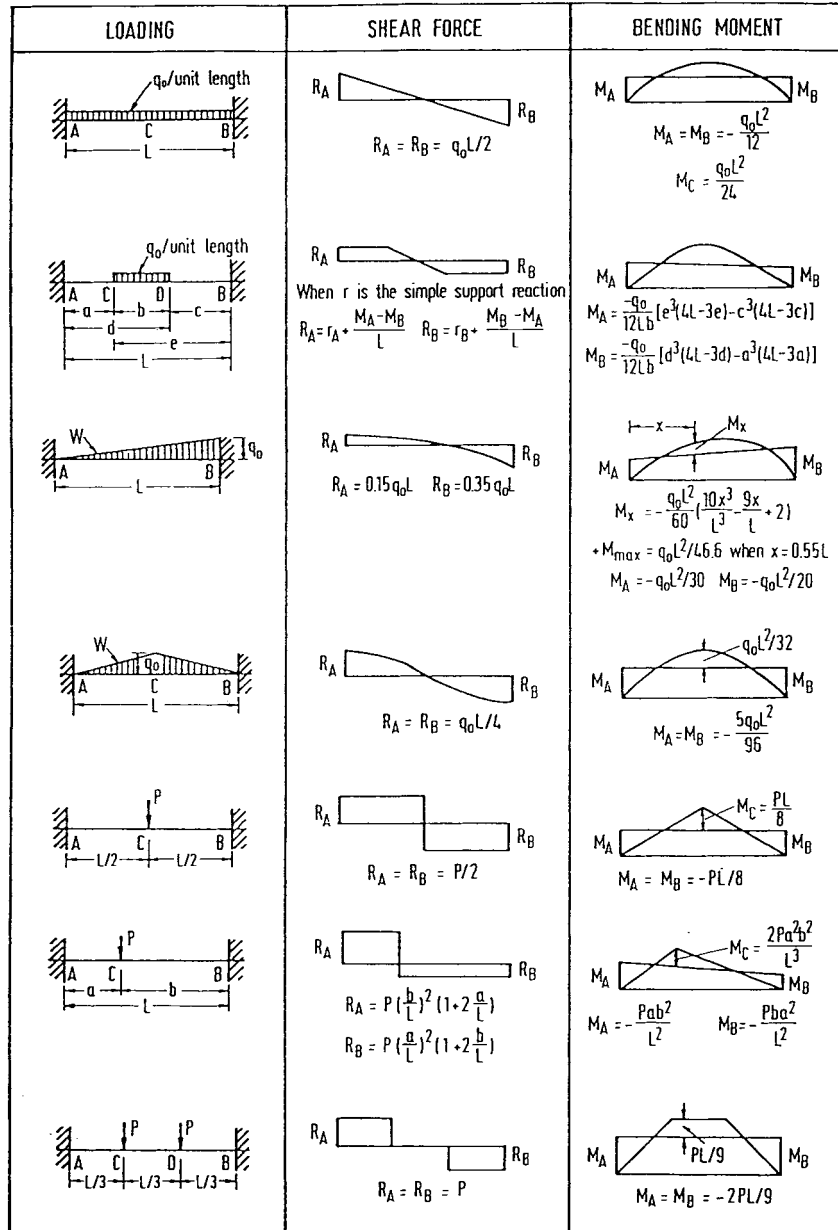


FIGURE 2.8: Shear force and bending moment diagrams for built-up beams subjected to typical loading cases.

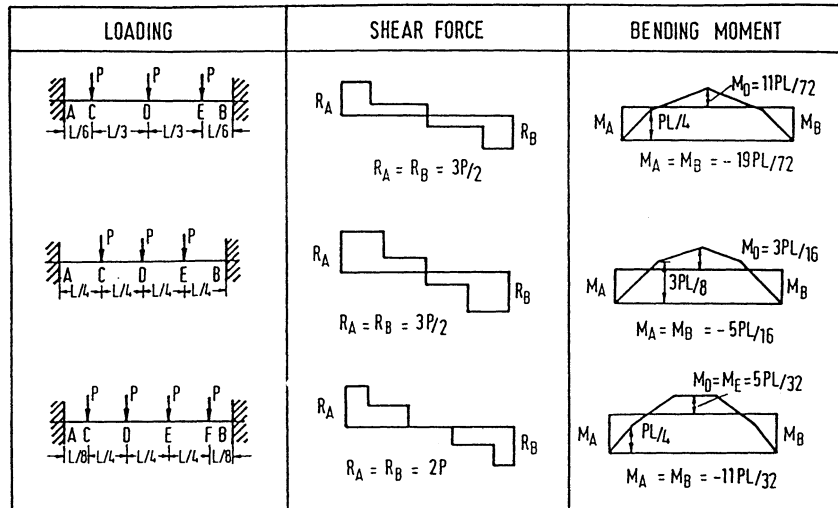


FIGURE 2.8: (Continued) Shear force and bending moment diagrams for built-up beams subjected to typical loading cases.

An example of a two-span continuous beam is solved by Clapeyron's Theorem of three moments. The theorem is applied to two adjacent spans at a time and the resulting equations in terms of unknown support moments are solved. The theorem states that

$$M_A L_1 + 2M_B(L_1 + L_2) + M_C L_2 = 6 \left( \frac{A_1 x_1}{L_1} + \frac{A_2 x_2}{L_2} \right) \quad (2.9)$$

in which  $M_A$ ,  $M_B$ , and  $M_C$  are the hogging moment at the supports A, B, and C, respectively, of two adjacent spans of length  $L_1$  and  $L_2$  (Figure 2.9);  $A_1$  and  $A_2$  are the area of bending moment diagrams produced by the vertical loads on the simple spans AB and BC, respectively;  $x_1$  is the centroid of  $A_1$  from A, and  $x_2$  is the distance of the centroid of  $A_2$  from C. If the beam section is constant within a

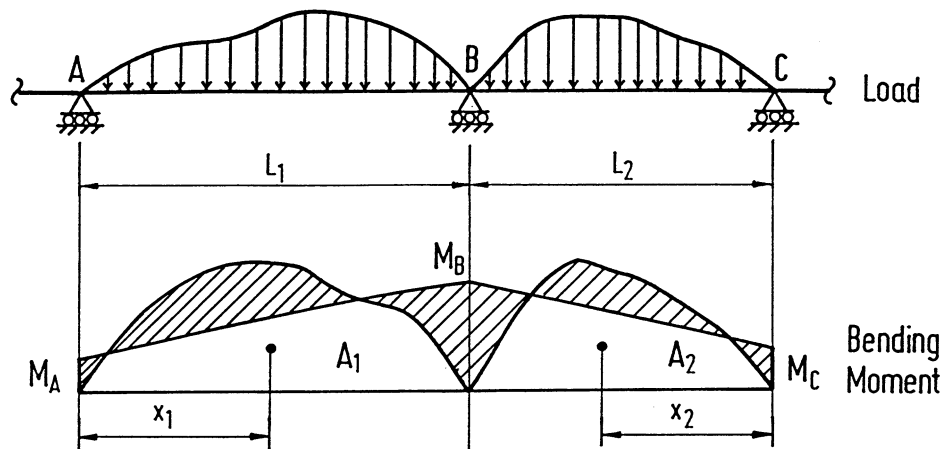


FIGURE 2.9: Continuous beams.

span but remains different for each of the spans, Equation 2.9 can be written as

$$M_A \frac{L_1}{I_1} + 2M_B \left( \frac{L_1}{I_1} + \frac{L_2}{I_2} \right) + M_C \frac{L_2}{I_2} = 6 \left( \frac{A_1 x_1}{L_1 I_1} + \frac{A_2 x_2}{L_2 I_2} \right) \quad (2.10)$$

in which  $I_1$  and  $I_2$  are the moments of inertia of beam section in span  $L_1$  and  $L_2$ , respectively.

**EXAMPLE 2.1:**

The example in Figure 2.10 shows the application of this theorem. For spans AC and BC

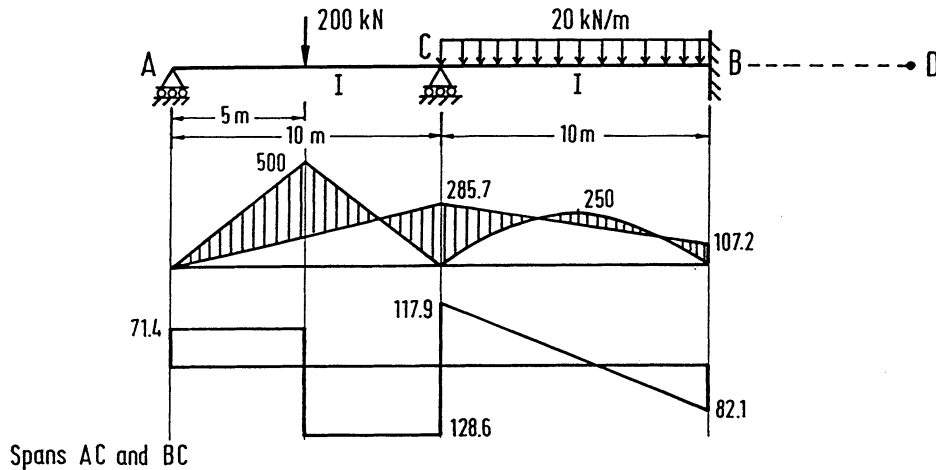


FIGURE 2.10: Example—continuous beam.

$$M_A \times 10 + 2M_C(10 + 10) + M_B \times 10 = 6 \left[ \frac{\frac{1}{2} \times 500 \times 10 \times 5}{10} + \frac{\frac{2}{3} \times 250 \times 10 \times 5}{10} \right]$$

Since the support at A is simply supported,  $M_A = 0$ . Therefore,

$$4M_C + M_B = 1250 \quad (2.11)$$

Considering an imaginary span BD on the right side of B, and applying the theorem for spans CB and BD

$$M_C \times 10 + 2M_B(10) + M_D \times 10 = 6 \times \frac{(2/3) \times 10 \times 5}{10} \times 2$$

$$M_C + 2M_B = 500 \quad (\text{because } M_C = M_D) \quad (2.12)$$

Solving Equations 2.11 and 2.12 we get

$$M_B = 107.2 \text{ kNm}$$

$$M_C = 285.7 \text{ kNm}$$

Shear force at A is

$$S_A = \frac{M_A - M_C}{L} + 100 = -28.6 + 100 = 71.4 \text{ kN}$$

Shear force at C is

$$\begin{aligned} S_C &= \left( \frac{M_C - M_A}{L} + 100 \right) + \left( \frac{M_C - M_B}{L} + 100 \right) \\ &= (28.6 + 100) + (17.9 + 100) = 246.5 \text{ kN} \end{aligned}$$

Shear force at B is

$$S_B = \left( \frac{M_B - M_C}{L} + 100 \right) = -17.9 + 100 = 82.1 \text{ kN}$$

The bending moment and shear force diagrams are shown in Figure 2.10.

### 2.2.6 Beam Deflection

There are several methods for determining beam deflections: (1) moment-area method, (2) conjugate-beam method, (3) virtual work, and (4) Castigliano's second theorem, among others.

The elastic curve of a member is the shape the neutral axis takes when the member deflects under load. The inverse of the radius of curvature at any point of this curve is obtained as

$$\frac{1}{R} = \frac{M}{EI} \quad (2.13)$$

in which  $M$  is the bending moment at the point and  $EI$  is the flexural rigidity of the beam section. Since the deflection is small,  $\frac{1}{R}$  is approximately taken as  $\frac{d^2y}{dx^2}$ , and Equation 2.13 may be rewritten as:

$$M = EI \frac{d^2y}{dx^2} \quad (2.14)$$

In Equation 2.14,  $y$  is the deflection of the beam at distance  $x$  measured from the origin of coordinate. The change in slope in a distance  $dx$  can be expressed as  $M dx/EI$  and hence the slope in a beam is obtained as

$$\theta_B - \theta_A = \int_A^B \frac{M}{EI} dx \quad (2.15)$$

Equation 2.15 may be stated as the change in slope between the tangents to the elastic curve at two points is equal to the area of the  $M/EI$  diagram between the two points.

Once the change in slope between tangents to the elastic curve is determined, the deflection can be obtained by integrating further the slope equation. In a distance  $dx$  the neutral axis changes in direction by an amount  $d\theta$ . The deflection of one point on the beam with respect to the tangent at another point due to this angle change is equal to  $d\delta = x d\theta$ , where  $x$  is the distance from the point at which deflection is desired to the particular differential distance.

To determine the total deflection from the tangent at one point A to the tangent at another point B on the beam, it is necessary to obtain a summation of the products of each  $d\theta$  angle (from A to B) times the distance to the point where deflection is desired, or

$$\delta_B - \delta_A = \int_A^B \frac{Mx}{EI} dx \quad (2.16)$$

The deflection of a tangent to the elastic curve of a beam with respect to a tangent at another point is equal to the moment of  $M/EI$  diagram between the two points, taken about the point at which deflection is desired.

## Moment Area Method

Moment area method is most conveniently used for determining slopes and deflections for beams in which the direction of the tangent to the elastic curve at one or more points is known, such as **cantilever** beams, where the tangent at the fixed end does not change in slope. The method is applied easily to beams loaded with concentrated loads because the moment diagrams consist of straight lines. These diagrams can be broken down into single triangles and rectangles. Beams supporting uniform loads or uniformly varying loads may be handled by integration. Properties of some of the shapes of  $\frac{M}{EI}$  diagrams designers usually come across are given in Figure 2.11.

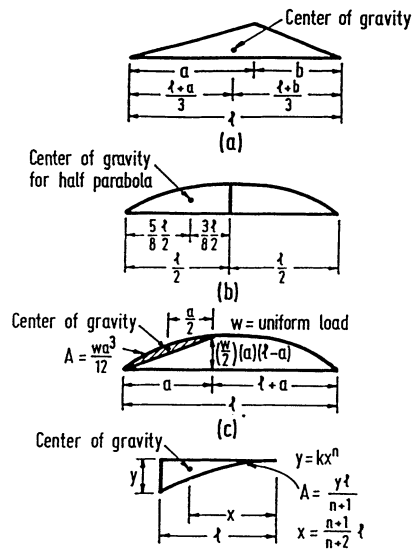


FIGURE 2.11: Typical  $M/EI$  diagram.

It should be understood that the slopes and deflections that are obtained using the moment area theorems are with respect to tangents to the elastic curve at the points being considered. The theorems do not directly give the slope or deflection at a point in the beam as compared to the horizontal axis (except in one or two special cases); they give the change in slope of the elastic curve from one point to another or the deflection of the tangent at one point with respect to the tangent at another point. There are some special cases in which beams are subjected to several concentrated loads or the combined action of concentrated and uniformly distributed loads. In such cases it is advisable to separate the concentrated loads and uniformly distributed loads and the moment area method can be applied separately to each of these loads. The final responses are obtained by the principle of superposition.

For example, consider a simply supported beam subjected to uniformly distributed load  $q$  as shown in Figure 2.12. The tangent to the elastic curve at each end of the beam is inclined. The deflection  $\delta_1$  of the tangent at the left end from the tangent at the right end is found as  $ql^4/24EI$ . The distance from the original chord between the supports and the tangent at right end,  $\delta_2$ , can be computed as  $ql^4/48EI$ . The deflection of a tangent at the center from a tangent at right end,  $\delta_3$ , is determined in this step as  $\frac{ql^4}{128EI}$ . The difference between  $\delta_2$  and  $\delta_3$  gives the centerline deflection as  $\frac{5}{384} \frac{ql^4}{EI}$ .

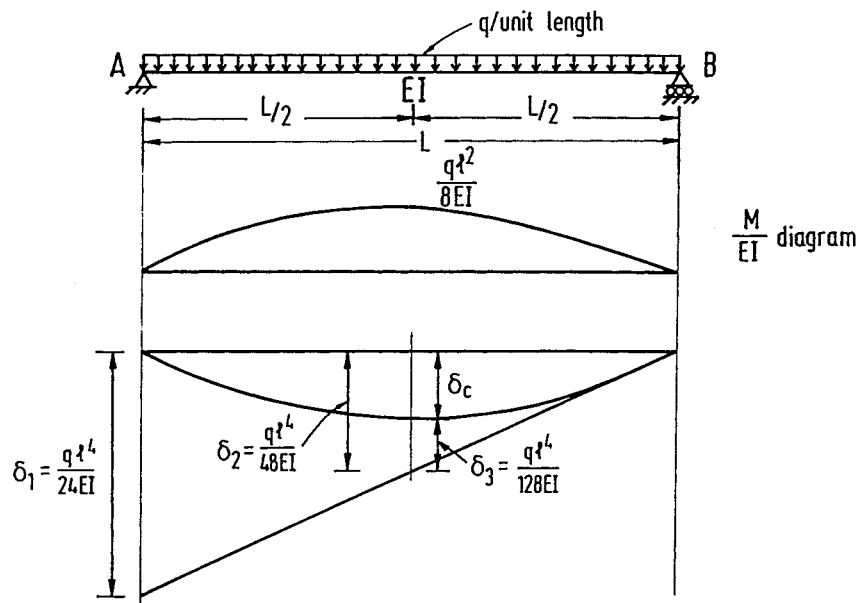


FIGURE 2.12: Deflection—simply supported beam under UDL.

### 2.2.7 Curved Flexural Members

The flexural formula is based on the assumption that the beam to which bending moment is applied is initially straight. Many members, however, are curved before a bending moment is applied to them. Such members are called curved beams. It is important to determine the effect of initial curvature of a beam on the stresses and deflections caused by loads applied to the beam in the plane of initial curvature. In the following discussion, all the conditions applicable to straight-beam formula are assumed valid except that the beam is initially curved.

Let the curved beam DOE shown in Figure 2.13 be subjected to the loads  $Q$ . The surface in which the fibers do not change in length is called the neutral surface. The total deformations of the fibers between two normal sections such as  $AB$  and  $A_1B_1$  are assumed to vary proportionally with the distances of the fibers from the neutral surface. The top fibers are compressed while those at the bottom are stretched, i.e., the plane section before bending remains plane after bending.

In Figure 2.13 the two lines  $AB$  and  $A_1B_1$  are two normal sections of the beam before the loads are applied. The change in the length of any fiber between these two normal sections after bending is represented by the distance along the fiber between the lines  $A_1B_1$  and  $A'B'$ ; the neutral surface is represented by  $NN_1$ , and the stretch of fiber  $PP_1$  is  $P_1P'_1$ , etc. For convenience it will be assumed that the line  $AB$  is a line of symmetry and does not change direction.

The total deformations of the fibers in the curved beam are proportional to the distances of the fibers from the neutral surface. However, the strains of the fibers are not proportional to these distances because the fibers are not of equal length. Within the elastic limit the stress on any fiber in the beam is proportional to the strain of the fiber, and hence the elastic stresses in the fibers of a curved beam are not proportional to the distances of the fibers from the neutral surface. The resisting moment in a curved beam, therefore, is not given by the expression  $\sigma I/c$ . Hence, the neutral axis in a curved beam does not pass through the centroid of the section. The distribution of stress over the section and the relative position of the neutral axis are shown in Figure 2.13b; if the beam were straight, the stress would be zero at the centroidal axis and would vary proportionally with the distance from the

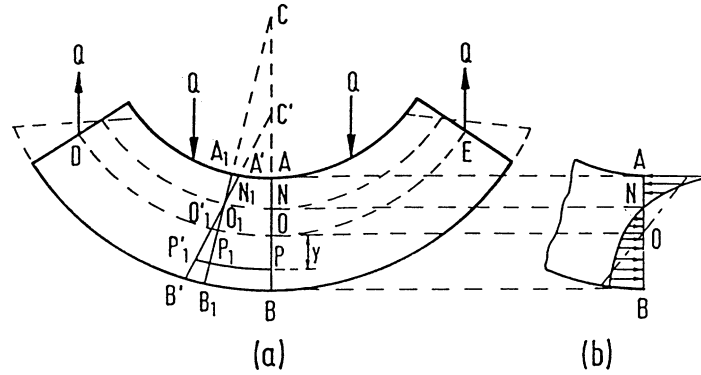


FIGURE 2.13: Bending of curved beams.

centroidal axis as indicated by the dot-dash line in the figure. The stress on a normal section such as  $AB$  is called the circumferential stress.

### Sign Conventions

The bending moment  $M$  is positive when it decreases the radius of curvature, and negative when it increases the radius of curvature;  $y$  is positive when measured toward the convex side of the beam, and negative when measured toward the concave side, that is, toward the center of curvature. With these sign conventions,  $\sigma$  is positive when it is a tensile stress.

### Circumferential Stresses

Figure 2.14 shows a free body diagram of the portion of the body on one side of the section; the equations of equilibrium are applied to the forces acting on this portion. The equations obtained are

$$\sum F_z = 0 \text{ or } \int \sigma da = 0 \quad (2.17)$$

$$\sum M_z = 0 \text{ or } M = \int y\sigma da \quad (2.18)$$

Figure 2.15 represents the part  $ABB_1A_1$  of Figure 2.13a enlarged; the angle between the two sections  $AB$  and  $A_1B_1$  is  $d\theta$ . The bending moment causes the plane  $A_1B_1$  to rotate through an angle  $\Delta d\theta$ , thereby changing the angle this plane makes with the plane  $BAC$  from  $d\theta$  to  $(d\theta + \Delta d\theta)$ ; the center of curvature is changed from  $C$  to  $C'$ , and the distance of the centroidal axis from the center of curvature is changed from  $R$  to  $\rho$ . It should be noted that  $y$ ,  $R$ , and  $\rho$  at any section are measured from the centroidal axis and not from the neutral axis.

It can be shown that the bending stress  $\sigma$  is given by the relation

$$\sigma = \frac{M}{aR} \left( 1 + \frac{1}{Z} \frac{y}{R+y} \right) \quad (2.19)$$

in which

$$Z = -\frac{1}{a} \int \frac{y}{R+y} da$$

$\sigma$  is the tensile or compressive (circumferential) stress at a point at the distance  $y$  from the centroidal axis of a transverse section at which the bending moment is  $M$ ;  $R$  is the distance from the centroidal

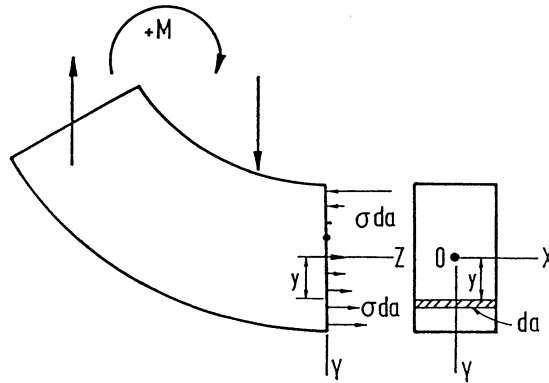


FIGURE 2.14: Free-body diagram of curved beam segment.

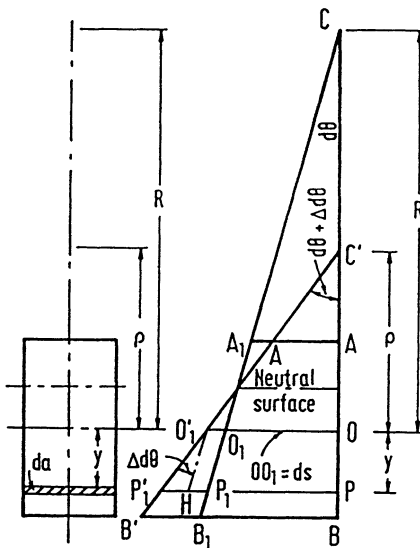


FIGURE 2.15: Curvature in a curved beam.

axis of the section to the center of curvature of the central axis of the unstressed beam;  $a$  is the area of the cross-section;  $Z$  is a property of the cross-section, the values of which can be obtained from the expressions for various areas given in Table 2.1. Detailed information can be obtained from [51].

**EXAMPLE 2.2:**

The bent bar shown in Figure 2.16 is subjected to a load  $P = 1780$  N. Calculate the circumferential stress at  $A$  and  $B$  assuming that the elastic strength of the material is not exceeded. We know from Equation 2.19

$$\sigma = \frac{P}{a} + \frac{M}{aR} \left( 1 + \frac{1}{Z} \frac{y}{R + y} \right)$$

TABLE 2.1 Analytical Expressions for Z

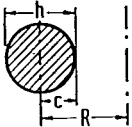
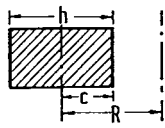
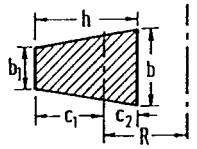
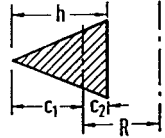
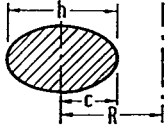
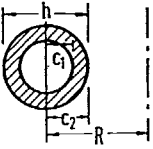
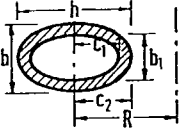
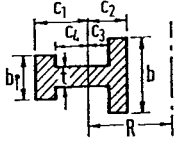
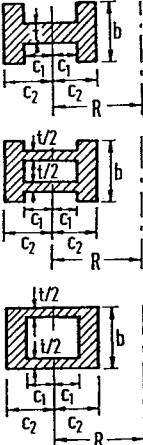
	$Z = \frac{1}{4} \left( \frac{c}{R} \right)^2 + \frac{1}{8} \left( \frac{c}{R} \right)^4 + \frac{5}{64} \left( \frac{c}{R} \right)^6 + \frac{7}{128} \left( \frac{c}{R} \right)^8 + \dots$ $Z = -1 + 2 \left( \frac{R}{c} \right)^2 - 2 \left( \frac{R}{c} \right) \sqrt{\left( \frac{R}{c} \right)^2 - 1}$
	$Z = \frac{1}{3} \left( \frac{c}{R} \right)^2 + \frac{1}{5} \left( \frac{c}{R} \right)^4 + \frac{1}{7} \left( \frac{c}{R} \right)^6 + \dots$ $Z = -1 + \frac{R}{h} \left[ \log_e \left( \frac{R+c}{R-c} \right) \right]$
	$Z = -1 + \frac{R}{ah} \left\{ [b_1 h + (R+c_1)(b-b_1)] \log_e \left( \frac{R+c_1}{R-c_2} \right) - (b-b_1)h \right\}$ $Z = -1 + \frac{2R}{(b+b_1)h} \left\{ \left[ b_1 + \frac{b-b_1}{h} (R+c_1) \right] \log_e \left( \frac{R+c_1}{R-c_2} \right) - (b-b_1) \right\}$
	$Z = -1 + 2 \frac{R}{h^2} \left[ (R+c_1) \log_e \left( \frac{R+c_1}{R-c_2} \right) - h \right]$
	$Z = \frac{1}{4} \left( \frac{c}{R} \right)^2 + \frac{1}{8} \left( \frac{c}{R} \right)^4 + \frac{5}{64} \left( \frac{c}{R} \right)^6 + \frac{7}{128} \left( \frac{c}{R} \right)^8 + \dots$ $Z = -1 + 2 \left( \frac{R}{c} \right)^2 - 2 \left( \frac{R}{c} \right) \sqrt{\left( \frac{R}{c} \right)^2 - 1}$

TABLE 2.1 Analytical Expressions for  $Z$  (continued)

	$Z = -1 + \frac{2R}{c_2^2 - c_1^2} \left[ \sqrt{R^2 - c_1^2} - \sqrt{R^2 - c_2^2} \right]$
	$Z = -1 + \frac{1}{bc_2 - b_1c_1} \left\{ bc_2 \left[ 2 \left( \frac{R}{c_2} \right)^2 - 2 \left( \frac{R}{c_2} \right) \sqrt{\left( \frac{R}{c_2} \right)^2 - 1} \right] - b_1c_1 \left[ 2 \left( \frac{R}{c_1} \right)^2 - 2 \left( \frac{R}{c_1} \right) \sqrt{\left( \frac{R}{c_1} \right)^2 - 1} \right] \right\}$
	$Z = -1 + \frac{R}{a} [b_1 \log_e(R + c_1) + (t - b_1) \log_e(R + c_4) + (b - t) \log_e(R - c_3) - b \log_e(R - c_2)]$
	<p>The value of <math>Z</math> for each of these three sections may be found from the expression above by making</p> <p><math>b_1 = b</math>, <math>c_2 = c_1</math>, and <math>c_3 = c_4</math></p> $Z = -1 + \frac{R}{a} \left[ b \log_e \left( \frac{R + c_2}{R - c_2} \right) + (t - b) \log_e \left( \frac{R + c_1}{R - c_1} \right) \right]$ <p>Area = <math>a = 2[(t - b)c_1 + bc_2]</math></p>

**TABLE 2.1** Analytical Expressions for  $Z$  (continued)

	<p>In the expression for the unequal I given above make <math>c_4 = c_1</math> and <math>b_1 = t</math>, then</p> $Z = -1 + \frac{R}{a} [t \log_e (R+c_1) + (b-t) \log_e (R-c_3) - b \log_e (R-c_2)]$ <p>Area = <math>a = tc_1 - (b-t)c_3 + bc_2</math></p>
	$Z = -1 + \frac{R}{a} \left\{ \left[ b_1 + \frac{b-b_1}{h_1} (R+c_1) \right] \log \frac{R+c_1}{R-c_2} + \left[ b_2 - \frac{b'-b_2}{h_2} (R-c_3) \right] \log \frac{R-c_2}{R-c_3} + (b'-b_2) - (b-b_1) \right\}$

From Seely, F.B. and Smith, J.O., *Advanced Mechanics of Materials*, John Wiley & Sons, New York, 1952. With permission.

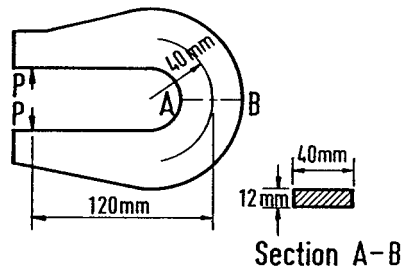


FIGURE 2.16: Bent bar.

in which

$$a = \text{area of rectangular section} = 40 \times 12 = 480 \text{ mm}^2$$

$$R = 40 \text{ mm}$$

$$y_A = -20$$

$$y_B = +20$$

$$P = 1780 \text{ N}$$

$$M = -1780 \times 120 = -213600 \text{ N mm}$$

From Table 2.1, for rectangular section

$$Z = -1 + \frac{R}{h} \left[ \log_e \frac{R+c}{R-c} \right]$$

$$h = 40 \text{ mm}$$

$$c = 20 \text{ mm}$$

Hence,

$$Z = -1 + \frac{40}{40} \left[ \log_e \frac{40+20}{40-20} \right] = 0.0986$$

Therefore,

$$\sigma_A = \frac{1780}{480} + \frac{-213600}{480 \times 40} \left( 1 + \frac{1}{0.0986} \frac{-20}{40-20} \right) = 105.4 \text{ N mm}^2 \text{ (tensile)}$$

$$\sigma_B = \frac{1780}{480} + \frac{-213600}{480 \times 40} \left( 1 + \frac{1}{0.0986} \frac{20}{40+20} \right) = -45 \text{ N mm}^2 \text{ (compressive)}$$

## 2.3 Trusses

A structure that is composed of a number of bars pin connected at their ends to form a stable framework is called a truss. If all the bars lie in a plane, the structure is a planar truss. It is generally assumed that loads and reactions are applied to the truss only at the joints. The centroidal axis of each member is straight, coincides with the line connecting the joint centers at each end of the member, and lies in a plane that also contains the lines of action of all the loads and reactions. Many truss structures are three dimensional in nature and a complete analysis would require consideration of the full spatial interconnection of the members. However, in many cases, such as bridge structures and simple roof systems, the three-dimensional framework can be subdivided into planar components for analysis as planar trusses without seriously compromising the accuracy of the results. Figure 2.17 shows some typical idealized planar truss structures.

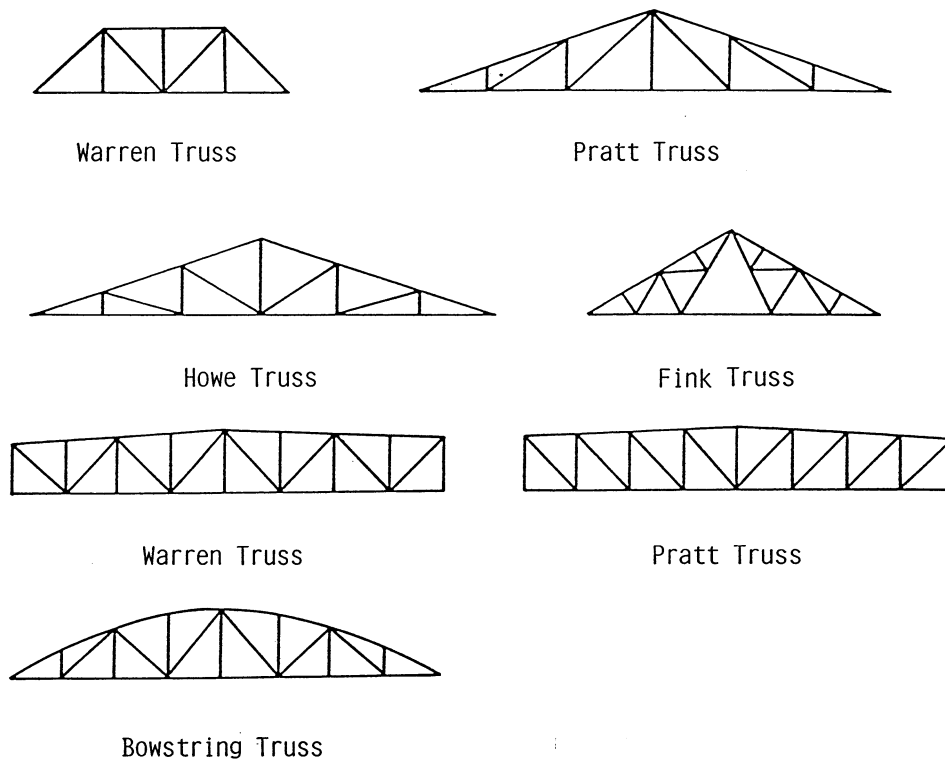


FIGURE 2.17: Typical planar trusses.

There exists a relation between the number of members,  $m$ , number of joints,  $j$ , and reaction components,  $r$ . The expression is

$$m = 2j - r \quad (2.20)$$

which must be satisfied if it is to be statically determinate internally. The least number of reaction components required for external stability is  $r$ . If  $m$  exceeds  $(2j - r)$ , then the excess members are called redundant members and the truss is said to be statically indeterminate.

Truss analysis gives the bar forces in a truss; for a statically determinate truss, these bar forces can be found by employing the laws of statics to assure internal equilibrium of the structure. The process requires repeated use of free-body diagrams from which individual bar forces are determined. The *method of joints* is a technique of truss analysis in which the bar forces are determined by the sequential isolation of joints—the unknown bar forces at one joint are solved and become known bar forces at subsequent joints. The other method is known as *method of sections* in which equilibrium of a part of the truss is considered.

### 2.3.1 Method of Joints

An imaginary section may be completely passed around a joint in a truss. The joint has become a free body in equilibrium under the forces applied to it. The equations  $\sum H = 0$  and  $\sum V = 0$  may be applied to the joint to determine the unknown forces in members meeting there. It is evident that no more than two unknowns can be determined at a joint with these two equations.

**EXAMPLE 2.3:**

A truss shown in Figure 2.18 is symmetrically loaded, and it is sufficient to solve half the truss by considering the joints 1 through 5. At Joint 1, there are two unknown forces. Summation of the

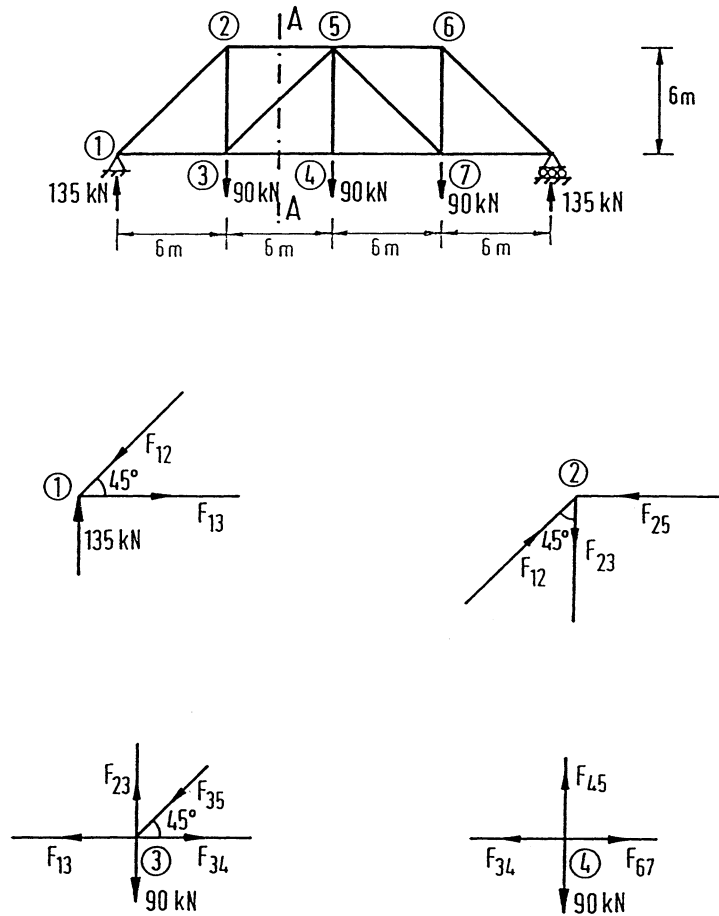


FIGURE 2.18: Example—methods of joints, planar truss.

vertical components of all forces at Joint 1 gives

$$135 - F_{12} \sin 45 = 0$$

which in turn gives the force in the member 1-2,  $F_{12} = 190.0$  kN (compressive). Similarly, summation of the horizontal components gives

$$F_{13} - F_{12} \cos 45 = 0$$

Substituting for  $F_{12}$  gives the force in the member 1-3 as

$$F_{13} = 135 \text{ kN (tensile).}$$

Now, Joint 2 is cut completely and it is found that there are two unknown forces  $F_{25}$  and  $F_{23}$ . Summation of the vertical components gives

$$F_{12} \cos 45^\circ - F_{23} = 0.$$

Therefore,

$$F_{23} = 135 \text{ kN (tensile).}$$

Summation of the horizontal components gives

$$F_{12} \sin 45^\circ - F_{25} = 0$$

and hence

$$F_{25} = 135 \text{ kN (compressive).}$$

After solving for Joints 1 and 2, one proceeds to take a section around Joint 3 at which there are now two unknown forces, namely,  $F_{34}$  and  $F_{35}$ . Summation of the vertical components at Joint 3 gives

$$F_{23} - F_{35} \sin 45^\circ - 90 = 0$$

Substituting for  $F_{23}$ , one obtains  $F_{35} = 63.6 \text{ kN (compressive)}$ . Summing the horizontal components and substituting for  $F_{13}$  one gets

$$-135 - 45 + F_{34} = 0$$

Therefore,

$$F_{34} = 180 \text{ kN (tensile).}$$

The next joint involving two unknowns is Joint 4. When we consider a section around it, the summation of the vertical components at Joint 4 gives

$$F_{45} = 90 \text{ kN (tensile).}$$

Now, the forces in all the members on the left half of the truss are known and by symmetry the forces in the remaining members can be determined. The forces in all the members of a truss can also be determined by making use of the method of section.

### 2.3.2 Method of Sections

If only a few member forces of a truss are needed, the quickest way to find these forces is by the Method of Sections. In this method, an imaginary cutting line called a section is drawn through a stable and determinate truss. Thus, a section subdivides the truss into two separate parts. Since the entire truss is in equilibrium, any part of it must also be in equilibrium. Either of the two parts of the truss can be considered and the three equations of equilibrium  $\sum F_x = 0$ ,  $\sum F_y = 0$ , and  $\sum M = 0$  can be applied to solve for member forces.

The example considered in Section 2.3.1 (Figure 2.19) is once again considered. To calculate the force in the member 3-5,  $F_{35}$ , a section  $AA$  should be run to cut the member 3-5 as shown in the figure. It is only required to consider the equilibrium of one of the two parts of the truss. In this case, the portion of the truss on the left of the section is considered. The left portion of the truss as shown in Figure 2.19 is in equilibrium under the action of the forces, namely, the external and internal forces. Considering the equilibrium of forces in the vertical direction, one can obtain

$$135 - 90 + F_{35} \sin 45^\circ = 0$$

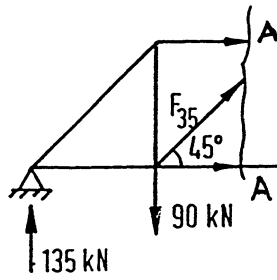


FIGURE 2.19: Example—method of sections, planar truss.

Therefore,  $F_{35}$  is obtained as

$$F_{35} = -45\sqrt{2} \text{ kN}$$

The negative sign indicates that the member force is compressive. This result is the same as the one obtained by the Method of Joints. The other member forces cut by the section can be obtained by considering the other equilibrium equations, namely,  $\sum M = 0$ . More sections can be taken in the same way so as to solve for other member forces in the truss. The most important advantage of this method is that one can obtain the required member force without solving for the other member forces.

### 2.3.3 Compound Trusses

A compound truss is formed by interconnecting two or more simple trusses. Examples of compound trusses are shown in Figure 2.20. A typical compound roof truss is shown in Figure 2.20a in which

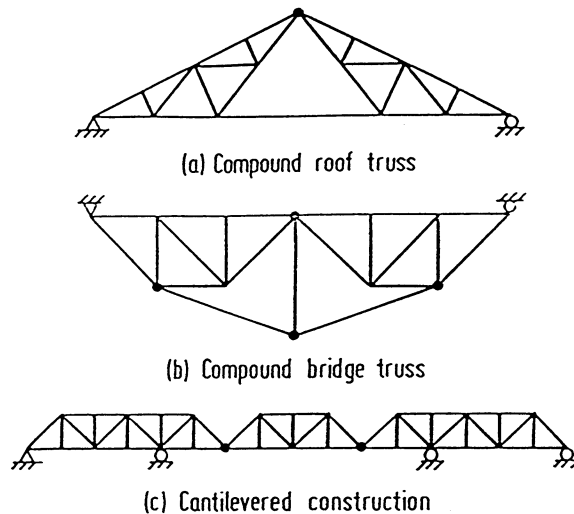


FIGURE 2.20: Compound truss.

two simple trusses are interconnected by means of a single member and a common joint. The compound truss shown in Figure 2.20b is commonly used in bridge construction and in this case,

three members are used to interconnect two simple trusses at a common joint. There are three simple trusses interconnected at their common joints as shown in Figure 2.20c.

The Method of Sections may be used to determine the member forces in the interconnecting members of compound trusses similar to those shown in Figure 2.20a and b. However, in the case of cantilevered truss, the middle simple truss is isolated as a free body diagram to find its reactions. These reactions are reversed and applied to the interconnecting joints of the other two simple trusses. After the interconnecting forces between the simple trusses are found, the simple trusses are analyzed by the Method of Joints or the Method of Sections.

### 2.3.4 Stability and Determinacy

A stable and statically determinate plane truss should have at least three members, three joints, and three reaction components. To form a stable and determinate plane truss of ' $n$ ' joints, the three members of the original triangle plus two additional members for each of the remaining  $(n - 3)$  joints are required. Thus, the minimum total number of members,  $m$ , required to form an internally stable plane truss is  $m = 2n - 3$ . If a stable, simple, plane truss of  $n$  joints and  $(2n - 3)$  members is supported by three independent reaction components, the structure is stable and determinate when subjected to a general loading. If the stable, simple, plane truss has more than three reaction components, the structure is externally indeterminate. That means not all of the reaction components can be determined from the three available equations of statics. If the stable, simple, plane truss has more than  $(2n - 3)$  members, the structure is internally indeterminate and hence all of the member forces cannot be determined from the  $2n$  available equations of statics in the Method of Joints. The analyst must examine the arrangement of the truss members and the reaction components to determine if the simple plane truss is stable. Simple plane trusses having  $(2n - 3)$  members are not necessarily stable.

## 2.4 Frames

---

Frames are statically indeterminate in general; special methods are required for their analysis. Slope deflection and moment distribution methods are two such methods commonly employed. Slope deflection is a method that takes into account the flexural displacements such as rotations and deflections and involves solutions of simultaneous equations. Moment distribution on the other hand involves successive cycles of computation, each cycle drawing closer to the "exact" answers. The method is more labor intensive but yields accuracy equivalent to that obtained from the "exact" methods. This method, however, remains the most important hand-calculation method for the analysis of frames.

### 2.4.1 Slope Deflection Method

This method is a special case of the stiffness method of analysis, and it is convenient for hand analysis of small structures. Moments at the ends of frame members are expressed in terms of the rotations and deflections of the joints. Members are assumed to be of constant section between each pair of supports. It is further assumed that the joints in a structure may rotate or deflect, but the angles between the members meeting at a joint remain unchanged.

The member force-displacement equations that are needed for the slope deflection method are written for a member  $AB$  in a frame. This member, which has its undeformed position along the  $x$  axis is deformed into the configuration shown in Figure 2.21. The positive axes, along with the positive member-end force components and displacement components, are shown in the figure.

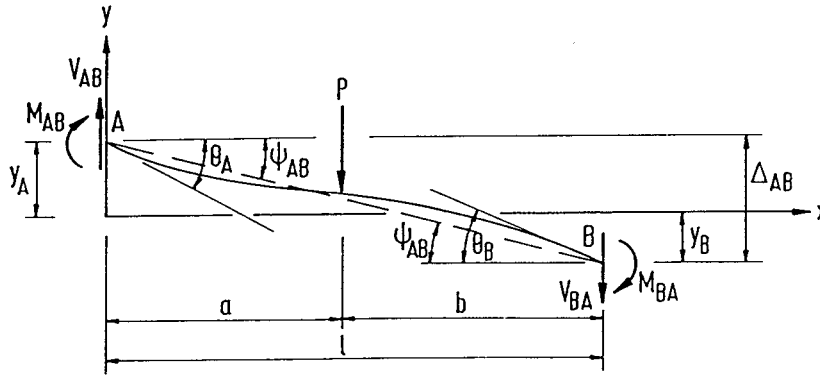


FIGURE 2.21: Deformed configuration of a beam.

The equations for end moments are written as

$$\begin{aligned}
 M_{AB} &= \frac{2EI}{l} (2\theta_A + \theta_B - 3\psi_{AB}) + M_{FAB} \\
 M_{BA} &= \frac{2EI}{l} (2\theta_B + \theta_A - 3\psi_{AB}) + M_{FBA}
 \end{aligned} \tag{2.21}$$

in which  $M_{FAB}$  and  $M_{FBA}$  are fixed-end moments at supports  $A$  and  $B$ , respectively, due to the applied load.  $\psi_{AB}$  is the rotation as a result of the relative displacement between the member ends  $A$  and  $B$  given as

$$\psi_{AB} = \frac{\Delta_{AB}}{l} = \frac{y_A + y_B}{l} \tag{2.22}$$

where  $\Delta_{AB}$  is the relative deflection of the beam ends.  $y_A$  and  $y_B$  are the vertical displacements at ends  $A$  and  $B$ . Fixed-end moments for some loading cases may be obtained from Figure 2.8. The slope deflection equations in Equation 2.21 show that the moment at the end of a member is dependent on member properties  $EI$ , dimension  $l$ , and displacement quantities. The fixed-end moments reflect the transverse loading on the member.

## 2.4.2 Application of Slope Deflection Method to Frames

The slope deflection equations may be applied to statically indeterminate frames with or without sidesway. A frame may be subjected to sidesway if the loads, member properties, and dimensions of the frame are not symmetrical about the centerline. Application of slope deflection method can be illustrated with the following example.

### EXAMPLE 2.4:

Consider the frame shown in Figure 2.22. subjected to sidesway  $\Delta$  to the right of the frame. Equation 2.21 can be applied to each of the members of the frame as follows:

Member  $AB$ :

$$M_{AB} = \frac{2EI}{20} \left( 2\theta_A + \theta_B - \frac{3\Delta}{20} \right) + M_{FAB}$$

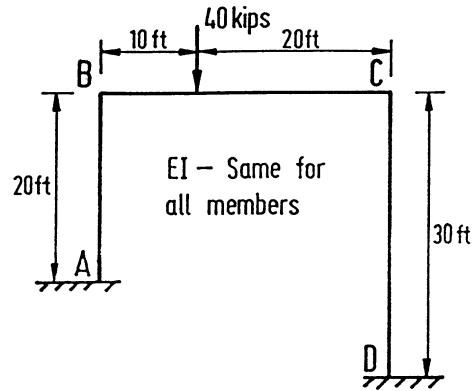


FIGURE 2.22: Example—slope deflection method.

$$M_{BA} = \frac{2EI}{20} \left( 2\theta_B + \theta_A - \frac{3\Delta}{20} \right) + M_{FBA}$$

$$\theta_A = 0, \quad M_{FAB} = M_{FBA} = 0$$

Hence,

$$M_{AB} = \frac{2EI}{20} (\theta_B - 3\psi) \quad (2.23)$$

$$M_{BA} = \frac{2EI}{20} (2\theta_B - 3\psi) \quad (2.24)$$

in which

$$\psi = \frac{\Delta}{20}$$

Member BC:

$$M_{BC} = \frac{2EI}{30} (2\theta_B + \theta_C - 3 \times 0) + M_{FBC}$$

$$M_{CB} = \frac{2EI}{30} (2\theta_C + \theta_B - 3 \times 0) + M_{FCB}$$

$$M_{FBC} = -\frac{40 \times 10 \times 20^2}{30^2} = -178 \text{ ft-kips}$$

$$M_{FCB} = -\frac{40 \times 10^2 \times 20}{30^2} = 89 \text{ ft-kips}$$

Hence,

$$M_{BC} = \frac{2EI}{30} (2\theta_B + \theta_C) - 178 \quad (2.25)$$

$$M_{CB} = \frac{2EI}{30} (2\theta_C + \theta_B) + 89 \quad (2.26)$$

Member CD:

$$M_{CD} = \frac{2EI}{30} \left( 2\theta_C + \theta_D - \frac{3\Delta}{30} \right) + M_{FCD}$$

$$M_{DC} = \frac{2EI}{30} \left( 2\theta_D + \theta_C - \frac{3\Delta}{30} \right) + M_{FDC}$$

$$M_{FCD} = M_{FDC} = 0$$

Hence,

$$M_{DC} = \frac{2EI}{30} \left( \theta_C - 3 \times \frac{2}{3} \psi \right) = \frac{2EI}{30} (2\theta_C - 2\psi) \quad (2.27)$$

$$M_{DC} = \frac{2EI}{30} \left( \theta_C - 3 \times \frac{2}{3} \psi \right) = \frac{2EI}{30} (\theta_C - 2\psi) \quad (2.28)$$

Considering moment equilibrium at Joint B

$$\sum M_B = M_{BA} + M_{BC} = 0$$

Substituting for  $M_{BA}$  and  $M_{BC}$ , one obtains

$$\frac{EI}{30} (10\theta_B + 2\theta_C - 9\psi) = 178$$

or

$$10\theta_B + 2\theta_C - 9\psi = \frac{267}{K} \quad (2.29)$$

where  $K = \frac{EI}{20}$ .

Considering moment equilibrium at Joint C

$$\sum M_C = M_{CB} + M_{CD} = 0$$

Substituting for  $M_{CB}$  and  $M_{CD}$  we get

$$\frac{2EI}{30} (4\theta_C + \theta_B - 2\psi) = -89$$

or

$$\theta_B + 4\theta_C - 2\psi = -\frac{66.75}{K} \quad (2.30)$$

Summation of base shear equals to zero, we have

$$\sum H = H_A + H_D = 0$$

or

$$\frac{M_{AB} + M_{BA}}{l_{AB}} + \frac{M_{CD} + M_{DC}}{l_{CD}} = 0$$

Substituting for  $M_{AB}$ ,  $M_{BA}$ ,  $M_{CD}$ , and  $M_{DC}$  and simplifying

$$2\theta_B + 12\theta_C - 70\psi = 0 \quad (2.31)$$

Solution of Equations 2.29 to 2.31 results in

$$\theta_B = \frac{42.45}{K}$$

$$\theta_C = \frac{20.9}{K}$$

and

$$\psi = \frac{12.8}{K} \quad (2.32)$$

Substituting for  $\theta_B$ ,  $\theta_C$ , and  $\psi$  from Equations 2.32 into Equations 2.23 to 2.28 we get,

$$\begin{aligned}M_{AB} &= 10.10 \text{ ft-kips} \\M_{BA} &= 93 \text{ ft-kips} \\M_{BC} &= -93 \text{ ft-kips} \\M_{CB} &= 90 \text{ ft-kips} \\M_{CD} &= -90 \text{ ft-kips} \\M_{DC} &= -62 \text{ ft-kips}\end{aligned}$$

### 2.4.3 Moment Distribution Method

The moment distribution method involves successive cycles of computation, each cycle drawing closer to the “exact” answers. The calculations may be stopped after two or three cycles, giving a very good approximate analysis, or they may be carried on to whatever degree of accuracy is desired. Moment distribution remains the most important hand-calculation method for the analysis of continuous beams and frames and it may be solely used for the analysis of small structures. Unlike the slope deflection method, this method does not require the solution to simultaneous equations.

The terms constantly used in moment distribution are fixed-end moments, unbalanced moment, distributed moments, and carry-over moments. When all of the joints of a structure are clamped to prevent any joint rotation, the external loads produce certain moments at the ends of the members to which they are applied. These moments are referred to as *fixed-end moments*. Initially the joints in a structure are considered to be clamped. When the joint is released, it rotates if the sum of the fixed-end moments at the joint is not zero. The difference between zero and the actual sum of the end moments is the *unbalanced moment*. The unbalanced moment causes the joint to rotate. The rotation twists the ends of the members at the joint and changes their moments. In other words, rotation of the joint is resisted by the members and resisting moments are built up in the members as they are twisted. Rotation continues until equilibrium is reached—when the resisting moments equal the unbalanced moment—at which time the sum of the moments at the joint is equal to zero. The moments developed in the members resisting rotation are the *distributed moments*. The distributed moments in the ends of the member cause moments in the other ends, which are assumed fixed, and these are the *carry-over moments*.

#### Sign Convention

The moments at the end of a member are assumed to be positive when they tend to rotate the member clockwise about the joint. This implies that the resisting moment of the joint would be counter-clockwise. Accordingly, under gravity loading condition the fixed-end moment at the left end is assumed as counter-clockwise ( $-ve$ ) and at the right end as clockwise ( $+ve$ ).

#### Fixed-End Moments

Fixed-end moments for several cases of loading may be found in Figure 2.8. Application of moment distribution may be explained with reference to a continuous beam example as shown in Figure 2.23. Fixed-end moments are computed for each of the three spans. At Joint  $B$  the unbalanced moment is obtained and the clamp is removed. The joint rotates, thus distributing the unbalanced moment to the  $B$ -ends of spans  $BA$  and  $BC$  in proportion to their distribution factors. The values of these distributed moments are carried over at one-half rate to the other ends of the members. When equilibrium is reached, Joint  $B$  is clamped in its new rotated position and Joint  $C$  is released afterwards. Joint  $C$  rotates under its unbalanced moment until it reaches equilibrium, the rotation causing distributed moments in the  $C$ -ends of members  $CB$  and  $CD$  and their resulting carry-over

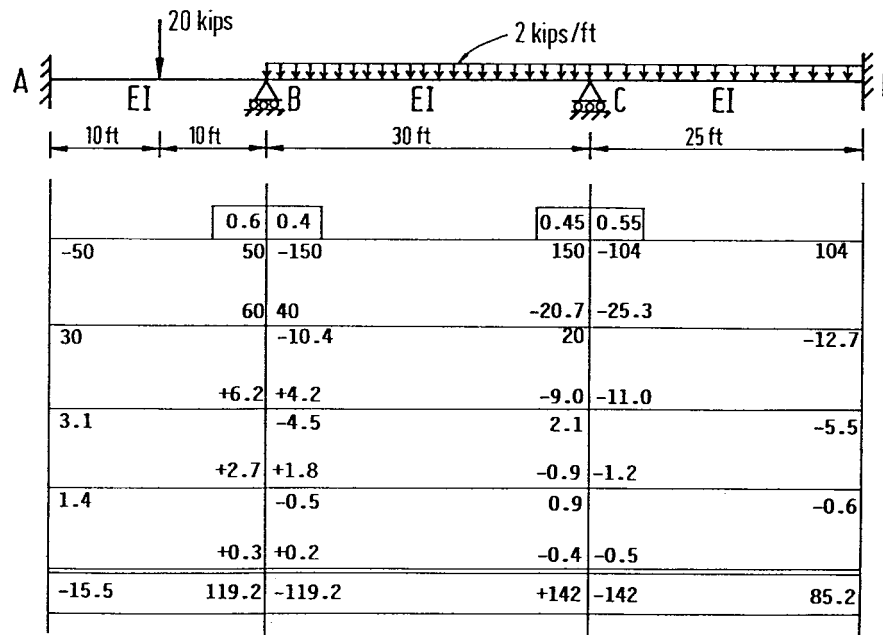


FIGURE 2.23: Example—continuous beam by moment distribution.

moments. Joint  $C$  is now clamped and Joint  $B$  is released. This procedure is repeated again and again for Joints  $B$  and  $C$ , the amount of unbalanced moment quickly diminishing, until the release of a joint causes negligible rotation. This process is called moment distribution.

The stiffness factors and distribution factors are computed as follows:

$$DF_{BA} = \frac{K_{BA}}{\sum K} = \frac{I/20}{I/20 + I/30} = 0.6$$

$$DF_{BC} = \frac{K_{BC}}{\sum K} = \frac{I/30}{I/20 + I/30} = 0.4$$

$$DF_{CB} = \frac{K_{CB}}{\sum K} = \frac{I/30}{I/30 + I/25} = 0.45$$

$$DF_{CD} = \frac{K_{CD}}{\sum K} = \frac{I/25}{I/30 + I/25} = 0.55$$

Fixed-end moments

$$M_{FAB} = -50 \text{ ft-kips}; \quad M_{FBC} = -150 \text{ ft-kips}; \quad M_{FCD} = -104 \text{ ft-kips}$$

$$M_{FBA} = 50 \text{ ft-kips}; \quad M_{FCB} = 150 \text{ ft-kips}; \quad M_{FDC} = 104 \text{ ft-kips}$$

When a clockwise couple is applied at the near end of a beam, a clockwise couple of half the magnitude is set up at the far end of the beam. The ratio of the moments at the far and near ends is defined as *carry-over factor*, and it is  $\frac{1}{2}$  in the case of a straight prismatic member. The carry-over factor was developed for carrying over to fixed ends, but it is applicable to simply supported ends, which must have final moments of zero. It can be shown that the beam simply supported at the far end is only three-fourths as stiff as the one that is fixed. If the stiffness factors for end spans that are simply supported are modified by three-fourths, the simple end is initially balanced to zero and no carry-overs are made to the end afterward. This simplifies the moment distribution process significantly.



The frame in Figure 2.25 shows a frame subjected to sway. The process of obtaining the final moments is illustrated for this frame.

The frame sways to the right and the sidesway moment can be assumed in the ratio

$$\frac{400}{20^2} : \frac{300}{20^2} \quad (\text{or}) \quad 1 : 0.7$$

Final moments are obtained by adding distributed fixed-end moments and  $\frac{13.06}{2.99}$  times the distributed assumed sidesway moments.

#### 2.4.4 Method of Consistent Deformations

The method of consistent deformations makes use of the principle of deformation compatibility to analyze indeterminate structures. This method employs equations that relate the forces acting on the structure to the deformations of the structure. These relations are formed so that the deformations are expressed in terms of the forces and the forces become the unknowns in the analysis.

Let us consider the beam shown in Figure 2.26a. The first step, in this method, is to determine the degree of indeterminacy or the number of redundants that the structure possesses. As shown in the figure, the beam has three unknown reactions,  $R_A$ ,  $R_C$ , and  $M_A$ . Since there are only two equations of equilibrium available for calculating the reactions, the beam is said to be indeterminate to the first degree. Restraints that can be removed without impairing the load-supporting capacity of the structure are referred to as *redundants*.

Once the number of redundants is known, the next step is to decide which reaction is to be removed in order to form a determinate structure. Any one of the reactions may be chosen to be the redundant provided that a stable structure remains after the removal of that reaction. For example, let us take the reaction  $R_C$  as the redundant. The determinate structure obtained by removing this restraint is the cantilever beam shown in Figure 2.26b. We denote the deflection at end  $C$  of this beam, due to  $P$ , by  $\Delta_{CP}$ . The first subscript indicates that the deflection is measured at  $C$  and the second subscript that the deflection is due to the applied load  $P$ . Using the moment area method, it can be shown that  $\Delta_{CP} = 5PL^3/48EI$ . The redundant  $R_C$  is then applied to the determinate cantilever beam, as shown in Figure 2.26c. This gives rise to a deflection  $\Delta_{CR}$  at point  $C$  the magnitude of which can be shown to be  $R_C L^3/3EI$ .

In the actual indeterminate structure, which is subjected to the combined effects of the load  $P$  and the redundant  $R_C$ , the deflection at  $C$  is zero. Hence the algebraic sum of the deflection  $\Delta_{CP}$  in Figure 2.26b and the deflection  $\Delta_{CR}$  in Figure 2.26c must vanish. Assuming downward deflections to be positive, we write

$$\Delta_{CP} - \Delta_{CR} = 0 \quad (2.33)$$

or

$$\frac{5PL^3}{48EI} - \frac{R_C L^3}{3EI} = 0$$

from which

$$R_C = \frac{5}{16}P$$

Equation 2.33, which is used to solve for the redundant, is referred to as an equation of consistent of deformation.

Once the redundant  $R_C$  has been evaluated, one can determine the remaining reactions by applying the equations of equilibrium to the structure in Figure 2.26a. Thus,  $\sum F_y = 0$  leads to

$$R_A = P - \frac{5}{16}P = \frac{11}{16}P$$

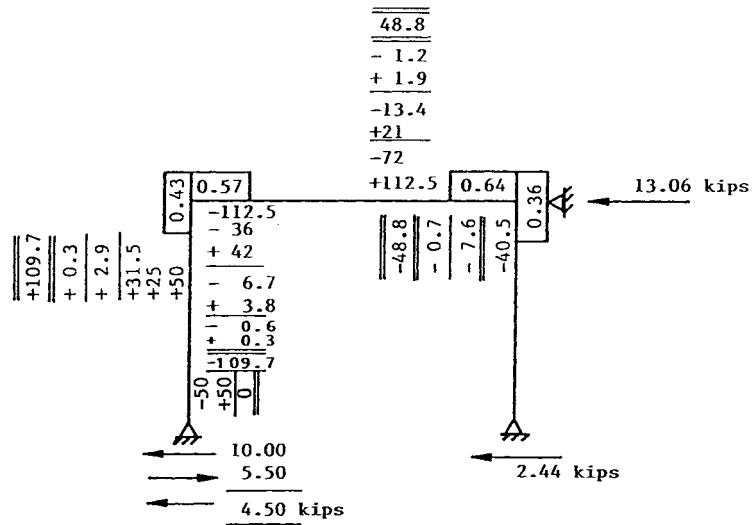
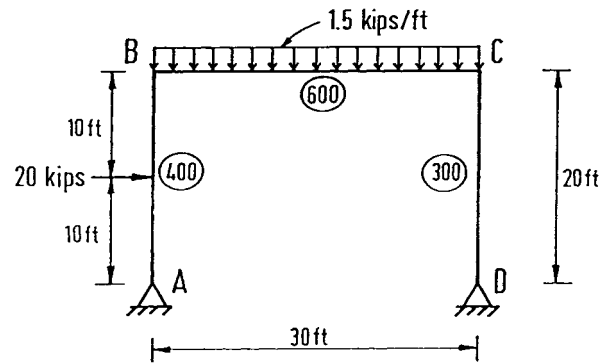


FIGURE 2.25: Example—sway frame by moment distribution.

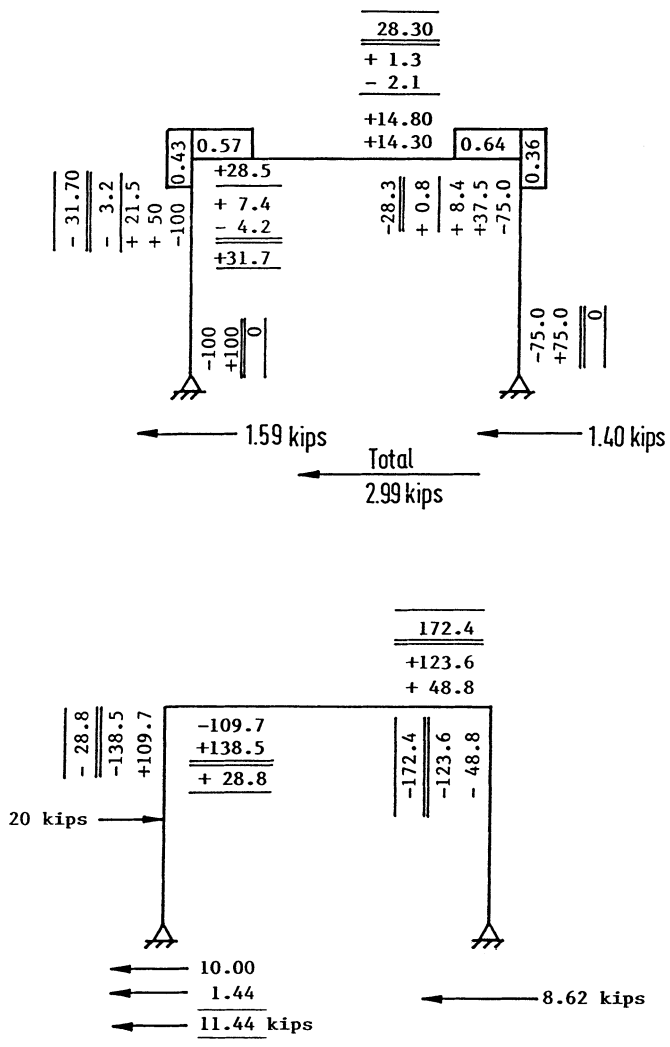


FIGURE 2.25: (Continued) Example—sway frame by moment distribution.

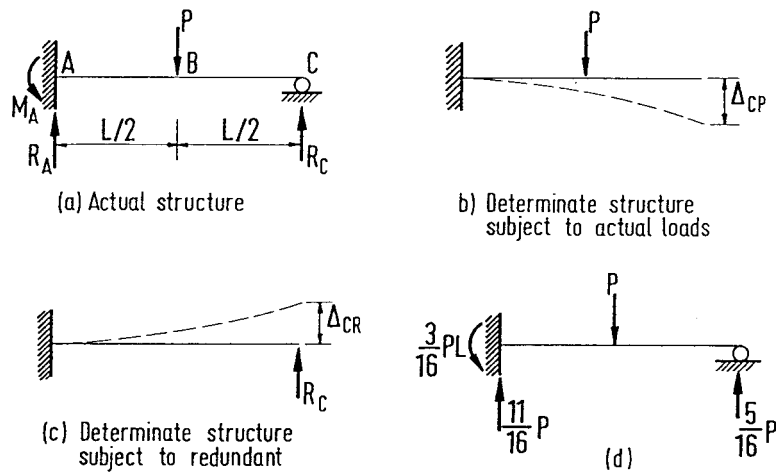


FIGURE 2.26: Beam with one redundant reaction.

and  $\sum M_A = 0$  gives

$$M_A = \frac{PL}{2} - \frac{5}{16}PL = \frac{3}{16}PL$$

A free body of the beam, showing all the forces acting on it, is shown in Figure 2.26d.

The steps involved in the method of consistent deformations are:

1. The number of redundants in the structure is determined.
2. Enough redundants are removed to form a determinate structure.
3. The displacements that the applied loads cause in the determinate structure at the points where the redundants have been removed are then calculated.
4. The displacements at these points in the determinate structure due to the redundants are obtained.
5. At each point where a redundant has been removed, the sum of the displacements calculated in Steps 3 and 4 must be equal to the displacement that exists at that point in the actual indeterminate structure. The redundants are evaluated using these relationships.
6. Once the redundants are known, the remaining reactions are determined using the equations of equilibrium.

### Structures with Several Redundants

The method of consistent deformations can be applied to structures with two or more redundants. For example, the beam in Figure 2.27a is indeterminate to the second degree and has two redundant reactions. If we let the reactions at B and C be the redundants, then the determinate structure obtained by removing these supports is the cantilever beam shown in Figure 2.27b. To this determinate structure we apply separately the given load (Figure 2.27c) and the redundants  $R_B$  and  $R_C$  one at a time (Figures 2.27d and e).

Since the deflections at B and C in the original beam are zero, the algebraic sum of the deflections in Figures 2.27c, d, and e at these same points must also vanish.

Thus,

$$\begin{aligned} \Delta_{BP} - \Delta_{BB} - \Delta_{BC} &= 0 \\ \Delta_{CP} - \Delta_{CB} - \Delta_{CC} &= 0 \end{aligned} \quad (2.34)$$

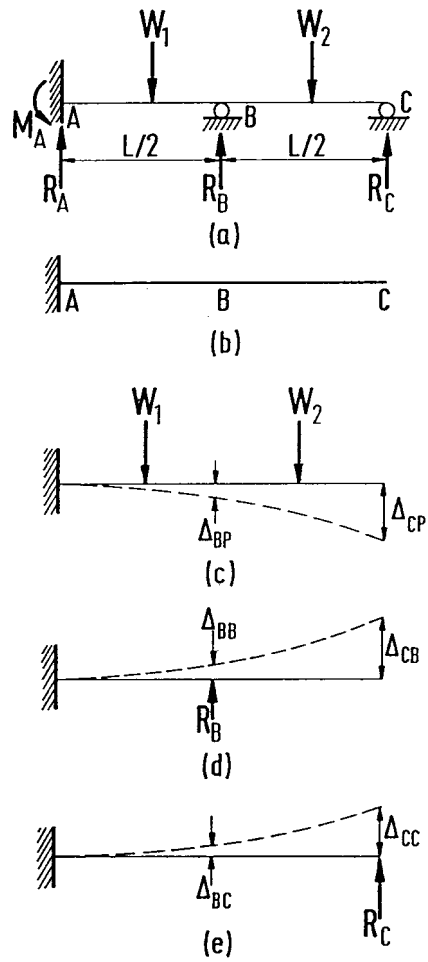


FIGURE 2.27: Beam with two redundant reactions.

It is useful in the case of complex structures to write the equations of consistent deformations in the form

$$\begin{aligned}\Delta_{BP} - \delta_{BB}R_B - \delta_{BC}R_C &= 0 \\ \Delta_{CP} - \delta_{CB}R_B - \delta_{CC}R_C &= 0\end{aligned}\quad (2.35)$$

in which  $\delta_{BC}$ , for example, denotes the deflection at  $B$  due to a unit load at  $C$  in the direction of  $R_C$ . Solution of Equation 2.35 gives the redundant reactions  $R_B$  and  $R_C$ .

#### EXAMPLE 2.5:

Determine the reactions for the beam shown in Figure 2.28 and draw its shear force and bending moment diagrams.

It can be seen from the figure that there are three reactions, namely,  $M_A$ ,  $R_A$ , and  $R_C$  one more than that required for a stable structure. The reaction  $R_C$  can be removed to make the structure determinate. We know that the deflection at support  $C$  of the beam is zero. One can determine the deflection  $\delta_{CP}$  at  $C$  due to the applied load on the cantilever in Figure 2.28b. The deflection  $\delta_{CR}$  at  $C$  due to the redundant reaction on the cantilever (Figure 2.28c) can be determined in the same way. The compatibility equation gives

$$\delta_{CP} - \delta_{CR} = 0$$

By moment area method,

$$\begin{aligned}\delta_{CP} &= \frac{20}{EI} \times 2 \times 1 + \frac{1}{2} \times \frac{20}{EI} \times 2 \times \frac{2}{3} \times 2 \\ &\quad + \frac{40}{EI} \times 2 \times 3 + \frac{1}{2} \times \frac{60}{EI} \times 2 \times \left(\frac{2}{3} \times 2 + 2\right) \\ &= \frac{1520}{3EI} \\ \delta_{CR} &= \frac{1}{2} \times \frac{4R_C}{EI} \times 4 \times \frac{2}{3} \times 4 = \frac{64R_C}{3EI}\end{aligned}$$

Substituting for  $\delta_{CP}$  and  $\delta_{CR}$  in the compatibility equation one obtains

$$\frac{1520}{3EI} - \frac{64R_C}{3EI} = 0$$

from which

$$R_C = 23.75 \text{ kN } \uparrow$$

By using statical equilibrium equations we get

$$R_A = 6.25 \text{ kN } \uparrow$$

and

$$M_A = 5 \text{ kNm.}$$

The shear force and bending moment diagrams are shown in Figure 2.28d.

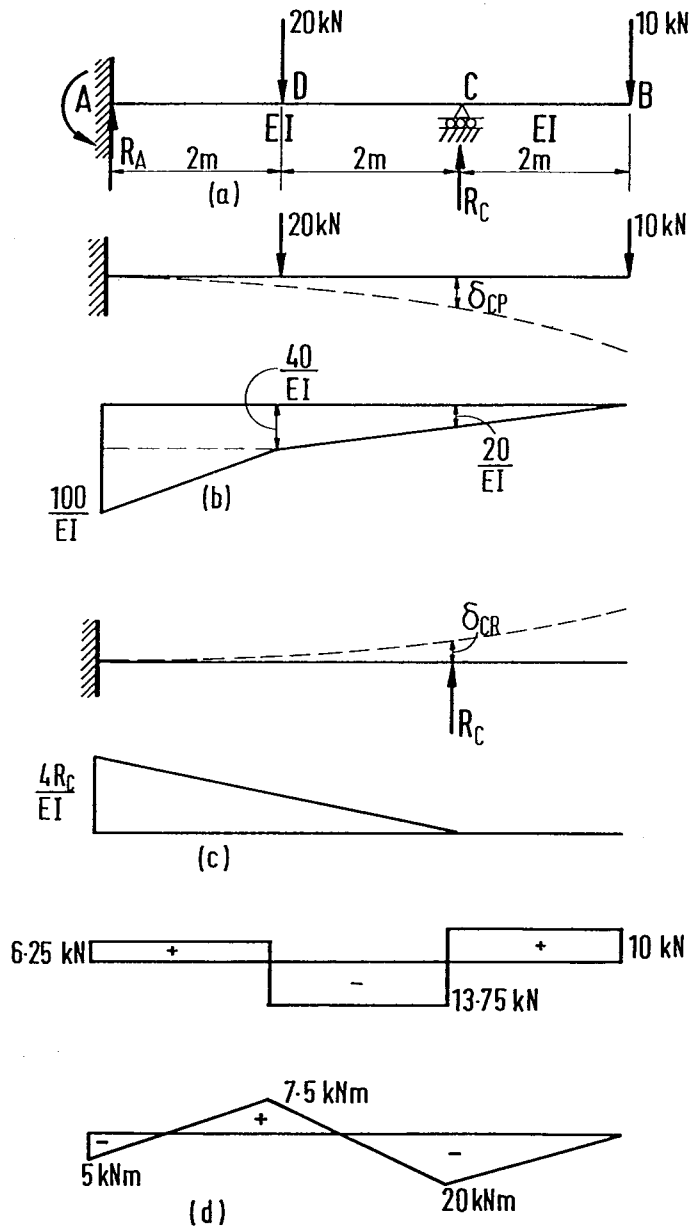


FIGURE 2.28: Example 2.5.

## 2.5 Plates

### 2.5.1 Bending of Thin Plates

When the thickness of an object is small compared to the other dimensions, it is called a **thin plate**. The plane parallel to the faces of the plate and bisecting the thickness of the plate, in the undeformed state, is called the middle plane of the plate. When the deflection of the middle plane is small compared with the thickness,  $h$ , it can be assumed that

1. There is no deformation in the middle plane.
2. The normal of the middle plane before bending is deformed into the normals of the middle plane after bending.
3. The normal stresses in the direction transverse to the plate can be neglected.

Based on these assumptions, all stress components can be expressed by deflection  $w'$  of the plate.  $w'$  is a function of the two coordinates  $(x, y)$  in the plane of the plate. This function has to satisfy a linear partial differential equation, which, together with the boundary conditions, completely defines  $w'$ .

Figure 2.29a shows a plate element cut from a plate whose middle plane coincides with the  $xy$  plane. The middle plane of the plate subjected to a lateral load of intensity ' $q$ ' is shown in Figure 2.29b. It can be shown, by considering the equilibrium of the plate element, that the stress resultants are given as

$$\begin{aligned} M_x &= -D \left( \frac{\partial^2 w}{\partial x^2} + \nu \frac{\partial^2 w}{\partial y^2} \right) \\ M_y &= -D \left( \frac{\partial^2 w}{\partial y^2} + \nu \frac{\partial^2 w}{\partial x^2} \right) \\ M_{xy} &= -M_{yx} = D(1 - \nu) \frac{\partial^2 w}{\partial x \partial y} \end{aligned} \quad (2.36)$$

$$V_x = \frac{\partial^3 w}{\partial x^3} + (2 - \nu) \frac{\partial^3 w}{\partial x \partial y^2} \quad (2.37)$$

$$V_y = \frac{\partial^3 w}{\partial y^3} + (2 - \nu) \frac{\partial^3 w}{\partial y \partial x^2} \quad (2.38)$$

$$Q_x = -D \frac{\partial}{\partial x} \left( \frac{\partial^2 w}{\partial x^2} + \frac{\partial^2 w}{\partial y^2} \right) \quad (2.39)$$

$$Q_y = -D \frac{\partial}{\partial y} \left( \frac{\partial^2 w}{\partial x^2} + \frac{\partial^2 w}{\partial y^2} \right) \quad (2.40)$$

$$R = 2D(1 - \nu) \frac{\partial^2 w}{\partial x \partial y} \quad (2.41)$$

where

- $M_x$  and  $M_y$  = bending moments per unit length in the  $x$  and  $y$  directions, respectively
- $M_{xy}$  and  $M_{yx}$  = twisting moments per unit length
- $Q_x$  and  $Q_y$  = shearing forces per unit length in the  $x$  and  $y$  directions, respectively
- $V_x$  and  $V_y$  = supplementary shear forces in the  $x$  and  $y$  directions, respectively
- $R$  = corner force
- $D$  =  $\frac{Eh^3}{12(1-\nu^2)}$ , flexural rigidity of the plate per unit length
- $E$  = modulus of elasticity

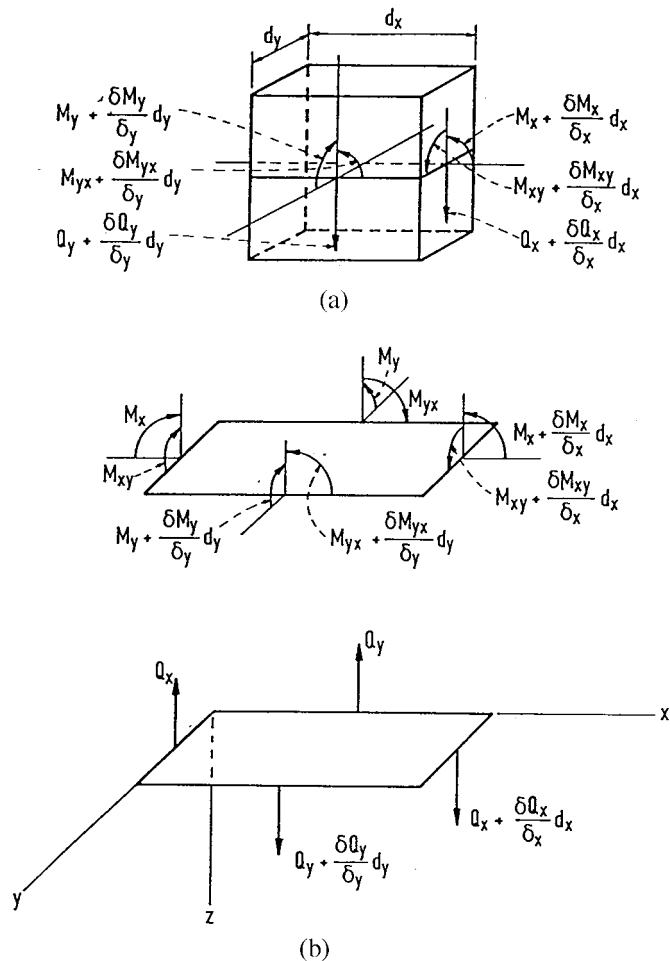


FIGURE 2.29: (a) Plate element; (b) stress resultants.

$\nu$  = Poisson's Ratio

The governing equation for the plate is obtained as

$$\frac{\partial^4 w}{\partial x^4} + 2 \frac{\partial^4 w}{\partial x^2 \partial y^2} + \frac{\partial^4 w}{\partial y^4} = \frac{q}{D} \tag{2.42}$$

Any plate problem should satisfy the governing Equation 2.42 and boundary conditions of the plate.

### 2.5.2 Boundary Conditions

There are three basic boundary conditions for plate problems. These are the clamped edge, the simply supported edge, and the free edge.

### Clamped Edge

For this boundary condition, the edge is restrained such that the deflection and slope are zero along the edge. If we consider the edge  $x = a$  to be clamped, we have

$$(w)_{x=a} = 0 \quad \left( \frac{\partial w}{\partial x} \right)_{x=a} = 0 \quad (2.43)$$

### Simply Supported Edge

If the edge  $x = a$  of the plate is simply supported, the deflection  $w$  along this edge must be zero. At the same time this edge can rotate freely with respect to the edge line. This means that

$$(w)_{x=a} = 0; \quad \left( \frac{\partial^2 w}{\partial x^2} \right)_{x=a} = 0 \quad (2.44)$$

### Free Edge

If the edge  $x = a$  of the plate is entirely free, there are no bending and twisting moments or vertical shearing forces. This can be written in terms of  $w$ , the deflection as

$$\begin{aligned} \left( \frac{\partial^2 w}{\partial x^2} + \nu \frac{\partial^2 w}{\partial y^2} \right)_{x=a} &= 0 \\ \left( \frac{\partial^3 w}{\partial x^3} + (2 - \nu) \frac{\partial^3 w}{\partial x \partial y^2} \right)_{x=a} &= 0 \end{aligned} \quad (2.45)$$

## 2.5.3 Bending of Simply Supported Rectangular Plates

A number of the plate bending problems may be solved directly by solving the differential Equation 2.42. The solution, however, depends on the loading and boundary condition. Consider a simply supported plate subjected to a sinusoidal loading as shown in Figure 2.30. The differential

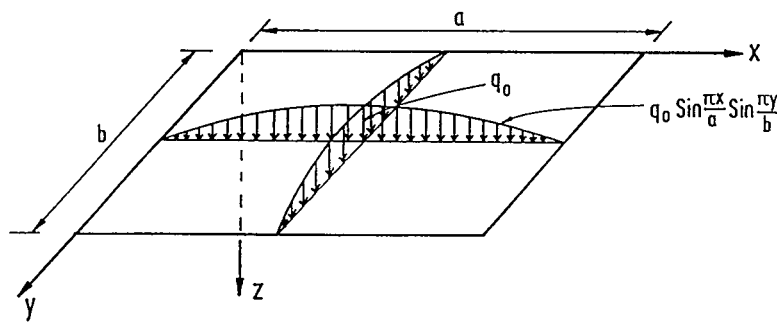


FIGURE 2.30: Rectangular plate under sinusoidal loading.

Equation 2.42 in this case becomes

$$\frac{\partial^4 w}{\partial x^4} + 2 \frac{\partial^4 w}{\partial x^2 \partial y^2} + \frac{\partial^4 w}{\partial y^4} = \frac{q_0}{D} \sin \frac{\pi x}{a} \sin \frac{\pi y}{b} \quad (2.46)$$

The boundary conditions for the simply supported edges are

$$\begin{aligned} w &= 0, & \frac{\partial^2 w}{\partial x^2} &= 0 \text{ for } x = 0 \text{ and } x = a \\ w &= 0, & \frac{\partial^2 w}{\partial y^2} &= 0 \text{ for } y = 0 \text{ and } y = b \end{aligned} \quad (2.47)$$

The deflection function becomes

$$w = w_0 \sin \frac{\pi x}{a} \sin \frac{\pi y}{b} \quad (2.48)$$

which satisfies all the boundary conditions in Equation 2.47.  $w_0$  must be chosen to satisfy Equation 2.46. Substitution of Equation 2.48 into Equation 2.46 gives

$$\pi^4 \left( \frac{1}{a^2} + \frac{1}{b^2} \right)^2 w_0 = \frac{q_o}{D}$$

The deflection surface for the plate can, therefore, be found as

$$w = \frac{q_o}{\pi^4 D \left( \frac{1}{a^2} + \frac{1}{b^2} \right)^2} \sin \frac{\pi x}{a} \sin \frac{\pi y}{b} \quad (2.49)$$

Using Equations 2.49 and 2.36, we find expression for moments as

$$\begin{aligned} M_x &= \frac{q_o}{\pi^2 \left( \frac{1}{a^2} + \frac{1}{b^2} \right)^2} \left( \frac{1}{a^2} + \frac{\nu}{b^2} \right) \sin \frac{\pi x}{a} \sin \frac{\pi y}{b} \\ M_y &= \frac{q_o}{\pi^2 \left( \frac{1}{a^2} + \frac{1}{b^2} \right)^2} \left( \frac{\nu}{a^2} + \frac{1}{b^2} \right) \sin \frac{\pi x}{a} \sin \frac{\pi y}{b} \\ M_{xy} &= \frac{q_o(1-\nu)}{\pi^2 \left( \frac{1}{a^2} + \frac{1}{b^2} \right)^2} \frac{\cos \frac{\pi x}{a} \cos \frac{\pi y}{b}}{ab} \end{aligned} \quad (2.50)$$

Maximum deflection and maximum bending moments that occur at the center of the plate can be written by substituting  $x = a/2$  and  $y = b/2$  in Equation 2.50 as

$$\begin{aligned} w_{\max} &= \frac{q_o}{\pi^4 D \left( \frac{1}{a^2} + \frac{1}{b^2} \right)^2} \\ (M_x)_{\max} &= \frac{q_o}{\pi^2 \left( \frac{1}{a^2} + \frac{1}{b^2} \right)^2} \left( \frac{1}{a^2} + \frac{\nu}{b^2} \right) \\ (M_y)_{\max} &= \frac{q_o}{\pi^2 \left( \frac{1}{a^2} + \frac{1}{b^2} \right)^2} \left( \frac{\nu}{a^2} + \frac{1}{b^2} \right) \end{aligned} \quad (2.51)$$

If the plate is square, then  $a = b$  and Equation 2.51 becomes

$$\begin{aligned} w_{\max} &= \frac{q_o a^4}{4\pi^4 D} \\ (M_x)_{\max} &= (M_y)_{\max} = \frac{(1+\nu)}{4\pi^2} q_o a^2 \end{aligned} \quad (2.52)$$

If the simply supported rectangular plate is subjected to any kind of loading given by

$$q = q(x, y) \quad (2.53)$$

the function  $q(x, y)$  should be represented in the form of a double trigonometric series as

$$q(x, y) = \sum_{m=1}^{\infty} \sum_{n=1}^{\infty} q_{mn} \sin \frac{m\pi x}{a} \sin \frac{n\pi y}{b} \quad (2.54)$$

in which  $q_{mn}$  is given by

$$q_{mn} = \frac{4}{ab} \int_0^a \int_0^b q(x, y) \sin \frac{m\pi x}{a} \sin \frac{n\pi y}{b} dx dy \quad (2.55)$$

From Equations 2.46, 2.53, 2.54, and 2.55 we can obtain the expression for deflection as

$$w = \frac{1}{\pi^4 D} \sum_{m=1}^{\infty} \sum_{n=1}^{\infty} \frac{q_{mn}}{\left(\frac{m^2}{a^2} + \frac{n^2}{b^2}\right)^2} \sin \frac{m\pi x}{a} \sin \frac{n\pi y}{b} \quad (2.56)$$

If the applied load is uniformly distributed of intensity  $q_o$ , we have

$$q(x, y) = q_o$$

and from Equation 2.55 we obtain

$$q_{mn} = \frac{4q_o}{ab} \int_0^a \int_0^b \sin \frac{m\pi x}{a} \sin \frac{n\pi y}{b} dx dy = \frac{16q_o}{\pi^2 mn} \quad (2.57)$$

in which 'm' and 'n' are odd integers.  $q_{mn} = 0$  if 'm' or 'n' or both of them are even numbers. We can, therefore, write the expression for deflection of a simply supported plate subjected to uniformly distributed load as

$$w = \frac{16q_o}{\pi^6 D} \sum_{m=1}^{\infty} \sum_{n=1}^{\infty} \frac{\sin \frac{m\pi x}{a} \sin \frac{n\pi y}{b}}{mn \left(\frac{m^2}{a^2} + \frac{n^2}{b^2}\right)^2} \quad (2.58)$$

where  $m = 1, 3, 5, \dots$  and  $n = 1, 3, 5, \dots$

The maximum deflection occurs at the center and it can be written by substituting  $x = \frac{a}{2}$  and  $y = \frac{b}{2}$  in Equation 2.58 as

$$w_{\max} = \frac{16q_o}{\pi^6 D} \sum_{m=1}^{\infty} \sum_{n=1}^{\infty} \frac{(-1)^{\frac{m+n}{2}-1}}{mn \left(\frac{m^2}{a^2} + \frac{n^2}{b^2}\right)^2} \quad (2.59)$$

Equation 2.59 is a rapid converging series and a satisfactory approximation can be obtained by taking only the first term of the series; for example, in the case of a square plate,

$$w_{\max} = \frac{4q_o a^4}{\pi^6 D} = 0.00416 \frac{q_o a^4}{D}$$

Assuming  $\nu = 0.3$ , we get for the maximum deflection

$$w_{\max} = 0.0454 \frac{q_o a^4}{Eh^3}$$

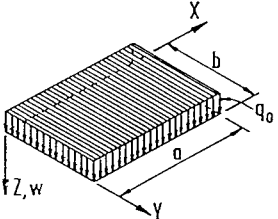
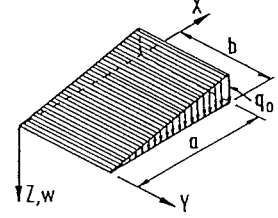
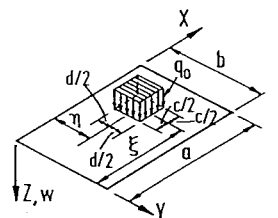
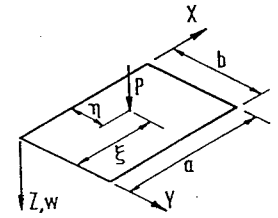
No.	Load $q(x,y) = \sum_m \sum_n q_{mn} \sin \frac{m\pi x}{a} \sin \frac{n\pi y}{b}$	Expansion Coefficients $q_{mn}$
1		$q_{mn} = \frac{16q_0}{\pi^2 mn}$ $(m, n = 1, 3, 5, \dots)$
2		$q_{mn} = \frac{-8q_0 \cos m\pi}{\pi^2 mn}$ $(m, n = 1, 3, 5, \dots)$
3		$p_{mn} = \frac{16q_0}{\pi^2 mn} \sin \frac{m\pi \xi}{a} \sin \frac{n\pi \eta}{b}$ $\times \sin \frac{m\pi c}{2a} \sin \frac{n\pi d}{2b}$ $(m, n = 1, 3, 5, \dots)$
4		$q_{mn} = \frac{4q_0}{ab} \sin \frac{m\pi \xi}{a} \sin \frac{n\pi \eta}{b}$ $(m, n = 1, 2, 3, \dots)$

FIGURE 2.31: Typical loading on plates and loading functions.

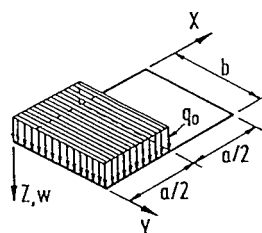
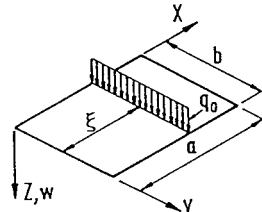
No.	Load $q(x,y) = \sum \sum q_{mn} \sin \frac{m\pi x}{a} \sin \frac{n\pi y}{b}$	Expansion coefficients $q_{mn}$
5		$q_{mn} = \frac{8q_0}{\pi^2 mn} \text{ for } m, n = 1, 3, 5, \dots$ $q_{mn} = \frac{16q_0}{\pi^2 mn} \text{ for } \begin{cases} m = 2, 6, 10, \dots \\ n = 1, 3, 5, \dots \end{cases}$
6		$q_{mn} = \frac{4q_0}{\pi a n} \sin \frac{m\pi \xi}{a}$ $(m, n = 1, 2, 3, \dots)$

FIGURE 2.31: (Continued) Typical loading on plates and loading functions.

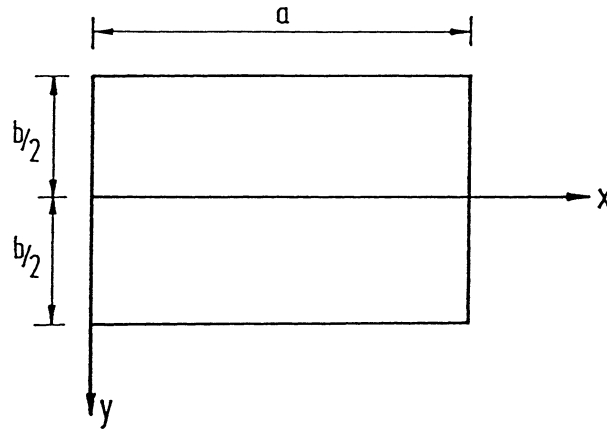


FIGURE 2.32: Rectangular plate.

The expressions for bending and twisting moments can be obtained by substituting Equation 2.58 into Equation 2.36. Figure 2.31 shows some loading cases and the corresponding loading functions.

The above solution for uniformly loaded cases is known as Navier solution. If two opposite sides (say  $x = 0$  and  $x = a$ ) of a rectangular plate are simply supported, the solution taking the deflection function as

$$w = \sum_{m=1}^{\infty} Y_m \sin \frac{m\pi x}{a} \quad (2.60)$$

can be adopted. This solution was proposed by Levy [53]. Equation 2.60 satisfies the boundary conditions  $w = 0$  and  $\frac{\partial^2 w}{\partial x^2} = 0$  on the two simply supported edges.  $Y_m$  should be determined such that it satisfies the boundary conditions along the edges  $y = \pm \frac{b}{2}$  of the plate shown in Figure 2.32 and also the equation of the deflection surface

$$\frac{\partial^4 w}{\partial x^4} + 2 \frac{\partial^4 w}{\partial x^2 \partial y^2} + \frac{\partial^4 w}{\partial y^4} = \frac{q_o}{D} \quad (2.61)$$

$q_o$  being the intensity of uniformly distributed load.

The solution for Equation 2.61 can be taken in the form

$$w = w_1 + w_2 \quad (2.62)$$

for a uniformly loaded simply supported plate.  $w_1$  can be taken in the form

$$w_1 = \frac{q_o}{24D} (x^4 - 2ax^3 + a^3x) \quad (2.63)$$

representing the deflection of a uniformly loaded strip parallel to the  $x$  axis. It satisfies Equation 2.61 and also the boundary conditions along  $x = 0$  and  $x = a$ .

The expression  $w_2$  has to satisfy the equation

$$\frac{\partial^4 w_2}{\partial x^4} + 2 \frac{\partial^4 w_2}{\partial x^2 \partial y^2} + \frac{\partial^4 w_2}{\partial y^4} = 0 \quad (2.64)$$

and must be chosen such that Equation 2.62 satisfies all boundary conditions of the plate. Taking  $w_2$  in the form of series given in Equation 2.60 it can be shown that the deflection surface takes the form

$$\begin{aligned} w\psi = & \frac{q_o}{24D} (x^4 - 2ax^3 + a^3x) + \frac{q_o a^4}{24D} \sum_{m=1}^{\infty} \left( A_m \cosh \frac{m\pi y}{a} \right. \\ & + B_m \frac{m\pi y}{a} \sinh \frac{m\pi y}{a} + C_m \sinh \frac{m\pi y}{a} \\ & \left. + D_m \frac{m\pi y}{a} \cosh \frac{m\pi y}{a} \right) \sin \frac{m\pi x}{a} \end{aligned} \quad (2.65)$$

Observing that the deflection surface of the plate is symmetrical with respect to the  $x$  axis, we keep in Equation 2.65 only an even function of  $y$ ; therefore,  $C_m = D_m = 0$ . The deflection surface takes the form

$$\begin{aligned} w = & \frac{q_o}{24D} (x^4 - 2ax^3 + a^3x) + \frac{q_o a^4}{24D} \sum_{m=1}^{\infty} \left( A_m \cosh \frac{m\pi y}{a} \right. \\ & \left. + B_m \frac{m\pi y}{a} \sinh \frac{m\pi y}{a} \right) \sin \frac{m\pi x}{a} \end{aligned} \quad (2.66)$$

Developing the expression in Equation 2.63 into a trigonometric series, the deflection surface in Equation 2.66 is written as

$$w = \frac{q_o a^4}{D} \sum_{m=1}^{\infty} \left( \frac{4}{\pi^5 m^5} + A_m \cosh \frac{m\pi y}{a} + B_m \frac{m\pi y}{a} \sin \frac{m\pi y}{a} \right) \sin \frac{m\pi x}{a} \quad (2.67)$$

Substituting Equation 2.67 in the boundary conditions

$$w = 0, \quad \frac{\partial^2 w}{\partial y^2} = 0 \quad (2.68)$$

one obtains the constants of integration  $A_m$  and  $B_m$  and the expression for deflection may be written as

$$w = \frac{4q_0 a^4}{\pi^5 D} \sum_{m=1,3,5,\dots}^{\infty} \frac{1}{m^5} \left( 1 - \frac{\alpha_m \tanh \alpha_m + 2}{2 \cosh \alpha_m} \cosh \frac{2\alpha_m y}{b} + \frac{\alpha_m}{2 \cosh \alpha_m} \frac{2y}{b} \sinh \frac{2\alpha_m y}{b} \right) \sin \frac{m\pi x}{a} \quad (2.69)$$

in which  $\alpha_m = \frac{m\pi b}{2a}$ .

Maximum deflection occurs at the middle of the plate,  $x = \frac{a}{2}$ ,  $y = 0$  and is given by

$$w = \frac{4q_0 a^4}{\pi^5 D} \sum_{m=1,3,5,\dots}^{\infty} \frac{(-1)^{\frac{m-1}{2}}}{m^5} \left( 1 - \frac{\alpha_m \tanh \alpha_m + 2}{2 \cosh \alpha_m} \right) \quad (2.70)$$

Solution of plates with arbitrary boundary conditions are complicated. It is possible to make some simplifying assumptions for plates with the same boundary conditions along two parallel edges in order to obtain the desired solution. Alternately, the energy method can be applied more efficiently to solve plates with complex boundary conditions. However, it should be noted that the accuracy of results depends upon the deflection function chosen. These functions must be so chosen that they satisfy at least the kinematics boundary conditions.

Figure 2.33 gives formulas for deflection and bending moments of rectangular plates with typical boundary and loading conditions.

## 2.5.4 Bending of Circular Plates

In the case of symmetrically loaded circular plate, the loading is distributed symmetrically about the axis perpendicular to the plate through its center. In such cases, the deflection surface to which the middle plane of the plate is bent will also be symmetrical. The solution of circular plates can be conveniently carried out by using polar coordinates.

Stress resultants in a circular plate element are shown in Figure 2.34. The governing differential equation is expressed in polar coordinates as

$$\frac{1}{r} \frac{d}{dr} \left\{ r \frac{d}{dr} \left[ \frac{1}{r} \frac{d}{dr} \left( r \frac{dw}{dr} \right) \right] \right\} = \frac{q}{D} \quad (2.71)$$

in which  $q$  is the intensity of loading.

In the case of uniformly loaded circular plates, Equation 2.71 can be integrated successively and the deflection at any point at a distance  $r$  from the center can be expressed as

$$w = \frac{q_0 r^4}{64D} + \frac{C_1 r^2}{4} + C_2 \log \frac{r}{a} + C_3 \quad (2.72)$$

in which  $q_0$  is the intensity of loading and  $a$  is the radius of the plate.  $C_1$ ,  $C_2$ , and  $C_3$  are constants of integration to be determined using the boundary conditions.

For a plate with clamped edges under uniformly distributed load  $q_0$ , the deflection surface reduces to

$$w = \frac{q_0}{64D} (a^2 - r^2)^2 \quad (2.73)$$

The maximum deflection occurs at the center where  $r = 0$ , and is given by

$$w = \frac{q_0 a^4}{64D} \quad (2.74)$$

Case No.	Structural System and Static Loading	Deflection and Internal Forces
1		$w = \frac{16q_0}{\pi^6 D} \sum_m \sum_n \frac{\sin \frac{m\pi x}{a} \sin \frac{n\pi y}{b}}{mn \left( \frac{m^2}{a^2} + \frac{n^2}{b^2} \right)^2}$ $m_x = \frac{16q_0 a^2}{\pi^4} \sum_m \sum_n \frac{\left( m^2 + \nu \frac{n^2}{e^2} \right) \sin \frac{m\pi x}{a} \sin \frac{n\pi y}{b}}{mn \left( m^2 + \frac{n^2}{e^2} \right)^2}$ $m_y = \frac{16q_0 a^2}{\pi^4} \sum_m \sum_n \frac{\left( \frac{n^2}{e^2} + \nu m^2 \right) \sin \frac{m\pi x}{a} \sin \frac{n\pi y}{b}}{mn \left( m^2 + \frac{n^2}{e^2} \right)^2}$ $e = \frac{b}{a}, \quad m = 1, 3, 5, \dots, \infty; \quad n = 1, 3, 5, \dots, \infty$
2		$w = \frac{a^4}{D \pi^4} \sum_{m=1}^{\infty} \frac{P_m}{m^4} \left( 1 - \frac{2 + \alpha_m \tanh \alpha_m}{2 \cosh \alpha_m} \cos \lambda_m y \right) + \frac{\lambda_m y \sinh \lambda_m y}{2 \cosh \alpha_m} \sin \lambda_m x$ <p>where</p> $P_m = \frac{2q_0}{a} \sin \frac{m\pi \xi}{a} \quad \lambda_m = \frac{m\pi}{a}$ $m = 1, 2, 3, \dots \quad \alpha_m = \frac{m\pi b}{2a}$
3		$w = \frac{16q_0}{D \pi^6} \sum_m \sum_n \frac{\sin \frac{m\pi \xi}{a} \sin \frac{n\pi \eta}{b} \sin \frac{m\pi c}{b} \sin \frac{n\pi d}{2b}}{mn \left( \frac{m^2}{a^2} + \frac{n^2}{b^2} \right)^2}$ $\times \sin \frac{m\pi x}{a} \sin \frac{n\pi y}{b}$ $m = 1, 2, 3, \dots$ $n = 1, 2, 3, \dots$
4		$w = \frac{4P}{D \pi^4 ab} \sum_m \sum_n \frac{\sin \frac{m\pi \xi}{a} \sin \frac{n\pi \eta}{b} \sin \frac{m\pi x}{a} \sin \frac{n\pi y}{b}}{\left( \frac{m^2}{a^2} + \frac{n^2}{b^2} \right)^2}$ $m = 1, 2, 3, \dots$ $n = 1, 2, 3, \dots$

FIGURE 2.33: Typical loading and boundary conditions for rectangular plates.

Bending moments in the radial and tangential directions are respectively given by

$$M_r = \frac{q_0}{16} \left[ a^2(1 + \nu) - r^2(3 + \nu) \right]$$

$$M_t = \frac{q_0}{16} \left[ a^2(1 + \nu) - r^2(1 + 3\nu) \right] \quad (2.75)$$

The method of superposition can be applied in calculating the deflections for circular plates with

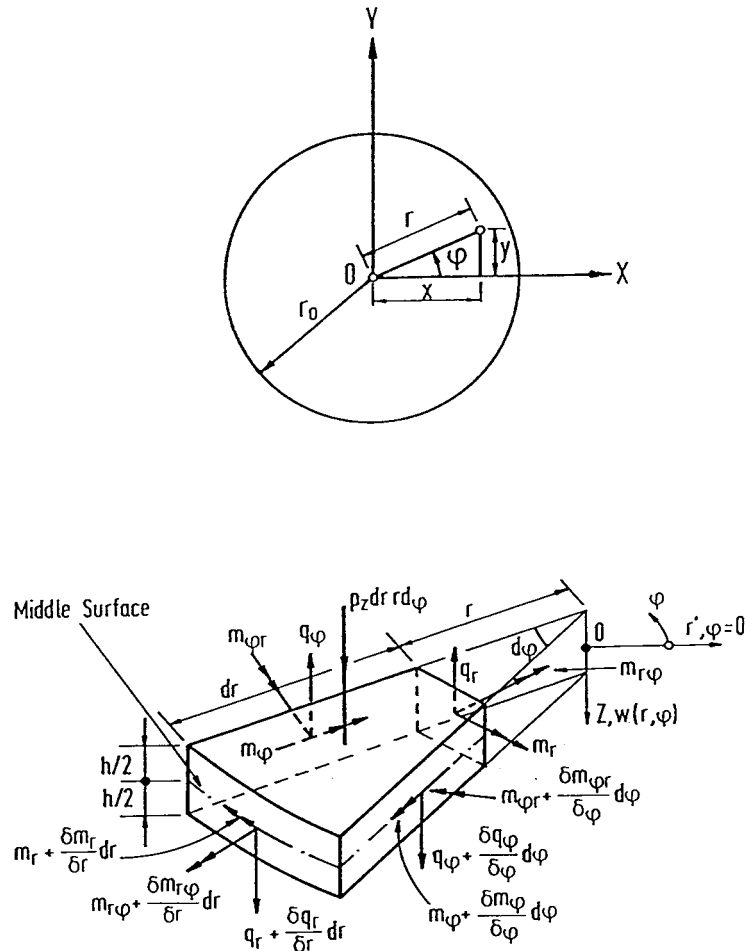


FIGURE 2.34: (a) Circular plate; (b) stress resultants.

simply supported edges. The expressions for deflection and bending moment are given as follows:

$$w = \frac{q_0(a^2 - r^2)}{64D} \left( \frac{5 + \nu}{1 + \nu} a^2 - r^2 \right)$$

$$w_{\max} = \frac{5 + \nu}{64(1 + \nu)} \frac{q_0 a^4}{D} \quad (2.76)$$

$$M_r = \frac{q_0}{16} (3 + \nu)(a^2 - r^2)$$

$$M_t = \frac{q_0}{16} [a^2(3 + \nu) - r^2(1 + 3\nu)] \quad (2.77)$$

This solution can be used to deal with plates with circular holes at the center and subjected to concentric moment and shearing forces. Plates subjected to concentric loading and concentrated loading also can be solved by this method. More rigorous solutions are available to deal with irregular loading on circular plates. Once again energy method can be employed advantageously to solve circular plate problems. Figure 2.35 gives deflection and bending moment expressions for typical cases of loading and boundary conditions on circular plates.

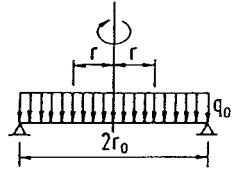
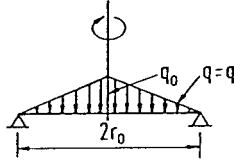
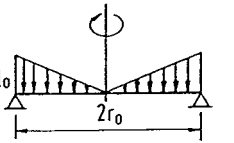
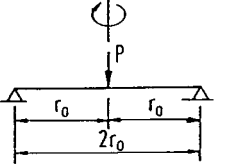
Case No.	Structural System and Static Loading	Deflection and Internal Forces
1		$w = \frac{q_0 r_0^4}{64D(1+\nu)} [2(3+\nu)C_1 - (1+\nu)C_0]$ $m_r = \frac{q_0 r_0^2}{16} (3+\nu)C_1 \quad \rho = \frac{r}{r_0}$ $m_\phi = \frac{q_0 r_0^2}{16} [2(1-\nu) - (1+3\nu)C_1] \quad C_0 = 1 - \rho^4$ $q_r = \frac{q_0 r_0}{2} \rho \quad C_1 = 1 - \rho^2$
2		$w = \frac{q_0 r_0^4}{14400D} \left[ \frac{3(183+43\nu)}{1+\nu} - \frac{10(71+29\nu)}{1+\nu} \rho^2 + 225\rho^4 - 64\rho^5 \right]$ $(m_r)_{\rho=0} = (m_\phi)_{\rho=0} = \frac{q_0 r_0^2}{720} (71+29\nu);$ $(q_r)_{\rho=1} = -\frac{q_0 r_0}{6} \quad \rho = \frac{r}{r_0}$
3		$w = \frac{q_0 r_0^4}{450D} \left[ \frac{3(6+\nu)}{1+\nu} - \frac{5(4+\nu)}{1+\nu} \rho^2 + 2\rho^5 \right]$ $(m_r)_{\rho=0} = (m_\phi)_{\rho=0} = \frac{q_0 r_0^2}{45} (4+\nu);$ $(q_r)_{\rho=1} = -\frac{q_0 r_0}{3} \quad \rho = \frac{r}{r_0}$
4		$w = \frac{P r_0^2}{16\pi D} \left[ \frac{3+\nu}{1+\nu} C_1 + 2C_2 \right] \quad C_1 = 1 - \rho^2$ $m_r = \frac{P}{4\pi} (1+\nu) C_3 \quad C_2 = \rho^2 \ln \rho$ $m_\phi = \frac{P}{4\pi} [(1-\nu) - (1+\nu)C_3] \quad C_3 = \ln \rho$ $q_r = \frac{P}{2\pi r_0 \rho} \quad \rho = \frac{r}{r_0}$

FIGURE 2.35: Typical loading and boundary conditions for circular plates.

Case No.	Structural System and Static Loading	Deflection and Internal Forces
5		$w = \frac{Mr_0^2}{2D(1+\nu)C_1}$ $m_r = m_\phi = M$ $q_r = 0$ $C_1 = 1 - \rho^2, \quad \rho = \frac{r}{r_0}$
6		$w = \frac{q_0 r_0^4}{64D} (1 - \rho^2)^2$ $m_r = \frac{q_0 r_0^2}{16} [1 + \nu - (3 + \nu)\rho^2]$ $m_\phi = \frac{q_0 r_0^2}{16} [1 + \nu - (1 + 3\nu)\rho^2]$ $q_r = -\frac{q_0 r_0}{2} \rho$ $\rho = \frac{r}{r_0}$
7		$w = \frac{q_0 r_0^4}{14400D} (129 - 290\rho^2 + 225\rho^4 - 64\rho^5)$ $(m_r)_{\rho=0} = (m_\phi)_{\rho=0} = \frac{29q_0 r_0^2}{720} (1 + \nu)$ $(q_r)_{\rho=1} = -\frac{q_0 r_0}{6}$ $(m_r)_{\rho=1} = (m_\phi)_{\rho=1} = -\frac{7q_0 r_0^2}{120}$ $\rho = \frac{r}{r_0}$
8		$w = \frac{q_0 r_0^4}{450D} (3 - 5\rho^2 + 2\rho^5)$ $m_r = \frac{q_0 r_0^2}{45} [1 + \nu - (4 + \nu)\rho^3]$ $m_\phi = \frac{q_0 r_0^2}{45} [1 + \nu - (1 + 4\nu)\rho^3]$ $q_r = -\frac{q_0 r_0}{3} \rho^2$ $\rho = \frac{r}{r_0}$
9		$w = \frac{Pr_0^2}{16\pi D} (1 - \rho^2 + 2\rho^2 \ln \rho)$ $m_r = -\frac{P}{4\pi} [1 + (1 + \nu) \ln \rho]$ $m_\phi = -\frac{P}{4\pi} [\nu + (1 + \nu) \ln \rho]$ $q_r = -\frac{P}{2\pi r_0 \rho}$ $\rho = \frac{r}{r_0}$

FIGURE 2.35: (Continued) Typical loading and boundary conditions for circular plates.

### 2.5.5 Strain Energy of Simple Plates

The strain energy expression for a simple rectangular plate is given by

$$U\psi = \frac{D}{2} \int \int_{\text{area}} \left\{ \left( \frac{\partial^2 w}{\partial x^2} + \frac{\partial^2 w}{\partial y^2} \right)^2 - 2(1 - \nu) \left[ \frac{\partial^2 w}{\partial x^2} \frac{\partial^2 w}{\partial y^2} - \left( \frac{\partial^2 w}{\partial x \partial y} \right)^2 \right] \right\} dx dy \psi \quad (2.78)$$

Suitable deflection function  $w(x, y)$  satisfying the boundary conditions of the given plate may be chosen. The strain energy,  $U$ , and the work done by the given load,  $q(x, y)$ ,

$$W = - \int \int_{\text{area}} q(x, y) w(x, y) dx dy \psi \quad (2.79)$$

can be calculated. The total potential energy is, therefore, given as  $V = U + W$ . Minimizing the total potential energy the plate problem can be solved.

$$\left[ \frac{\partial^2 w}{\partial x^2} \frac{\partial^2 w}{\partial y^2} - \left( \frac{\partial^2 w}{\partial x \partial y} \right)^2 \right]$$

The term is known as the Gaussian curvature.

If the function  $w(x, y) = f(x) \cdot \phi(y)$  (product of a function of  $x$  only and a function of  $y$  only) and  $w = 0$  at the boundary are assumed, then the integral of the Gaussian curvature over the entire plate equals zero. Under these conditions

$$U = \frac{D}{2} \int \int_{\text{area}} \left( \frac{\partial^2 w}{\partial x^2} + \frac{\partial^2 w}{\partial y^2} \right)^2 dx dy$$

If polar coordinates instead of rectangular coordinates are used and axial symmetry of loading and deformation is assumed, the equation for strain energy,  $U$ , takes the form

$$U = \frac{D}{2} \int \int_{\text{area}} \left\{ \left( \frac{\partial^2 w}{\partial r^2} + \frac{1}{r} \frac{\partial w}{\partial r} \right)^2 - \frac{2(1 - \nu)}{r} \frac{\partial w}{\partial r} \frac{\partial^2 w}{\partial r^2} \right\} r dr d\theta \psi \quad (2.80)$$

and the work done,  $W$ , is written as

$$W = - \int \int_{\text{area}} qwr dr d\theta \psi \quad (2.81)$$

Detailed treatment of the Plate Theory can be found in [56].

### 2.5.6 Plates of Various Shapes and Boundary Conditions

#### Simply Supported Isosceles Triangular Plate Subjected to a Concentrated Load

Plates of shapes other than circle and rectangle are used in some situations. A rigorous solution of the deflection for a plate with a more complicated shape is likely to be very difficult. Consider, for example, the bending of an isosceles triangular plate with simply supported edges under concentrated load  $P$  acting at an arbitrary point (Figure 2.36). A solution can be obtained for this plate by considering a mirror image of the plate as shown in the figure. The deflection of  $OBC$  of the square

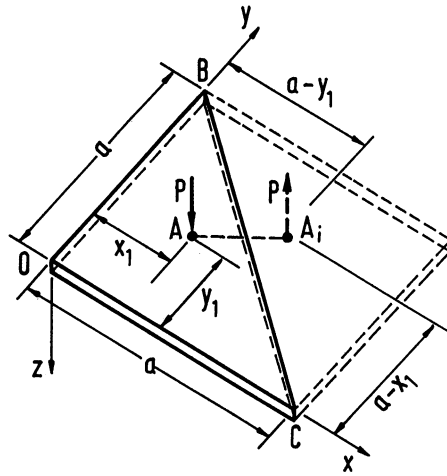


FIGURE 2.36: Isosceles triangular plate.

plate is identical with that of a simply supported triangular plate  $OB C$ . The deflection owing to the force  $P$  can be written as

$$w_1 = \frac{4Pa^2}{\pi^4 D} \sum_{m=1}^{\infty} \sum_{n=1}^{\infty} \frac{\sin(m\pi x_1/a) \sin(n\pi y_1/a)}{(m^2 + n^2)^2} \sin \frac{m\pi x}{a} \sin \frac{n\pi y}{a} \quad (2.82)$$

Upon substitution of  $-P$  for  $P$ ,  $(a - y_1)$  for  $x_1$ , and  $(a - x_1)$  for  $y_1$  in Equation 2.82 we obtain the deflection due to the force  $-P$  at  $A_i$ :

$$w_2 = -\frac{4Pa^2}{\pi^4 D} \sum_{m=1}^{\infty} \sum_{n=1}^{\infty} (-1)^{m+n} \frac{\sin(m\pi x_1/a) \sin(n\pi y_1/a)}{(m^2 + n^2)^2} \sin \frac{m\pi x}{a} \sin \frac{n\pi y}{a} \quad (2.83)$$

The deflection surface of the triangular plate is then

$$w = w_1 + w_2 \quad (2.84)$$

### Equilateral Triangular Plates

The deflection surface of a simply supported plate loaded by uniform moment  $M_o$  along its boundary and the surface of a uniformly loaded membrane, uniformly stretched over the same triangular boundary, are identical. The deflection surface for such a case can be obtained as

$$w = \frac{M_o}{4aD} \left[ x^3 - 3xy^2 - a(x^2 + y^2) + \frac{4}{27}a^3 \right] \quad (2.85)$$

If the simply supported plate is subjected to uniform load  $p_o$  the deflection surface takes the form

$$w = \frac{p_o}{64aD} \left[ x^3 - 3xy^2 - a(x^2 + y^2) + \frac{4}{27}a^3 \right] \left( \frac{4}{9}a^2 - x^2 - y^2 \right) \quad (2.86)$$

For the equilateral triangular plate (Figure 2.37) subjected to uniform load and supported at the corners approximate solutions based on the assumption that the total bending moment along each

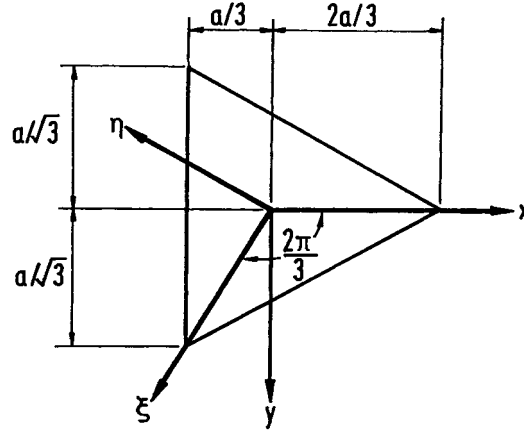


FIGURE 2.37: Equilateral triangular plate with coordinate axes.

side of the triangle vanishes were obtained by Vijakhana et al. [58] who derived an equation for deflection surface as

$$\begin{aligned}
 w = & \frac{qa^4}{144(1-\nu^2)D} \left[ \frac{8}{27}(7+\nu)(2-\nu) - (7+\nu)(1-\nu) \right. \\
 & \left. \left( \frac{x^2}{a^2} + \frac{y^2}{a^2} \right) - (5-\nu)(1+\nu) \left( \frac{x^3}{a^3} - 3\frac{xy^2}{a^3} \right) \right. \\
 & \left. + \frac{9}{4}(1-\nu^2) \left( \frac{x^4}{a^4} + 2\frac{x^2y^2}{a^4} + \frac{y^4}{a^4} \right) \right] \quad (2.87)
 \end{aligned}$$

The errors introduced by the approximate boundary condition, i.e., the total bending moment along each side of the triangle vanishes, are not significant because its influence on the maximum deflection and stress resultants is small for practical design purposes. The value of the twisting moment on the edge at the corner given by this solution is found to be exact.

The details of the mathematical treatment may be found in [58].

### Rectangular Plate Supported at Corners

Approximate solutions for rectangular plates supported at the corners and subjected to uniformly distributed load were obtained by Lee and Ballesteros [36]. The approximate deflection surface is given as

$$\begin{aligned}
 w = & \frac{qa^4}{48(1-\nu^2)D} \left[ (10+\nu-\nu^2) \left( 1 + \frac{b^4}{a^4} \right) - 2(7\nu-1) \frac{b^2}{a^2} \right. \\
 & + 2 \left( (1+5\nu) \frac{b^2}{a^2} - (6+\nu-\nu^2) \right) \frac{x}{a} \\
 & + 2 \left( (1+5\nu) - (6+\nu-\nu^2) \frac{b^2}{a^2} \right) \frac{y^2}{a^2} \\
 & \left. + (2+\nu-\nu^2) \frac{x^4+y^4}{a^4} - 6(1+\nu) \frac{x^2y^2}{a^4} \right] \quad (2.88)
 \end{aligned}$$

The details of the mathematical treatment may be found in [36].

### 2.5.7 Orthotropic Plates

Plates of anisotropic materials have important applications owing to their exceptionally high bending stiffness. A nonisotropic or anisotropic material displays direction-dependent properties. Simplest among them are those in which the material properties differ in two mutually perpendicular directions. A material so described is orthotropic, e.g., wood. A number of manufactured materials are approximated as orthotropic. Examples include corrugated and rolled metal sheets, fillers in sandwich plate construction, plywood, fiber reinforced composites, reinforced concrete, and gridwork. The latter consists of two systems of equally spaced parallel ribs (beams), mutually perpendicular, and attached rigidly at the points of intersection.

The governing equation for orthotropic plates similar to that of isotropic plates (Equation 2.42) takes the form

$$D_x \frac{\delta^4 w}{\delta x^4} + 2H \frac{\delta^4 w}{\delta x^2 \delta y^2} + D_y \frac{\delta^4 w}{\delta y^4} = q \quad (2.89)$$

In which

$$D_x = \frac{h^3 E_x}{12}, \quad D_y = \frac{h^3 E_y}{12}, \quad H = D_{xy} + 2G_{xy}, \quad D_{xy} = \frac{h^3 E_{xy}}{12}, \quad G_{xy} = \frac{h^3 G}{12}$$

The expressions for  $D_x$ ,  $D_y$ ,  $D_{xy}$ , and  $G_{xy}$  represent the flexural rigidities and the torsional rigidity of an orthotropic plate, respectively.  $E_x$ ,  $E_y$ , and  $G$  are the orthotropic plate moduli. Practical considerations often lead to assumptions, with regard to material properties, resulting in approximate expressions for elastic constants. The accuracy of these approximations is generally the most significant factor in the orthotropic plate problem. Approximate rigidities for some cases that are commonly encountered in practice are given in Figure 2.38.

General solution procedures applicable to the case of isotropic plates are equally applicable to the orthotropic plates as well. Deflections and stress-resultants can thus be obtained for orthotropic plates of different shapes with different support and loading conditions. These problems have been researched extensively and solutions concerning plates of various shapes under different boundary and loading conditions may be found in the references, namely [37, 52, 53, 56, 57].

### 2.5.8 Buckling of Thin Plates

#### Rectangular Plates

Buckling of a plate involves bending in two planes and is therefore fairly complicated. From a mathematical point of view, the main difference between columns and plates is that quantities such as deflections and bending moments, which are functions of a single independent variable, in columns become functions of two independent variables in plates. Consequently, the behavior of plates is described by partial differential equations, whereas ordinary differential equations suffice for describing the behavior of columns. A significant difference between columns and plates is also apparent if one compares their buckling characteristics. For a column, buckling terminates the ability of the member to resist axial load, and the critical load is thus the failure load of the member. However, the same is not true for plates. These structural elements can, subsequently to reaching the critical load, continue to resist increasing axial force, and they do not fail until a load considerably in excess of the critical load is reached. The critical load of a plate is, therefore, not its failure load. Instead, one must determine the load-carrying capacity of a plate by considering its postbuckling behavior.

To determine the critical in-plane loading of a plate by the concept of neutral equilibrium, a governing equation in terms of biaxial compressive forces  $N_x$  and  $N_y$  and constant shear force  $N_{xy}$  as shown in Figure 2.39 can be derived as

$$D \left( \frac{\delta^4 w}{\delta x^4} + 2 \frac{\delta^4 w}{\delta x^2 \delta y^2} + \frac{\delta^4 w}{\delta y^4} \right) + N_x \frac{\delta^2 w}{\delta x^2} + N_y \frac{\delta^2 w}{\delta y^2} + 2N_{xy} \frac{\delta^2 w}{\delta x \delta y} = 0 \quad (2.90)$$

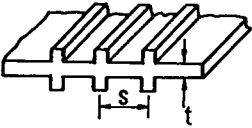
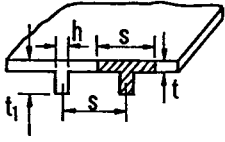
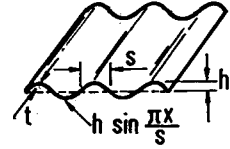
Geometry	Rigidities
<p>A. Reinforced concrete slab with x and y directed reinforcement steel bars</p> 	$D_x = \frac{E_c}{1-\nu_c^2} \left[ I_{cx} + \left( \frac{E_s}{E_c} - 1 \right) I_{sx} \right] \quad D_y = \frac{E_c}{1-\nu_c^2} \left[ I_{cy} + \left( \frac{E_s}{E_c} - 1 \right) I_{sy} \right]$ $G_{xy} = \frac{1-\nu_c}{2} \sqrt{D_x D_y} \quad H = \sqrt{D_x D_y} \quad D_{xy} = \nu_c \sqrt{D_x D_y}$ <p><math>\nu_c</math>: Poisson's ratio for concrete  <math>E_c, E_s</math>: Elastic modulus of concrete and steel, respectively  <math>I_{cx}(I_{sx}), I_{cy}(I_{sy})</math>: Moment of inertia of the slab (steel bars) about neutral axis in the section <math>x = \text{constant}</math> and <math>y = \text{constant}</math>, respectively</p>
<p>B. Plate reinforced by equidistant stiffeners</p> 	$D_x = H = \frac{Et^3}{12(1-\nu^2)} \quad D_y = \frac{Et^3}{12(1-\nu^2)} + \frac{E'I}{s}$ <p><math>E, E'</math>: Elastic modulus of plating and stiffeners, respectively  <math>\nu</math>: Poisson's ratio of plating  <math>s</math>: Spacing between centerlines of stiffeners  <math>I</math>: Moment of inertia of the stiffener cross section with respect to midplane of plating</p>
<p>C. Plate reinforced by a set of equidistant ribs</p> 	$D_x = \frac{Est^3}{12[s-h+h(t t_1)^3]} \quad D_y = \frac{EI}{s}$ $H = 2G'_{xy} + \frac{C}{s} \quad D_{xy} = 0$ <p><math>C</math>: Torsional rigidity of one rib  <math>I</math>: Moment of inertia about neutral axis of a T-section of width <math>s</math> (shown as shaded)  <math>G'_{xy}</math>: Torsional rigidity of the plating  <math>E</math>: Elastic modulus of the plating</p>
<p>D. Corrugated plate</p> 	$D_x = \frac{s}{\lambda} \frac{Et^3}{12(1-\nu^2)} \quad D_y = EI, H = \frac{\lambda}{a} \frac{Et^3}{12(1+\nu)} \quad D_{xy} = 0$ <p>where</p> $\lambda = s \left( 1 + \frac{\pi^2 h^2}{4s^2} \right) \quad I = 0.5h^2 t \left[ 1 - \frac{0.81}{1 + 2.5(h/2s)^2} \right]$

FIGURE 2.38: Various orthotropic plates.

The critical load for uniaxial compression can be determined from the differential equation

$$D \left( \frac{\delta^4 w}{\delta x^4} + 2 \frac{\delta^4 w}{\delta x^2 \delta y^2} + \frac{\delta^4 w}{\delta y^4} \right) + N_x \frac{\delta^2 w}{\delta x^2} = 0 \quad (2.91)$$

which is obtained by setting  $N_y = N_{xy} = 0$  in Equation 2.90.

For example, in the case of a simply supported plate Equation 2.91 can be solved to give

$$N_x = \frac{\pi^2 a^2 D}{m^2} \left( \frac{m^2}{a^2} + \frac{n^2}{b^2} \right)^2 \quad (2.92)$$

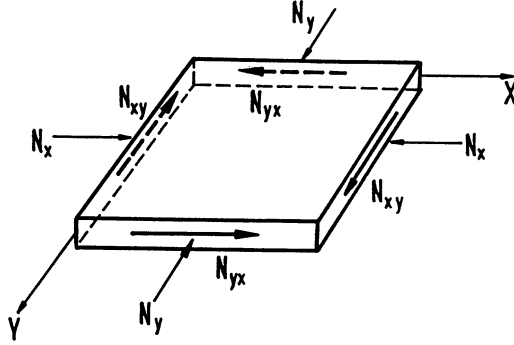


FIGURE 2.39: Plate subjected to in-plane forces.

The critical value of  $N_x$ , i.e., the smallest value, can be obtained by taking  $n$  equal to 1. The physical meaning of this is that a plate buckles in such a way that there can be several half-waves in the direction of compression but only one half-wave in the perpendicular direction. Thus, the expression for the critical value of the compressive force becomes

$$(N_x)_{cr} = \frac{\pi^2 D}{a^2} \left( m + \frac{1}{m} \frac{a^2}{b^2} \right)^2 \quad (2.93)$$

The first factor in this expression represents the Euler load for a strip of unit width and of length  $a$ . The second factor indicates in what proportion the stability of the continuous plate is greater than the stability of an isolated strip. The magnitude of this factor depends on the magnitude of the ratio  $a/b$  and also on the number  $m$ , which gives the number of half-waves into which the plate buckles. If ' $a$ ' is smaller than ' $b$ ', the second term in the parenthesis of Equation 2.93 is always smaller than the first and the minimum value of the expression is obtained by taking  $m = 1$ , i.e., by assuming that the plate buckles in one half-wave. The critical value of  $N_x$  can be expressed as

$$N_{cr} = \frac{k\pi^2 D}{b^2} \quad (2.94)$$

The factor  $k$  depends on the aspect ratio  $a/b$  of the plate and  $m$ , the number of half-waves into which the plate buckles in the  $x$  direction. The variation of  $k$  with  $a/b$  for different values of  $m$  can be plotted, as shown in Figure 2.40. The critical value of  $N_x$  is the smallest value that is obtained for  $m = 1$  and the corresponding value of  $k$  is equal to 4.0. This formula is analogous to Euler's formula for buckling of a column.

In the more general case in which normal forces  $N_x$  and  $N_y$  and the shearing forces  $N_{xy}$  are acting on the boundary of the plate, the same general method can be used. The critical stress for the case of a uniaxially compressed simply supported plate can be written as

$$\sigma_{cr} = 4 \frac{\pi^2 E}{12(1 - \nu^2)} \left( \frac{h}{b} \right)^2 \quad (2.95)$$

The critical stress values for different loading and support conditions can be expressed in the form

$$f_{cr} = k \frac{\pi^2 E}{12(1 - \nu^2)} \left( \frac{h}{b} \right)^2 \quad (2.96)$$

in which  $f_{cr}$  is the critical value of different loading cases. Values of  $k$  for plates with several different boundary and loading conditions are given in Figure 2.41.

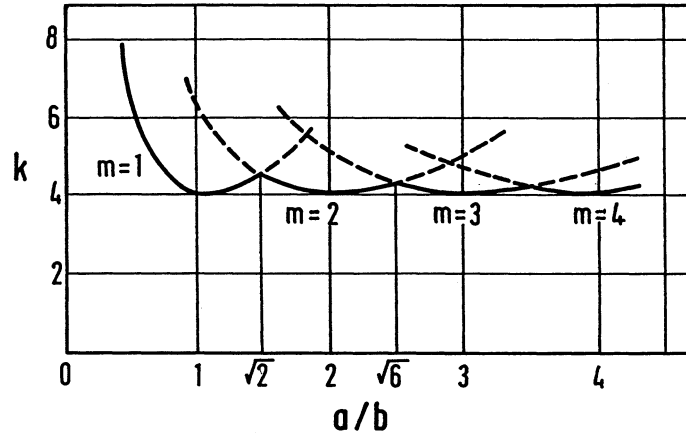


FIGURE 2.40: Buckling stress coefficients for uniaxially compressed plate.

### Circular Plates

The critical value of the compressive forces  $N_r$  uniformly distributed around the edge of a circular plate of radius  $r_0$ , clamped along the edge (Figure 2.42) can be determined by using the governing equation

$$r^2 \frac{d^2 \phi}{dr^2} + r \frac{d\phi}{dr} - \phi = -\frac{Qr^2}{D} \quad (2.97)$$

in which  $\phi$  is the angle between the axis of revolution of the plate surface and any normal to the plate,  $r$  is the distance of any point measured from the center of the plate, and  $Q$  is the shearing force per unit of length. When there are no lateral forces acting on the plate, the solution of Equation 2.97 involves a Bessel function of the first order of the first and second kind and the resulting critical value of  $N_r$  is obtained as

$$(N_r)_{cr} = \frac{14.68D}{r_0^2} \quad (2.98)$$

The critical value of  $N_r$  for the plate when the edge is simply supported can be obtained in the same way as

$$(N_r)_{cr} = \frac{4.20D}{r_0^2} \quad (2.99)$$

## 2.6 Shell

### 2.6.1 Stress Resultants in Shell Element

A **thin shell** is defined as a shell with a thickness that is relatively small compared to its other dimensions. Also, deformations should not be large compared to the thickness. The primary difference between a shell structure and a plate structure is that the former has a curvature in the unstressed state, whereas the latter is assumed to be initially flat. The presence of initial curvature is of little consequence as far as flexural behavior is concerned. The membrane behavior, however, is affected significantly by the curvature. Membrane action in a surface is caused by in-plane forces. These forces may be primary forces caused by applied edge loads or edge deformations, or they may be secondary forces resulting from flexural deformations.

Case	Boundary condition	Type of stress	Value of k for long plate
(a)		Compression	4.0
(b)		Compression	6.97
(c)		Compression	0.425
(d)		Compression	1.277
(e)		Compression	5.42
(f)		Shear	5.34
(g)		Shear	8.98
(h)		Bending	23.9
(i)		Bending	41.8

FIGURE 2.41: Values of  $K$  for plate with different boundary and loading conditions.

In the case of the flat plates, secondary in-plane forces do not give rise to appreciable membrane action unless the bending deformations are large. Membrane action due to secondary forces is, therefore, neglected in small deflection theory. If the surface, as in the case of shell structures, has an initial curvature, membrane action caused by secondary in-plane forces will be significant regardless of the magnitude of the bending deformations.

A plate is likened to a two-dimensional beam and resists transverse loads by two dimensional bending and shear. A membrane is likened to a two-dimensional equivalent of the cable and resists loads through tensile stresses. Imagine a membrane with large deflections (Figure 2.43a), reverse the load and the membrane and we have the structural shell (Figure 2.43b) provided that the shell is stable for the type of load shown. The membrane resists the load through tensile stresses but the ideal thin shell must be capable of developing both tension and compression.

Consider an infinitely small shell element formed by two pairs of adjacent planes which are normal to the middle surface of the shell and which contain its principal curvatures as shown in Figure 2.44a. The thickness of the shell is denoted as  $h$ . Coordinate axes  $x$  and  $y$  are taken tangent at 'O' to the lines of principal curvature and the axis  $z$  normal to the middle surface.  $r_x$  and  $r_y$  are the principal

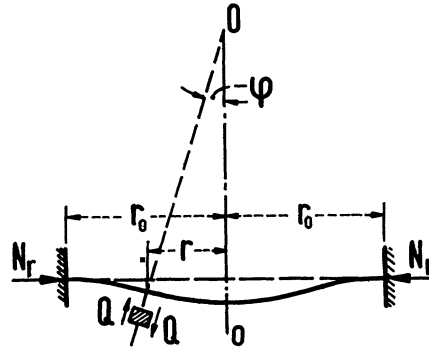


FIGURE 2.42: Circular plate under compressive loading.

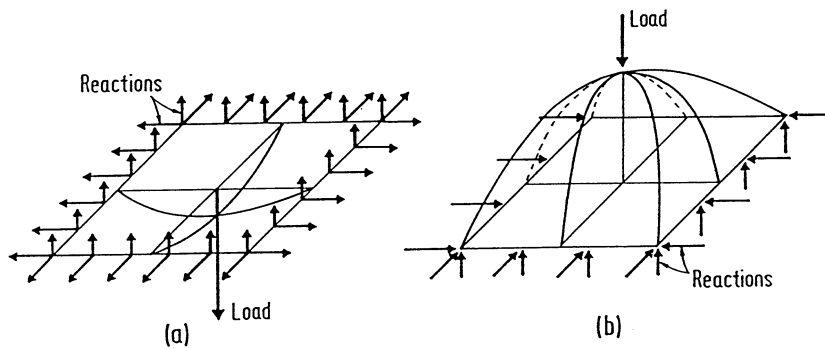


FIGURE 2.43: Membrane with large deflections.

radii of curvature lying in the  $xz$  and  $yz$  planes, respectively. The resultant forces per unit length of the normal sections are given as

$$\begin{aligned}
 N_x &= \int_{-h/2}^{h/2} \sigma_x \left(1 - \frac{z}{r_y}\right) dz, & N_y &= \int_{-h/2}^{h/2} \sigma_y \left(1 - \frac{z}{r_x}\right) dz \\
 N_{xy} &= \int_{-h/2}^{h/2} \tau_{xy} \left(1 - \frac{z}{r_y}\right) dz, & N_{yx} &= \int_{-h/2}^{h/2} \tau_{yx} \left(1 - \frac{z}{r_x}\right) dz \\
 Q_x &= \int_{-h/2}^{h/2} \tau_{xz} \left(1 - \frac{z}{r_y}\right) dz, & Q_y &= \int_{-h/2}^{h/2} \tau_{yz} \left(1 - \frac{z}{r_x}\right) dz
 \end{aligned} \tag{2.100}$$

The bending and twisting moments per unit length of the normal sections are given by

$$\begin{aligned}
 M_x &= \int_{-h/2}^{h/2} \sigma_x z \left(1 - \frac{z}{r_y}\right) dz, & M_y &= \int_{-h/2}^{h/2} \sigma_y z \left(1 - \frac{z}{r_x}\right) dz \\
 M_{xy} &= - \int_{-h/2}^{h/2} \tau_{xy} z \left(1 - \frac{z}{r_y}\right) dz, & M_{yx} &= \int_{-h/2}^{h/2} \tau_{yx} z \left(1 - \frac{z}{r_x}\right) dz
 \end{aligned} \tag{2.101}$$

It is assumed, in bending of the shell, that linear elements as  $AD$  and  $BC$  (Figure 2.44), which are normal to the middle surface of the shell, remain straight and become normal to the deformed middle surface of the shell. If the conditions of a shell are such that bending can be neglected, the

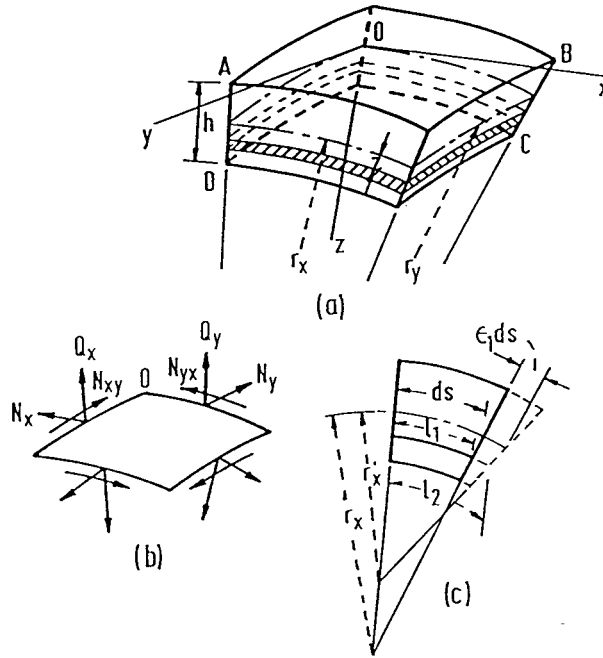


FIGURE 2.44: A shell element.

problem of stress analysis is greatly simplified because the resultant moments (Equation 2.101) vanish along with shearing forces  $Q_x$  and  $Q_y$  in Equation 2.100. Thus, the only unknowns are  $N_x$ ,  $N_y$ , and  $N_{xy} = N_{yx}$  and these are called membrane forces.

### 2.6.2 Membrane Theory of Shells of Revolution

Shells having the form of surfaces of revolution find extensive application in various kinds of containers, tanks, and domes. Consider an element of a shell cut by two adjacent meridians and two parallel circles as shown in Figure 2.45. There will be no shearing forces on the sides of the element because of the symmetry of loading. By considering the equilibrium in the direction of the tangent to the meridian and  $z$ , two equations of equilibrium are written, respectively, as

$$\begin{aligned} \frac{d}{d\phi}(N_\phi r_0) - N_\theta r_1 \cos \phi + Y r_1 r_0 &= 0 \\ N_\phi r_0 + N_\theta r_1 \sin \phi + Z r_1 r_0 &= 0 \end{aligned} \quad (2.102)$$

The force  $N_\theta$  and  $N_\phi$  can be calculated from Equation 2.102 if the radii  $r_0$  and  $r_1$  and the components  $Y$  and  $Z$  of the intensity of the external load are given.

### 2.6.3 Spherical Dome

The spherical shell shown in Figure 2.46 is assumed to be subjected to its own weight; the intensity of the self weight is assumed as a constant value  $q_o$  per unit area. Considering an element of the shell at an angle  $\phi$ , the self weight of the portion of the shell above this element is obtained as

$$r = 2\pi \int_0^\phi a^2 q_o \sin \phi d\phi$$

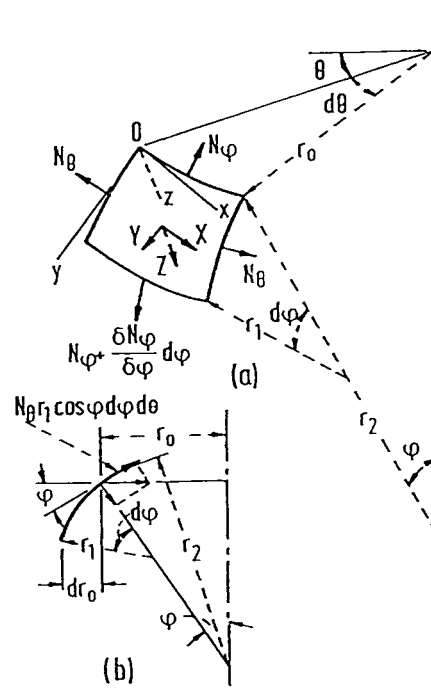


FIGURE 2.45: An element from shells of revolution—symmetrical loading.

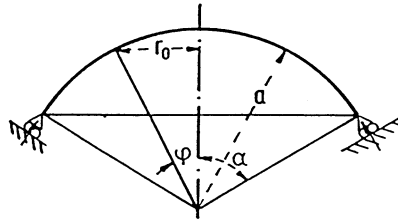


FIGURE 2.46: Spherical dome.

$$= 2\pi a^2 q_o (1 - \cos \phi)$$

Considering the equilibrium of the portion of the shell above the parallel circle defined by the angle  $\phi$ , we can write

$$2\pi r_0 N_\phi \sin \phi + R = 0 \quad (2.103)$$

Therefore,

$$N_\phi = -\frac{aq(1 - \cos \phi)}{\sin^2 \phi} = -\frac{aq}{1 + \cos \phi}$$

We can write from Equation 2.102

$$\frac{N_\phi}{r_1} + \frac{N_\theta}{r_2} = -Z \quad (2.104)$$

Substituting for  $N_\phi$  and  $R$  into Equation 2.104

$$N_\theta = -aq \left( \frac{1}{1 + \cos \phi} - \cos \phi \right)$$

It is seen that the forces  $N_\phi$  are always negative. Thus, there is a compression along the meridians that increases as the angle  $\phi$  increases. The forces  $N_\theta$  are also negative for small angles  $\phi$ . The stresses as calculated above will represent the actual stresses in the shell with great accuracy if the supports are of such a type that the reactions are tangent to meridians as shown in the figure.

### 2.6.4 Conical Shells

If a force  $P$  is applied in the direction of the axis of the cone as shown in Figure 2.47, the stress distribution is symmetrical and we obtain

$$N_\phi = -\frac{P}{2\pi r_0 \cos \alpha}$$

By Equation 2.104, one obtains  $N_\theta = 0$ .

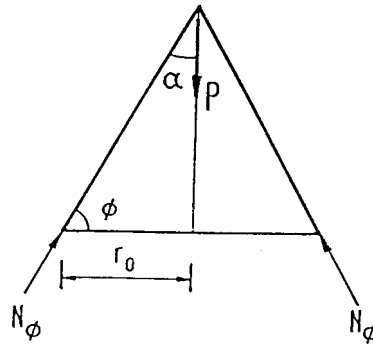


FIGURE 2.47: Conical shell.

In the case of a conical surface in which the lateral forces are symmetrically distributed, the membrane stresses can be obtained by using Equations 2.103 and 2.104. The curvature of the meridian in the case of a cone is zero and hence  $r_1 = \infty$ ; Equations 2.103 and 2.104 can, therefore, be written as

$$N_\phi = -\frac{R}{2\pi r_0 \sin \phi}$$

and

$$N_\theta = -r_2 Z = -\frac{Z r_0}{\sin \phi}$$

If the load distribution is given,  $N_\phi$  and  $N_\theta$  can be calculated independently.

For example, a conical tank filled with a liquid of specific weight  $\gamma$  is considered as shown in Figure 2.48. The pressure at any parallel circle  $mn$  is

$$p = -Z = \gamma(d - y)$$

For the tank,  $\phi = \alpha + \frac{\pi}{2}$  and  $r_0 = y \tan \alpha$ .  
Therefore,

$$N_\theta = \frac{\gamma(d - y)y \tan \alpha}{\cos \alpha}$$

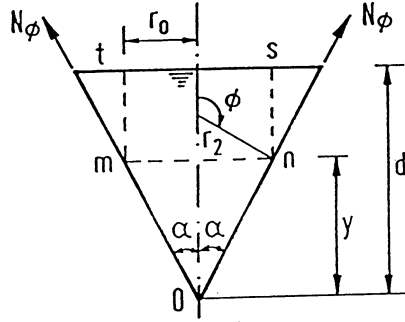


FIGURE 2.48: Inverted conical tank.

$N_\theta$  is maximum when  $y = \frac{d}{2}$  and hence

$$(N_\theta)_{\max} = \frac{\gamma d^2 \tan \alpha}{4 \cos \alpha}$$

The term  $R$  in the expression for  $N_\phi$  is equal to the weight of the liquid in the conical part  $mno$  and the cylindrical part must be as shown in Figure 2.47. Therefore,

$$\begin{aligned} R &= - \left[ \frac{1}{3} \pi y^3 \tan^2 \alpha + \pi y^2 (d - y) \tan^2 \alpha \right] \gamma \\ &= -\pi \gamma y^2 \left( d - \frac{2}{3} y \right) \tan^2 \alpha \end{aligned}$$

Hence,

$$N_\phi = \frac{\gamma y \left( d - \frac{2}{3} y \right) \tan \alpha}{2 \cos \alpha}$$

$N_\phi$  is maximum when  $y = \frac{3}{4} d$  and

$$(N_\phi)_{\max} = \frac{3}{16} \frac{d^2 \gamma \tan \alpha}{\cos \alpha}$$

The horizontal component of  $N_\phi$  is taken by the reinforcing ring provided along the upper edge of the tank. The vertical components constitute the reactions supporting the tank.

### 2.6.5 Shells of Revolution Subjected to Unsymmetrical Loading

Consider an element cut from a shell by two adjacent meridians and two parallel circles (Figure 2.49). In the general case, shear forces  $N_{\phi\theta} = N_{\theta\phi}$  in addition to normal forces  $N_\phi$  and  $N_\theta$  will act on the sides of the element. Projecting the forces on the element in the  $y$  direction we obtain the equation

$$\frac{\partial}{\partial \phi} (N_\phi r_0) + \frac{\partial N_{\theta\phi}}{\partial \theta} r_1 - N_{\theta r_1} \cos \phi + Y r_1 r_0 = 0 \quad (2.105)$$

Similarly the forces in the  $x$  direction can be summed up to give

$$\frac{\partial}{\partial \phi} (r_0 N_{\phi\theta}) + \frac{\partial N_\theta}{\partial \theta} r_1 + N_{\theta\phi} r_1 \cos \phi + X r_0 r_1 = 0 \quad (2.106)$$

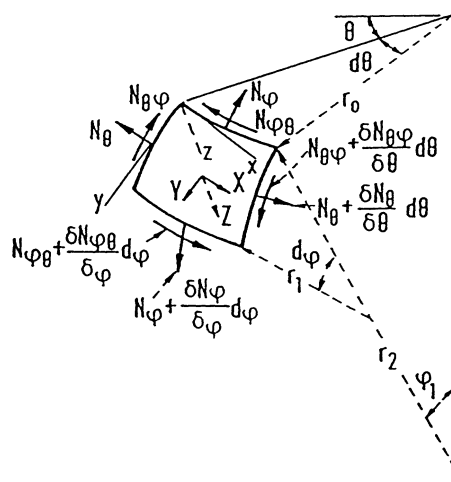


FIGURE 2.49: An element from shells of revolution—unsymmetrical loading.

Since the projection of shearing forces on the  $z$  axis vanishes, the third equation is the same as Equation 2.104. The problem of determining membrane stresses under unsymmetrical loading reduces to the solution of Equations 2.104, 2.105, and 2.106 for given values of the components  $X$ ,  $Y$ , and  $Z$  of the intensity of the external load.

### 2.6.6 Membrane Theory of Cylindrical Shells

It is assumed that the generator of the shell is horizontal and parallel to the  $x$  axis. An element is cut from the shell by two adjacent generators and two cross-sections perpendicular to the  $x$  axis, and its position is defined by the coordinate  $x$  and the angle  $\varphi$ . The forces acting on the sides of the element are shown in Figure 2.50b.

The components of the distributed load over the surface of the element are denoted as  $X$ ,  $Y$ , and  $Z$ . Considering the equilibrium of the element and summing up the forces in the  $x$  direction, we obtain

$$\frac{\partial N_x}{\partial x} r d\varphi dx + \frac{\partial N_{x\varphi}}{\partial \varphi} d\varphi dx + X r d\varphi dx = 0$$

The corresponding equations of equilibrium in the  $y$  and  $z$  directions are given, respectively, as

$$\begin{aligned} \frac{\partial N_{x\varphi}}{\partial x} r d\varphi dx + \frac{\partial N_\varphi}{\partial \varphi} d\varphi dx + Y r d\varphi dx &= 0 \\ N_\varphi d\varphi dx + Z r d\varphi dx &= 0 \end{aligned}$$

The three equations of equilibrium can be simplified and represented in the following form:

$$\begin{aligned} \frac{\partial N_x}{\partial x} + \frac{1}{r} \frac{\partial N_{x\varphi}}{\partial \varphi} &= -X \\ \frac{\partial N_{x\varphi}}{\partial x} + \frac{1}{r} \frac{\partial N_\varphi}{\partial \varphi} &= -Y \\ N_\varphi &= -Z_r \end{aligned} \tag{2.107}$$

In each particular case we readily find the value of  $N_\varphi$ . Substituting this value in the second of the equations, we then obtain  $N_{x\varphi}$  by integration. Using the value of  $N_{x\varphi}$  thus obtained we find  $N_x$  by integrating the first equation.

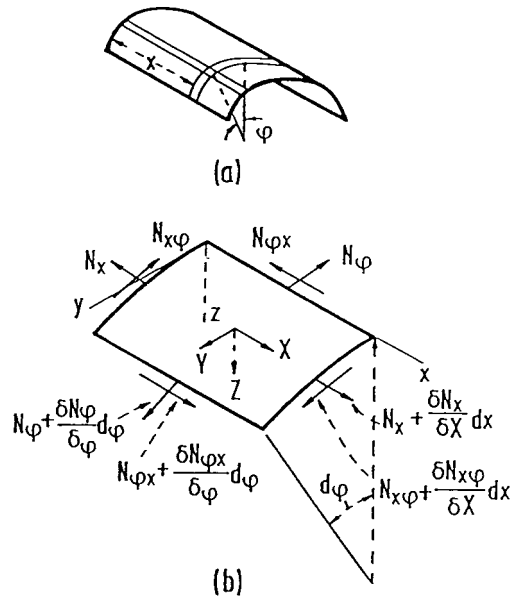


FIGURE 2.50: Membrane forces on a cylindrical shell element.

### 2.6.7 Symmetrically Loaded Circular Cylindrical Shells

In practical applications problems in which a circular shell is subjected to the action of forces distributed symmetrically with respect to the axis of the cylinder are common. To establish the equations required for the solution of these problems, we consider an element, as shown in Figures 2.50a and 2.51, and consider the equations of equilibrium. From symmetry, the membrane shearing forces

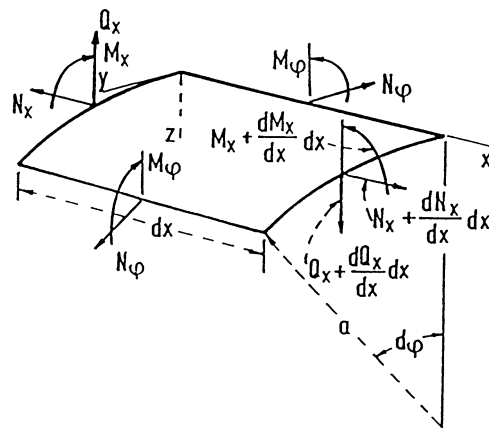


FIGURE 2.51: Stress resultants in a cylindrical shell element.

$N_{x\phi} = N_{\phi x}$  vanish in this case; forces  $N_\phi$  are constant along the circumference. From symmetry, only the forces  $Q_z$  do not vanish. Considering the moments acting on the element in Figure 2.51,

from symmetry it can be concluded that the twisting moments  $M_{x\varphi} = M_{\varphi x}$  vanish and the bending moments  $M_\varphi$  are constant along the circumference. Under such conditions of symmetry three of the six equations of equilibrium of the element are identically satisfied. We have to consider only the equations obtained by projecting the forces on the  $x$  and  $z$  axes and by taking the moment of the forces about the  $y$  axis. For example, consider a case in which external forces consist only of a pressure normal to the surface. The three equations of equilibrium are

$$\begin{aligned}\frac{dN}{dx}adx d\varphi &= 0 \\ \frac{dQ_x}{dx}adx d\varphi + N_\varphi dx d\varphi + Zadx d\varphi &= 0 \\ \frac{dM_x}{dx}adx d\varphi - Q_x adx d\varphi &= 0\end{aligned}\quad (2.108)$$

The first one indicates that the forces  $N_x$  are constant, and they are taken equal to zero in the further discussion. If they are different from zero, the deformation and stress corresponding to such constant forces can be easily calculated and superposed on stresses and deformations produced by lateral load. The remaining two equations are written in the simplified form:

$$\begin{aligned}\frac{dQ_x}{dx} + \frac{1}{a}N_\varphi &= -Z \\ \frac{dM_x}{dx} - Q_x &= 0\end{aligned}\quad (2.109)$$

These two equations contain three unknown quantities:  $N_\varphi$ ,  $Q_x$ , and  $M_x$ . We need, therefore, to consider the displacements of points in the middle surface of the shell.

The component  $v$  of the displacement in the circumferential direction vanishes because of symmetry. Only the components  $u$  and  $w$  in the  $x$  and  $z$  directions, respectively, are to be considered. The expressions for the strain components then become

$$\varepsilon_x = \frac{du}{dx} \quad \varepsilon_\varphi = -\frac{w}{a}\quad (2.110)$$

By Hooke's law, we obtain

$$\begin{aligned}N_x &= \frac{Eh}{1-\nu^2}(\varepsilon_x + \nu\varepsilon_\varphi) = \frac{Eh}{1-\nu^2}\left(\frac{du}{dx} - \nu\frac{w}{a}\right) = 0 \\ N_\varphi &= \frac{Eh}{1-\nu^2}(\varepsilon_\varphi + \nu\varepsilon_x) = \frac{Eh}{1-\nu^2}\left(-\frac{w}{a} + \nu\frac{du}{dx}\right) = 0\end{aligned}\quad (2.111)$$

From the first of these equation it follows that

$$\frac{du}{dx} = \nu\frac{w}{a}$$

and the second equation gives

$$N_\varphi = -\frac{Ehw}{a}\quad (2.112)$$

Considering the bending moments, we conclude from symmetry that there is no change in curvature in the circumferential direction. The curvature in the  $x$  direction is equal to  $-d^2w/dx^2$ . Using the same equations as for plates, we then obtain

$$\begin{aligned}M_\varphi &= \nu M_x \\ M_x &= -D\frac{d^2w}{dx^2}\end{aligned}\quad (2.113)$$

where

$$D = \frac{Eh^3}{12(1-\nu^2)}$$

is the flexural rigidity per unit length of the shell.

Eliminating  $Q_x$  from Equation 2.109, we obtain

$$\frac{d^2 M_x}{dx^2} + \frac{1}{a} N_\phi = -Z$$

from which, by using Equations 2.112 and 2.113, we obtain

$$\frac{d^2}{dx^2} \left( D \frac{d^2 w}{dx^2} \right) + \frac{Eh}{a^2} w = Z \quad (2.114)$$

All problems of symmetrical deformation of circular cylindrical shells thus reduce to the integration of Equation 2.114.

The simplest application of this equation is obtained when the thickness of the shell is constant. Under such conditions, Equation 2.114 becomes

$$D \frac{d^4 w}{dx^4} + \frac{Eh}{a^2} w = Z$$

Using the notation

$$\beta^4 = \frac{Eh}{4a^2 D} = \frac{3(1-\nu^2)}{a^2 h^2} \quad (2.115)$$

Equation 2.115 can be represented in the simplified form

$$\frac{d^4 w}{dx^4} + 4\beta^4 w = \frac{Z}{D} \quad (2.116)$$

The general solution of this equation is

$$w = e^{\beta x} (C_1 \cos \beta x + C_2 \sin \beta x) + e^{-\beta x} (C_3 \cos \beta x + C_4 \sin \beta x) + f(x) \quad (2.117)$$

Detailed treatment of shell theory can be obtained from Timoshenko and Woinowsky-Krieger [56].

## 2.6.8 Buckling of Shells

If a circular cylindrical shell is uniformly compressed in the axial direction, buckling symmetrical with respect to the axis of the cylinder (Figure 2.52) may occur at a certain value of the compressive load. The critical value of the compressive force  $N_{cr}$  per unit length of the edge of the shell can be obtained by solving the differential equation

$$D \frac{d^4 w}{dx^4} + N \frac{d^2 w}{dx^2} + Eh \frac{w}{a^2} = 0 \quad (2.118)$$

in which  $a$  is the radius of the cylinder and  $h$  is the wall thickness.

Alternatively, the critical force per unit length may also be obtained by using the energy method. For a cylinder of length  $L$  simply supported at both ends one obtains

$$N_{cr} = D \left( \frac{m^2 \pi^2}{L^2} + \frac{EhL^2}{Da^2 m^2 \pi^2} \right) \quad (2.119)$$

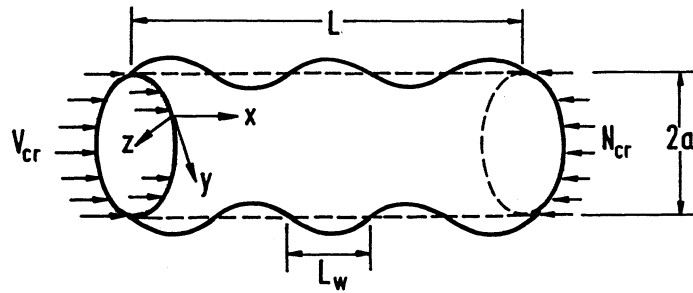


FIGURE 2.52: Buckling of a cylindrical shell.

For each value of  $m$  there is a unique buckling mode shape and a unique buckling load. The lowest value is of greatest interest and is thus found by setting the derivative of  $N_{cr}$  with respect to  $L$  equal to zero for  $m = 1$ . With Poisson's Ratio,  $\nu = 0.3$ , the buckling load is obtained as

$$N_{cr} = 0.605 \frac{Eh^2}{a} \quad (2.120)$$

It is possible for a cylindrical shell be subjected to uniform external pressure or to the combined action of axial and uniform lateral pressure. In such cases the mathematical treatment is more involved and it requires special considerations.

More detailed treatment of such cases may be found in Timoshenko and Gere [55].

## 2.7 Influence Lines

Structures such as bridges, industrial buildings with travelling cranes, and frames supporting conveyor belts are subjected to moving loads. Each member of these structures must be designed for the most severe conditions that can possibly be developed in that member. Live loads should be placed at the position where they will produce these severe conditions. The critical positions for placing live loads will not be the same for every member. On some occasions it is possible to determine by inspection where to place the loads to give the most critical forces, but on many other occasions it is necessary to resort to certain criteria to find the locations. The most useful of these methods is influence lines.

An influence line for a particular response such as reaction, shear force, bending moment, and axial force is defined as a diagram the ordinate to which at any point equals the value of that response attributable to a unit load acting at that point on the structure. Influence lines provide a systematic procedure for determining how the force in a given part of a structure varies as the applied load moves about on the structure. Influence lines of responses of [statically determinate structures](#) consist only of straight lines whereas they are curves for [statically indeterminate structures](#). They are primarily used to determine where to place live loads to cause maximum force and to compute the magnitude of those forces. The knowledge of influence lines helps to study the structural response under different moving load conditions.

### 2.7.1 Influence Lines for Shear in Simple Beams

Figure 2.53 shows influence lines for shear at two sections of a simply supported beam. It is assumed that positive shear occurs when the sum of the transverse forces to the left of a section is in the upward direction or when the sum of the forces to the right of the section is downward. A unit force is placed at various locations and the shear force at sections 1-1 and 2-2 are obtained for each position of the

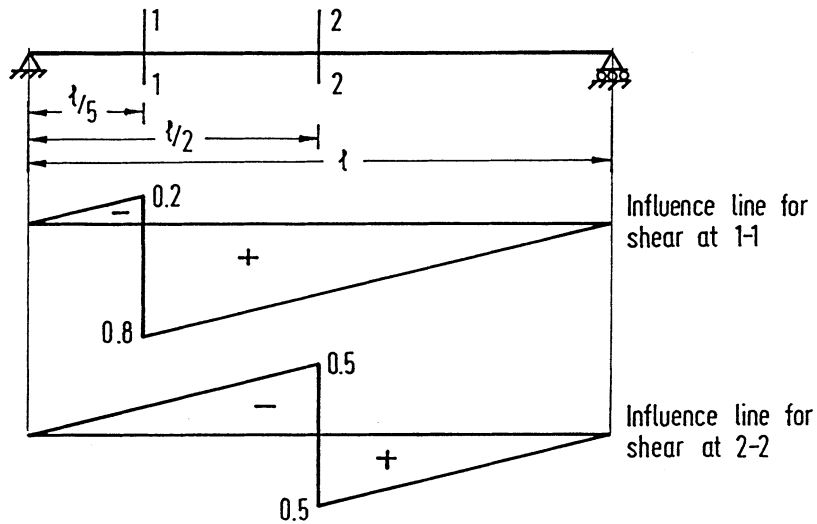


FIGURE 2.53: Influence line for shear force.

unit load. These values give the ordinate of influence line with which the influence line diagrams for shear force at sections 1-1 and 2-2 can be constructed. Note that the slope of the influence line for shear on the left of the section is equal to the slope of the influence line on the right of the section. This information is useful in drawing shear force influence line in other cases.

### 2.7.2 Influence Lines for Bending Moment in Simple Beams

Influence lines for bending moment at the same sections, 1-1 and 2-2 of the simple beam considered in Figure 2.53, are plotted as shown in Figure 2.54. For a section, when the sum of the moments of

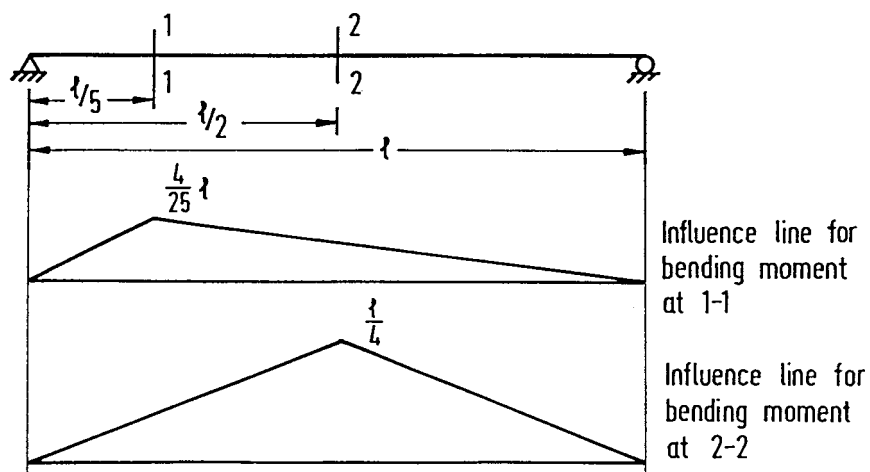


FIGURE 2.54: Influence line for bending moment.

all the forces to the left is clockwise or when the sum to the right is counter-clockwise, the moment is taken as positive. The values of bending moment at sections 1-1 and 2-2 are obtained for various positions of unit load and plotted as shown in the figure.

It should be understood that a shear or bending moment diagram shows the variation of shear or moment across an entire structure for loads fixed in one position. On the other hand, an influence line for shear or moment shows the variation of that response at one particular section in the structure caused by the movement of a unit load from one end of the structure to the other.

Influence lines can be used to obtain the value of a particular response for which it is drawn when the beam is subjected to any particular type of loading. If, for example, a uniform load of intensity  $q_o$  per unit length is acting over the entire length of the simple beam shown in Figure 2.53, then the shear force at section 1-1 is given by the product of the load intensity,  $q_o$ , and the net area under the influence line diagram. The net area is equal to  $0.3l$  and the shear force at section 1-1 is, therefore, equal to  $0.3q_o l$ . In the same way, the bending moment at the section can be found as the area of the corresponding influence line diagram times the intensity of loading,  $q_o$ . The bending moment at the section is, therefore,  $(0.08l^2 \times q_o =) 0.08q_o l^2$ .

### 2.7.3 Influence Lines for Trusses

Influence lines for support reactions and member forces may be constructed in the same manner as those for various beam functions. They are useful to determine the maximum load that can be applied to the truss. The unit load moves across the truss, and the ordinates for the responses under consideration may be computed for the load at each panel point. Member force, in most cases, need not be calculated for every panel point because certain portions of influence lines can readily be seen to consist of straight lines for several panels. One method used for calculating the forces in a chord member of a truss is by the Method of Sections discussed earlier.

The truss shown in Figure 2.55 is considered for illustrating the construction of influence lines for trusses.

The member forces in  $U_1U_2$ ,  $L_1L_2$ , and  $U_1L_2$  are determined by passing a section 1-1 and considering the equilibrium of the free body diagram of one of the truss segments. Unit load is placed at  $L_1$  first and the force in  $U_1U_2$  is obtained by taking moment about  $L_2$  of all the forces acting on the right-hand segment of the truss and dividing the resulting moment by the lever arm (the perpendicular distance of the force in  $U_1U_2$  from  $L_2$ ). The value thus obtained gives the ordinate of the influence diagram at  $L_1$  in the truss. The ordinate at  $L_2$  obtained similarly represents the force in  $U_1U_2$  for unit load placed at  $L_2$ . The influence line can be completed with two other points, one at each of the supports. The force in the member  $L_1L_2$  due to unit load placed at  $L_1$  and  $L_2$  can be obtained in the same manner and the corresponding influence line diagram can be completed. By considering the horizontal component of force in the diagonal of the panel, the influence line for force in  $U_1L_2$  can be constructed. Figure 2.55 shows the respective influence diagram for member forces in  $U_1U_2$ ,  $L_1L_2$ , and  $U_1L_2$ . Influence line ordinates for the force in a chord member of a “curved-chord” truss may be determined by passing a vertical section through the panel and taking moments at the intersection of the diagonal and the other chord.

### 2.7.4 Qualitative Influence Lines

One of the most effective methods of obtaining influence lines is by the use of Müller-Breslau’s principle, which states that “the ordinates of the influence line for any response in a structure are equal to those of the deflection curve obtained by releasing the restraint corresponding to this response and introducing a corresponding unit displacement in the remaining structure”. In this way, the shape of the influence lines for both statically determinate and indeterminate structures can be easily obtained especially for beams.

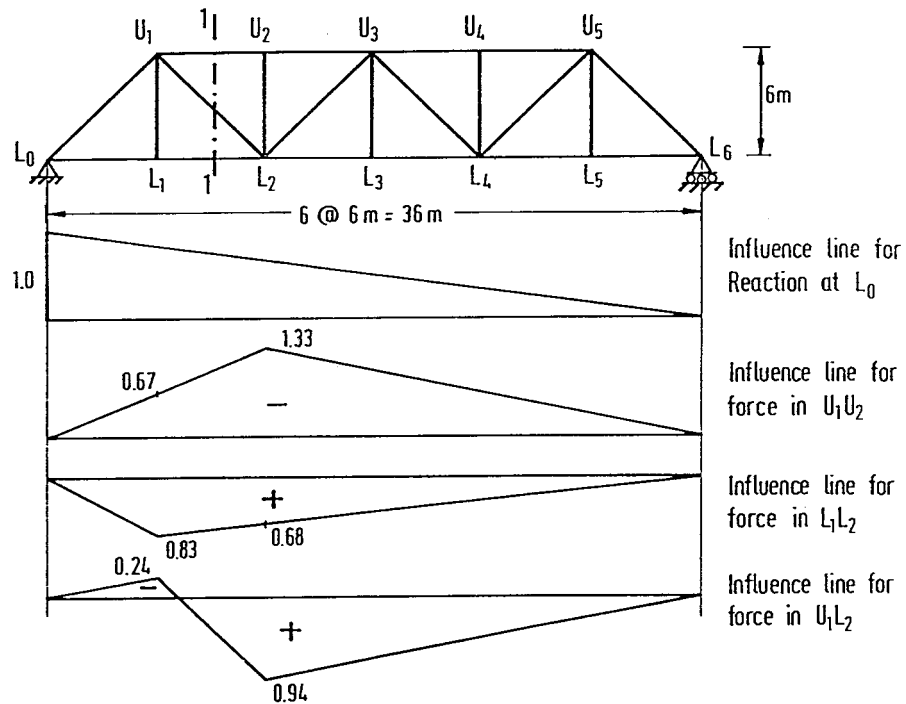


FIGURE 2.55: Influence line for truss.

To draw the influence lines of

1. Support reaction: Remove the support and introduce a unit displacement in the direction of the corresponding reaction to the remaining structure as shown in Figure 2.56 for a symmetrical overhang beam.

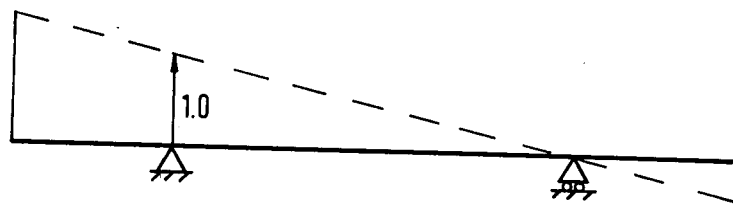


FIGURE 2.56: Influence line for support reaction.

2. Shear: Make a cut at the section and introduce a unit relative translation (in the direction of positive shear) without relative rotation of the two ends at the section as shown in Figure 2.57.
3. Bending moment: Introduce a hinge at the section (releasing the bending moment) and apply bending (in the direction corresponding to positive moment) to produce a unit relative rotation of the two beam ends at the hinged section as shown in Figure 2.58.

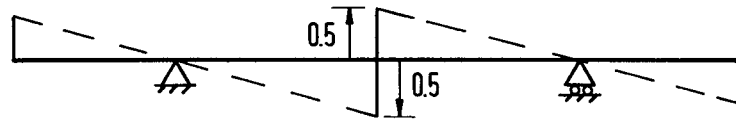


FIGURE 2.57: Influence line for midspan shear force.

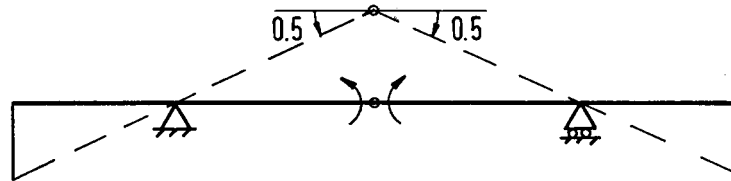


FIGURE 2.58: Influence line for midspan bending moment.

### 2.7.5 Influence Lines for Continuous Beams

Using Müller-Breslau's principle, the shape of the influence line of any response of a continuous beam can be sketched easily. One of the methods for beam deflection can then be used for determining the ordinates of the influence line at critical points. Figures 2.59 to 2.61 show the influence lines of bending moment at various points of two, three, and four span continuous beams.

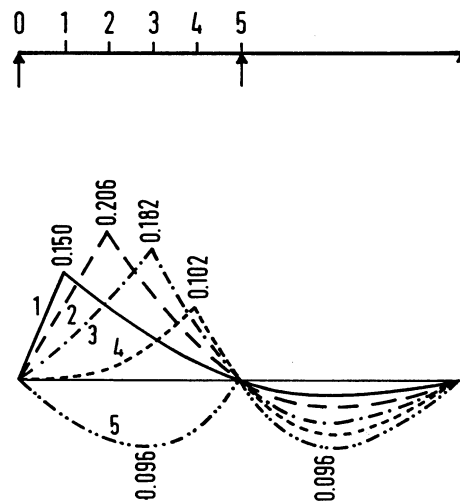


FIGURE 2.59: Influence lines for bending moments—two span beam.

## 2.8 Energy Methods in Structural Analysis

Energy methods are a powerful tool in obtaining numerical solutions of statically indeterminate problems. The basic quantity required is the *strain energy*, or work stored due to deformations, of the structure.

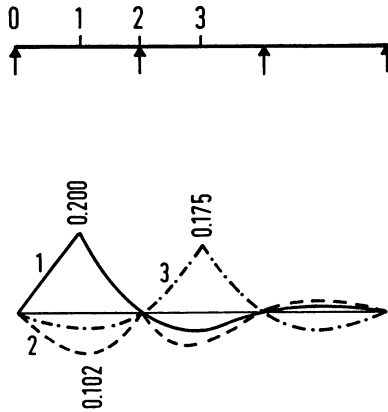


FIGURE 2.60: Influence lines for bending moments—three span beam.

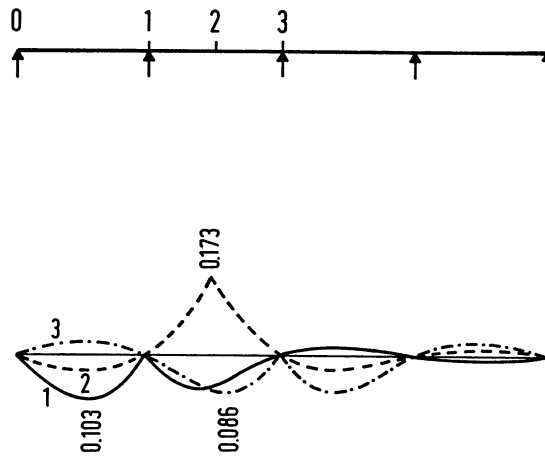


FIGURE 2.61: Influence lines for bending moments—four span beam.

### 2.8.1 Strain Energy Due to Uniaxial Stress

In an axially loaded bar with constant cross-section, the applied load causes normal stress  $\sigma_y$  as shown in Figure 2.62. The tensile stress  $\sigma_y$  increases from zero to a value  $\sigma_y$  as the load is gradually applied. The original, unstrained position of any section such as  $C - C$  will be displaced by an amount  $v$ . A section  $D - D$  located a differential length below  $C - C$  will have been displaced by an amount  $v + \left(\frac{\partial v}{\partial y}\right) dy$ . As  $\sigma_y$  varies with the applied load, from zero to  $\sigma_y$ , the work done by the forces external to the element can be shown to be

$$dV = \frac{1}{2E} \sigma_y^2 A dy = \frac{1}{2} \sigma_y \varepsilon_y A dy \quad (2.121)$$

in which  $A$  is the area of cross-section of the bar and  $\varepsilon_y$  is the strain in the direction of  $\sigma_y$ .

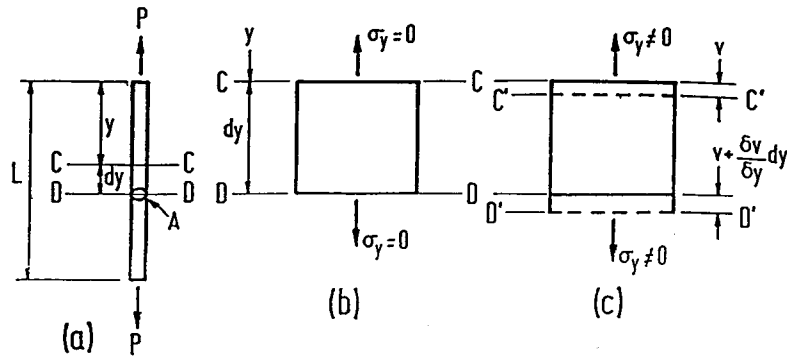


FIGURE 2.62: Axially loaded bar.

### 2.8.2 Strain Energy in Bending

It can be shown that the strain energy of a differential volume  $dx dy dz$  stressed in tension or compression in the  $x$  direction only by a normal stress  $\sigma_x$  will be

$$dV = \frac{1}{2E} \sigma_x^2 dx dy dz = \frac{1}{2} \sigma_x \epsilon_x dx dy dz \quad (2.122)$$

When  $\sigma_x$  is the bending stress given by  $\sigma_x = \frac{My}{I}$  (see Figure 2.63), then  $dV = \frac{1}{2E} \frac{M^2 y^2}{I^2} dx dy dz$ , where  $I$  is the **moment of inertia** of the cross-sectional area about the neutral axis.

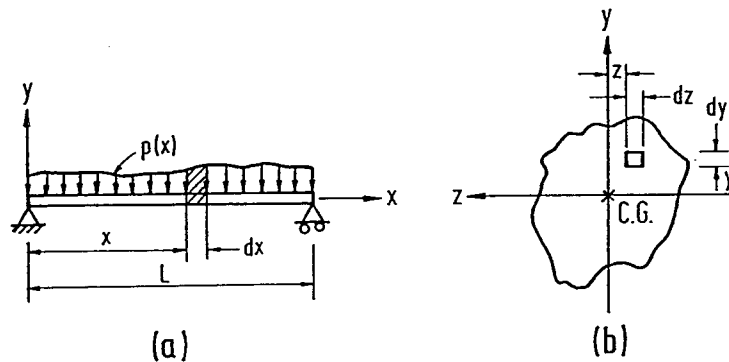


FIGURE 2.63: Beam under arbitrary bending load.

The total strain energy of bending of a beam is obtained as

$$V = \int \int \int_{\text{volume}} \frac{1}{2E} \frac{M^2}{I^2} y^2 dz dy dx$$

where

$$I = \int \int_{\text{area}} y^2 dz dy$$

Therefore,

$$V = \int_{\text{length}} \frac{M^2}{2EI} dx \quad (2.123)$$

### 2.8.3 Strain Energy in Shear

Figure 2.64 shows an element of volume  $dx dy dz$  subjected to shear stress  $\tau_{xy}$  and  $\tau_{yx}$ .

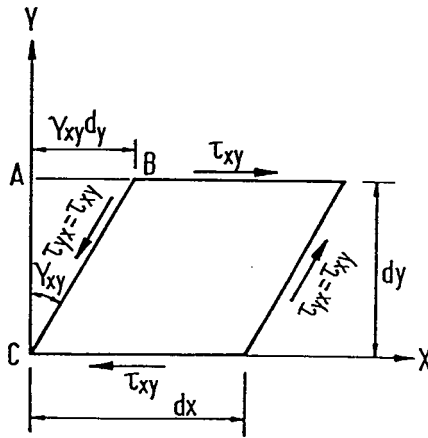


FIGURE 2.64: Shear loading.

For static equilibrium, it can readily be shown that

$$\tau_{xy} = \tau_{yx}$$

The shear strain,  $\gamma$  is defined as  $AB/AC$ . For small deformations, it follows that

$$\gamma_{xy} = \frac{AB}{AC}$$

Hence, the angle of deformation  $\gamma_{xy}$  is a measure of the shear strain. The strain energy for this differential volume is obtained as

$$dV = \frac{1}{2} (\tau_{xy} dz dx) \gamma_{xy} dy = \frac{1}{2} \tau_{xy} \gamma_{xy} dx dy dz \quad (2.124)$$

Hooke's Law for shear stress and strain is

$$\gamma_{xy} = \frac{\tau_{xy}}{G} \quad (2.125)$$

where  $G$  is the shear modulus of elasticity of the material. The expression for strain energy in shear reduces to

$$dV = \frac{1}{2G} \tau_{xy}^2 dx dy dz \quad (2.126)$$

## 2.8.4 The Energy Relations in Structural Analysis

The energy relations or laws such as (1) Law of Conservation of Energy, (2) Theorem of Virtual Work, (3) Theorem of Minimum Potential Energy, and (4) Theorem of Complementary Energy are of fundamental importance in structural engineering and are used in various ways in structural analysis.

### The Law of Conservation of Energy

There are many ways of stating this law. For the purpose of structural analysis it will be sufficient to state it in the following way:

If a structure and the external loads acting on it are isolated so that these neither receive nor give out energy, then the total energy of this system remains constant.

A typical application of the Law of Conservation of Energy can be made by referring to Figure 2.65 which shows a cantilever beam of constant cross-sections subjected to a concentrated load at its end. If only bending strain energy is considered,

$$\begin{aligned} \text{External work} &= \text{Internal work} \\ \frac{P\delta}{2} &= \int_0^L \frac{M^2 dx}{2EI} \end{aligned}$$

Substituting  $M = -Px$  and integrating along the length gives

$$\delta = \frac{PL^3}{3EI} \quad (2.127)$$

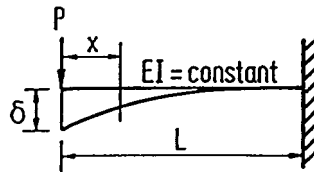


FIGURE 2.65: Cantilever beam.

### The Theorem of Virtual Work

The Theorem of Virtual Work can be derived by considering the beam shown in Figure 2.66. The full curved line represents the equilibrium position of the beam under the given loads. Assume the beam to be given an additional small deformation consistent with the boundary conditions. This is called a virtual deformation and corresponds to increments of deflection  $\Delta y_1, \Delta y_2, \dots, \Delta y_n$  at loads  $P_1, P_2, \dots, P_n$  as shown by the broken line.

The change in potential energy of the loads is given by

$$\Delta(P.E.) = \sum_{i=1}^n P_i \Delta y_i \quad (2.128)$$

By the Law of Conservation of Energy this must be equal to the internal strain energy stored in the beam. Hence, we may state the Theorem of Virtual Work in the following form:

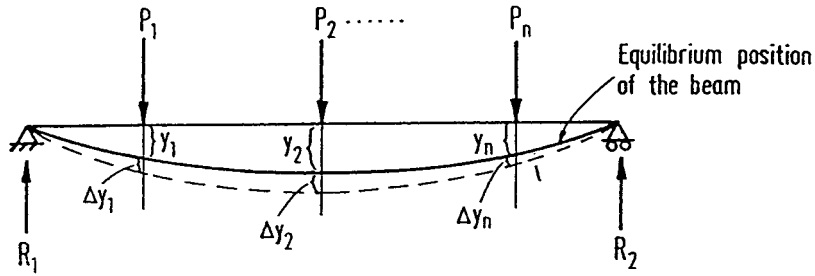


FIGURE 2.66: Equilibrium of a simply supported beam under loading.

If a body in equilibrium under the action of a system of external loads is given any small (virtual) deformation, then the work done by the external loads during this deformation is equal to the increase in internal strain energy stored in the body.

### The Theorem of Minimum Potential Energy

Let us consider the beam shown in Figure 2.67. The beam is in equilibrium under the action

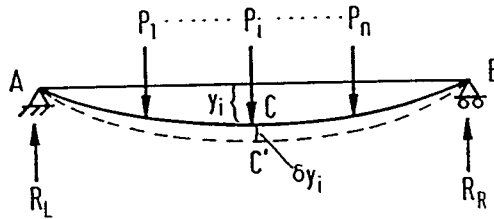


FIGURE 2.67: Simply supported beam under point loading.

of loads,  $P_1, P_2, P_3, \dots, P_i, \dots, P_n$ . The curve  $ACB$  defines the equilibrium positions of the loads and reactions. Now apply by some means an additional small displacement to the curve so that it is defined by  $AC'B$ . Let  $y_i$  be the original equilibrium displacement of the curve beneath a particular load  $P_i$ . The additional small displacement is called  $\delta y_i$ . The potential energy of the system while it is in the equilibrium configuration is found by comparing the potential energy of the beam and loads in equilibrium and in the undeflected position. If the change in potential energy of the loads is  $W$  and the strain energy of the beam is  $V$ , the total energy of the system is

$$U = W + V \quad (2.129)$$

If we neglect the second-order terms, then

$$\delta U = \delta(W + V) = 0 \quad (2.130)$$

The above is expressed as the Principle or Theorem of Minimum Potential Energy which can be stated as

Of all displacements satisfying given boundary conditions, those that satisfy the equilibrium conditions make the potential energy a minimum.

### Castigliano's Theorem

An example of application of energy methods to the field of structural engineering is Castigliano's Theorem. The theorem applies only to structures stressed within the elastic limit. Also, all deformations must be linear homogeneous functions of the loads. Castigliano's Theorem can be derived using the expression for total potential energy as follows: For a beam in equilibrium loaded as in Figure 2.66, the total energy is

$$U = -[P_1y_1 + P_2y_2 + \dots P_jy_j + \dots P_ny_n] + V \quad (2.131)$$

For an elastic system, the strain energy,  $V$ , turns out to be one half the change in the potential energy of the loads.

$$V = \frac{1}{2} \sum_{i=1}^{i=n} P_i y_i \quad (2.132)$$

Castigliano's Theorem results from studying the variation in the strain energy,  $V$ , produced by a differential change in one of the loads, say  $P_j$ .

If the load  $P_j$  is changed by a differential amount  $\delta P_j$  and if the deflections  $y$  are linear functions of the loads, then

$$\frac{\partial V}{\partial P_j} = \frac{1}{2} \sum_{i=1}^{i=n} P_i \frac{\partial y_i}{\partial P_j} + \frac{1}{2} y_j = y_j \quad (2.133)$$

Castigliano's Theorem is stated as follows:

The partial derivatives of the total strain energy of any structure with respect to any one of the applied forces is equal to the displacement of the point of application of the force in the direction of the force.

To find the deflection of a point in a beam that is not the point of application of a concentrated load, one should apply a load  $P = 0$  at that point and carry the term  $P$  into the strain energy equation. Finally, introduce the true value of  $P = 0$  into the expression for the answer.

#### EXAMPLE 2.6:

For example, it is required to determine the bending deflection at the free end of a cantilever loaded as shown in Figure 2.68.

#### Solution

$$\begin{aligned} V &= \int_0^L \frac{M^2}{2EI} dx \\ \Delta &= \frac{\partial V}{\partial W_1} = \int_0^L \frac{M}{EI} \frac{\partial M}{\partial W_1} dx \\ M &= W_1 x \quad 0 < x < \frac{L}{2} \\ &= W_1 x + W_2 \left( x - \frac{\ell}{2} \right) \quad \frac{L}{2} < x < L \\ \Delta &= \frac{1}{EI} \int_0^{\ell/2} W_1 x \times x dx + \frac{1}{EI} \int_{\ell/2}^{\ell} \left[ W_1 x + W_2 \left( x - \frac{\ell}{2} \right) \right] x dx \\ &= \frac{W_1 \ell^3}{24EI} + \frac{7W_1 \ell^3}{24EI} + \frac{5W_2 \ell^3}{48EI} \end{aligned}$$

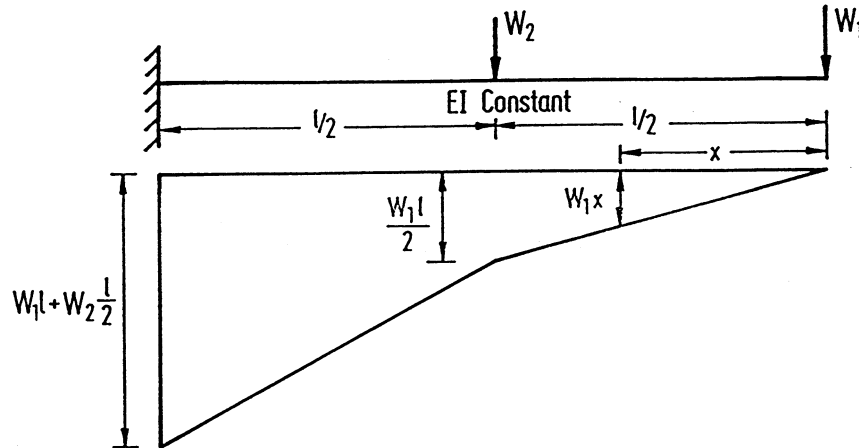


FIGURE 2.68: Example 2.6

$$= \frac{W_1 \ell^3}{3EI} + \frac{5W_2 \ell^3}{48EI}$$

Castigliano's Theorem can be applied to determine deflection of trusses as follows: We know that the increment of strain energy for an axially loaded bar is given as

$$dV = \frac{1}{2E} \sigma_y^2 A dy$$

Substituting,  $\sigma_y = \frac{S}{A}$ , where  $S$  is the axial load in the bar and integrating over the length of the bar the total strain energy of the bar is given as

$$V = \frac{S^2 L}{2AE} \quad (2.134)$$

The deflection component  $\Delta_i$  of the point of application of a load  $P_i$  in the direction of  $P_i$  is given as

$$\Delta_i = \frac{\partial V}{\partial P_i} = \frac{\partial}{\partial P_i} \sum \frac{S^2 L}{2AE} = \sum \frac{S}{AE} \frac{\partial S}{\partial P_i} L$$

**EXAMPLE 2.7:**

Let us consider the truss shown in Figure 2.69. It is required to determine the vertical deflection at 'g' of the truss when loaded as shown in the figure. Let us first replace 20 k load at 'g' by  $P$  and carry out the calculations in terms of  $P$ . At the end,  $P$  will be replaced by the actual value, namely 20 k.

Member	A in. <sup>2</sup>	L ft	S	$\frac{\partial S}{\partial P}$	n	$nS \frac{\partial S}{\partial P} \frac{L}{A}$
ab	2	25	$-(33.3 + 0.83P)$	-0.83	2	$(691 + 17.2P)$
af	2	20	$(26.7 + 0.67P)$	0.67	2	$(358 + 9P)$
fg	2	20	$(26.7 + 0.67P)$	0.67	2	$(358 + 9P)$
bf	1	15	20	0	2	0
bg	1	25	$0.83P$	0.83	2	$34.4P$
bc	2	20	$-26.7 - 1.33P$	-1.33	2	$(710 + 35.4P)$
cg	1	15	0	0	1	0
'n' indicates the number of similar members				$\sum \frac{S \frac{\partial S}{\partial P} L}{A}$		2117 + 105P

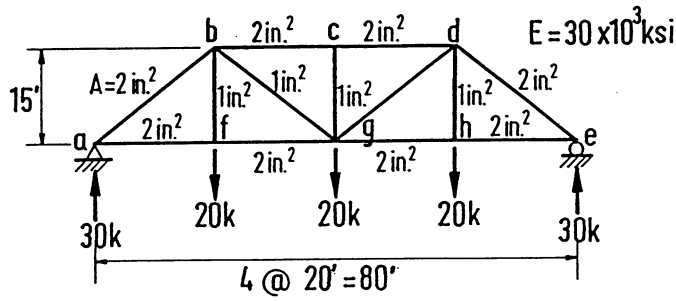


FIGURE 2.69: Example 2.7.

With

$$P = 20k$$

$$\Delta_g = \sum \frac{S \frac{\delta S}{\delta P} L}{AE} = \frac{(2117 + 105 \times 20) \times 12}{30 \times 10^3} = 1.69 \text{ in.}$$

## 2.8.5 Unit Load Method

The unit load method is a versatile tool in the solution of deflections of both trusses and beams. Consider an elastic body in equilibrium under loads  $P_1, P_2, P_3, P_4, \dots, P_n$  and a load  $p$  applied at point  $O$ , as shown in Figure 2.70. By Castigliano's Theorem, the component of the deflection of

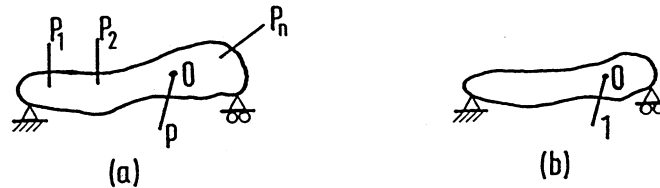


FIGURE 2.70: Elastic body in equilibrium under load.

point  $O$  in the direction of the applied force  $p$  is

$$\delta_{o_p} = \frac{\partial V}{\partial p} \quad (2.135)$$

in which  $V$  is the strain energy of the body. It has been shown in Equation 2.123, that the strain energy of a beam, neglecting shear effects, is given by

$$V = \int_0^L \frac{M^2}{2EI} dx$$

Also it was shown that if the elastic body is a truss, from Equation 2.134

$$V = \sum \frac{S^2 L}{2AE}$$

For a beam, therefore, from Equation 2.135

$$\delta_{o_p} = \int_L \frac{M \frac{\partial M}{\partial p} dx}{EI} \quad (2.136)$$

and for a truss,

$$\delta_{o_p} = \sum \frac{S \frac{\partial S}{\partial p} L}{AE} \quad (2.137)$$

The bending moments  $M$  and the axial forces  $S$  are functions of the load  $p$  as well as of the loads  $P_1, P_2, \dots, P_n$ . Let a unit load be applied at  $O$  on the elastic body and the corresponding moment be  $m$  if the body is a beam, and the forces in the members of the body be  $u$  if the body is a truss. For the body in Figure 2.70, the moments  $M$  and the forces  $S$  due to the system of forces  $P_1, P_2, \dots, P_n$  and  $p$  at  $O$  applied separately can be obtained by superposition as

$$M = M_p + pm \quad (2.138)$$

$$S = S_p + pu \quad (2.139)$$

in which  $M_p$  and  $S_p$  are, respectively, moments and forces produced by  $P_1, P_2, \dots, P_n$ . Then

$$\frac{\partial M}{\partial p} = m = \text{moments produced by a unit load at } O \quad (2.140)$$

$$\frac{\partial S}{\partial p} = u = \text{stresses produced by a unit load at } O \quad (2.141)$$

Using Equations 2.140 and 2.141 in Equations 2.136 and 2.137, respectively,

$$\delta_{o_p} = \int_L \frac{M m dx}{EI} \quad (2.142)$$

$$\delta_{o_p} = \sum \frac{S u L}{AE} \quad (2.143)$$

### EXAMPLE 2.8:

Determine, using the unit load method, the deflection at  $C$  of a simple beam of constant cross-section loaded as shown in Figure 2.71a.

**Solution** The bending moment diagram for the beam due to the applied loading is shown in Figure 2.71b. A unit load is applied at  $C$  where it is required to determine the deflection as shown in Figure 2.71c and the corresponding bending moment diagram is shown in Figure 2.71d. Now, using Equation 2.142, we have

$$\begin{aligned} \delta_c &= \int_0^L \frac{M m dx}{EI} \\ &= \frac{1}{EI} \int_0^{\frac{L}{4}} (Wx) \left(\frac{3}{4}x\right) dx + \frac{1}{EI} \int_{\frac{L}{4}}^{\frac{3L}{4}} \left(\frac{WL}{4}\right) \frac{1}{4}(L-x) dx \\ &\quad + \frac{1}{EI} \int_{\frac{3L}{4}}^L W(L-x) \frac{1}{4}(L-x) dx \\ &= \frac{WL^3}{48EI} \end{aligned}$$

Further details on energy methods in structural analysis may be found in [10].

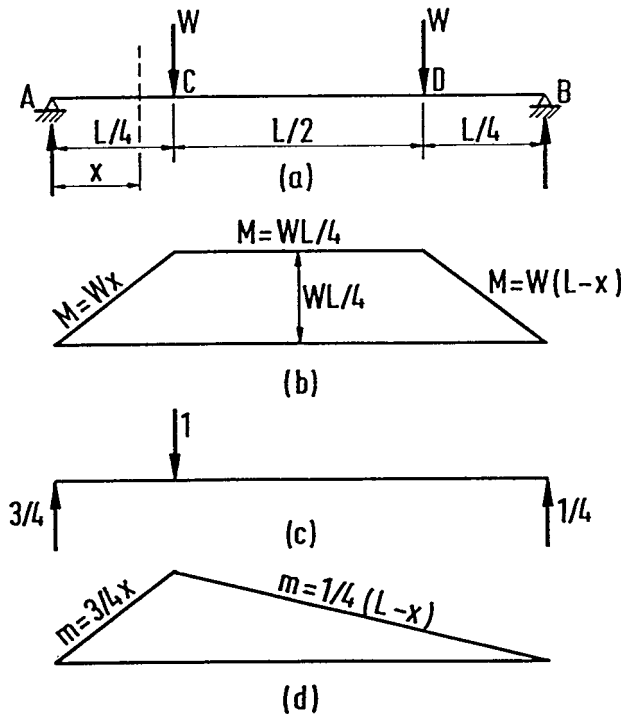


FIGURE 2.71: Example 2.8.

## 2.9 Matrix Methods

In this method of structural analysis, a set of simultaneous equations that describe the load-deformation characteristics of the structure under consideration are formed. These equations are solved using the matrix algebra to obtain the load-deformation characteristics of discrete or finite elements into which the structure has been subdivided. Matrix algebra is ideally suited for setting up and solving equations on the computer. Matrix structural analysis has two methods of approach. The first is called the flexibility method in which forces are used as independent variables and the second is called the stiffness method; the second method employs deformations as the independent variables. The two methods are also called the force method and the displacement method, respectively.

### 2.9.1 Flexibility Method

In a structure, the forces and displacements are related to one another by using stiffness influence coefficients. Let us consider, for example, a simple beam in which three concentrated loads  $W_1$ ,  $W_2$ , and  $W_3$  are applied at sections 1, 2, and 3, respectively as shown in Figure 2.72. Now, the deflection at section 1,  $\Delta_1$  can be expressed as

$$\Delta_1 = F_{11}W_1 + F_{12}W_2 + F_{13}W_3$$

in which  $F_{11}$ ,  $F_{12}$ , and  $F_{13}$  are called flexibility coefficients and they are, respectively, defined as the deflection at section 1 due to unit loads applied at sections 1, 2, and 3. Deflections at sections 2 and 3 are similarly given as

$$\Delta_2 = F_{21}W_1 + F_{22}W_2 + F_{23}W_3$$

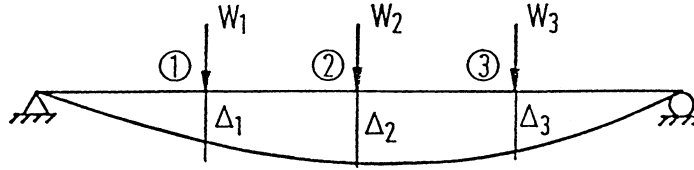


FIGURE 2.72: Simple beam under concentrated loads.

and

$$\Delta_3 = F_{31}W_1 + F_{32}W_2 + F_{33}W_3 \quad (2.144)$$

These expressions are written in the matrix form as

$$\begin{Bmatrix} \Delta_1 \\ \Delta_2 \\ \Delta_3 \end{Bmatrix} = \begin{bmatrix} F_{11} & F_{12} & F_{13} \\ F_{21} & F_{22} & F_{23} \\ F_{31} & F_{32} & F_{33} \end{bmatrix} \begin{Bmatrix} W_1 \\ W_2 \\ W_3 \end{Bmatrix}$$

(or)

$$\{\Delta\} = [F]\{W\} \quad (2.145)$$

The matrix  $[F]$  is called the flexibility matrix. It can be shown, by applying Maxwell's reciprocal theorem [10], that the matrix  $[F]$  is a symmetric matrix.

The flexibility matrix for a cantilever beam loaded as shown in Figure 2.73 can be constructed as follows.

The first column in the flexibility matrix can be generated by applying a unit vertical load at the free end of the cantilever as shown in Figure 2.73b and making use of the moment area method. We get

$$F_{11} = \frac{8L^3}{3EI}, \quad F_{21} = \frac{2L^2}{EI}, \quad F_{31} = \frac{5L^3}{6EI}, \quad F_{41} = \frac{3L^2}{2EI}$$

Columns 2, 3, and 4 are, similarly, generated by applying unit moment at the free end and unit force and unit moment at the mid-span as shown in Figures 2.73c, d, and e, respectively. Combining the results thus obtained, one gets the flexibility matrix as

$$\begin{Bmatrix} \Delta_1 \\ \Delta_2 \\ \Delta_3 \\ \Delta_4 \end{Bmatrix} = \frac{1}{EI} \begin{bmatrix} \frac{8L^3}{3} & 2L^2 & \frac{5L^3}{6} & \frac{3L^2}{2} \\ 2L^2 & 2L & \frac{L^2}{2} & L \\ \frac{5L^3}{6} & \frac{L^2}{2} & \frac{L^3}{3} & \frac{L^2}{2} \\ \frac{3L^2}{2} & L & \frac{L^2}{2} & L \end{bmatrix} \begin{Bmatrix} W_1 \\ W_2 \\ W_3 \\ W_4 \end{Bmatrix} \quad (2.146)$$

The above method to generate the flexibility matrix for a given structure is extremely impractical. It is therefore recommended to subdivide a given structure into several elements and to form the flexibility matrix for each of the elements. The flexibility matrix for the entire structure is then obtained by combining the flexibility matrices of the individual elements.

Force transformation matrix relates what occurs in these elements to the behavior of the entire structure. Using the conditions of equilibrium, it relates the element forces to the structure forces. The principle of conservation of energy may be used to generate transformation matrices.

## 2.9.2 Stiffness Method

Forces and deformations in a structure are related to one another by means of stiffness influence coefficients. Let us consider, for example, a simply supported beam subjected to end moments  $W_1$

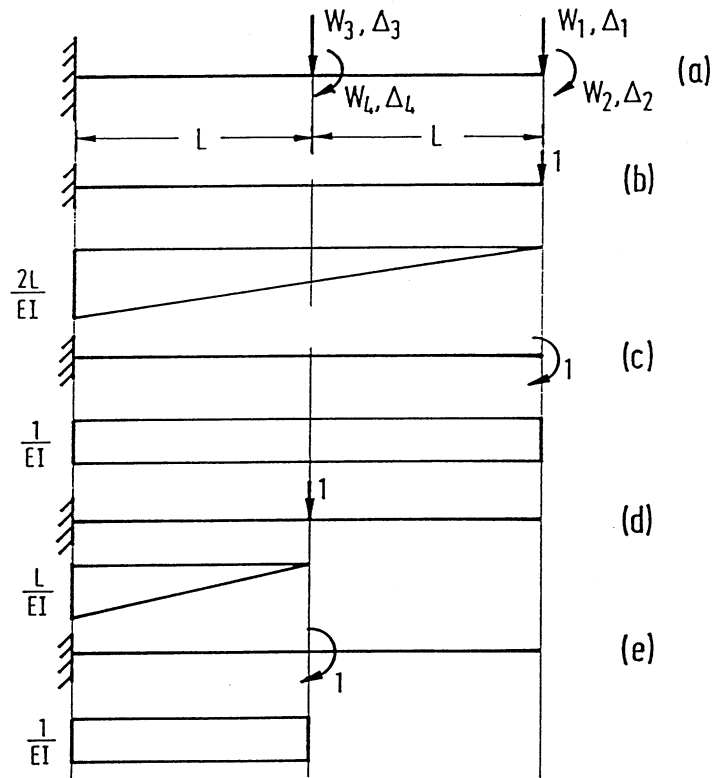


FIGURE 2.73: Cantilever beam.

and  $W_2$  applied at supports 1 and 2 and let the respective rotations be denoted as  $\Delta_1$  and  $\Delta_2$  as shown in Figure 2.74. We can now write the expressions for end moments  $W_1$  and  $W_2$  as

$$\begin{aligned} W_1 &= K_{11}\Delta_1 + K_{12}\Delta_2 \\ W_2 &= K_{21}\Delta_1 + K_{22}\Delta_2 \end{aligned} \quad (2.147)$$

in which  $K_{11}$  and  $K_{12}$  are called stiffness influence coefficients defined as moments at 1 due to unit rotation at 1 and 2, respectively. The above equations can be written in matrix form as

$$\begin{Bmatrix} W_1 \\ W_2 \end{Bmatrix} = \begin{bmatrix} K_{11} & K_{12} \\ K_{21} & K_{22} \end{bmatrix} \begin{Bmatrix} \Delta_1 \\ \Delta_2 \end{Bmatrix}$$

or

$$\{W\} = [K]\{\Delta\} \quad (2.148)$$

The matrix  $[K]$  is referred to as stiffness matrix. It can be shown that the flexibility matrix of a structure is the inverse of the stiffness matrix and vice versa. The stiffness matrix of the whole structure is formed out of the stiffness matrices of the individual elements that make up the structure.

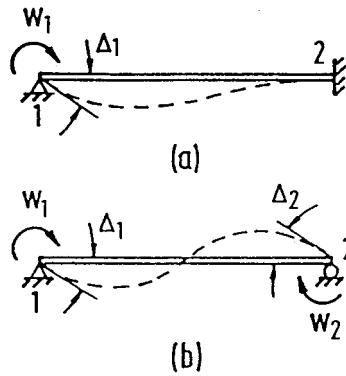


FIGURE 2.74: Simply supported beam.

### 2.9.3 Element Stiffness Matrix

#### Axially Loaded Member

Figure 2.75 shows an axially loaded member of constant cross-sectional area with element forces  $q_1$  and  $q_2$  and displacements  $\delta_1$  and  $\delta_2$ . They are shown in their respective positive directions.

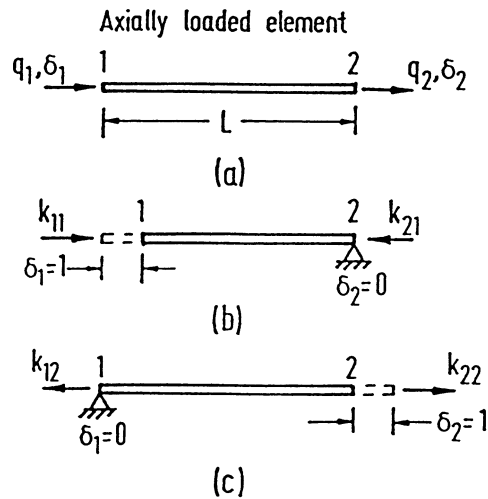


FIGURE 2.75: Axially loaded member.

With unit displacement  $\delta_1 = 1$  at node 1, as shown in Figure 2.75, axial forces at nodes 1 and 2 are obtained as

$$K_{11} = \frac{EA}{L}, \quad K_{21} = -\frac{EA}{L}$$

In the same way by setting  $\delta_2 = 1$  as shown in Figure 2.75 the corresponding forces are obtained as

$$K_{12} = -\frac{EA}{L}, \quad K_{22} = \frac{EA}{L}$$

The stiffness matrix is written as

$$\begin{Bmatrix} q_1 \\ q_2 \end{Bmatrix} = \begin{bmatrix} K_{11} & K_{12} \\ K_{21} & K_{22} \end{bmatrix} \begin{Bmatrix} \delta_1 \\ \delta_2 \end{Bmatrix}$$

or

$$\begin{Bmatrix} q_1 \\ q_2 \end{Bmatrix} = \frac{EA}{L} \begin{bmatrix} 1 & -1 \\ -1 & 1 \end{bmatrix} \begin{Bmatrix} \delta_1 \\ \delta_2 \end{Bmatrix}. \quad (2.149)$$

### Flexural Member

The stiffness matrix for the flexural element shown in Figure 2.76 can be constructed as follows. The forces and the corresponding displacements, namely the moments, the shears, and the

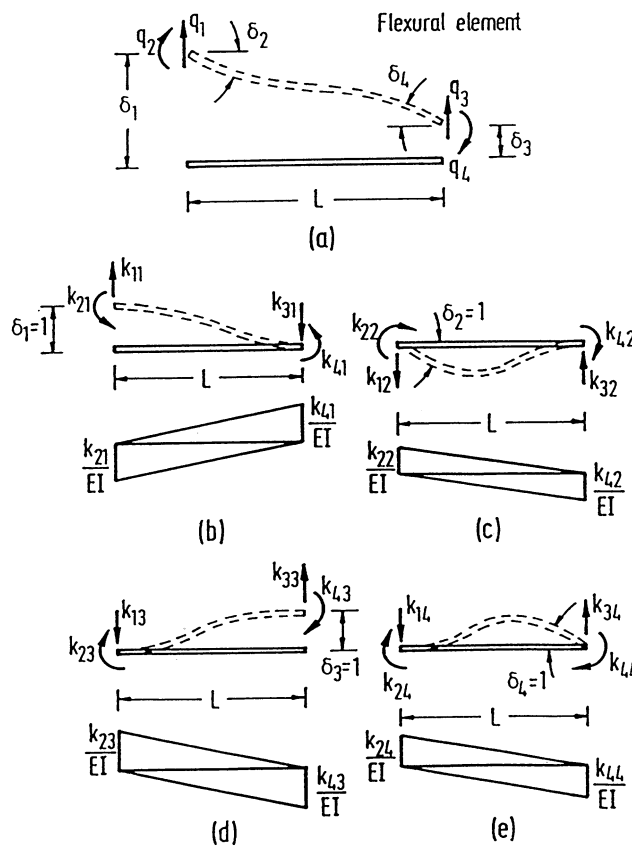


FIGURE 2.76: Beam element—stiffness matrix.

corresponding rotations and translations at the ends of the member, are defined in the figure. The matrix equation that relates these forces and displacements can be written in the form

$$\begin{Bmatrix} q_1 \\ q_2 \\ q_3 \\ q_4 \end{Bmatrix} = \begin{bmatrix} K_{11} & K_{12} & K_{13} & K_{14} \\ K_{21} & K_{22} & K_{23} & K_{24} \\ K_{31} & K_{32} & K_{33} & K_{34} \\ K_{41} & K_{42} & K_{43} & K_{44} \end{bmatrix} \begin{Bmatrix} \delta_1 \\ \delta_2 \\ \delta_3 \\ \delta_4 \end{Bmatrix}$$

The terms in the first column consist of the element forces  $q_1$  through  $q_4$  that result from displacement  $\delta_1 = 1$  when  $\delta_2 = \delta_3 = \delta_4 = 0$ . This means that a unit vertical displacement is imposed at the left end of the member while translation at the right end and rotation at both ends are prevented as shown in Figure 2.76. The four member forces corresponding to this deformation can be obtained using the moment-area method.

The change in slope between the two ends of the member is zero and the area of the  $M/EI$  diagram between these point must, therefore, vanish. Hence,

$$\frac{K_{41}L}{2EI} - \frac{K_{21}L}{2EI} = 0$$

and

$$K_{21} = K_{41} \quad (2.150)$$

The moment of the  $M/EI$  diagram about the left end of the member is equal to unity. Hence,

$$\frac{K_{41}L}{2EI} \left( \frac{2L}{3} \right) - \frac{K_{21}L}{2EI} \left( \frac{L}{3} \right) = 1$$

and in view of Equation 2.150,

$$K_{41} = K_{21} = \frac{6EI}{L^2}$$

Finally, moment equilibrium of the member about the right end leads to

$$K_{11} = \frac{K_{21} + K_{41}}{L} = \frac{12EI}{L^3}$$

and from equilibrium in the vertical direction we obtain

$$K_{31} = K_{11} = \frac{12EI}{L^3}$$

The forces act in the directions indicated in Figure 2.76b. To obtain the correct signs, one must compare the forces with the positive directions defined in Figure 2.76a. Thus,

$$K_{11} = \frac{12EI}{L^3}, \quad K_{21} = -\frac{6EI}{L^2}, \quad K_{31} = -\frac{12EI}{L^3}, \quad K_{41} = -\frac{6EI}{L^2}$$

The second column of the stiffness matrix is obtained by letting  $\delta_2 = 1$  and setting the remaining three displacements equal to zero as indicated in Figure 2.76c. The area of the  $M/EI$  diagram between the ends of the member for this case is equal to unity, and hence,

$$\frac{K_{22}L}{2EI} - \frac{K_{42}L}{2EI} = 1$$

The moment of the  $M/EI$  diagram about the left end is zero, so that

$$\frac{K_{22}L}{2EI} \left( \frac{L}{3} \right) - \frac{K_{42}L}{2EI} \left( \frac{2L}{3} \right) = 0$$

Therefore, one obtains

$$K_{22} = \frac{4EI}{L}, \quad K_{42} = \frac{2EI}{L}$$

From vertical equilibrium of the member,

$$K_{12} = K_{32}$$

and moment equilibrium about the right end of the member leads to

$$K_{12} = \frac{K_{22} + K_{42}}{L} = \frac{6EI}{L^2}$$

Comparison of the forces in Figure 2.76c with the positive directions defined in Figure 2.76a indicates that all the influence coefficients except  $k_{12}$  are positive. Thus,

$$K_{12} = -\frac{6EI}{L^2}, \quad K_{22} = \frac{4EI}{L}, \quad K_{32} = \frac{6EI}{L^2}, \quad K_{42} = \frac{2EI}{L}$$

Using Figures 2.76d and e, the influence coefficients for the third and fourth columns can be obtained. The results of these calculations lead to the following element-stiffness matrix:

$$\begin{bmatrix} q_1 \\ q_2 \\ q_3 \\ q_4 \end{bmatrix} = \begin{bmatrix} \frac{12EI}{L^3} & -\frac{6EI}{L^2} & -\frac{12EI}{L^3} & -\frac{6EI}{L^2} \\ -\frac{6EI}{L^2} & \frac{4EI}{L} & \frac{6EI}{L^2} & \frac{2EI}{L} \\ -\frac{12EI}{L^3} & \frac{6EI}{L^2} & \frac{12EI}{L^3} & \frac{6EI}{L^2} \\ -\frac{6EI}{L^2} & \frac{2EI}{L} & \frac{6EI}{L^2} & \frac{4EI}{L} \end{bmatrix} \begin{bmatrix} \delta_1 \\ \delta_2 \\ \delta_3 \\ \delta_4 \end{bmatrix} \quad (2.151)$$

Note that Equation 2.150 defines the element-stiffness matrix for a flexural member with constant flexural rigidity  $EI$ .

If axial load in a frame member is also considered the general form of an element, then the stiffness matrix for an element shown in Figure 2.77 becomes

$$\begin{bmatrix} q_1 \\ q_2 \\ q_3 \\ q_4 \\ q_5 \\ q_6 \end{bmatrix} = \begin{bmatrix} \frac{EA}{L} & 0 & 0 & -\frac{EA}{L} & 0 & 0 \\ 0 & \frac{12EI}{L^3} & -\frac{6EI}{L^2} & 0 & -\frac{12EI}{L^3} & -\frac{6EI}{L^2} \\ 0 & -\frac{6EI}{L^2} & \frac{4EI}{L} & 0 & \frac{6EI}{L^2} & \frac{2EI}{L} \\ -\frac{EA}{L} & 0 & 0 & \frac{EA}{L} & 0 & 0 \\ 0 & -\frac{12EI}{L^3} & \frac{6EI}{L^2} & 0 & \frac{12EI}{L^3} & \frac{6EI}{L^2} \\ 0 & -\frac{6EI}{L^2} & \frac{2EI}{L} & 0 & \frac{6EI}{L^2} & \frac{4EI}{L} \end{bmatrix} \begin{bmatrix} \delta_1 \\ \delta_2 \\ \delta_3 \\ \delta_4 \\ \delta_5 \\ \delta_6 \end{bmatrix}$$

(or)

$$[q] = [k_c][\delta] \quad (2.152)$$

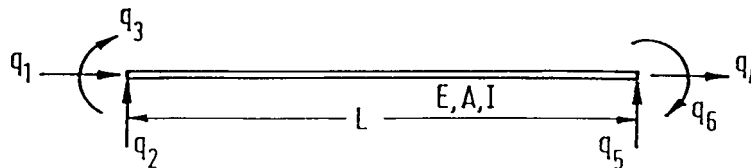


FIGURE 2.77: Beam element with axial force.

### 2.9.4 Grillages

Another common type of structure is one in which the members all lie in one plane with loads being applied in the direction normal to this plane. This type of structure is commonly adopted in building floor systems, bridge decks, ship decks, floors, etc. The grid floor, for purposes of analysis by using matrix method, can be treated as a **space frame**. However, the solution can be simplified by considering the grid member as a planar grid. A typical grid floor is shown in Figure 2.78a. The significant member forces in a member and the corresponding deformations are as shown in Figure 2.78b.

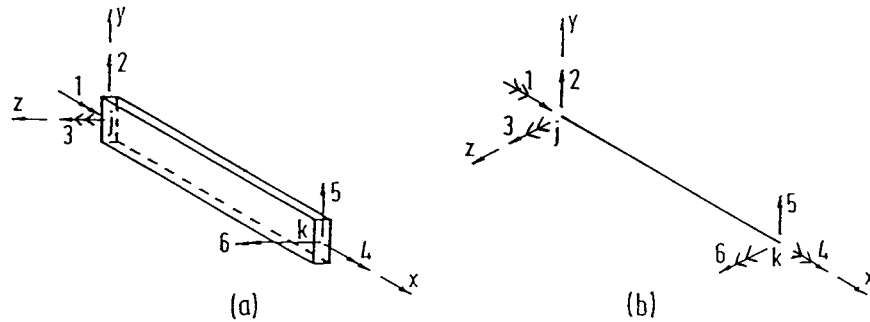


FIGURE 2.78: A grid member.

The member stiffness matrix can be written as

$$K = \begin{bmatrix} \frac{GJ}{L} & 0 & 0 & -\frac{GJ}{L} & 0 & 0 \\ 0 & \frac{12EI_z}{L^3} & \frac{6EI_z}{L^2} & 0 & -\frac{12EI_z}{L^3} & \frac{6EI_z}{L^2} \\ 0 & \frac{6EI_z}{L^2} & \frac{4EI_z}{L} & 0 & -\frac{6EI_z}{L^2} & \frac{2EI_z}{L} \\ 0 & -\frac{GJ}{L} & 0 & 0 & \frac{GJ}{L} & 0 \\ 0 & -\frac{12EI_z}{L^3} & -\frac{6EI_z}{L^2} & 0 & \frac{12EI_z}{L^3} & -\frac{6EI_z}{L^2} \\ 0 & \frac{6EI_z}{L^2} & \frac{2EI_z}{L} & 0 & -\frac{6EI_z}{L^2} & \frac{4EI_z}{L} \end{bmatrix} \quad (2.153)$$

### 2.9.5 Structure Stiffness Matrix

Equation 2.152 has been expressed in terms of the coordinate system of the individual members. In a structure consisting of many members there would be as many systems of coordinates as the number of members. Before the internal actions in the members of the structure can be related, all forces and deflections must be stated in terms of one single system of axes common to all—the structure axes. The transformation from element to structure coordinates is carried out separately for each element and the resulting matrices are then combined to form the structure-stiffness matrix. A separate transformation matrix  $[T]$  is written for each element and a relation of the form

$$[\delta]_n = [T]_n[\Delta]_n \quad (2.154)$$

is written in which  $[T]_n$  defines the matrix relating the element deformations of element 'n' to the structure deformations at the ends of that particular element. The element and structure forces are

related in the same way as the corresponding deformations as

$$[q]_n = [T]_n[W]_n \quad (2.155)$$

where  $[q]_n$  contains the element forces for element 'n' and  $[W]_n$  contains the structure forces at the extremities of the element. The transformation matrix  $[T]_n$  can be used to transform element 'n' from its local coordinates to structure coordinates. We know, for an element  $n$ , the force-deformation relation is given as

$$[q]_n = [k]_n[\delta]_n$$

Substituting for  $[q]_n$  and  $[\delta]_n$  from Equations 2.153 and 2.154 one obtains

$$[T]_n[W]_n = [k]_n[T]_n[\Delta]_n$$

or

$$\begin{aligned} [W]_n &= [T]_n^{-1}[k]_n[T]_n[\Delta]_n \\ &= [T]_n^T[k]_n[T]_n[\Delta]_n \\ &= [K]_n[\Delta]_n \\ [K]_n &= [T]_n^T[k]_n[T]_n \end{aligned} \quad (2.156)$$

$[K]_n$  is the stiffness matrix which transforms any element 'n' from its local coordinate to structure coordinates. In this way, each element is transformed individually from element coordinate to structure coordinate and the resulting matrices are combined to form the stiffness matrix for the entire structure.

Member stiffness matrix  $[K]_n$  in structure coordinates for a truss member shown in Figure 2.79, for example, is given as

$$[K]_n = \frac{AE}{L} \begin{bmatrix} \lambda^2\mu & \lambda\mu & -\lambda^2 & -\lambda\mu \\ \lambda\mu & \mu^2 & -\lambda\mu & -\mu^2 \\ -\lambda^2 & -\lambda\mu & \lambda^2 & \lambda\mu \\ -\lambda\mu & -\mu^2 & \lambda\mu & \mu^2 \end{bmatrix} \begin{matrix} i \\ j \\ k \\ \ell \end{matrix} \quad (2.157)$$

in which  $\lambda = \cos \phi$  and  $\mu = \sin \phi$ .

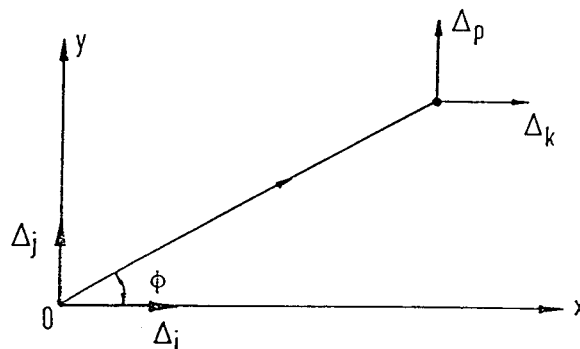


FIGURE 2.79: A grid member.

To construct  $[K]_n$  for a given member it is necessary to have the values of  $\lambda$  and  $\mu$  for the member. In addition, the structure coordinates  $i$ ,  $j$ ,  $k$ , and  $\ell$  at the extremities of the member must be known.



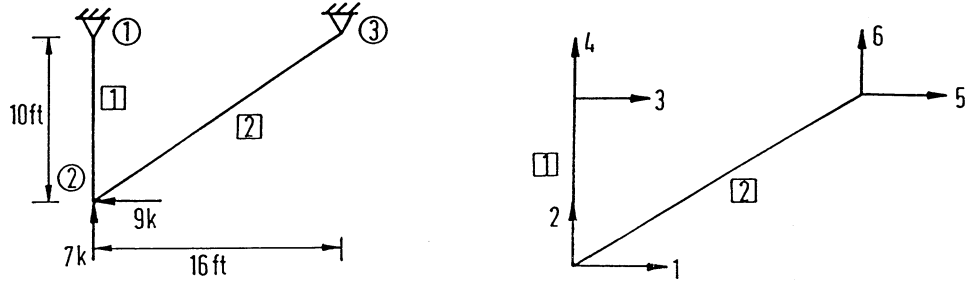


FIGURE 2.81: Example 2.9.

$$[K]_1 = \begin{bmatrix} 1 & 2 & 3 & 4 \\ 0 & 0 & 0 & 0 \\ 0 & 750 & 0 & -750 \\ 0 & 0 & 0 & 0 \\ 0 & -750 & 0 & 750 \end{bmatrix} \begin{matrix} 1 \\ 2 \\ 3 \\ 4 \end{matrix}$$

For member 2,

$$\frac{AE}{L} = \frac{3 \times 30 \times 10^3}{18.9 \times 12} = 397$$

$$[K]_2 = \begin{bmatrix} 1 & 2 & 5 & 6 \\ 286 & 179 & -286 & -179 \\ 179 & 111 & -179 & -111 \\ -286 & -179 & 286 & 179 \\ -179 & -111 & 179 & 111 \end{bmatrix} \begin{matrix} 1 \\ 2 \\ 5 \\ 6 \end{matrix}$$

Combining the element stiffness matrices,  $[K]_1$  and  $[K]_2$ , one obtains the structure stiffness matrix as follows:

$$\begin{bmatrix} W_1 \\ W_2 \\ W_3 \\ W_4 \\ W_5 \\ W_6 \end{bmatrix} = \begin{bmatrix} 286 & 179 & 0 & 0 & -286 & -179 \\ 179 & 861 & 0 & -750 & -179 & -111 \\ 0 & 0 & 0 & 0 & 0 & 0 \\ 0 & -750 & 0 & 750 & 0 & 0 \\ -286 & -179 & 0 & 0 & 286 & 179 \\ -179 & -111 & 0 & 0 & 179 & 111 \end{bmatrix} \begin{bmatrix} \Delta_1 \\ \Delta_2 \\ \Delta_3 \\ \Delta_4 \\ \Delta_5 \\ \Delta_6 \end{bmatrix}$$

The stiffness matrix can now be subdivided to determine the unknowns. Let us consider  $\Delta_1$  and  $\Delta_2$  the deflections at joint 2 which can be determined in view of  $\Delta_3 = \Delta_4 = \Delta_5 = \Delta_6 = 0$  as follows:

$$\begin{bmatrix} \Delta_1 \\ \Delta_2 \end{bmatrix} = \begin{bmatrix} 286 & 179 \\ 179 & 861 \end{bmatrix}^{-1} \begin{bmatrix} -9 \\ 7 \end{bmatrix}$$

or

$$\begin{aligned} \Delta_1 &= 0.042 \text{ in. to the left} \\ \Delta_2 &= 0.0169 \text{ in. upward} \end{aligned}$$

**EXAMPLE 2.10:**

A simple triangular frame is loaded at the tip by 20 kips as shown in Figure 2.82. Assemble the structure stiffness matrix and determine the displacements at the loaded node.

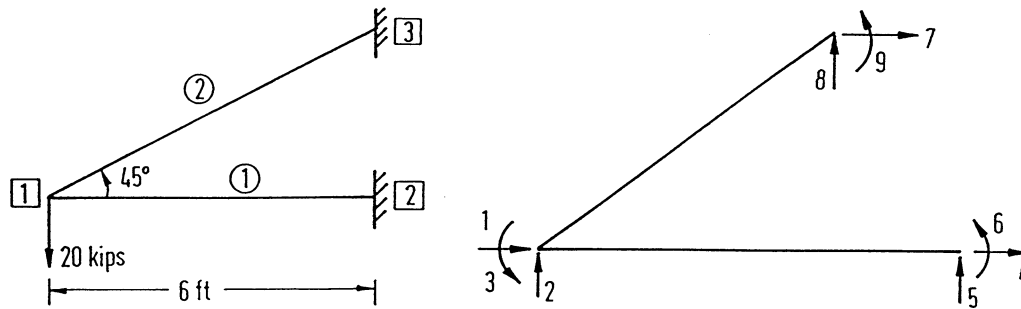


FIGURE 2.82: Example 2.10.

Member	Length (in.)	A (in. <sup>2</sup> )	I (in. <sup>4</sup> )	$\phi$	$\lambda$	$\mu$
1	72	2.4	1037	0	1	0
2	101.8	3.4	2933	45°	0.707	0.707

For members 1 and 2 the stiffness matrices in structure coordinates can be written by making use of Equation 2.158.

$$[K]_1 = 10^3 \times \begin{bmatrix} 1 & 2 & 3 & 4 & 5 & 6 \\ 1 & 0 & 0 & -1 & 0 & 0 \\ 0 & 1 & 36 & 0 & -1 & 36 \\ 0 & 36 & 1728 & 0 & -36 & 864 \\ -1 & 0 & 0 & 1 & 0 & 0 \\ 0 & -1 & -36 & 0 & 1 & -36 \\ 0 & 36 & 864 & 0 & -36 & 1728 \end{bmatrix} \begin{matrix} 1 \\ 2 \\ 3 \\ 4 \\ 5 \\ 6 \end{matrix}$$

and

$$[K]_2 = 10^3 \times \begin{bmatrix} 1 & 2 & 3 & 7 & 8 & 9 \\ 1 & 0 & -36 & -1 & 0 & -36 \\ 0 & 1 & 36 & 0 & 1 & 36 \\ -36 & 36 & 3457 & 36 & -36 & 1728 \\ -1 & 0 & 36 & 1 & 0 & 36 \\ 0 & 1 & -36 & 0 & 1 & -36 \\ -36 & 36 & 1728 & 36 & -36 & 3457 \end{bmatrix} \begin{matrix} 1 \\ 2 \\ 3 \\ 7 \\ 8 \\ 9 \end{matrix}$$

Combining the element stiffness matrices  $[K]_1$  and  $[K]_2$ , one obtains the structure stiffness matrix

as follows:

$$[K] = 10^3 \times \begin{bmatrix} 2 & 0 & -36 & -1 & 0 & 0 & -1 & 0 & -36 \\ 0 & 2 & 72 & 0 & -1 & 36 & 0 & 1 & 36 \\ -36 & 72 & 5185 & 0 & -36 & 864 & 36 & -36 & 1728 \\ -1 & 0 & 0 & 1 & 0 & 0 & 0 & 0 & 0 \\ 0 & -1 & -36 & 0 & 1 & -36 & 0 & 0 & 0 \\ 0 & 36 & 864 & 0 & -36 & 1728 & 0 & 0 & 0 \\ -1 & 0 & 36 & 0 & 0 & 0 & 1000 & 0 & 36 \\ 0 & 1 & -36 & 0 & 0 & 0 & 0 & 1 & -36 \\ -36 & 36 & 1728 & 0 & 0 & 0 & 36 & 36 & 3457 \end{bmatrix} \begin{matrix} 1 \\ 2 \\ 3 \\ 4 \\ 5 \\ 6 \\ 7 \\ 8 \\ 9 \end{matrix}$$

The deformations at joints 2 and 3 corresponding to  $\Delta_5$  to  $\Delta_9$  are zero since joints 2 and 4 are restrained in all directions. Cancelling the rows and columns corresponding to zero deformations in the structure stiffness matrix, one obtains the force deformation relation for the structure:

$$\begin{bmatrix} F_1 \\ F_2 \\ F_3 \end{bmatrix} = \begin{bmatrix} 2 & 0 & -36 \\ 0 & 2 & 72 \\ -36 & 72 & 5185 \end{bmatrix} \times 10^3 \begin{bmatrix} \Delta_1 \\ \Delta_2 \\ \Delta_3 \end{bmatrix}$$

Substituting for the applied load  $F_2 = -20$  kips, the deformations are given as

$$\begin{bmatrix} \Delta_1 \\ \Delta_2 \\ \Delta_3 \end{bmatrix} = \begin{bmatrix} 2 & 0 & -36 \\ 0 & 2 & 72 \\ -36 & 72 & 5185 \end{bmatrix}^{-1} \times 10^3 \begin{bmatrix} 0 \\ -20 \\ 0 \end{bmatrix}$$

or

$$\begin{bmatrix} \Delta_1 \\ \Delta_2 \\ \Delta_3 \end{bmatrix} = \begin{bmatrix} 6.66 \text{ in.} \\ -23.334 \text{ in.} \\ 0.370 \text{ rad} \end{bmatrix} \times 10^3$$

## 2.9.6 Loading Between Nodes

The problems discussed thus far have involved concentrated forces and moments applied to nodes only. But real structures are subjected to distributed or concentrated loading between nodes as shown in Figure 2.83. Loading may range from a few concentrated loads to an infinite variety of uniform

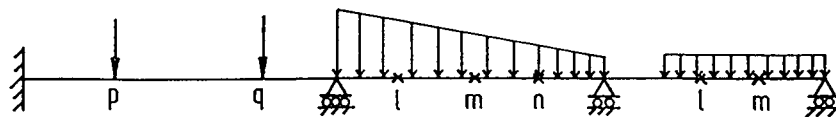


FIGURE 2.83: Loading between nodes.

or nonuniformly distributed loads. The solution method of matrix analysis must be modified to account for such load cases.

One way to treat such loads in the matrix analysis is to insert artificial nodes, such as  $p$  and  $q$  as shown in Figure 2.83. The degrees of freedom corresponding to the additional nodes are added to the total structure and the necessary additional equations are written by considering the requirements of equilibrium at these nodes. The internal member forces on each side of nodes  $p$  and  $q$  must

equilibrate the external loads applied at these points. In the case of distributed loads, suitable nodes such as  $l$ ,  $m$ , and  $n$  shown in Figure 2.83 are selected arbitrarily and the distributed loads are lumped as concentrated loads at these nodes. The degrees of freedom corresponding to the arbitrary and real nodes are treated as unknowns of the problem. There are different ways of obtaining equivalence between the lumped and the distributed loading. In all cases the lumped loads must be statically equivalent to the distributed loads they replace.

The method of introducing arbitrary nodes is not a very elegant procedure because the number of unknown degrees of freedom made the solution procedure laborious. The approach that is of most general use with the displacement method is one employing the related concepts of artificial joint restraint, fixed-end forces, and equivalent nodal loads.

### 2.9.7 Semi-Rigid End Connection

A rigid connection holds unchanged the original angles between intersecting members; a simple connection allows the member end to rotate freely under gravity load, a **semi-rigid connection** possesses a moment capacity intermediate between the simple and the rigid. A simplified linear relationship between the moment  $m$  acting on the connection and the resulting connection rotation  $\psi$  in the direction of  $m$  is assumed giving

$$M = R \frac{EI}{L} \psi \quad (2.159)$$

where  $EI$  and  $L$  are the flexural rigidity and length of the member, respectively. The non-dimensional quantity  $R$ , which is a measure of the degree of rigidity of the connection, is called the rigidity index. For a simple connection,  $R$  is zero and for a rigid connection,  $R$  is infinity. Considering the semi-rigidity of joints, the member flexibility matrix for flexure is derived as

$$\begin{bmatrix} \phi_1 \\ \phi_2 \end{bmatrix} = \frac{L}{EI} \begin{bmatrix} \frac{1}{3} + \frac{1}{R_1} & -\frac{1}{6} \\ -\frac{1}{6} & \frac{1}{3} + \frac{1}{R_2} \end{bmatrix} \begin{bmatrix} M_1 \\ M_2 \end{bmatrix} \quad (2.160)$$

or

$$[\phi] = [F][M] \quad (2.161)$$

where  $\phi_1$  and  $\phi_2$  are as shown in Figure 2.84.

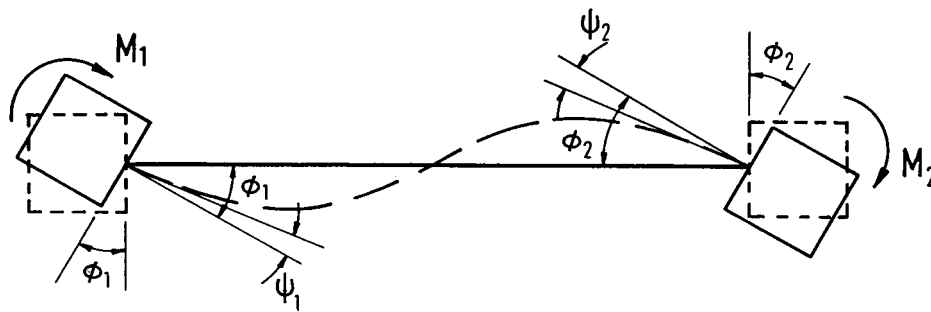


FIGURE 2.84: A flexural member with semi-rigid end connections.

For convenience, two parameters are introduced as follows:

$$p_1 = \frac{1}{1 + \frac{3}{R_1}}$$

and

$$p_2 = \frac{1}{1 + \frac{3}{R_2}}$$

where  $p_1$  and  $p_2$  are called the fixity factors. For hinged connections, both the fixity factors ( $p$ ) and the rigidity index ( $R$ ) are zero; but for rigid connections, the fixity factor is 1 and the rigidity index is infinity. Since the fixity factor can only vary from 0 to 1, its use is more convenient in the analyses of structures with semi-rigid connections.

Equation 2.160 can be rewritten to give

$$[F] = \frac{L}{EI} \begin{bmatrix} \frac{1}{3p_1} & -\frac{1}{6} \\ -\frac{1}{6} & \frac{1}{3p_2} \end{bmatrix} \quad (2.162)$$

From Equation 2.162, the modified member stiffness matrix  $[K]$  for a member with semi-rigid and connections expresses the member end moments,  $M_1$  and  $M_2$ , in terms of the member end rotations,  $\phi_1$  and  $\phi_2$ , as

$$[K] = EI \begin{bmatrix} k_{11} & k_{12} \\ k_{21} & k_{22} \end{bmatrix} \quad (2.163a)$$

Expressions for  $k_{11}$ , and  $k_{12} = k_{21}$  and  $k_{22}$  may be obtained by inverting the  $[F]$  matrix. Thus,

$$k_{11} = \frac{12/p_2}{4/(p_1 p_2) - 1} \quad (2.163b)$$

$$k_{12} = k_{21} = \frac{6}{4(p_1 p_2) - 1} \quad (2.163c)$$

$$k_{22} = \frac{12/p_1}{4/(p_1 p_2) - 1} \quad (2.163d)$$

The modified member stiffness matrix  $[K]$ , as expressed by Equations 2.163 will be needed in the stiffness method of analysis of frames in which there are semi-rigid member-end connections.

## 2.10 The Finite Element Method

Many problems that confront the design analyst, in practice, cannot be solved by analytical methods. This is particularly true for problems involving complex material properties and boundary conditions. Numerical methods, in such cases, provide approximate but acceptable solutions. Of the many numerical methods developed before and after the advent of computers, the finite element method has proven to be a powerful tool. This method can be regarded as a natural extension of the matrix methods of structural analysis. It can accommodate complex and difficult problems such as nonhomogeneity, nonlinear stress-strain behavior, and complicated boundary conditions. The finite element method is applicable to a wide range of boundary value problems in engineering and it dates back to the mid-1950s with the pioneering work by Argyris [4], Clough [21], and others. The method was first applied to the solution of plane stress problems and extended subsequently to the solution of plates, shells, and axisymmetric solids.

### 2.10.1 Basic Concept

The finite element method is based on the representation of a body or a structure by an assemblage of subdivisions called finite elements as shown in Figure 2.85. These elements are considered to be con-

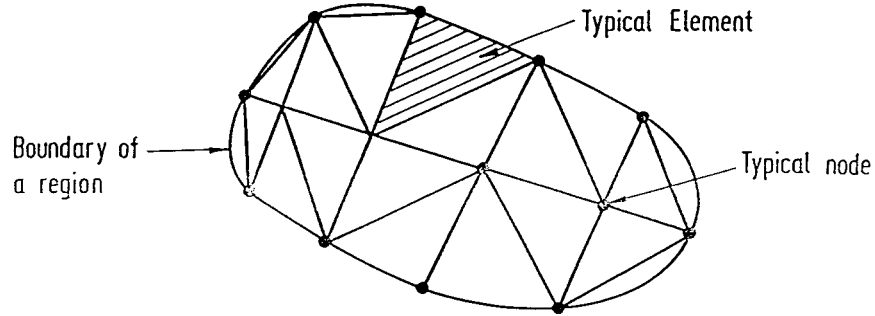


FIGURE 2.85: Assemblage of subdivisions.

nected at nodes. Displacement functions are chosen to approximate the variation of displacements over each finite element. Polynomials are commonly employed to express these functions. Equilibrium equations for each element are obtained by means of the principle of minimum potential energy. These equations are formulated for the entire body by combining the equations for the individual elements so that the continuity of displacements is preserved at the nodes. The resulting equations are solved satisfying the boundary conditions in order to obtain the unknown displacements.

The entire procedure of the finite element method involves the following steps: (1) the given body is subdivided into an equivalent system of finite elements, (2) suitable displacement function is chosen, (3) element stiffness matrix is derived using variational principle of mechanics such as the principle of minimum potential energy, (4) global stiffness matrix for the entire body is formulated, (5) the algebraic equations thus obtained are solved to determine unknown displacements, and (6) element strains and stresses are computed from the nodal displacements.

### 2.10.2 Basic Equations from Theory of Elasticity

Figure 2.86 shows the state of stress in an elemental volume of a body under load. It is defined in terms of three normal stress components  $\sigma_x$ ,  $\sigma_y$ , and  $\sigma_z$  and three shear stress components  $\tau_{xy}$ ,  $\tau_{yz}$ , and  $\tau_{zx}$ . The corresponding strain components are three normal strains  $\epsilon_x$ ,  $\epsilon_y$ , and  $\epsilon_z$  and three shear strains  $\gamma_{xy}$ ,  $\gamma_{yz}$ , and  $\gamma_{zx}$ . These strain components are related to the displacement components  $u$ ,  $v$ , and  $w$  at a point as follows:

$$\begin{aligned} \epsilon_x &= \frac{\partial u}{\partial x} & \gamma_{xy} &= \frac{\partial v}{\partial x} + \frac{\partial u}{\partial y} \\ \epsilon_y &= \frac{\partial v}{\partial y} & \gamma_{yz} &= \frac{\partial w}{\partial y} + \frac{\partial v}{\partial z} \\ \epsilon_z &= \frac{\partial w}{\partial z} & \gamma_{zx} &= \frac{\partial u}{\partial z} + \frac{\partial w}{\partial x} \end{aligned} \quad (2.164)$$

The relations given in Equation 2.164 are valid in the case of the body experiencing small deformations. If the body undergoes large or finite deformations, higher order terms must be retained.

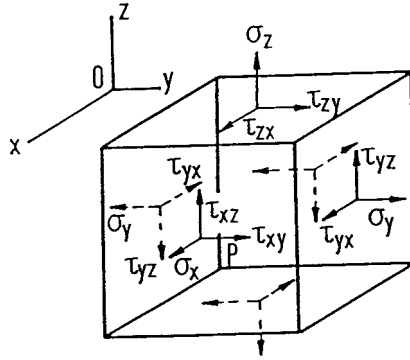


FIGURE 2.86: State of stress in an elemental volume.

The stress-strain equations for isotropic materials may be written in terms of the Young's modulus and Poisson's ratio as

$$\begin{aligned}
 \sigma_x &= \frac{E}{1-\nu^2} [\varepsilon_x + \nu(\varepsilon_y + \varepsilon_z)] \\
 \sigma_y &= \frac{E}{1-\nu^2} [\varepsilon_y + \nu(\varepsilon_z + \varepsilon_x)] \\
 \sigma_z &= \frac{E}{1-\nu^2} [\varepsilon_z + \nu(\varepsilon_x + \varepsilon_y)] \\
 \tau_{xy} &= G\gamma_{xy}, \quad \tau_{yz} = G\gamma_{yz}, \quad \tau_{zx} = G\gamma_{zx}
 \end{aligned} \tag{2.165}$$

### 2.10.3 Plane Stress

When the elastic body is very thin and there are no loads applied in the direction parallel to the thickness, the state of stress in the body is said to be plane stress. A thin plate subjected to in-plane loading as shown in Figure 2.87 is an example of a plane stress problem. In this case,  $\sigma_z = \tau_{yz} = \tau_{zx} = 0$  and the constitutive relation for an isotropic continuum is expressed as

$$\begin{bmatrix} \sigma_x \\ \sigma_y \\ \sigma_{xy} \end{bmatrix} = \frac{E}{1-\nu^2} \begin{bmatrix} 1 & \nu & 0 \\ \nu & 1 & 0 \\ 0 & 0 & \frac{1-\nu}{2} \end{bmatrix} \begin{bmatrix} \varepsilon_x \\ \varepsilon_y \\ \gamma_{xy} \end{bmatrix} \tag{2.166}$$

### 2.10.4 Plane Strain

The state of plane strain occurs in members that are not free to expand in the direction perpendicular to the plane of the applied loads. Examples of some plane strain problems are retaining walls, dams, long cylinder, tunnels, etc. as shown in Figure 2.88. In these problems  $\varepsilon_z$ ,  $\gamma_{yz}$ , and  $\gamma_{zx}$  will vanish and hence,

$$\sigma_z = \nu(\sigma_x + \sigma_y)$$

The constitutive relations for an isotropic material are written as

$$\begin{bmatrix} \sigma_x \\ \sigma_y \\ \tau_{xy} \end{bmatrix} = \frac{E}{(1+\nu)(1-2\nu)} \begin{bmatrix} (1-\nu) & \nu & 0 \\ \nu & (1-\nu) & 0 \\ 0 & 0 & \frac{1-2\nu}{2} \end{bmatrix} \begin{bmatrix} \varepsilon_x \\ \varepsilon_y \\ \gamma_{xy} \end{bmatrix} \tag{2.167}$$

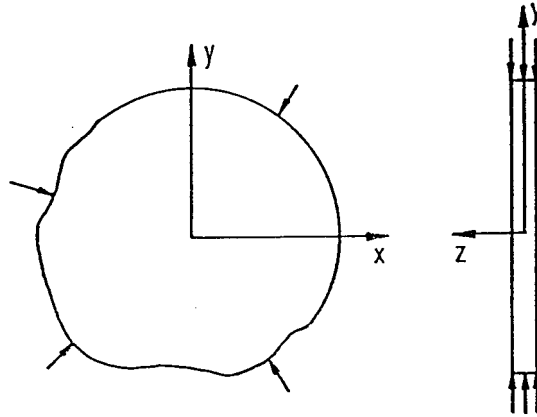


FIGURE 2.87: Plane-stress problem.

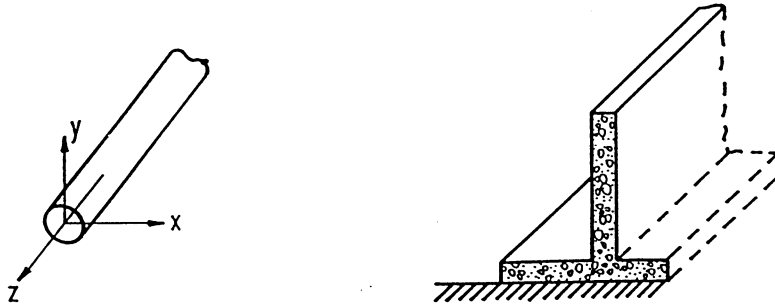


FIGURE 2.88: Practical examples of plane-strain problems.

### 2.10.5 Element Shapes and Discretization

The process of subdividing a continuum is an exercise of engineering judgement. The choice depends on the geometry of the body. A finite element generally has a simple one-, two-, or three-dimensional configuration. The boundaries of elements are often straight lines and the elements can be one, two, or three dimensional as shown in Figure 2.89. While subdividing the continuum, one has to decide the number, shape, size, and configuration of the elements in such a way that the original body is simulated as closely as possible. Nodes must be located in locations where abrupt changes in geometry, loading, and material properties occur. A node must be placed at the point of application of a concentrated load because all loads are converted into equivalent nodal-point loads.

It is easy to subdivide a continuum into a completely regular one having the same shape and size. But problems encountered in practice do not involve regular shape; they may have regions of steep gradients of stresses. A finer subdivision may be necessary in regions where stress concentrations are expected in order to obtain a useful approximate solution. Typical examples of mesh selection are shown in Figure 2.90.

### 2.10.6 Choice of Displacement Function

Selection of displacement function is the important step in the finite element analysis because it determines the performance of the element in the analysis. Attention must be paid to select a

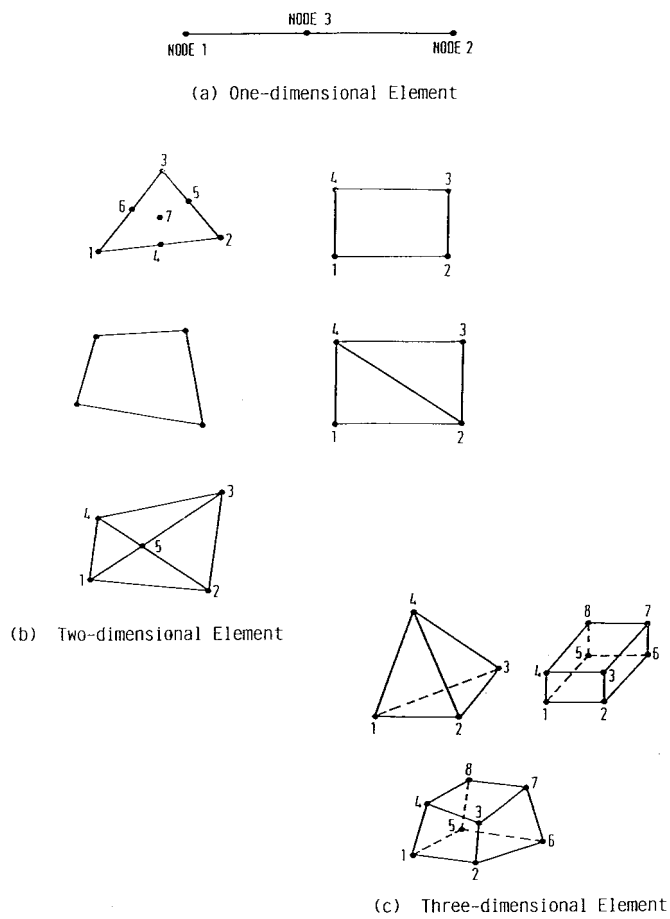


FIGURE 2.89: (a) One-dimensional element; (b) two-dimensional elements; (c) three-dimensional elements.

displacement function which (1) has the number of unknown constants as the total number of degrees of freedom of the element, (2) does not have any preferred directions, (3) allows the element to undergo rigid-body movement without any internal strain, (4) is able to represent states of constant stress or strain, and (5) satisfies the compatibility of displacements along the boundaries with adjacent elements. Elements that meet both the third and fourth requirements are known as *complete elements*.

A polynomial is the most common form of displacement function. Mathematics of polynomials are easy to handle in formulating the desired equations for various elements and convenient in digital computation. The degree of approximation is governed by the stage at which the function is truncated. Solutions closer to exact solutions can be obtained by including more number of terms. The polynomials are of the general form

$$w(x) = a_1 + a_2x + a_3x^2 + \dots a_{n+1}x^n \tag{2.168}$$

The coefficients 'a's are known as *generalized displacement amplitudes*. The general polynomial form for a two-dimensional problem can be given as

$$u(x, y) = a_1 + a_2x + a_3y + a_4x^2 + a_5xy + a_6y^2 + \dots a_my^n$$

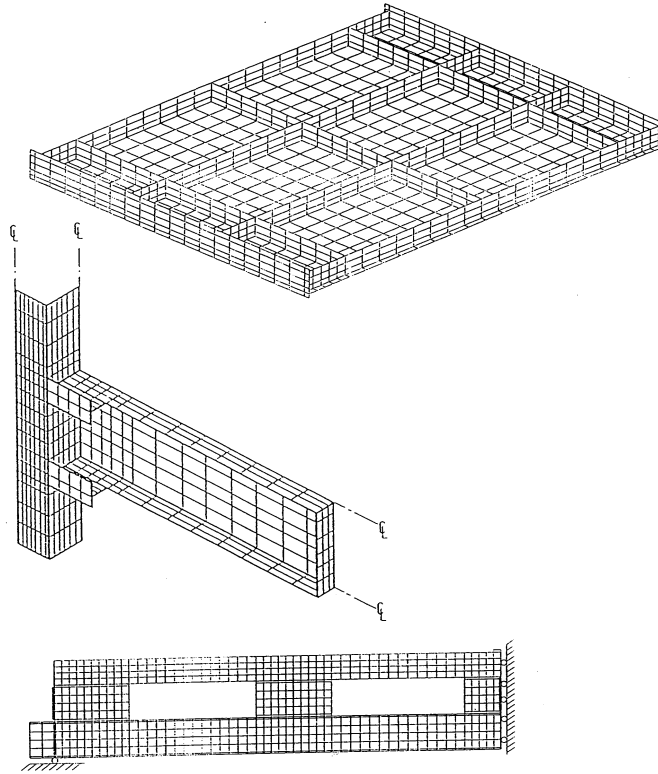


FIGURE 2.90: Typical examples of finite element mesh.

$$v(x, y) = a_{m+1} + a_{m+2}x + a_{m+3}y + a_{m+4}x^2 + a_{m+5}xy + a_{m+6}y^2 + \dots + a_{2m}y^n$$

in which

$$m = \sum_{i=1}^{n+1} i \quad (2.169)$$

These polynomials can be truncated at any desired degree to give constant, linear, quadratic, or higher order functions. For example, a linear model in the case of a two-dimensional problem can be given as

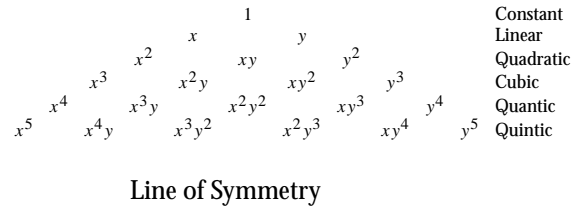
$$\begin{aligned} u &= a_1 + a_2x + a_3y \\ v &= a_4 + a_5x + a_6y \end{aligned} \quad (2.170)$$

A quadratic function is given by

$$\begin{aligned} u &= a_1 + a_2x + a_3y + a_4x^2 + a_5xy + a_6y^2 \\ v &= a_7 + a_8x + a_9y + a_{10}x^2 + a_{11}xy + a_{12}y^2 \end{aligned} \quad (2.171)$$

The Pascal triangle shown below can be used for the purpose of achieving isotropy, i.e., to avoid

displacement shapes that change with a change in local coordinate system.



### 2.10.7 Nodal Degrees of Freedom

The deformation of the finite element is specified completely by the nodal displacement, rotations, and/or strains which are referred to as *degrees of freedom*. Convergence, geometric isotropy, and potential energy function are the factors that determine the minimum number of degrees of freedom necessary for a given element. Additional degrees of freedom beyond the minimum number may be included for any element by adding secondary external nodes. Such elements with additional degrees of freedom are called higher order elements. The elements with more additional degrees of freedom become more flexible.

### 2.10.8 Isoparametric Elements

The scope of finite element analysis is also measured by the variety of element geometries that can be constructed. Formulation of element stiffness equations requires the selection of displacement expressions with as many parameters as there are node-point displacements. In practice, for planar conditions, only the four-sided (quadrilateral) element finds as wide an application as the triangular element. The simplest form of quadrilateral, the rectangle, has four node points and involves two displacement components at each point for a total of eight degrees of freedom. In this case one would choose four-term expressions for both  $u$  and  $v$  displacement fields. If the description of the element is expanded to include nodes at the mid-points of the sides, an eight-term expression would be chosen for each displacement component.

The triangle and rectangle can approximate the curved boundaries only as a series of straight line segments. A closer approximation can be achieved by means of *isoparametric* coordinates. These are non-dimensionalized curvilinear coordinates whose description is given by the same coefficients as are employed in the displacement expressions. The displacement expressions are chosen to ensure continuity across element interfaces and along supported boundaries, so that geometric continuity is ensured when the same forms of expressions are used as the basis of description of the element boundaries. The elements in which the geometry and displacements are described in terms of the same parameters and are of the same order are called *isoparametric elements*. The isoparametric concept enables one to formulate elements of any order which satisfy the completeness and compatibility requirements and which have isotropic displacement functions.

### 2.10.9 Isoparametric Families of Elements

#### Definitions and Justifications

For example, let  $u_i$  represent nodal displacements and  $x_i$  represent nodal  $x$ -coordinates. The interpolation formulas are

$$u = \sum_{i=1}^m N_i u_i \quad x = \sum_{i=1}^n N'_i x_i$$

where  $N_i$  and  $N$  are shape functions written in terms of the intrinsic coordinates. The value of  $u$  and the value of  $x$  at a point within the element are obtained in terms of nodal values of  $u_i$  and  $x_i$  from the above equations when the (intrinsic) coordinates of the internal point are given. Displacement components  $v$  and  $w$  in the  $y$  and  $z$  directions are treated in a similar manner.

The element is *isoparametric* if  $m = n$ ,  $N_i = N$ , and the same nodal points are used to define both element geometry and element displacement (Figure 2.91a); the element is *subparametric* if  $m > n$

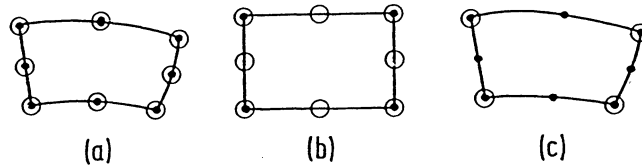


FIGURE 2.91: (a) Isoparametric element; (b) subparametric element; (c) superparametric element.

and the order of  $N_i$  is larger than  $N'_i$  (Figure 2.91b); the element is *superparametric* if  $m < n$  and the order of  $N_i$  is smaller than  $N'_i$  (Figure 2.91c). The isoparametric elements can correctly display rigid-body and constant-strain modes.

### 2.10.10 Element Shape Functions

The finite element method is not restricted to the use of linear elements. Most finite element codes, commercially available, allow the user to select between elements with linear or quadratic interpolation functions. In the case of quadratic elements, fewer elements are needed to obtain the same degree of accuracy in the nodal values. Also, the two-dimensional quadratic elements can be shaped to model a curved boundary. Shape functions can be developed based on the following properties: (1) each shape function has a value of one at its own node and is zero at each of the other nodes, (2) the shape functions for two-dimensional elements are zero along each side that the node does not touch, and (3) each shape function is a polynomial of the same degree as the interpolation equation. Shape function for typical elements are given in Figures 2.92a and b.

### 2.10.11 Formulation of Stiffness Matrix

It is possible to obtain all the strains and stresses within the element and to formulate the stiffness matrix and a consistent load matrix once the displacement function has been determined. This consistent load matrix represents the equivalent nodal forces which replace the action of external distributed loads.

As an example, let us consider a linearly elastic element of any of the types shown in Figure 2.93. The displacement function may be written in the form

$$\{f\} = [P]\{A\} \quad (2.172)$$

in which  $\{f\}$  may have two components  $\{u, v\}$  or simply be equal to  $w$ ,  $[P]$  is a function of  $x$  and  $y$  only, and  $\{A\}$  is the vector of undetermined constants. If Equation 2.172 is applied repeatedly to the nodes of the element one after the other, we obtain a set of equations of the form

$$\{D^*\} = [C]\{A\} \quad (2.173)$$

Element name	Configuration	DOF	Shape functions
Two-node linear element		+	$N_i = \frac{1}{2}(1 + \xi_i)$ $i = 1, 2$
Three-node parabolic element		+	$N_i = \frac{1}{2}\xi_i(1 + \xi_i); i = 1, 3$ $N_i = (1 - \xi^2); i = 2$
Four-node cubic element		+	$N_i = \frac{1}{16}(1 + \xi_i)(9\xi_i^2 - 1)$ $i = 1, 4$ $N_i = \frac{9}{16}(1 + 9\xi_i)(1 - \xi^2)$ $i = 2, 3$
Five-node quartic element		+	$N_i = \frac{1}{6}(1 + \xi_i)(4\xi_i(1 - \xi^2) + 3\xi_i)$ $i = 1, 5$ $N_i = 4\xi_i(1 - \xi^2)(1 + 4\xi_i)$ $i = 2, 4$ $N_3 = (1 - 4\xi^2)(1 - \xi^2)$

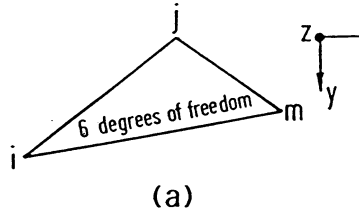
Figure 2.92a Shape functions for typical elements.

Element name	Configuration	DOF	Shape functions
Four-node plane quadrilateral		u, v	$N_i = \frac{1}{4}(1 + \xi_0)(1 + \eta_0);$ $i = 1, 2, 3, 4$
Eight-node plane quadrilateral		u, v	$N_i = \frac{1}{4}(1 + \xi_0)(1 + \eta_0)$ $(\xi_0 + \eta_0 - 1);$ $i = 1, 3, 5, 7$ $N_i = \frac{1}{2}(1 - \xi^2)(1 + \eta_0)$ $i = 2, 6$ $N_i = \frac{1}{2}(1 - \eta^2)(1 + \xi_0)$ $i = 4, 8$
Twelve-node plane quadrilateral		u, v	$N_i = \frac{1}{32}(1 + \xi_0)(1 + \eta_0)$ $(-10 + 9(\xi^2 + \eta^2))$ $i = 1, 4, 7, 10$ $N_i = \frac{9}{32}(1 + \xi_0)(1 + \eta^2)$ $(1 + 9\eta_0)$ $i = 5, 6, 11, 12$ $N_i = \frac{9}{32}(1 + \eta_0)(1 - \xi^2)$ $(1 + 9\xi_0)$ $i = 2, 3, 8, 9$

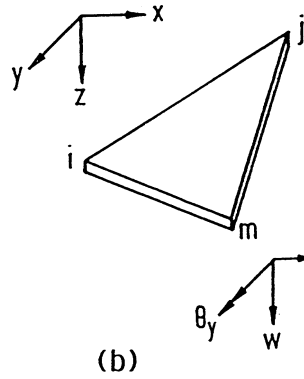
Figure 2.92b Shape functions for typical elements.

Serial no.	Element name	Configuration	DOF	Shape functions
4	Six-node linear Quadrilateral		u, v	$N_i = \frac{\xi_0}{4}(1 + \xi_0)(1 + \eta_0)$ $i = 1, 3, 4, 6$ $N_i = \frac{1}{2}(1 - \xi^2)(1 + \eta_0)$ $i = 2, 5$
5	Eight-node plane quadrilateral		u, v	$N_i = \frac{1}{32}(1 + \xi_0)(-1 + 9\xi^2)$ $(1 + \eta_0)$ $i = 1, 4, 5, 8$ $N_i = \frac{9}{32}(1 - \xi^2)(1 + 9\xi_0)$ $(1 + \eta_0)$ $i = 2, 3, 6, 7$
6	Seven-node plane quadrilateral		u, v	$N_1 = \frac{1}{4}(1 - \xi)(1 - \eta)$ $(1 + \xi + \eta)$ $N_2 = \frac{1}{2}(1 - \eta)(1 - \xi^2)$ $N_3 = \frac{\xi}{4}(1 + \xi)(1 - \eta)$ $N_4 = \frac{\xi}{4}(1 + \xi)(1 + \eta)$ $N_5 = \frac{1}{2}(1 + \eta)(1 - \xi^2)$ $N_6 = -\frac{1}{4}(1 - \xi)(1 + \eta)$ $(1 + \xi - \eta)$ $N_7 = \frac{1}{2}(1 - \xi)(1 - \eta^2)$

Figure 2.92b (Continued) Shape functions for typical elements.



(a)



(b)

FIGURE 2.93: Degrees of freedom. (a) Triangular plane-stress element; (b) triangular bending element.

in which  $\{D^*\}$  is the nodal parameters and  $[C]$  is the relevant nodal coordinates. The undetermined constants  $\{A\}$  can be expressed in terms of the nodal parameters  $\{D^*\}$  as

$$\{A\} = [C]^{-1}\{D^*\} \quad (2.174)$$

Substituting Equation 2.174 into Equation 2.172

$$\{f\} = [P][C]^{-1}\{D^*\} \quad (2.175)$$

Constructing the displacement function directly in terms of the nodal parameters one obtains

$$\{f\} = [L]\{D^*\} \quad (2.176)$$

where  $[L]$  is a function of both  $(x, y)$  and  $(x, y)_{i,j,m}$  given by

$$[L] = [P][C]^{-1} \quad (2.177)$$

The various components of strain can be obtained by appropriate differentiation of the displacement function. Thus,

$$\{\varepsilon\} = [B]\{D^*\} \quad (2.178)$$

$[B]$  is derived by differentiating appropriately the elements of  $[L]$  with respect to  $x$  and  $y$ . The stresses  $\{\sigma\}$  in a linearly elastic element are given by the product of the strain and a symmetrical elasticity matrix  $[E]$ . Thus,

$$\begin{aligned} \{\sigma\} &= [E]\{\varepsilon\} \\ \text{or } \{\sigma\} &= [E][B]\{D^*\} \end{aligned} \quad (2.179)$$

The stiffness and the consistent load matrices of an element can be obtained using the principle of minimum total potential energy. The potential energy of the external load in the deformed configuration of the element is written as

$$W = -\{D^*\}^T \{Q^*\} - \int_a \{f\}^T \{q\} da \quad (2.180)$$

In Equation 2.180  $\{Q^*\}$  represents concentrated loads at nodes and  $\{q\}$  represents the distributed loads per unit area. Substituting for  $\{f\}^T$  from Equation 2.176 one obtains

$$W = -\{D^*\}^T \{Q^*\} - \{D^*\}^T \int_a [L]^T \{q\} da \quad (2.181)$$

Note that the integral is taken over the area  $a$  of the element. The strain energy of the element integrated over the entire volume  $v$  is given as

$$U = \frac{1}{2} \int_v \{\varepsilon\}^T \{\sigma\} dv$$

Substituting for  $\{\varepsilon\}$  and  $\{\sigma\}$  from Equations 2.178 and 2.179, respectively,

$$U = \frac{1}{2} \{D^*\}^T \left( \int_v [B]^T [E] [B] dv \right) \{D^*\} \quad (2.182)$$

The total potential energy of the element is

$$V = U + W$$

or

$$\begin{aligned} V &= \frac{1}{2} \{D^*\}^T \left( \int_v [B]^T [E] [B] dv \right) \{D^*\} - \{D^*\}^T \{Q^*\} \\ &\quad - \{D^*\}^T \int_a [L]^T \{q\} da \end{aligned} \quad (2.183)$$

Using the principle of minimum total potential energy, we obtain

$$\left( \int_v [B]^T [E] [B] dv \right) \{D^*\} = \{Q^*\} + \int_a [L]^T \{q\} da$$

or

$$[K] \{D^*\} = \{F^*\} \quad (2.184)$$

where

$$[K] = \int_v [B]^T [E] [B] dv \quad (2.185a)$$

and

$$\{F^*\} = \{Q^*\} + \int_a [L]^T \{q\} da \quad (2.185b)$$

### 2.10.12 Plates Subjected to In-Plane Forces

The simplest element available in two-dimensional stress analysis is the triangular element. The stiffness and consistent load matrices of such an element will now be obtained by applying the equation derived in the previous section.

Consider the triangular element shown in Figure 2.93a. There are two degrees of freedom per node and a total of six degrees of freedom for the entire element. We can write

$$u = A_1 + A_2x + A_3y$$

and

$$v = A_4 + A_5x + A_6y$$

expressed as

$$\{f\} = \begin{Bmatrix} u \\ v \end{Bmatrix} = \begin{bmatrix} 1 & x & y & 0 & 0 & 0 \\ 0 & 0 & 0 & 1 & x & y \end{bmatrix} \begin{Bmatrix} A_1 \\ A_2 \\ A_3 \\ A_4 \\ A_5 \\ A_6 \end{Bmatrix} \quad (2.186)$$

or

$$\{f\} = [P]\{A\} \quad (2.187)$$

Once the displacement function is available, the strains for a plane problem are obtained from

$$\varepsilon_x = \frac{\partial u}{\partial x} \quad \varepsilon_y = \frac{\partial v}{\partial y}$$

and

$$\gamma_{xy} = \frac{\partial u}{\partial y} + \frac{\partial v}{\partial x}$$

The matrix  $[B]$  relating the strains to the nodal displacement  $\{D^*\}$  is thus given as

$$[B] = \frac{1}{2\Delta} \begin{bmatrix} b_i & 0 & b_j & 0 & b_m & 0 \\ 0 & c_i & 0 & c_j & 0 & c_m \\ c_i & b_j & c_j & b_j & c_m & b_m \end{bmatrix} \quad (2.188)$$

$b_i, c_i$ , etc. are constants related to the nodal coordinates only. The strains inside the element must all be constant and hence the name of the element.

For derivation of strain matrix, only isotropic material is considered. The plane stress and plane strain cases can be combined to give the following elasticity matrix which relates the stresses to the strains

$$[E] = \begin{bmatrix} C_1 & C_1C_2 & 0 \\ C_1C_2 & C_1 & 0 \\ 0 & 0 & C_{12} \end{bmatrix} \quad (2.189)$$

where

$$C_1 = \bar{E}/(1 - \nu^2) \quad \text{and} \quad C_2 = \nu \quad \text{for plane stress}$$

and

$$C_1 = \frac{\bar{E}(1 - \nu)}{(1 + \nu)(1 - 2\nu)} \quad \text{and} \quad C_2 = \frac{\nu}{(1 - \nu)} \quad \text{for plane strain}$$

and for both cases,

$$C_{12} = C_1(1 - C_2)/2$$





or

$$[K] = \bar{E}I \begin{bmatrix} \frac{12}{\ell^3} & & & & & \\ & \frac{6}{\ell^2} & & & & \\ & & \frac{4}{\ell} & & & \\ & -\frac{12}{\ell^3} & & & \frac{12}{\ell^3} & \\ & \frac{6}{\ell^2} & & & & \frac{4}{\ell} \\ & & \frac{2}{\ell} & & & \\ & & & & & & \text{symmetrical} \end{bmatrix} \quad (2.193)$$

### 2.10.14 Plates in Bendings—Rectangular Element

For the rectangular bending element shown in Figure 2.94 with three degrees of freedom (one

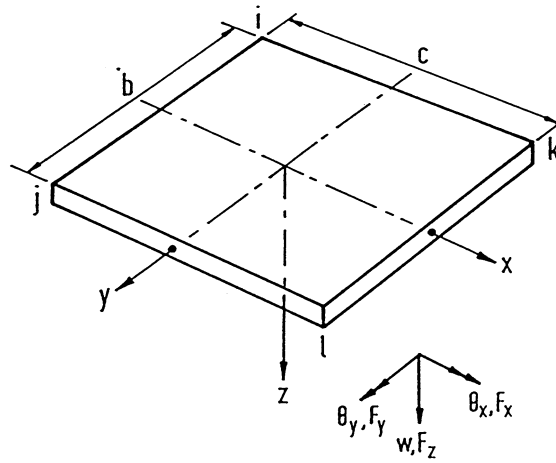


FIGURE 2.94: Rectangular bending element.

deflection and two rotations) at each node, the displacement function can be chosen as a polynomial with 12 undetermined constants as

$$\{f\} = w = A_1 + A_2x + A_3y + A_4x^2 + A_5xy + A_6y^2 + A_7x^3 + A_8x^2y + A_9xy^2 + A_{10}y^3 + A_{11}x^3y + A_{12}xy^3 \quad (2.194)$$

or

$$\{f\} = \{P\}\{A\}$$

The displacement parameter vector is defined as

$$\{D^*\} = \{w_i, \theta_{xi}, \theta_{yi} \mid w_j, \theta_{xj}, \theta_{yj} \mid w_k, \theta_{xk}, \theta_{yk} \mid w_l, \theta_{xl}, \theta_{yl}\}$$

where

$$\theta_x = \frac{\partial w}{\partial y} \quad \text{and} \quad \theta_y = -\frac{\partial w}{\partial x}$$

As in the case of beam it is possible to derive from Equation 2.194 a system of 12 equations relating  $\{D^*\}$  to constants  $\{A\}$ . The last equation

$$w = [L]_i \mid [L]_j \mid [L]_k \mid [L]_l \{D^*\} \quad (2.195)$$

The curvatures of the plate element at any point  $(x, y)$  are given by

$$\{\varepsilon\} = \left\{ \begin{array}{c} -\frac{\partial^2 w}{\partial x^2} \\ -\frac{\partial^2 w}{\partial y^2} \\ 2\frac{\partial^2 w}{\partial x \partial y} \end{array} \right\}$$

By differentiating Equation 2.195, we obtain

$$\{\varepsilon\} = [[B]_i | [B]_j | [B]_k | [B]_l] \{D^*\} \quad (2.196)$$

or

$$\{\varepsilon\} = \sum_{r=i,j,k,l} [B]_r \{D^*\}_r \quad (2.197)$$

where

$$[B]_r = \begin{bmatrix} -\frac{\partial^2}{\partial x^2} [L]_r \\ -\frac{\partial^2}{\partial y^2} [L]_r \\ 2\frac{\partial^2}{\partial x \partial y} [L]_r \end{bmatrix} \quad (2.198)$$

and

$$\{D^*\}_r = \{w_r, \theta_{xr}, \theta_{yr}\} \quad (2.199)$$

For an isotropic slab, the moment-curvature relationship is given by

$$\{\sigma\} = \{M_x M_y M_{xy}\} \quad (2.200)$$

$$[E] = N \begin{bmatrix} 1 & \nu & 0 \\ \nu & 1 & 0 \\ 0 & 0 & \frac{1-\nu}{2} \end{bmatrix} \quad (2.201)$$

and

$$N = \frac{\bar{E} h^3}{12(1-\nu^2)} \quad (2.202)$$

For orthotropic slabs with the principal directions of orthotropy coinciding with the  $x$  and  $y$  axes, no additional difficulty is experienced. In this case we have

$$[E] = \begin{bmatrix} D_x & D_1 & 0 \\ D_1 & D_y & 0 \\ 0 & 0 & D_{xy} \end{bmatrix} \quad (2.203)$$

where  $D_x$ ,  $D_1$ ,  $D_y$ , and  $D_{xy}$  are the orthotropic constants used by Timoshenko and Woinowsky-Krieger [56],

$$\left. \begin{array}{l} D_x = \frac{E_x h^3}{12(1-\nu_x \nu_y)} \\ D_y = \frac{E_y h^3}{12(1-\nu_x \nu_y)} \\ D_1 = \frac{\nu_x E_y h^3}{12(1-\nu_x \nu_y)} = \frac{\nu_y E_x h^3}{12(1-\nu_x \nu_y)} \\ D_{xy} = \frac{G h^3}{12} \end{array} \right\} \quad (2.204)$$

where  $E_x$ ,  $E_y$ ,  $\nu_x$ ,  $\nu_y$ , and  $G$  are the orthotropic material constants, and  $h$  is the plate thickness.

Unlike the strain matrix for the plane stress triangle (see Equation 2.188), the stress and strain in the present element vary with  $x$  and  $y$ . In general we calculate the stresses (moments) at the four corners. These can be expressed in terms of the nodal displacements by Equation 2.179 which, for an isotropic element, takes the form

$$\begin{aligned}
 & \left\{ \begin{array}{c} \{\sigma\}_i \\ \{\sigma\}_j \\ \{\sigma\}_k \\ \{\sigma\}_r \end{array} \right\} = \frac{N}{cb} \\
 & \left[ \begin{array}{cccccccccccc}
 6p^{-1} + 6vp & 4vc & -4b & -6vp & 2vc & 0 & -6p^{-1} & 0 & -2b & 0 & 0 & 0 \\
 6p + 6vp^{-1} & 4c & -4vb & -6p & 2c & 0 & -6vp^{-1} & 0 & -2vb & 0 & 0 & 0 \\
 -(1-v) & -(1-v)b & (1-v)c & (1-v) & 0 & -(1-v)c & (1-v) & (1-v)b & 0 & -(1-v) & 0 & 0 \\
 -6vp & -2vc & 0 & 6p^{-1} + 6vp & -4vc & -4b & 0 & 0 & 0 & -6p^{-1} & 0 & -2b \\
 -6p & -2c & 0 & 6p + 6vp^{-1} & -4c & -4vb & 0 & 0 & 0 & -6vp^{-1} & 0 & -2vb \\
 -(1-v) & 0 & (1-v)c & (1-v) & -(1-v)b & (1-v) & 0 & 0 & -(1-v) & (1-v)b & 0 & 0 \\
 -6p^{-1} & 0 & 2b & 0 & 0 & 0 & 6p^{-1} + 6vp & 4vc & 4b & -6vp & 2vc & 0 \\
 -6vp^{-1} & 0 & 2b & 0 & 0 & 0 & 6p + 6vp^{-1} & 4c & 4vb & -6p & 2c & 0 \\
 -(1-v) & -(1-v)b & 0 & (1-v) & 0 & 0 & (1-v) & (1-v)b & (1-v)c & -(1-vv) & 0 & -(1-v)c \\
 0 & 0 & 0 & -6p^{-1} & 0 & 2b & -6vp & -2vc & 0 & 6p^{-1} + 6vp & -4vv & 4b \\
 0 & 0 & 0 & -6vp^{-1} & 0 & 2vb & -6p & -2c & 0 & 6p + 6vp^{-1} & -4c & 4vb \\
 -(1-v) & 0 & 0 & (1-v) & -(1-v)b & 0 & (1-v) & 0 & (1-v)c & -(1-v) & (1-v)b & -(1-v)c
 \end{array} \right] \\
 & \left\{ \begin{array}{c} \{D^*\}_i \\ \{D^*\}_j \\ \{D^*\}_k \\ \{D^*\}_r \end{array} \right\}
 \end{aligned}$$

(2.205)

where  $p = c/b$ .

The stiffness matrix corresponding to the 12 nodal coordinates can be calculated by

$$[K] = \int_{-b/2}^{b/2} \int_{-c/2}^{c/2} [B]^T [E] [B] dx dy \quad (2.206)$$

For an isotropic element, this gives

$$[K^*] = \frac{N}{15cb} [T] [\bar{k}] [T] \quad (2.207)$$

where

$$[T] = \begin{bmatrix} [T_s] \text{ Submatrices not} \\ [T_s] \text{ shown are} \\ [T_s] \text{ zero} \\ [T_s] \end{bmatrix} \quad (2.208)$$

$$[T_s] = \begin{bmatrix} 1 & 0 & 0 \\ 0 & b & 0 \\ 0 & 0 & c \end{bmatrix} \quad (2.209)$$

and  $[\bar{k}]$  is given by the matrix shown in Equation 2.210.



If the element is subjected to a uniform load in the  $z$  direction of intensity  $q$ , the consistent load vector becomes

$$\{Q_q^*\} = q \int_{-b/2}^{b/2} \int_{-c/2}^{c/2} [L]^T dx dy \quad (2.211)$$

where  $\{Q_q^*\}$  are 12 forces corresponding to the nodal displacement parameters. Evaluating the integrals in this equation gives

$$\{Q_q^*\} = qcb \begin{pmatrix} 1/4 \\ b/24 \\ -c/24 \\ - \\ - \\ 1/4 \\ -b/24 \\ -c/24 \\ - \\ - \\ 1/4 \\ b/24 \\ c/24 \\ - \\ - \\ 1/4 \\ -b/24 \\ c/24 \end{pmatrix} \quad (2.212)$$

More details on the Finite Element Method can be found in [23] and [27].

## 2.11 Inelastic Analysis

### 2.11.1 An Overall View

Inelastic analysis can be generalized into two main approaches. The first approach is known as *plastic hinge analysis*. The analysis assumes that structural elements remain elastic except at critical regions where zero-length [plastic hinges](#) are allowed to form. The second approach is known as *plastic-zone analysis*. The analysis follows explicitly the gradual spread of yielding throughout the volume of the structure. Material yielding in the member is modeled by discretization of members into several beam-column elements, and subdivision of the cross-sections into many “fibers”. The plastic-zone analysis can predict accurately the inelastic response of the structure. However, the plastic hinge analysis is considered to be more efficient than the plastic-zone analysis since it requires, in most cases, one beam-column element per member to capture the stability of column members subject to end loading.

If geometric nonlinear effect is not considered, the plastic hinge analysis predicts the maximum load of the structure corresponding to the formation of a plastic collapse mechanism [16]. First-order plastic hinge analysis is finding considerable application in continuous beams and low-rise building frames where members are loaded primarily in flexure. For tall building frames and for frames with slender columns subjected to sidesway, the interaction between structural inelasticity and instability may lead to collapse prior to the formation of a plastic mechanism [54]. If equilibrium equations are formulated based on deformed geometry of the structure, the analysis is termed *second order*. The need for a [second-order analysis](#) of steel frame is increasing in view of the American Specifications [3] which give explicit permission for the engineer to compute load effects from a direct second-order analysis.

This section presents the virtual work principle to explain the fundamental theorems of plastic hinge analysis. Simple and approximate techniques of practical [plastic analysis](#) methods are then

introduced. The concept of hinge-by-hinge analysis is presented. The more advanced topics such as second-order elastic plastic hinge, refined plastic hinge analysis, and plastic zone analysis are covered in Section 2.12.

### 2.11.2 Ductility

Plastic analysis is strictly applicable for materials that can undergo large deformation without fracture. Steel is one such material with an idealized stress-strain curve as shown in Figure 2.95. When steel is

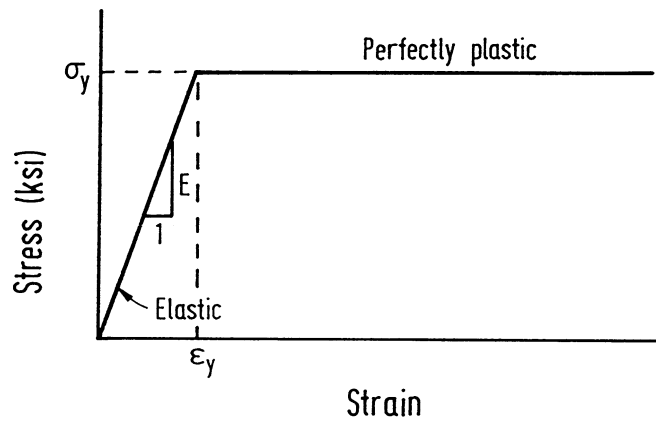


FIGURE 2.95: Idealized stress-strain curve.

subjected to tensile force, it will elongate elastically until the yield stress is reached. This is followed by an increase in strain without much increase in stress. Fracture will occur at very large deformation. This material idealization is generally known as *elastic-perfectly plastic* behavior. For a compact section, the attainment of initial yielding does not result in failure of a section. The compact section will have reserved plastic strength that depends on the shape of the cross-section. The capability of the material to deform under constant load without decrease in strength is the *ductility* characteristic of the material.

### 2.11.3 Redistribution of Forces

The benefit of using a ductile material can be demonstrated from an example of a three-bar system shown in Figure 2.96. From the equilibrium condition of the system,

$$2T_1 + T_2 = P \quad (2.213)$$

Assuming elastic stress-strain law, the displacement and force relationship of the bars may be written as:

$$\delta = \frac{T_1 L_1}{AE} = \frac{T_2 L_2}{AE} \quad (2.214)$$

Since  $L_2 = L_1/2 = L/2$ , Equation 2.214 can be written as

$$T_1 = \frac{T_2}{2} \quad (2.215)$$

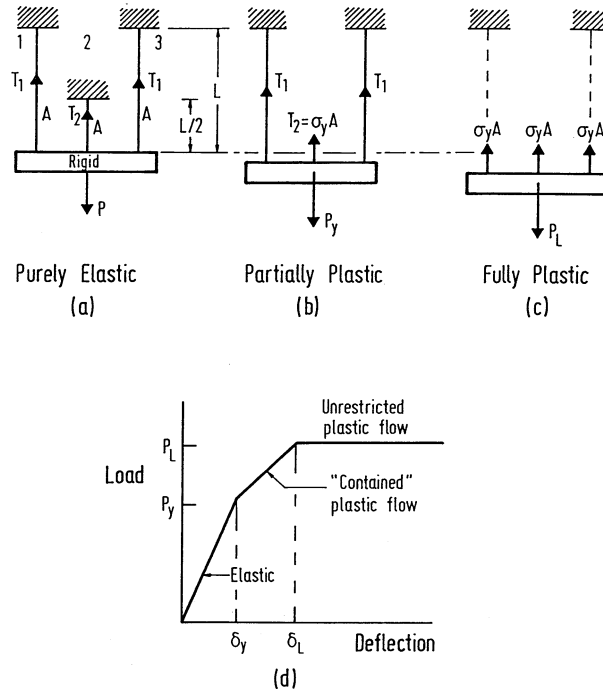


FIGURE 2.96: Force redistribution in a three-bar system: (a) elastic, (b) partially yielded, (c) fully plastic, (d) load-deflection curve.

where  $T_1$  and  $T_2$  are the tensile forces in the rods,  $L_1$  and  $L_2$  are length of the rods,  $A$  is a cross-section area, and  $E$  = elastic modulus. Solving Equations 2.214 and 2.215 for  $T_2$ :

$$T_2 = \frac{P}{2} \quad (2.216)$$

The load at which the structure reaches the first yield (in Figure 2.96b) is determined by letting  $T_2 = \sigma_y A$ . From Equation 2.216:

$$P_y = 2T_2 = 2\sigma_y A \quad (2.217)$$

The corresponding displacement at first yield is

$$\delta_y = \varepsilon_y L = \frac{\sigma_y L}{2E} \quad (2.218)$$

After Bar 2 is yielded, the system continues to take additional load until all three bars reach their maximum strength of  $\sigma_y A$ , as shown in Figure 2.96c. The plastic limit load of the system is thus written as

$$P_L = 3\sigma_y A \quad (2.219)$$

The process of successive yielding of bars in this system is known as inelastic redistribution of forces. The displacement at the incipient of collapse is

$$\delta_L = \varepsilon_y L = \frac{\sigma_y L}{E} \quad (2.220)$$

Figure 2.96d shows the load-displacement behavior of the system when subjected to increasing force. As load increases, Bar 2 will reach its maximum strength first. As it yielded, the force in the

member remains constant, and additional loads on the system are taken by the less critical bars. The system will eventually fail when all three bars are fully yielded. This is based on an assumption that material strain-hardening does not take place.

### 2.11.4 Plastic Hinge

A plastic hinge is said to form in a structural member when the cross-section is fully yielded. If material strain hardening is not considered in the analysis, a fully yielded cross-section can undergo indefinite rotation at a constant restraining plastic moment  $M_p$ .

Most of the plastic analyses assume that plastic hinges are concentrated at zero length plasticity. In reality, the yield zone is developed over a certain length, normally called the *plastic hinge length*, depending on the loading, boundary conditions, and geometry of the section. The hinge lengths of beams ( $\Delta L$ ) with different support and loading conditions are shown in Figures 2.97a, b, and c. Plastic hinges are developed first at the sections subjected to the greatest curvature. The possible

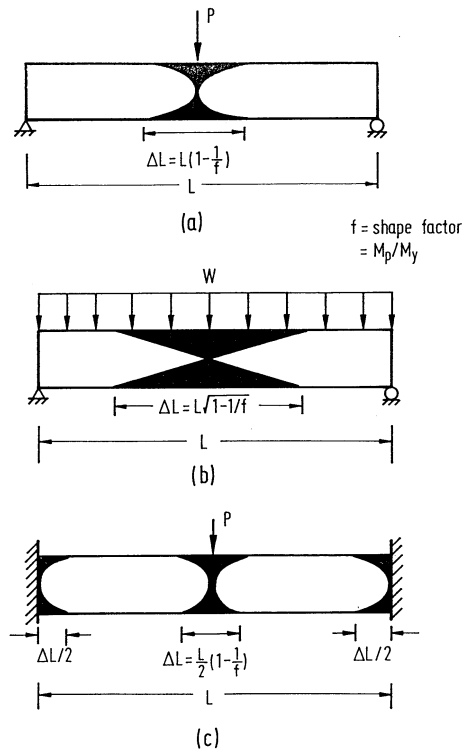


FIGURE 2.97: Hinge lengths of beams with different support and loading conditions.

locations for plastic hinges to develop are at the points of concentrated loads, at the intersections of members involving a change in geometry, and at the point of zero shear for member under uniform distributed load.

### 2.11.5 Plastic Moment

A knowledge of full plastic moment capacity of a section is important in plastic analysis. It forms the basis for limit load analysis of the system. Plastic moment is the moment resistance of a fully yielded cross-section. The cross-section must be fully compact in order to develop its plastic strength. The component plates of a section must not buckle prior to the attainment of full moment capacity.

The plastic moment capacity,  $M_p$ , of a cross-section depends on the material yield stress and the section geometry. The procedure for the calculation of  $M_p$  may be summarized in the following two steps:

1. The plastic neutral axis of a cross-section is located by considering equilibrium of forces normal to the cross-section. Figure 2.98a shows a cross-section of arbitrary shape subjected to increasing moment. The plastic neutral axis is determined by equating the force

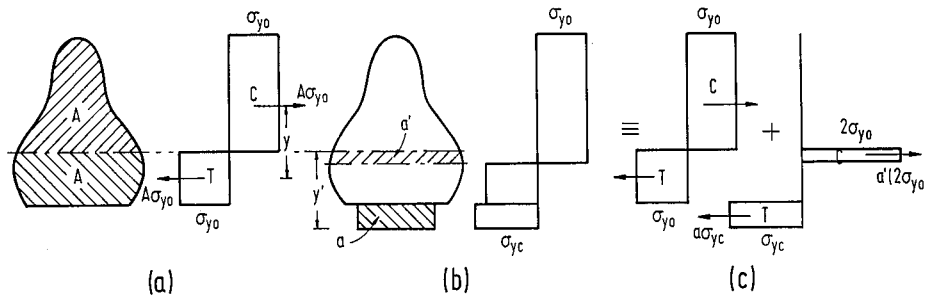


FIGURE 2.98: Cross-section of arbitrary shape subjected to bending.

in compression ( $C$ ) to that in tension ( $T$ ). If the entire cross-section is made of the same material, the plastic neutral axis can be determined by dividing the cross-sectional area into two equal parts. If the cross-section is made of more than one type of material, the plastic neutral axis must be determined by summing the normal force and letting the force equal zero.

2. The plastic moment capacity is determined by obtaining the moment generated by the tensile and compressive forces.

Consider an arbitrary section with area  $2A$  and with one axis of symmetry of which the section is strengthened by a cover plate of area " $a$ " as shown in Figure 2.98b. Further assume that the yield strength of the original section and the cover plate is  $\sigma_{y0}$  and  $\sigma_{yc}$ , respectively. At the full plastic state, the total axial force acting on the cover plate is  $a\sigma_{yc}$ . In order to maintain equilibrium of force in axial direction, the plastic neutral axis must shift down from its original position by  $a'$ , i.e.,

$$a' = \frac{a\sigma_{yc}}{2\sigma_{y0}} \quad (2.221)$$

The resulting plastic capacity of the "built-up" section may be obtained by summing the full plastic moment of the original section and the moment contribution by the cover plate. The additional capacity is equal to the moment caused by the cover plate force  $a\sigma_{yc}$  and a force due to the fictitious stress  $2\sigma_{y0}$  acting on the area  $a'$  resulting from the shifting of plastic neutral axis from tension zone to compression zone as shown in Figure 2.98c.

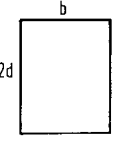
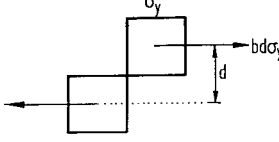
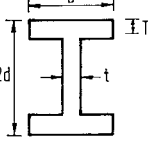
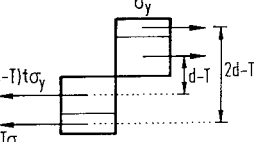
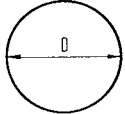
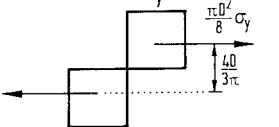
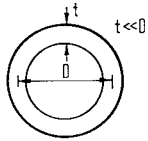
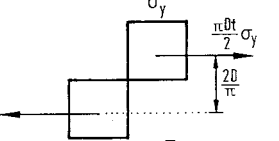
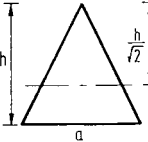
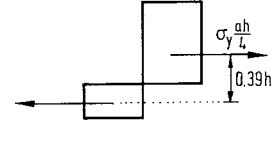
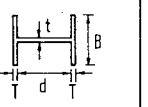
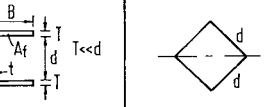
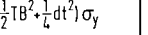
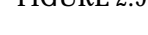
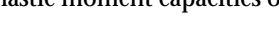
Cross-section	Stress Distribution	Plastic Moment, $M_p$
		$bd^2\sigma_y$
		$bT(2d-T)\sigma_y + (d-T)^2t\sigma_y$
		$\frac{1}{6}D^3\sigma_y$
		$tD^2\sigma_y$
		$0.0975ah^2\sigma_y$
		$(\frac{1}{2}tB^2 + \frac{1}{6}dt^2)\sigma_y$
		$\frac{d}{4}(A_w + 4A_f)\sigma_y$
		$\frac{d^3}{3\sqrt{2}}\sigma_y$
		$\frac{bd^3}{12}\sigma_y$

FIGURE 2.99: Plastic moment capacities of sections.

Figure 2.99 shows the computation of plastic moment capacity of several shapes of cross-section. Based on the principle developed in this section, the plastic moment capacities of typical cross-sections may be generated. Additional information for sections subjected to combined bending, torsion, shear, and axial load can be found in Mrazik et al. [43].

### 2.11.6 Theory of Plastic Analysis

There are two main assumptions for first-order plastic analysis:

1. The structure is made of ductile material that can undergo large deformations beyond elastic limit without fracture or buckling.
2. The deflections of the structure under loading are small so that second-order effects can be ignored.

An “exact” plastic analysis solution must satisfy three basic conditions. They are *equilibrium*, *mechanism*, and *plastic moment* conditions. The plastic analysis disregards the continuity condition as required by the elastic analysis of indeterminate structures. The formation of plastic hinge in members leads to discontinuity of slope. If sufficient plastic hinges are formed to allow the structure to deform into a mechanism, it is called a *mechanism* condition. Since plastic analysis utilizes the limit of resistance of the member’s plastic strength, the plastic moment condition is required to ensure that the resistance of the cross-sections is not violated anywhere in the structure. Lastly, the equilibrium condition, which is the same condition to be satisfied in elastic analysis, requires that the sum of all applied forces and reactions should be equal to zero, and all internal forces should be self-balanced.

When all the three conditions are satisfied, then the resulting plastic analysis for limiting load is the “correct” limit load. The collapse loads for simple structures such as beams and **portal frames** can be solved easily using a direct approach or through visualization of the formation of “correct” collapse mechanism. However, for more complex structures, the exact solution satisfying all three conditions may be difficult to predict. Thus, simple techniques using approximate methods of analysis are often used to assess these solutions. These techniques, called equilibrium and mechanism methods, will be discussed in the subsequent sections.

#### Principle of Virtual Work

The virtual work principle may be applied to relate a system of forces in equilibrium to a system of compatible displacements. For example, if a structure in equilibrium is given a set of small compatible displacement, then the work done by the external loads on these external displacements is equal to the work done by the internal forces on the internal deformation. In plastic analysis, internal deformations are assumed to be concentrated at plastic hinges. The virtual work equation for hinged structures can be written in an explicit form as

$$\sum P_i \delta_j = \sum M_i \theta_j \quad (2.222)$$

where  $P_i$  is an external load and  $M_i$  is an internal moment at a hinge location. Both the  $P_i$  and  $M_i$  constitute an equilibrium set and they must be in equilibrium.  $\delta_j$  are the displacements under the point loads  $P_i$  and in the direction of the loads.  $\theta_j$  are the plastic hinge rotations under the moment  $M_i$ . Both  $\delta_j$  and  $\theta_j$  constitute a displacement set and they must be compatible with each other.

#### Lower Bound Theorem

For a given structure, if there exists any distribution of bending moments in the structure that satisfies both the equilibrium and plastic moment conditions, then the load factor,  $\lambda_L$ , computed from this moment diagram must be equal to or less than the collapse load factor,  $\lambda_c$ , of the structure. Lower bound theorem provides a safe estimate of the collapse limit load, i.e.,  $\lambda_L \leq \lambda_c$ .

### Upper Bound Theorem

For a given structure subjected to a set of applied loads, a load factor,  $\lambda_u$ , computed based on an assumed collapse mechanism must be greater than or equal to the true collapse load factor,  $\lambda_c$ . Upper bound theorem, which uses only the mechanism condition, over-estimates or is equal to the collapse limit load, i.e.,  $\lambda_u \geq \lambda_c$ .

### Uniqueness Theorem

A structure at collapse has to satisfy three conditions. First, a sufficient number of plastic hinges must be formed to turn the structure, or part of it, into a mechanism; this is called the mechanism condition. Second, the structure must be in equilibrium, i.e., the bending moment distribution must satisfy equilibrium with the applied loads. Finally, the bending moment at any cross-section must not exceed the full plastic value of that cross-section; this is called the plastic moment condition. The theorem simply implies that the collapse load factor,  $\lambda_c$ , obtained from the three basic conditions (mechanism, equilibrium, and plastic moment) has a unique value.

The proof of the three theorems can be found in Chen and Sohal [16]. A useful corollary of the lower bound theorem is that if at a load factor,  $\lambda$ , it is possible to find a bending moment diagram that satisfies both the equilibrium and moment conditions but not necessarily the mechanism condition, then the structure will not collapse at that load factor unless the load happens to be the collapse load. A corollary of the upper bound theorem is that the true load factor at collapse is the smallest possible one that can be determined from a consideration of all possible mechanisms of collapse. This concept is very useful in finding the collapse load of the system from various combinations of mechanisms. From these theorems, it can be seen that the lower bound theorem is based on the equilibrium approach while the upper bound technique is based on the mechanism approach. These two alternative approaches to an exact solution, called the *equilibrium method* and the *mechanism method*, will be discussed in the sections that follow.

#### 2.11.7 Equilibrium Method

The equilibrium method, which employs the lower bound theorem, is suitable for the analysis of continuous beams and frames in which the structural redundancies are not exceeding two. The procedures for obtaining the equilibrium equations of a statically indeterminate structure and to evaluate its plastic limit load are as follows:

*To obtain the equilibrium equations of a statically indeterminate structure:*

1. Select the redundant(s).
2. Free the redundants and draw a moment diagram for the determinate structure under the applied loads.
3. Draw a moment diagram for the structure due to the redundant forces.
4. Superimpose the moment diagrams in Steps 2 and 3.
5. Obtain the maximum moment at critical sections of the structure utilizing the moment diagram in Step 4.

*To evaluate the plastic limit load of the structure:*

6. Select value(s) of redundant(s) such that the plastic moment condition is not violated at any section in the structure.
7. Determine the load corresponding to the selected redundant(s).

8. Check for the formation of a mechanism. If a collapse mechanism condition is met, then the computed load is the exact plastic limit load. Otherwise, it is a lower bound solution.
9. Adjust the redundant(s) and repeat Steps 6 to 9 until the exact plastic limit load is obtained.

**EXAMPLE 2.11:** Continuous Beam

Figure 2.100a shows a two-span continuous beam which is analyzed using the equilibrium method. The plastic limit load of the beam is calculated based on the step-by-step procedure described in the

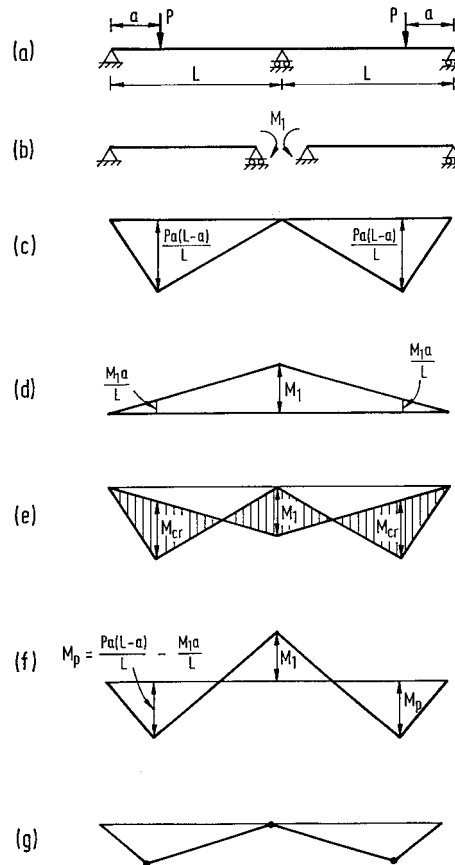


FIGURE 2.100: Analysis of a two-span continuous using the equilibrium method.

previous section as follows:

1. Select the redundant force as  $M_1$  which is the bending moment at the intermediate support, as shown in Figure 2.100b.
2. Free the redundants and draw the moment diagram for the determinate structure under the applied loads, as shown in Figure 2.100c.

3. Draw the moment diagram for the structure due to the redundant moment  $M_1$  as shown in Figure 2.100d.
4. Superimpose the moment diagrams in Figures 2.100c and d. The results are shown in Figure 2.100e. The moment diagram in Figure 2.100e is redrawn on a single straight base line. The critical moment in the beam is

$$M_{cr} = \frac{Pa(L-a)}{L} - \frac{M_1a}{L} \quad (2.223)$$

The maximum moment at the critical sections of the structure utilizing the moment diagram in Figure 2.100e is obtained. By letting  $M_{cr} = M_p$ , the resulting moment distribution is shown in Figure 2.100f.

5. A lower bound solution may be obtained by selecting a value of redundant moment  $M_1$ . For example, if  $M_1 = 0$  is selected, the moment diagram is reduced to that shown in Figure 2.100c. By equating the maximum moment in the diagram to the plastic moment,  $M_p$ , we have

$$M_{cr} = \frac{Pa(L-a)}{L} = M_p \quad (2.224)$$

which gives  $P = P_1$  as

$$P_1 = \frac{M_p L}{a(L-a)} \quad (2.225)$$

The moment diagram in Figure 2.100c shows a plastic hinge formed at each span. Since two plastic hinges in each span are required to form a plastic mechanism, the load  $P_1$  is a lower bound solution. However, if the redundant moment  $M_1$  is set equal to the plastic moment  $M_p$ , and letting the maximum moment in Figure 2.100f be equal to the plastic moment, we have

$$M_{cr} = \frac{Pa(L-a)}{L} - \frac{M_p a}{L} = M_p \quad (2.226)$$

which gives  $P = P_2$  as

$$P_2 = \frac{M_p(L+a)}{a(L-a)} \quad (2.227)$$

6. Since a sufficient number of plastic hinges has formed in the beams (Figure 2.100g) to arrive at a collapse mechanism, the computed load,  $P_2$ , is the exact plastic limit load.

### EXAMPLE 2.12: Portal Frame

A pinned-base rectangular frame subjected to vertical load  $V$  and horizontal load  $H$  is shown in Figure 2.101a. All the members of the frame,  $AB$ ,  $BD$ , and  $DE$  are made of the same section with moment capacity  $M_p$ . The objective is to determine the limit value of  $H$  if the frame's width-to-height ratio  $L/h$  is 1.0.

*Procedure:* The frame has one degree of redundancy. The redundancy for this structure can be chosen as the horizontal reaction at  $E$ . Figures 2.101b and c show the resulting determinate frame loaded by the applied loads and redundant force. The moment diagrams corresponding to these two loading

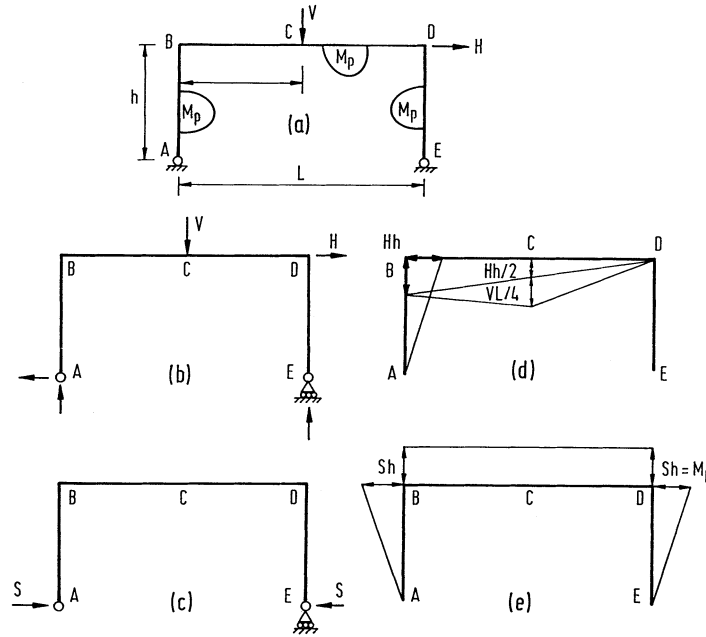


FIGURE 2.101: Analysis of portal frame using the equilibrium method.

conditions are shown in Figures 2.101d and e.

The horizontal reaction  $S$  should be chosen in such a manner that all three conditions (equilibrium, plastic moment, and mechanism) are satisfied. Formation of two plastic hinges is necessary to form a mechanism. The plastic hinges may be formed at  $B$ ,  $C$ , and  $D$ . Assuming that a plastic hinge is formed at  $D$ , as shown in Figure 2.101e, we have

$$S = \frac{M_p}{h} \quad (2.228)$$

Corresponding to this value of  $S$ , the moments at  $B$  and  $C$  can be expressed as

$$M_B = Hh - M_p \quad (2.229)$$

$$M_C = \frac{Hh}{2} + \frac{VL}{4} - M_p \quad (2.230)$$

The condition for the second plastic hinge to form at  $B$  is  $|M_B| > |M_C|$ . From Equations 2.229 and 2.230 we have

$$Hh - M_p > \frac{Hh}{2} + \frac{VL}{4} - M_p \quad (2.231)$$

and

$$\frac{V}{H} < \frac{h}{L} \quad (2.232)$$

The condition for the second plastic hinge to form at  $C$  is  $|M_C| > |M_B|$ . From Equations 2.229 and 2.230 we have

$$Hh - M_p < \frac{Hh}{2} + \frac{VL}{4} - M_p \quad (2.233)$$

and

$$\frac{V}{H} > \frac{h}{L} \quad (2.234)$$

For a particular combination of  $V$ ,  $H$ ,  $L$ , and  $h$ , the collapse load for  $H$  can be calculated.

(a) When  $L/h = 1$  and  $V/H = 1/3$ , we have

$$M_B = Hh - M_p \quad (2.235)$$

$$M_C = \frac{Hh}{2} + \frac{Hh}{12} - M_p = \frac{7}{12}Hh - M_p \quad (2.236)$$

Since  $|M_B| > |M_C|$ , the second plastic hinge will form at  $B$ , and the corresponding value for  $H$  is

$$H = \frac{2M_p}{h} \quad (2.237)$$

(b) When  $L/h = 1$  and  $V/H = 3$ , we have

$$M_B = Hh - M_p \quad (2.238)$$

$$M_C = \frac{Hh}{2} + \frac{3}{4}Hh - M_p = \frac{5}{4}Hh - M_p \quad (2.239)$$

Since  $|M_C| > |M_B|$ , the second plastic hinge will form at  $C$ , and the corresponding value for  $H$  is

$$H = \frac{1.6M_p}{h} \quad (2.240)$$

### 2.11.8 Mechanism Method

This method, which is based on the upper bound theorem, states that the load computed on the basis of an assumed failure mechanism is never less than the exact plastic limit load of a structure. Thus, it always predicts the upper bound solution of the collapse limit load. It can also be shown that the minimum upper bound is the limit load itself. The procedure for using the mechanism method has the following two steps:

1. Assume a failure mechanism and form the corresponding work equation from which an upper bound value of the plastic limit load can be estimated.
2. Write the equilibrium equations for the assumed mechanism and check the moments to see whether the plastic moment condition is met everywhere in the structure.

To obtain the true limit load using the mechanism method, it is necessary to determine every possible collapse mechanism of which some are the combinations of a certain number of independent mechanisms. Once the independent mechanisms have been identified, a work equation may be established for each combination and the corresponding collapse load is determined. The lowest load among those obtained by considering all the possible combination of independent mechanisms is the correct plastic limit load.

#### Number of Independent Mechanisms

The number of possible independent mechanisms  $n$ , for a structure, can be determined from

$$n = N - R \quad (2.241)$$

where  $N$  is the number of critical sections at which plastic hinges might form, and  $R$  is the degrees of redundancy of the structure.

Critical sections generally occur at the points of concentrated loads, at joints where two or more members are meeting at different angles, and at sections where there is an abrupt change in section

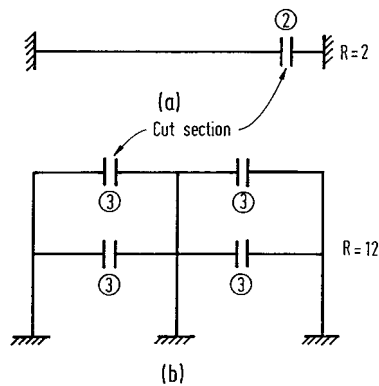


FIGURE 2.102: Number of redundants in (a) a beam and (b) a frame.

geometries or properties. To determine the number of redundant  $R$ s of a structure, it is necessary to free sufficient supports or restraining forces in structural members so that the structure becomes an assembly of several determinate sub-structures.

Figure 2.102 shows two examples. The cuts that are made in each structure reduce the structural members to either cantilevers or simply supported beams. The fixed-end beam requires a shear force and a moment to restore continuity at the cut section, and thus  $R = 2$ . For the two-story frame, an axial force, shear, and moment are required at each cut section for full continuity, and thus  $R = 12$ .

### Types of Mechanism

Figure 2.103a shows a frame structure subjected to a set of loading. The frame may fail by different types of collapse mechanisms dependent on the magnitude of loading and the frame's configurations. The collapse mechanisms are:

- (a) *Beam Mechanism*: Possible mechanisms of this type are shown in Figure 2.103b.
- (b) *Panel Mechanism*: The collapse mode is associated with sidesway as shown in Figure 2.103c.
- (c) *Gable Mechanism*: The collapse mode is associated with the spreading of column tops with respect to the column bases as shown in Figure 2.103d.
- (d) *Joint Mechanism*: The collapse mode is associated with the rotation of joints of which the adjoining members developed plastic hinges and deformed under an applied moment as shown in Figure 2.103e.
- (e) *Combined Mechanism*: It can be a partial collapse mechanism as shown in Figure 2.103f or it may be a complete collapse mechanism as shown in Figure 2.103g.

The principal rule for combining independent mechanisms is to obtain a lower value of collapse load. The combinations are selected in such a way that the external work becomes a maximum and the internal work becomes a minimum. Thus, the work equation would require that the mechanism involve as many applied loads as possible and at the same time to eliminate as many plastic hinges as possible. This procedure will be illustrated in the following example.

### EXAMPLE 2.13: Rectangular Frame

A fixed-end rectangular frame has a uniform section with  $M_p = 20$  and carries the load shown in Figure 2.104. Determine the value of load ratio  $\lambda$  at collapse.

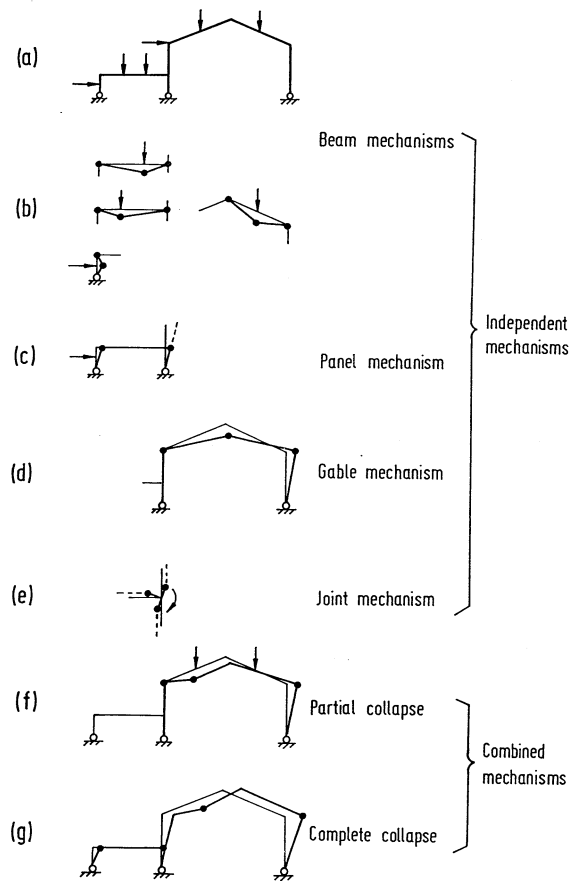


FIGURE 2.103: Typical plastic mechanisms.

**Solution**

Number of possible plastic hinges	$N = 5$
Number of redundancies	$R = 3$
Number of independent mechanisms	$N - R = 2.$

The two independent mechanisms are shown in Figures 2.104b and c, and the corresponding work equations are

Panel mechanism	$20\lambda = 4(20) = 80$	$\Rightarrow \lambda = 4$
Beam mechanism	$30\lambda = 4(20) = 80$	$\Rightarrow \lambda = 2.67$

The combined mechanisms are now examined to see whether they will produce a lower  $\lambda$  value. It is observed that only one combined mechanism is possible. The mechanism is shown in Figure 2.104c involving cancellation of a plastic hinge at B. The calculation of the limit load is described below:

Panel mechanism	$20\lambda = 4(20)$
Beam mechanism	$30\lambda = 4(20)$
Addition	$50\lambda = 8(20)$
Cancellation of plastic hinge	$-2(20)$
Combined mechanism	$50\lambda = 6(20)$
	$\Rightarrow \lambda = 2.4$

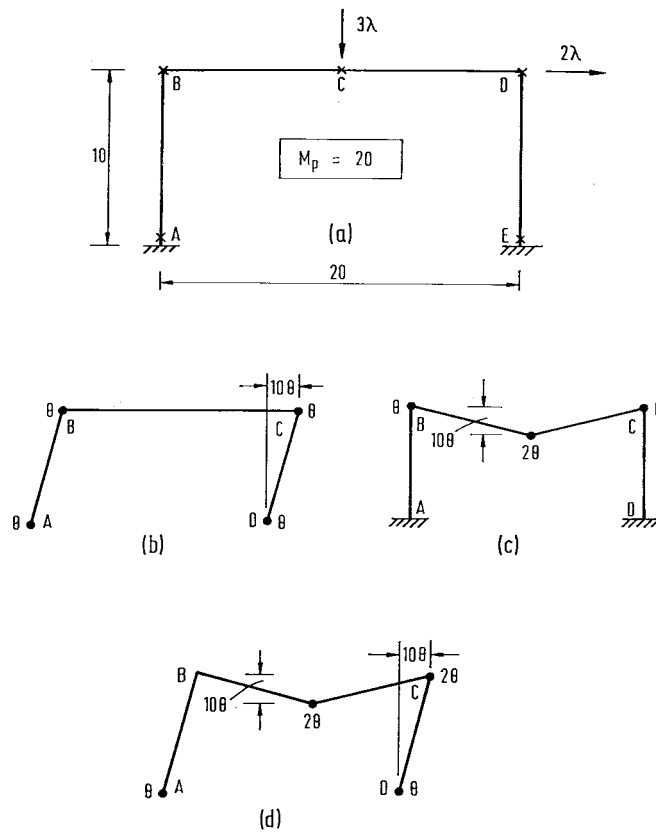


FIGURE 2.104: Collapse mechanisms of a fixed base portal frame.

The combined mechanism results in a smaller value for  $\lambda$  and no other possible mechanism can produce a lower load. Thus,  $\lambda = 2.4$  is the collapse load.

**EXAMPLE 2.14:** Frame Subjected to Distributed Load

When a frame is subjected to distributed loads, the maximum moment and hence the plastic hinge location is not known in advance. The exact location of the plastic hinge may be determined by writing the work equation in terms of the unknown distance and then maximizing the plastic moment by formal differentiation.

Consider the frame shown in Figure 2.105a. The sidesway collapse mode in Figure 2.105b leads to the following work equation:

$$4M_p = 24(10\theta)$$

which gives

$$M_p = 60 \text{ kip-ft}$$

The beam mechanism of Figure 2.105c gives

$$4M_p\theta = \frac{1}{2}(10\theta)32$$

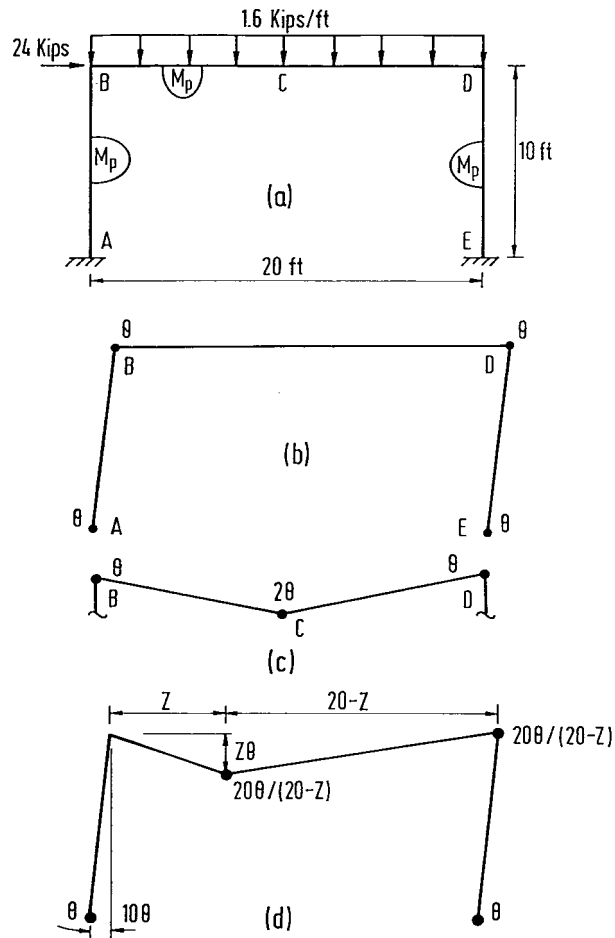


FIGURE 2.105: A portal frame subjected to a combined uniform distributed load and a horizontal load.

which gives

$$M_p = 40 \text{ kip-ft}$$

In fact, the correct mechanism is shown in Figure 2.105d in which the distance  $Z$  from the plastic hinge location is unknown. The work equation is

$$24(10\theta) + \frac{1}{2}(1.6)(20)(z\theta) = M_p \left( 2 + 2 \left( \frac{20}{20-z} \right) \right) \theta$$

which gives

$$M_p = \frac{(240 + 16z)(20 - z)}{80 - 2z}$$

To maximize  $M_p$ , the derivative of  $M_p$  is set to zero, i.e.,

$$(80 - 2z)(80 - 32z) + (4800 + 80z - 16z^2)(2) = 0$$

which gives

$$z = 40 - \sqrt{1100} = 6.83 \text{ ft}$$

and

$$M_p = 69.34 \text{ kip-ft}$$

In practice, uniform load is often approximated by applying several equivalent point loads to the member under consideration. Plastic hinges thus can be assumed to form only at the concentrated load points, and the calculations become simpler when the structural system becomes more complex.

### 2.11.9 Gable Frames

The mechanism method is used to determine the plastic limit load of the gable frame shown in Figure 2.106. The frame is composed of members with plastic moment capacity of 270 kip-in. The column bases are fixed. The frame is loaded by a horizontal load  $H$  and vertical concentrated load  $V$ . A graph from which  $V$  and  $H$  cause the collapse of the frame is to be produced.

**Solution** Consider the three modes of collapse as follows:

1. Plastic hinges form at  $A$ ,  $C$ ,  $D$ , and  $E$

The mechanism is shown in Figure 2.106b. The instantaneous center  $O$  for member  $CD$  is located at the intersection of  $AC$  and  $ED$  extended. From similar triangles  $ACC_1$  and  $OCC_2$ , we have

$$\frac{OC_2}{CC_2} = \frac{C_1A}{C_1C}$$

which gives

$$OC_2 = \frac{C_1A}{C_1C} CC_2 = \frac{22.5(9)}{18} = 11.25 \text{ ft}$$

From triangles  $ACC'$  and  $CC'O$ , we have

$$AC(\phi) = OC(\theta)$$

which gives

$$\phi = \frac{OC}{AC} \theta = \frac{CC_2}{C_1C} \theta = \frac{9}{8} \theta = \frac{1}{2} \theta$$

Similarly, from triangles  $ODD'$  and  $EDD'$ , the rotation at  $E$  is given as

$$DE(\Psi) = OD(\theta)$$

which gives

$$\Psi = \frac{OD}{DE} \theta = 1.5\theta$$

From the hinge rotations and displacements, the work equation for this mechanism can be written as

$$V(9\theta) + H(13.5\Psi) = M_p[\phi + (\phi + \theta) + (\theta + \Psi) + \Psi]$$

Substituting values for  $\psi$  and  $\phi$  and simplifying, we have

$$V + 2.25H = 180$$

2. Mechanism with Hinges at  $B$ ,  $C$ ,  $D$ , and  $E$

Figure 2.106c shows the mechanism in which the plastic hinge rotations and displacements at the load points can be expressed in terms of the rotation of member  $CD$  about the instantaneous center  $O$ .

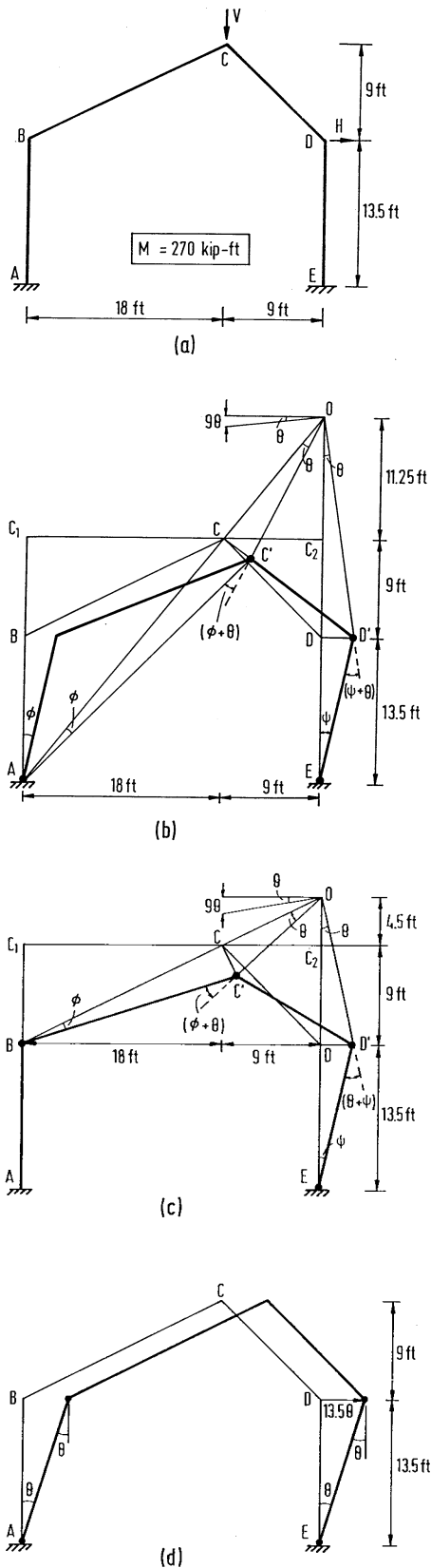


FIGURE 2.106: Collapse mechanisms of a fixed base gable frame.

From similar triangles  $BCC_1$  and  $OCC_2$ , we have

$$\frac{OC_2}{CC_2} = \frac{BC_1}{C_1C}$$

which gives

$$OC_2 = \frac{BC_1}{C_1C} CC_2 = \frac{9}{18}(9) = 4.5 \text{ ft}$$

From triangles  $BCC'$  and  $CC'O$ , we have

$$BC(\phi) = OC(\theta)$$

which gives

$$\phi = \frac{OC}{BC}\theta = \frac{OC_2}{BC_1}\theta = \frac{4.5}{9}\theta = \frac{1}{2}\theta$$

Similarly, from triangles  $ODD'$  and  $EDD'$ , the rotation at  $E$  is given as

$$DE(\Psi) = OD(\theta)$$

which gives

$$\Psi = \frac{OD}{DE}\theta = \theta$$

The work equation for this mechanism can be written as

$$V(9\theta) + H(13.5\Psi) = M_p[\phi + (\phi + \theta) + (\theta + \Psi) + \Psi]$$

Substituting values of  $\psi$  and  $\phi$  and simplifying, we have

$$V + 1.5H = 150$$

### 3. Mechanism with Hinges at $A$ , $B$ , $D$ , and $E$

The hinge rotations and displacements corresponding to this mechanism are shown in Figure 2.106d. The rotation of all hinges is  $\theta$ . The horizontal load moves by  $13.5\theta$  but the horizontal load has no vertical displacement. The work equation becomes

$$H(13.5\theta) = M_p(\theta + \theta + \theta + \theta)$$

or

$$H = 80 \text{ kips}$$

The interaction equations corresponding to the three mechanisms are plotted in Figure 2.107. By carrying out moment checks, it can be shown that Mechanism 1 is valid for portion  $AB$  of the curve, Mechanism 2 is valid for portion  $BC$ , and Mechanism 3 is valid only when  $V = 0$ .

## 2.11.10 Analysis Charts for Gable Frames

### Pinned-Base Gable Frames

Figure 2.108a shows a pinned-end gable frame subjected to a uniform gravity load  $\lambda w L$  and a horizontal load  $\lambda 1 H$  at the column top. The collapse mechanism is shown in Figure 2.108b. The

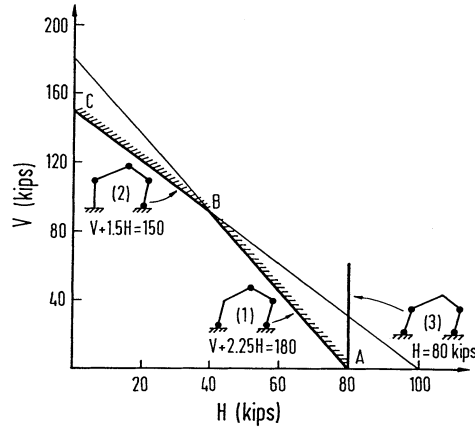


FIGURE 2.107: Vertical load and horizontal force interaction curve for collapse analysis of a gable frame.

work equation is used to determine the plastic limit load. First, the instantaneousness of rotation  $O$  is determined by considering similar triangles,

$$\frac{OE}{CF} = \frac{L}{xL} \quad \text{and} \quad \frac{OE}{CF} = \frac{OE}{h_1 + 2xh_2} \quad (2.242)$$

and

$$OD = OE - h_1 = \frac{(1-x)h_1 + 2xh_2}{x} \quad (2.243)$$

From the horizontal displacement of  $D$ ,

$$\theta h_1 = \phi OD \quad (2.244)$$

of which

$$\phi = \frac{x}{(1-x) + 2xk} \theta \quad (2.245)$$

where  $k = h_2/h_1$ . From the vertical displacement at  $C$ ,

$$\beta = \frac{1-x}{(1-x) + 2xk} \theta \quad (2.246)$$

The work equation for the assumed mechanism is

$$\lambda_1 H h_1 \beta + \frac{\lambda w L^2}{2} (1-x) \phi = M_p (\beta + 2\phi + \theta) \quad (2.247)$$

which gives

$$M_p = \frac{(1-x)\lambda_1 H h_1 + (1-x)x\lambda w L^2/2}{2(1+kx)} \quad (2.248)$$

Differentiating  $M_p$  in Equation 2.248 with respect to  $x$  and solve for  $x$ ,

$$x = \frac{A-1}{k} \quad (2.249)$$

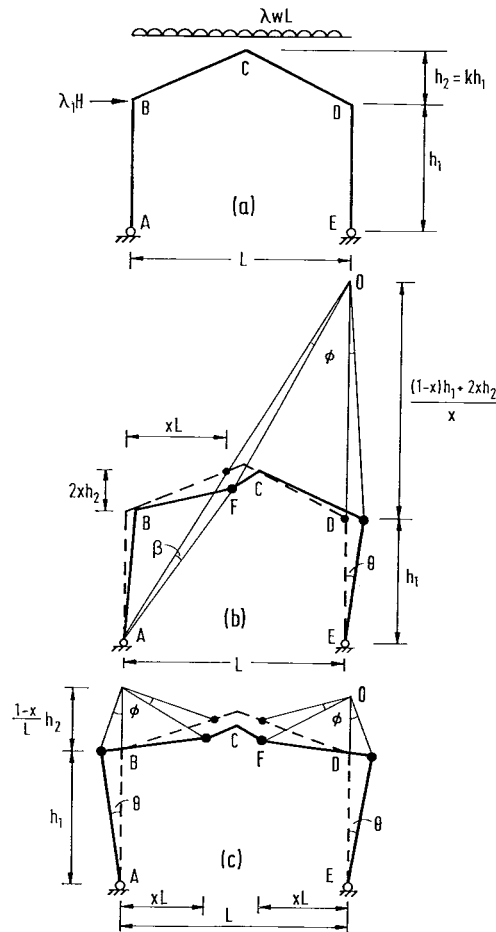


FIGURE 2.108: Pinned base gable frame subjected to a combined uniform distributed load and horizontal load.

where

$$A = \sqrt{(1+k)(1-Uk)} \quad \text{and} \quad U = \frac{2\lambda_1 H h_1}{\lambda w L^2} \quad (2.250)$$

Substituting for  $x$  in the expression for  $M_p$  gives

$$M_p = \frac{\lambda w L^2}{8} \left[ \frac{U(2+U)}{A^2 + 2A - Uk^2 + 1} \right] \quad (2.251)$$

In the absence of horizontal loading, the gable mechanism, as shown in Figure 2.108c, is the failure mode. In this case, letting  $H = 0$  and  $U = 0$  gives [31]:

$$M_p = \frac{\lambda w L^2}{8} \left[ \frac{1}{1+k+\sqrt{1+k}} \right] \quad (2.252)$$

Equation 2.251 can be used to produce a chart as shown in Figure 2.109 by which the value of  $M_p$

can be determined rapidly by knowing the values of

$$k = \frac{h_2}{h_1} \quad \text{and} \quad U = \frac{2\lambda_1 H h_1}{\lambda w L^2} \quad (2.253)$$

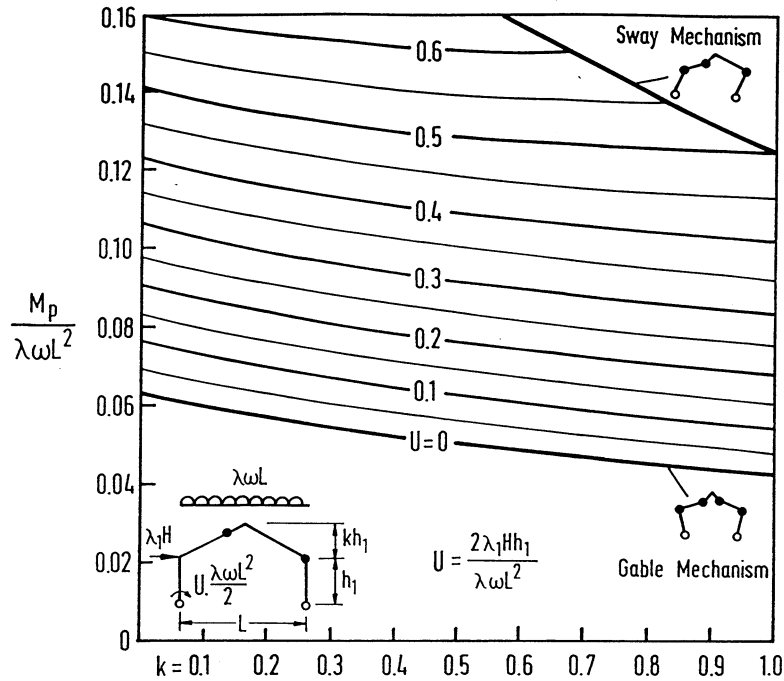


FIGURE 2.109: Analysis chart for pinned base gable frame.

### Fixed-Base Gable Frames

Similar charts can be generated for fixed-base gable frames as shown in Figure 2.110. Thus, if the values of loading,  $\lambda w$  and  $\lambda_1 H$ , and frame geometry,  $h_1$ ,  $h_2$ , and  $L$ , are known, the parameters  $k$  and  $U$  can be evaluated and the corresponding value of  $M_p / (\lambda w L^2)$  can be read directly from the appropriate chart. The required value of  $M_p$  is obtained by multiplying the value of  $M_p / (\lambda w L^2)$  by  $\lambda w L^2$ .

### 2.11.11 Grillages

Grillage is a type of structure consisting of straight beams lying on the same plane, subjected to loads acting perpendicular to the plane. An example of such structure is shown in Figure 2.111. The grillage consists of two equal simply supported beams of span length  $2L$  and full plastic moment  $M_p$ . The two beams are connected rigidly at their centers where a concentrated load  $W$  is carried.

The collapse mechanism consists of four plastic hinges formed at the beams adjacent to the point load as shown in Figure 2.111. The work equation is

$$WL\theta = 4M_p\theta$$

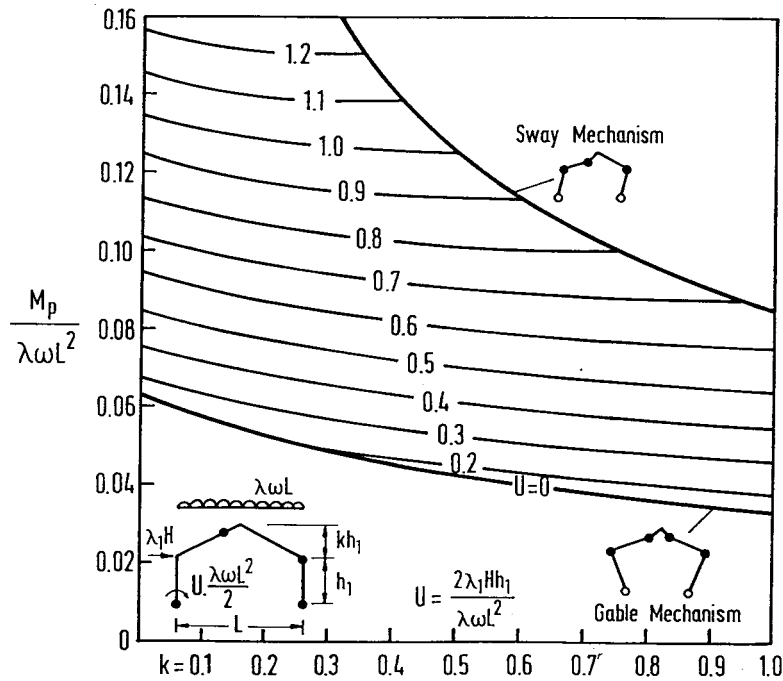


FIGURE 2.110: Analysis chart for fixed base gable frame.

of which the collapse load is

$$W = \frac{4M_p}{L}$$

### Six-Beam Grillage

A grillage consisting of six beams of span length  $4L$  each and full plastic moment  $M_p$  is shown in Figure 2.112. A total load of  $9W$  acts on the grillage, splitting into concentrated loads  $W$  at the nine nodes. Three collapse mechanisms are possible. Ignoring member twisting due to torsional forces, the work equations associated with the three collapse mechanisms are computed as follows:

Mechanism 1 (Figure 2.113a)	
Work equation	$9wL\theta = 12M_p\theta$
of which	$w = \frac{12}{9} \frac{M_p}{L} = \frac{4M_p}{3L}$
Mechanism 2 (Figure 2.113b)	
Work equation	$wL\theta = 8M_p\theta$
of which	$w = \frac{8M_p}{L}$
Mechanism 3 (Figure 2.113c)	
Work equation	$w2L2\theta + 4 \times w2L\theta = M_p(4\theta + 8\theta)$
of which	$w = \frac{M_p}{L}$

The lowest upper bound load corresponds to Mechanism 3. This can be confirmed by conducting a moment check to ensure that bending moments anywhere are not violating the plastic moment condition. Additional discussion of plastic analysis of grillages can be found in [6] and [29].

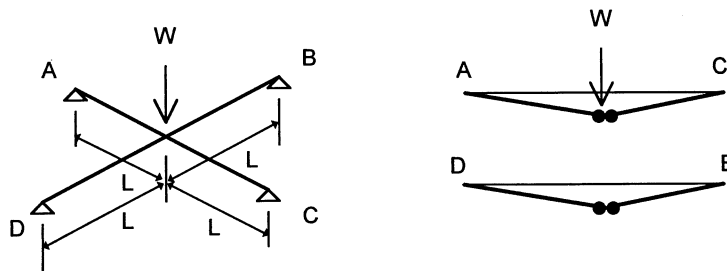


FIGURE 2.111: Two-beam grillage system.

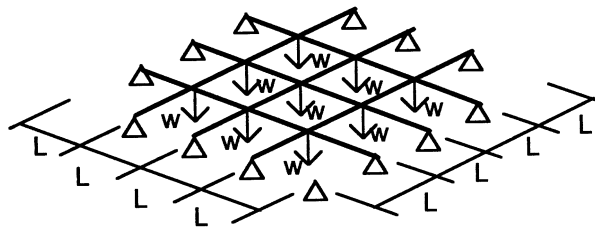


FIGURE 2.112: Six-beam grillage system.

### 2.11.12 Vierendeel Girders

Figure 2.114 shows a simply supported girder in which all members are rigidly joined and have the same plastic moment  $M_p$ . It is assumed that axial loads in the members do not cause member instability. Two possible collapse mechanisms are considered as shown in Figures 2.114b and c. The work equation for Mechanism 1 is

$$W3\theta L = 20M_p\theta$$

so that

$$W = \frac{20M_p}{3L}$$

The work equation for Mechanism 2 is

$$W3\theta L = 16M_p\theta$$

or

$$W = \frac{16M_p}{3L}$$

It can be easily proved that the collapse load associated with Mechanism 2 is the correct limit load. This is done by constructing an equilibrium set of bending moments and checking that they are not violating the plastic moment condition.

### 2.11.13 First-Order Hinge-By-Hinge Analysis

Instead of finding the collapse load of the frame, it may be useful to obtain information about the distribution and redistribution of forces prior to reaching the collapse load. Elastic-plastic hinge analysis (also known as hinge-by-hinge analysis) determines the order of plastic hinge formation, the load factor associated with each plastic-hinge formation, and member forces in the frame between each hinge formation. Thus, the state of the frame can be defined at any load factor rather than only

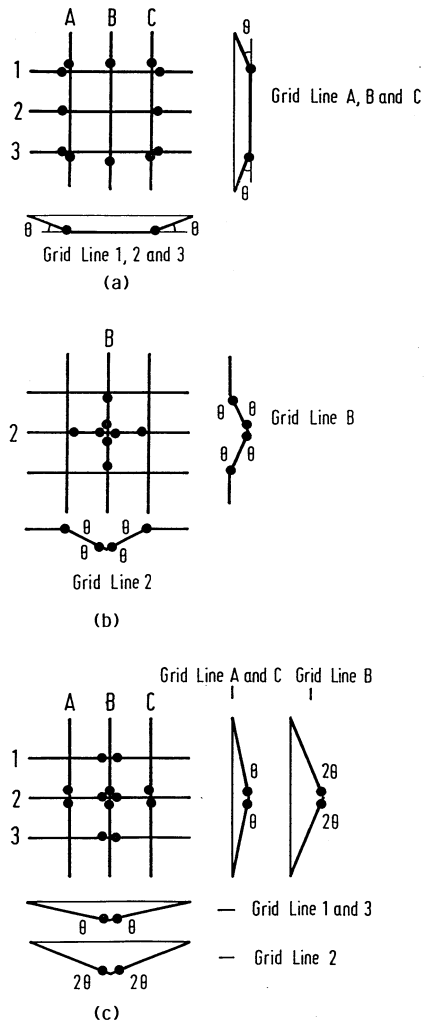


FIGURE 2.113: Six-beam grillage system. (a) Mechanism 1. (b) Mechanism 2. (c) Mechanism 3.

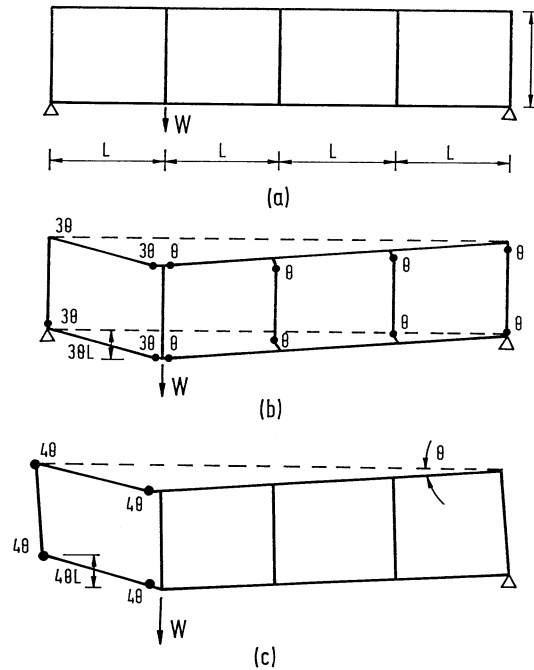


FIGURE 2.114: Collapse mechanisms of a Vierendeel girder.

at the state of collapse. This allows for a more accurate determination of member forces at the design load level.

Educational and commercial software are now available for elastic-plastic hinge analysis [16]. The computations of deflections for simple beams and multi-story frames can be done using the virtual work method [5, 8, 16, 34]. The basic assumption of first-order elastic-plastic hinge analysis is that the deformations of the structure are insufficient to alter radically the equilibrium equations. This assumption ceases to be true for slender members and structures, and the method gives unsafe predictions of limit loads.

## 2.12 Frame Stability

### 2.12.1 Categorization of Analysis Methods

Several stability analysis methods have been utilized in research and practice. Figure 2.115 shows schematic representations of the load-displacement results of a sway frame obtained from each type of analysis to be considered.

#### Elastic Buckling Analysis

The elastic buckling load is calculated by linear buckling or bifurcation (or eigenvalue) analysis. The buckling loads are obtained from the solutions of idealized elastic frames subjected to idealized loads which do not produce direct bending in the structure. The only displacements that occur before buckling occurs are those in the directions of the applied loads. When buckling (bifurcation) occurs, the displacements increase without bound, assuming linearized theory of elasticity and small displacement as shown by the horizontal straight line in Figure 2.115. The load at which these

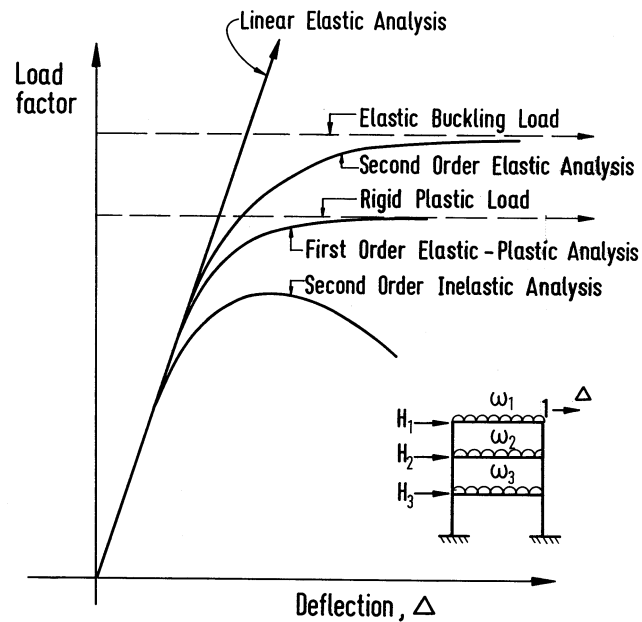


FIGURE 2.115: Categorization of stability analysis methods.

displacements occur is known as the buckling load, or commonly referred to as bifurcation load. For structural models that actually exhibit a bifurcation from the primary load path, the elastic buckling load is the largest load that the model can sustain, at least within the vicinity of the bifurcation point, provided that the post-buckling path is in unstable equilibrium. If the secondary path is in stable equilibrium, the load can still increase beyond the critical load value.

Buckling analysis is a common tool for calculations of column effective lengths. The effective length factor of a column member can be calculated using the procedure described in Section 2.12.2. The buckling analysis provides useful indices of the stability behavior of structures; however, it does not predict actual behavior of all but idealized structures with gravity loads applied only at the joints.

### Second-Order Elastic Analysis

The analysis is formulated based on the deformed configuration of the structure. When derived rigorously, a second-order analysis can include both the member curvature ( $P - \delta$ ) and the sidesway ( $P - \Delta$ ) stability effects. The  $P - \delta$  effect is associated with the influence of the axial force acting through the member displacement with respect to the rotated chord, whereas the  $P - \Delta$  effect is the influence of axial force acting through the relative sidesway displacements of the member ends. It is interesting to note that a structural system will become stiffer when its members are subjected to tension. Conversely, the structure will become softer when its members are in compression. Such behavior can be illustrated for a simple model shown in Figure 2.116. There is a clear advantage for a designer to take advantage of the stiffer behavior for tension structures. However, the detrimental effects associated with second-order deformations due to the compression forces must be considered in designing structures subjected to predominant gravity loads.

Unlike the first-order analysis in which solutions can be obtained in a rather simple and direct manner, a second-order analysis often requires an iterative procedure to obtain solutions. Although second-order analysis can account for all the stability effects, it does not provide information on the actual inelastic strength of the structure. In design, the combined effects due to stability and inelasticity must be considered for a proper evaluation of member and system strengths. The load-

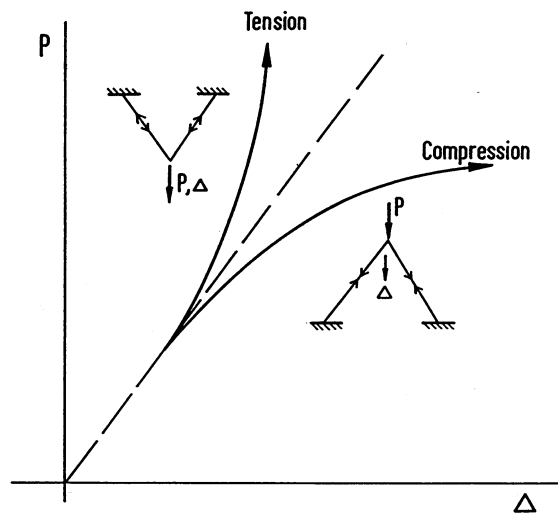


FIGURE 2.116: Behavior of frame in compression and tension.

displacement curve generated from a second-order analysis will gradually approach the horizontal straight line which represents the buckling load obtained from the elastic buckling analysis, as shown in Figure 2.115. Differences in the two loads may arise from the fact that the elastic stability limit is calculated for equilibrium based on the deformed configuration whereas the elastic critical load is calculated as a bifurcation from equilibrium on the undeformed geometry of the frame.

The load-displacement response of most frame structures usually does not involve any actual bifurcation or branch from one equilibrium solution to another equilibrium path. In some cases, the second-order elastic incremental response may not have any limit. The reader is referred to Chapter 1 of [14] for a basic discussion of these behavioral issues.

Recent works on second-order elastic analysis have been reported in Liew et al. [40]; White and Hajjar [64]; Chen and Lui [15], Liew and Chen [39], and Chen and Kim [17], among others. Second-order analysis programs which can take into consideration connection flexibility are also available [1, 24, 26, 28, 30, 41, 42].

### Second-Order Inelastic Analysis

Second-order inelastic analysis refers to any method of analysis that can capture geometrical and material nonlinearities in the analysis. The most refined inelastic analysis method is called spread-of-plasticity analysis. It involves discretization of members into many line segments, and the cross-section of each segment into a number of finite elements. Inelasticity is captured within the cross-sections and along the member length. The calculation of forces and deformations in the structure after yielding requires iterative trial-and-error processes because of the nonlinearity of the load-deformation response, and the change in cross-section effective stiffness at inelastic regions associated with the increase in the applied loads and the change in structural geometry. Although most of the plastic-zone analysis methods have been developed for planar analysis [59, 62], three-dimensional plastic-zone techniques are also available involving various degrees of refinements [12, 20, 60, 63].

The simplest second-order inelastic analysis is the elastic-plastic hinge approach. The analysis assumes that the element remains elastic except at its ends where zero-length plastic hinges are allowed to form [15, 18, 19, 41, 42, 45, 66, 69, 70]. Second-order plastic hinge analysis allows efficient analysis of large scale building frames. This is particularly true for structures in which

the axial forces in the component members are small and the predominate behavior is associated with bending actions. Although elastic-plastic hinge approaches can provide essentially the same load-displacement predictions as second-order plastic-zone methods for many frame problems, they cannot be classified as advanced analysis for use in frame design. Some modifications to the elastic-plastic hinge are required to qualify the methods as advanced analysis, and they are discussed in Section 2.12.8.

Figure 2.115 shows the load-displacement curve (a smooth curve with a descending branch) obtained from the second-order inelastic analysis. The computed limit load should be close to that obtained from the plastic-zone analysis.

## 2.12.2 Columns Stability

### Stability Equations

The stability equation of a column can be obtained by considering an infinitesimal deformed segment of the column as shown in Figure 2.117. By summing the moment about point  $b$ , we obtain

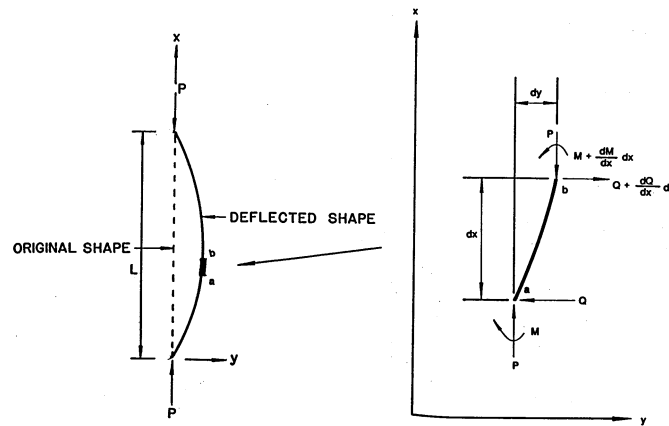


FIGURE 2.117: Stability equations of a column segment.

$$Qdx + Pdy + M - \left( M + \frac{dM}{dx} dx \right) = 0$$

or, upon simplification

$$Q = \frac{dM}{dx} - P \frac{dy}{dx} \quad (2.254)$$

Summing force horizontally, we can write

$$-Q + \left( Q + \frac{dQ}{dx} dx \right) = 0$$

or, upon simplification

$$\frac{dQ}{dx} = 0 \quad (2.255)$$

Differentiating Equation 2.254 with respect to  $x$ , we obtain

$$\frac{dQ}{dx} = \frac{d^2M}{dx^2} - P \frac{d^2y}{dx^2} \quad (2.256)$$

which, when compared with Equation 2.255, gives

$$\frac{d^2M}{dx^2} - P \frac{d^2y}{dx^2} = 0 \quad (2.257)$$

Since  $M = -EI \frac{d^2y}{dx^2}$ , Equation 2.257 can be written as

$$EI \frac{d^4y}{dx^4} + P \frac{d^2y}{dx^2} = 0 \quad (2.258)$$

or

$$y^{IV} + k^2 y'' = 0 \quad (2.259)$$

Equation 2.259 is the general fourth-order differential equation that is valid for all support conditions. The general solution to this equation is

$$y = A \sin kx + B \cos kx + Cx + D \quad (2.260)$$

To determine the critical load, it is necessary to have four boundary conditions: two at each end of the column. In some cases, both geometric and force boundary conditions are required to eliminate the unknown coefficients ( $A, B, C, D$ ) in Equation 2.260.

### Column with Pinned Ends

For a column pinned at both ends as shown in Figure 2.118a, the four boundary conditions are

$$y(x=0) = 0, \quad M(x=0) = 0 \quad (2.261)$$

$$y(x=L) = 0, \quad M(x=L) = 0 \quad (2.262)$$

Since  $M = -EIy''$ , the moment conditions can be written as

$$y''(0) = 0 \text{ and } y''(x=L) = 0 \quad (2.263)$$

Using these conditions, we have

$$B = D = 0 \quad (2.264)$$

The deflection function (Equation 2.260) reduces to

$$y = A \sin kx + Cx \quad (2.265)$$

Using the conditions  $y(L) = y''(L) = 0$ , Equation 2.265 gives

$$A \sin kL + CL = 0 \quad (2.266)$$

and

$$-Ak^2 \sin kL = 0 \quad (2.267)$$

$$\begin{bmatrix} \sin kL & L \\ -k^2 \sin kL & 0 \end{bmatrix} \begin{bmatrix} A \\ C \end{bmatrix} = \begin{bmatrix} 0 \\ 0 \end{bmatrix} \quad (2.268)$$

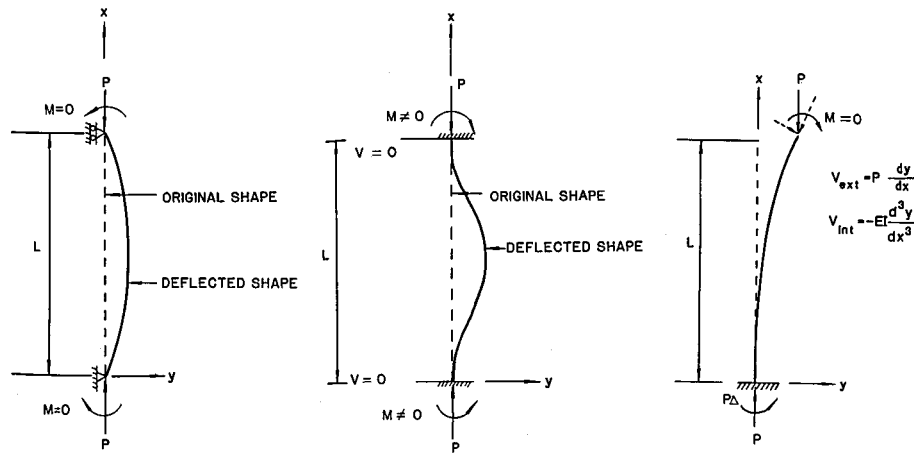


FIGURE 2.118: Column with (a) pinned ends, (b) fixed ends, and (c) fixed-free ends.

If  $A = C = 0$ , the solution is trivial. Therefore, to obtain a nontrivial solution, the determinant of the coefficient matrix of Equation 2.268 must be zero, i.e.,

$$\det \begin{vmatrix} \sin kL & L \\ -k^2 \sin kL & 0 \end{vmatrix} = 0 \quad (2.269)$$

or

$$k^2 L \sin kL = 0 \quad (2.270)$$

Since  $k^2 L$  cannot be zero, we must have

$$\sin kL = 0 \quad (2.271)$$

or

$$kL = n\pi, \quad n = 1, 2, 3, \dots \quad (2.272)$$

The lowest buckling load corresponds to the first mode obtained by setting  $n = 1$ :

$$P_{cr} = \frac{\pi^2 EI}{L^2} \quad (2.273)$$

### Column with Fixed Ends

The four boundary conditions for a fixed-end column are (Figure 2.118b):

$$y(x = 0) = y'(x = 0) = 0 \quad (2.274)$$

$$y(x = L) = y'''(x = L) = 0 \quad (2.275)$$

Using the first two boundary conditions, we obtain

$$D = -B, \quad C = -Ak \quad (2.276)$$

The deflection function (Equation 2.260) becomes

$$y = A(\sin kx - kx) + B(\cos kx - 1) \quad (2.277)$$

Using the last two boundary conditions, we have

$$\begin{bmatrix} \sin kL - kL & \cos kL - 1 \\ \cos kL - 1 & -\sin kL \end{bmatrix} \begin{bmatrix} A \\ B \end{bmatrix} = \begin{bmatrix} 0 \\ 0 \end{bmatrix} \quad (2.278)$$

For a nontrivial solution, we must have

$$\det \begin{vmatrix} \sin kL - kL & \cos kL - 1 \\ \cos kL - 1 & -\sin kL \end{vmatrix} = 0 \quad (2.279)$$

or, after expanding

$$kL \sin kL + 2 \cos kL - 2 = 0 \quad (2.280)$$

Using trigonometrical identities  $\sin kL = 2 \sin(kL/2) \cos(kL/2)$  and  $\cos kL = 1 - 2 \sin^2(kL/2)$ , Equation 2.280 can be written as

$$\sin \frac{kL}{2} \left( \frac{kL}{2} \cos \frac{kL}{2} - \sin \frac{kL}{2} \right) = 0 \quad (2.281)$$

The critical load for the symmetric buckling mode is  $P_{cr} = 4\pi^2 EI/L^2$  by letting  $\sin(kL/2) = 0$ . The buckling load for the antisymmetric buckling mode is  $P_{cr} = 80.766 EI/L^2$  by letting the bracket term in Equation 2.281 equal zero.

### Column with One End Fixed and One End Free

The boundary conditions for a fixed-free column are (Figure 2.118c):  
at the fixed end

$$y(x=0) = y'(x=0) = 0 \quad (2.282)$$

and, at the free end, the moment  $M = EIy''$  is equal to zero

$$y''(x=L) = 0 \quad (2.283)$$

and the shear force  $V = -dM/dx = -EIy'''$  is equal to  $P y'$  which is the transverse component of  $P$  acting at the free end of the column.

$$V = -EIy''' = P y' \quad (2.284)$$

It follows that the shear force condition at the free end has the form

$$y''' + k^2 y' = 0 \quad (2.285)$$

Using the boundary conditions at the fixed end, we have

$$B + D = 0, \quad \text{and} \quad Ak + C = 0 \quad (2.286)$$

The boundary conditions at the free end give

$$A \sin kL + B \cos kL = 0 \quad \text{and} \quad C = 0 \quad (2.287)$$

In matrix form, Equations 2.286 and 2.287 can be written as

$$\begin{bmatrix} 0 & 1 & 1 \\ k & 0 & 0 \\ \sin kL & \cos kL & 0 \end{bmatrix} \begin{bmatrix} A \\ B \\ C \end{bmatrix} = \begin{bmatrix} 0 \\ 0 \\ 0 \end{bmatrix} \quad (2.288)$$

For a nontrivial solution, we must have

$$\det \begin{vmatrix} 0 & 1 & 1 \\ k & 0 & 0 \\ \sin kL & \cos kL & 0 \end{vmatrix} = 0 \quad (2.289)$$

the characteristic equation becomes

$$k \cos kL = 0 \quad (2.290)$$

Since  $k$  cannot be zero, we must have  $\cos kL = 0$  or

$$kL = \frac{n\pi}{2} \quad n = 1, 3, 5, \dots \quad (2.291)$$

The smallest root ( $n = 1$ ) gives the lowest critical load of the column

$$P_{cr} = \frac{\pi^2 EI}{4L^2} \quad (2.292)$$

The boundary conditions for columns with various end conditions are summarized in Table 2.2.

**TABLE 2.2** Boundary Conditions for Various End Conditions

End conditions	Boundary conditions	
Pinned	$y = 0$	$y'' = 0$
Fixed	$y = 0$	$y' = 0$
Guided	$y' = 0$	$y''' = 0$
Free	$y'' = 0$	$y''' + k^2 y' = 0$

### Column Effective Length Factor

The effective length factor,  $K$ , of columns with different end boundary conditions can be obtained by equating the  $P_{cr}$  load obtained from the buckling analysis with the Euler load of a pinned-ended column of effective length  $KL$ .

$$P_{cr} = \frac{\pi^2 EI}{(KL)^2}$$

The effective length factor can be obtained as

$$K = \sqrt{\frac{\pi^2 EI/L^2}{P_{cr}}} \quad (2.293)$$

The  $K$  factor is a factor that can be multiplied to the actual length of the end-restrained column to give the length of an equivalent pinned-ended column whose buckling load is the same as that of the end-restrained column. Table 2.3 [2, 3] summarizes the theoretical  $K$  factors for columns with different boundary conditions. Also shown in the table are the recommended  $K$  factors for design applications. The recommended values for design are equal or larger than the theoretical values to account for semi-rigid effects of the connections used in practice.

**TABLE 2.3** Comparison of Theoretical and Design *K* Factors

Buckled shape of column is shown by dashed line	(a)	(b)	(c)	(d)	(e)	(f)
Theoretical <i>K</i> value	0.5	0.7	1.0	1.0	2.0	2.0
Recommended design value when ideal conditions are approximated	0.65	0.80	1.2	1.0	2.10	2.0
End condition code						
						Rotation fixed and translation fixed Rotation free and translation fixed Rotation fixed and translation free Rotation free and translation free

### 2.12.3 Beam-Column Stability

Figure 2.119a shows a beam-column subjected to an axial compressive force  $P$  at the ends, a lateral load  $w$  along the entire length and end moments  $M_A$  and  $M_B$ . The stability equation can be derived by considering the equilibrium of an infinitesimal element of length  $ds$  as shown in Figure 2.119b. The cross-section forces  $S$  and  $H$  act in the vertical and horizontal directions.

Considering equilibrium of forces

(a) Horizontal equilibrium

$$H + \frac{dH}{ds}ds - H = 0 \quad (2.294)$$

(b) Vertical equilibrium

$$S + \frac{dS}{ds}ds - S + wds = 0 \quad (2.295)$$

(c) Moment equilibrium

$$M + \frac{dM}{ds}ds - M - \left( S + \frac{dS}{ds} + S \right) \cos \theta \left( \frac{ds}{2} \right) + \left( H + \frac{dH}{ds}ds + H \right) \sin \theta \left( \frac{ds}{2} \right) = 0 \quad (2.296)$$

Since  $(dS/ds)ds$  and  $(dH/ds)ds$  are negligibly small compared to  $S$  and  $H$ , the above equilibrium equations can be reduced to

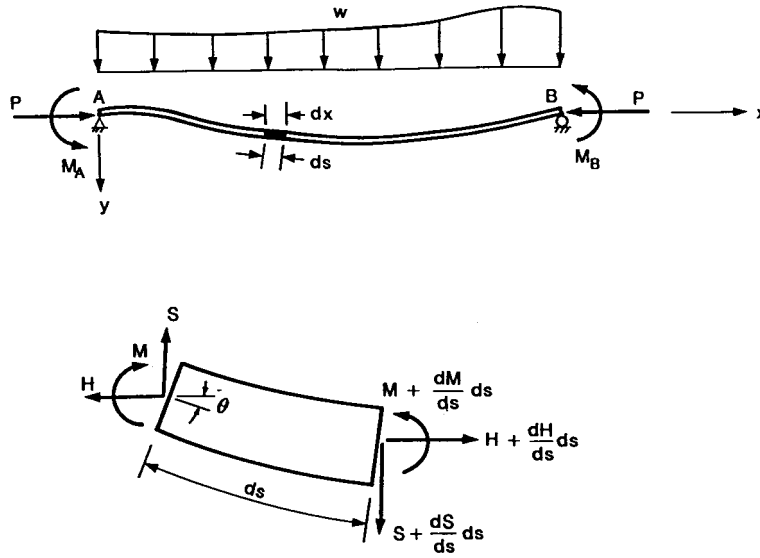


FIGURE 2.119: Basic differential equation of a beam-column.

$$\frac{dH}{ds} = 0 \quad (2.297a)$$

$$\frac{dS}{ds} + w = 0 \quad (2.297b)$$

$$\frac{dM}{ds} - S \cos \theta + H \sin \theta = 0 \quad (2.297c)$$

For small deflections and neglecting shear deformations

$$ds \cong dx, \quad \cos \theta \cong 1 \quad \sin \theta \cong \theta \cong \frac{dy}{dx} \quad (2.298)$$

where  $y$  is the lateral displacement of the member. Using the above approximations, Equation 2.297c can be written as

$$\frac{dM}{dx} - S + H \frac{dy}{dx} = 0 \quad (2.299)$$

Differentiating Equation 2.299 and substituting Equations 2.297a and 2.297b into the resulting equation, we have

$$\frac{d^2 M}{dx^2} + w + H \frac{d^2 y}{dx^2} = 0 \quad (2.300)$$

From elementary mechanics of materials, it can easily be shown that

$$M = -EI \frac{d^2 y}{dx^2} \quad (2.301)$$

Upon substitution of Equation 2.301 into Equation 2.300 and realizing that  $H = -P$ , we obtain

$$EI \frac{d^4 y}{dx^4} + P \frac{d^2 y}{dx^2} = w \quad (2.302)$$

The general solution to this differential equation has the form

$$y = A \sin kx + B \cos kx + Cx + D + f(x) \quad (2.303)$$

where  $k = \sqrt{P/EI}$  and  $f(x)$  is a particular solution satisfying the differential equation. The constants  $A$ ,  $B$ ,  $C$ , and  $D$  can be determined from the boundary conditions of the beam-column under investigation.

### Beam-Column Subjected to Transverse Loading

Figure 2.120 shows a fixed-ended beam-column with uniformly distributed load  $w$ .

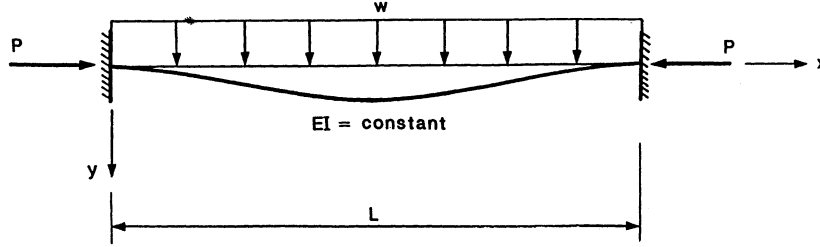


FIGURE 2.120: Beam-column subjected to uniform loading.

The general solution to Equation 2.302 is

$$y = A \sin kx + B \cos kx + Cx + D + \frac{w}{2EI k^2} x^2 \quad (2.304)$$

Using the boundary conditions

$$y_{x=0} = 0 \quad y'_{x=0} = 0 \quad y_{x=L} = 0 \quad y'_{x=L} = 0 \quad (2.305)$$

in which a prime denotes differentiation with respect to  $x$ , it can be shown that

$$A = \frac{wL}{2EI k^3} \quad (2.306a)$$

$$B = \frac{wL}{2EI k^3 \tan(kL/2)} \quad (2.306b)$$

$$C = -\frac{wL}{2EI k^2} \quad (2.306c)$$

$$D = -\frac{wL}{2EI k^3 \tan(kL/2)} \quad (2.306d)$$

Upon substitution of these constants into Equation 2.304, the deflection function can be written as

$$y = \frac{wL}{2EI k^3} \left[ \sin kx + \frac{\cos kx}{\tan(kL/2)} - kx - \frac{1}{\tan(kL/2)} + \frac{kx^2}{L} \right] \quad (2.307)$$

The maximum moment for this beam-column occurs at the fixed ends and is equal to

$$M_{\max} = -EI y''|_{x=0} = -EI y''|_{x=L} = -\frac{wL^2}{12} \left[ \frac{3(\tan u - u)}{u^2 \tan u} \right] \quad (2.308)$$

where  $u = kL/2$ .

Since  $wL^2/12$  is the maximum first-order moment at the fixed ends, the term in the bracket represents the theoretical moment amplification factor due to the  $P$ - $\delta$  effect.

For beam-columns with other transverse loading and boundary conditions, a similar approach can be followed to determine the moment amplification factor. Table 2.4 summarizes the expressions for the theoretical and design moment amplification factors for some loading conditions [2, 3].

**TABLE 2.4** Theoretical and Design Moment Amplification Factor  
 $\left(u = kL/2 = \frac{1}{2}\sqrt{(PL^2/EI)}\right)$

Boundary conditions	$P_{cr}$	Location of $M_{max}$	Moment amplification factor
Hinged-hinged	$\frac{\pi^2 EI}{L^2}$	Mid-span	$\frac{2(\sec u - 1)}{u^2}$
Hinged-fixed	$\frac{\pi^2 EI}{(0.7L)^2}$	End	$\frac{2(\tan u - u)}{u^2(1/2u - 1/\tan 2u)}$
Fixed-fixed	$\frac{\pi^2 EI}{(0.5L)^2}$	End	$\frac{3(\tan u - u)}{u^2 \tan u}$
Hinged-hinged	$\frac{\pi^2 EI}{L^2}$	Mid-span	$\frac{\tan u}{u}$
Hinged-fixed	$\frac{\pi^2 EI}{(0.7L)^2}$	End	$\frac{4u(1 - \cos u)}{3u^2 \cos u(1/2u - 1/\tan 2u)}$
Fixed-fixed	$\frac{\pi^2 EI}{(0.5L)^2}$	Mid-span and end	$\frac{2(1 - \cos u)}{u \sin u}$

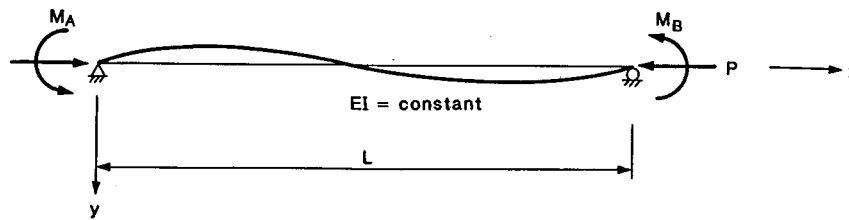


FIGURE 2.121: Beam-column subjected to end moments.

### Beam-Column Subjected to End Moments

Consider the beam-column shown in Figure 2.121. The member is subjected to an axial force of  $P$  and end moments  $M_A$  and  $M_B$ . The differential equation for this beam-column can be obtained from Equation 2.302 by setting  $w = 0$ :

$$EI \frac{d^4 y}{dx^4} + P \frac{d^2 y}{dx^2} = 0 \quad (2.309)$$

The general solution is

$$y = A \sin kx + B \cos kx + Cx + D \quad (2.310)$$

The constants  $A$ ,  $B$ ,  $C$ , and  $D$  are determined by enforcing the four boundary conditions

$$y|_{x=0} = 0, \quad y''|_{x=0} = \frac{M_A}{EI}, \quad y|_{x=L} = 0, \quad y''|_{x=L} = \frac{-M_B}{EI} \quad (2.311)$$

to give

$$A = \frac{M_A \cos kL + M_B}{EI k^2 \sin kL} \quad (2.312a)$$

$$B = -\frac{M_A}{EI k^2} \quad (2.312b)$$

$$C = -\left(\frac{M_A + M_B}{EI k^2 L}\right) \quad (2.312c)$$

$$D = \frac{M_A}{EI k^2} \quad (2.312d)$$

Substituting Equations 2.312 into the deflection function Equation 2.310 and rearranging gives

$$y = \frac{1}{EI k} \left[ \frac{\cos kL}{\sin kL} \sin kx - \cos kx - \frac{x}{L} + 1 \right] M_A + \frac{1}{EI k^2} \left[ \frac{1}{\sin kL} \sin kx - \frac{x}{L} \right] M_B \quad (2.313)$$

The maximum moment can be obtained by first locating its position by setting  $dM/dx = 0$  and substituting the result into  $M = -EI y''$  to give

$$M_{\max} = \frac{\sqrt{(M_A^2 + 2M_A M_B \cos kL + M_B^2)}}{\sin kL} \quad (2.314)$$

Assuming that  $M_B$  is the larger of the two end moments, Equation 2.314 can be expressed as

$$M_{\max} = M_B \left[ \frac{\sqrt{\{(M_A/M_B)^2 + 2(M_A/M_B) \cos kL + 1\}}}{\sin kL} \right] \quad (2.315)$$

Since  $M_B$  is the maximum first-order moment, the expression in brackets is therefore the theoretical moment amplification factor. In Equation 2.315, the ratio  $(M_A/M_B)$  is positive if the member is bent in double (or reverse) curvature and the ratio is negative if the member is bent in single curvature. A special case arises when the end moments are equal and opposite (i.e.,  $M_B = -M_A$ ). By setting  $M_B = -M_A = M_0$  in Equation 2.315, we have

$$M_{\max} = M_0 \left[ \frac{\sqrt{\{2(1 - \cos kL)\}}}{\sin kL} \right] \quad (2.316)$$

For this special case, the maximum moment always occurs at mid-span.

#### 2.12.4 Slope Deflection Equations

The slope-deflection equations of a beam-column can be derived by considering the beam-column shown in Figure 2.121. The deflection function for this beam-column can be obtained from Equation 2.313 in terms of  $M_A$  and  $M_B$  as:

$$y = \frac{1}{EI k^2} \left[ \frac{\cos kL}{\sin kL} \sin kx - \cos kx - \frac{x}{L} + 1 \right] M_A$$

$$+ \frac{1}{EI k^2} \left[ \frac{1}{\sin kL} \sin kx - \frac{x}{L} \right] M_B \quad (2.317)$$

from which

$$y' = \frac{1}{EI k} \left[ \frac{\cos kL}{\sin kL} \cos kx + \sin kx - \frac{1}{kL} \right] M_A + \frac{1}{EI k} \left[ \frac{\cos kx}{\sin kL} - \frac{1}{kL} \right] M_B \quad (2.318)$$

The end rotations  $\theta_A$  and  $\theta_B$  can be obtained from Equation 2.318 as

$$\begin{aligned} \theta_A &= y'(x=0) = \frac{1}{EI k} \left[ \frac{\cos kL}{\sin kL} - \frac{1}{kL} \right] M_A + \frac{1}{EI k} \left[ \frac{1}{\sin kL} - \frac{1}{kL} \right] M_B \\ &= \frac{L}{EI} \left[ \frac{kL \cos kL - \sin kL}{(kL)^2 \sin kL} \right] M_A + \frac{L}{EI} \left[ \frac{kL - \sin kL}{(kL)^2 \sin kL} \right] M_B \end{aligned} \quad (2.319)$$

and

$$\begin{aligned} \theta_B &= y'(x=L) = \frac{1}{EI k} \left[ \frac{1}{\sin kL} - \frac{1}{kL} \right] M_A + \frac{1}{EI k} \left[ \frac{\cos kL}{\sin kL} - \frac{1}{kL} \right] M_B \\ &= \frac{L}{EI} \left[ \frac{kL - \sin kL}{(kL)^2 \sin kL} \right] M_A + \frac{L}{EI} \left[ \frac{kL \cos kL - \sin kL}{(kL)^2 \sin kL} \right] M_B \end{aligned} \quad (2.320)$$

The moment rotation relationship can be obtained from Equations 2.319 and 2.320 by arranging  $M_A$  and  $M_B$  in terms of  $\theta_A$  and  $\theta_B$  as:

$$M_A = \frac{EI}{L} (s_{ii} \theta_A + s_{ij} \theta_B) \quad (2.321)$$

$$M_B = \frac{EI}{L} (s_{ji} \theta_A + s_{jj} \theta_B) \quad (2.322)$$

where

$$s_{ii} = s_{jj} = \frac{kL \sin kL - (kL)^2 \cos kL}{2 - 2 \cos kL - kL \sin kL} \quad (2.323)$$

$$s_{ij} = s_{ji} = \frac{(kL)^2 - kL \sin kL}{2 - 2 \cos kL - kL \sin kL} \quad (2.324)$$

are referred to as the *stability functions*.

Equations 2.321 and 2.322 are the slope-deflection equations for a beam-column that is not subjected to transverse loading and relative joint translation. It should be noted that when  $P$  approaches zero,  $kL = \sqrt{(P/EI)L}$  approaches zero, and by using L'Hospital's rule, it can be shown that  $s_{ij} = 4$  and  $s_{ji} = 2$ . Values for  $s_{ii}$  and  $s_{ij}$  for various values of  $kL$  are plotted as shown in Figure 2.122.

Equations 2.322 and 2.323 are valid if the following conditions are satisfied:

1. The beam is prismatic.
2. There is no relative joint displacement between the two ends of the member.
3. The member is continuous, i.e., there is no internal hinge or discontinuity in the member.
4. There is no in-span transverse loading on the member.
5. The axial force in the member is compressive.

If these conditions are not satisfied, some modifications to the slope-deflection equations are necessary.

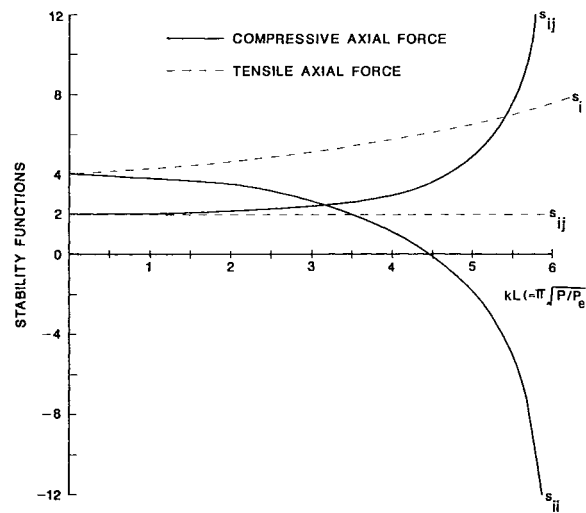


FIGURE 2.122: Plot of stability functions.

### Members Subjected to Sidesway

If there is a relative joint translation,  $\Delta$ , between the member ends, as shown in Figure 2.123, the slope-deflection equations are modified as

$$\begin{aligned}
 M_A &= \frac{EI}{L} \left[ s_{ii} \left( \theta_A - \frac{\Delta}{L} \right) + s_{ij} \left( \theta_B - \frac{\Delta}{L} \right) \right] \\
 &= \frac{EI}{L} \left[ s_{ii} \theta_A + s_{ij} \theta_B - (s_{ii} + s_{ij}) \frac{\Delta}{L} \right] \quad (2.325)
 \end{aligned}$$

$$\begin{aligned}
 M_B &= \frac{EI}{L} \left[ s_{ij} \left( \theta_A - \frac{\Delta}{L} \right) + s_{ii} \left( \theta_B - \frac{\Delta}{L} \right) \right] \\
 &= \frac{EI}{L} \left[ s_{ij} \theta_A + s_{ii} \theta_B - (s_{ii} + s_{ij}) \frac{\Delta}{L} \right] \quad (2.326)
 \end{aligned}$$

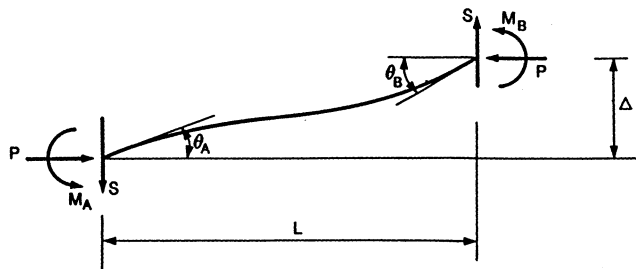


FIGURE 2.123: Beam-column subjected to end moments and sidesway.

### Member with a Hinge at One End

If a hinge is present at  $B$  end of the member, the end moment there is zero, i.e.,

$$M_B = \frac{EI}{L} (s_{ij}\theta_A + s_{ii}\theta_B) = 0 \quad (2.327)$$

from which

$$\theta_B = -\frac{s_{ij}}{s_{ii}}\theta_A \quad (2.328)$$

Upon substituting Equation 2.328 into Equation 2.325, we have

$$M_A = \frac{EI}{L} \left( s_{ii} - \frac{s_{ij}^2}{s_{ii}} \right) \theta_A \quad (2.329)$$

If the member is hinged at  $A$  rather than at  $B$ , Equation 2.329 is still valid provided that the subscript  $A$  is changed to  $B$ .

### Member with End Restraints

If the member ends are connected by two linear elastic springs, as in Figure 2.124, with spring constants,  $R_{kA}$  and  $R_{kB}$  at the  $A$  and  $B$  ends, respectively, the end rotations of the linear spring are  $M_A/R_{kA}$  and  $M_B/R_{kB}$ . If we denote the total end rotations at joints  $A$  and  $B$  by  $\theta_A$  and  $\theta_B$ ,

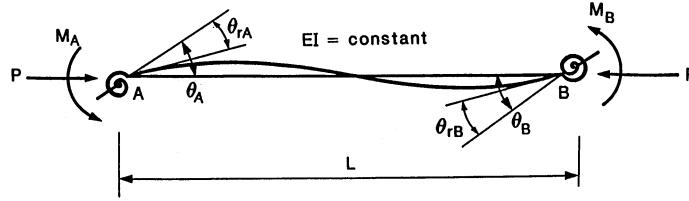


FIGURE 2.124: Beam-column with end springs.

respectively, then the member end rotations, with respect to its chord, will be  $(\theta_A - M_A/R_{kA})$  and  $(\theta_B - M_B/R_{kB})$ . As a result, the slope-deflection equations are modified to

$$M_A = \frac{EI}{L} \left[ s_{ii} \left( \theta_A - \frac{M_A}{R_{kA}} \right) + s_{ij} \left( \theta_B - \frac{M_B}{R_{kB}} \right) \right] \quad (2.330)$$

$$M_B = \frac{EI}{L} \left[ s_{ij} \left( \theta_A - \frac{M_A}{R_{kA}} \right) + s_{jj} \left( \theta_B - \frac{M_B}{R_{kB}} \right) \right] \quad (2.331)$$

Solving Equations 2.330 and 2.331 simultaneously for  $M_A$  and  $M_B$  gives

$$M_A = \frac{EI}{LR^*} \left[ \left( s_{ii} + \frac{EIs_{ii}^2}{LR_{kB}} - \frac{EIs_{ij}^2}{LR_{kB}} \right) \theta_A + s_{ij}\theta_B \right] \quad (2.332)$$

$$M_B = \frac{EI}{LR^*} \left[ s_{ij}\theta_A + \left( s_{ii} + \frac{EIs_{ii}^2}{LR_{kA}} - \frac{EIs_{ij}^2}{LR_{kA}} \right) \theta_B \right] \quad (2.333)$$

where

$$R^* = \left( 1 + \frac{EIs_{ii}}{LR_{kA}} \right) \left( 1 + \frac{EIs_{ii}}{LR_{kB}} \right) - \left( \frac{EI}{L} \right)^2 \frac{s_{ij}^2}{R_{kA}R_{kB}} \quad (2.334)$$

In writing Equations 2.332 to 2.333, the equality  $s_{jj} = s_{ii}$  has been used. Note that as  $R_{kA}$  and  $R_{kB}$  approach infinity, Equations 2.332 and 2.333 reduce to Equations 2.321 and 2.322, respectively.

### Member with Transverse Loading

For members subjected to transverse loading, the slope-deflection Equations 2.321 and 2.322 can be modified by adding an extra term for the fixed-end moment of the member.

$$M_A = \frac{EI}{L} (s_{ii}\theta_A + s_{ij}\theta_B) + M_{FA} \quad (2.335)$$

$$M_B = \frac{EI}{L} (s_{ij}\theta_A + s_{jj}\theta_B) + M_{FB} \quad (2.336)$$

Table 2.5 give the expressions for the fixed-end moments of five commonly encountered cases of transverse loading. Readers are referred to [14, 15] for more details.

### Member with Tensile Axial Force

For members subjected to tensile force, Equations 2.321 and 2.322 can be used provided that the stability functions are redefined as

$$s_{ii} = s_{jj} = \frac{(kL)^2 \cosh kL - kL \sinh kL}{2 - 2 \cosh kL + kL \sinh kL} \quad (2.337)$$

$$s_{ij} = s_{ji} = \frac{kL \sinh kL - (kL)^2}{2 - 2 \cosh kL + kL \sinh kL} \quad (2.338)$$

### Member Bent in Single Curvature with $\theta_B = -\theta_A$

For the member bent in single curvature in which  $\theta_B = -\theta_A$ , the slope-deflection equations reduce to

$$M_A = \frac{EI}{L} (s_{ii} - s_{ij}) \theta_A \quad (2.339)$$

$$M_B = -M_A \quad (2.340)$$

### Member Bent in Double Curvature with $\theta_B = \theta_A$

For the member bent in double curvature such that  $\theta_B = \theta_A$ , the slope-deflection equations become

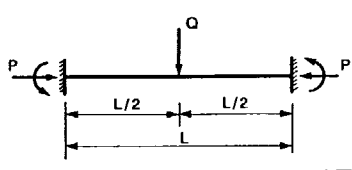
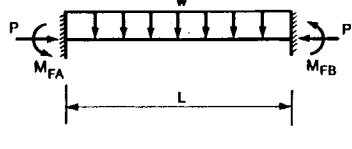
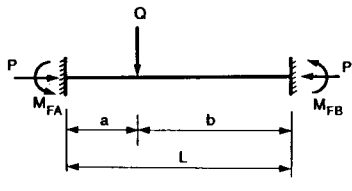
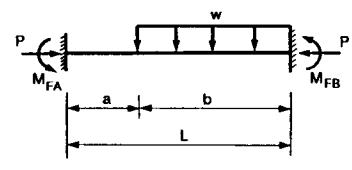
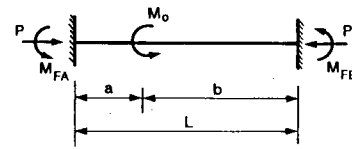
$$M_A = \frac{EI}{L} (s_{ii} + s_{ij}) \theta_A \quad (2.341)$$

$$M_B = M_A \quad (2.342)$$

## 2.12.5 Second-Order Elastic Analysis

The basis of the formulation is that the beam-column element is prismatic and initially straight. An update-Lagrangian approach [7] is assumed. There are two methods to incorporate second-order effects: (1) the stability function approach and (2) the geometric stiffness (or finite element) approach. The stability function approach is based directly on the governing differential equations of the problem as described in Section 2.12.4, whereas the stiffness approach is based on an assumed cubic polynomial variation of the transverse displacement along the element length. Therefore, the stability function approach is more exact in terms of representing the member stability behavior. However, the geometric stiffness approach is easier to implement for three-dimensional analysis.

**TABLE 2.5** Beam-Column Fixed-End Moments [15]  $\left( u = kL/2 = \frac{L}{2} \sqrt{\frac{P}{EI}} \right)$

Case	Fixed-End Moments
	$M_{FA} = \frac{QL}{8} \left[ \frac{2(1-\cos u)}{u \sin u} \right]$ $M_{FB} = -M_{FA}$
	$M_{FA} = \frac{wL^2}{12} \left[ \frac{3(\tan u - u)}{u^2 \tan u} \right]$ $M_{FB} = -M_{FA}$
	$M_{FA} = \frac{QL}{d} \left[ \frac{2ub}{L} \cos 2u - 2u \cos \frac{2ub}{L} - \sin 2u \right. \\ \left. + \sin \frac{2ua}{L} + \sin \frac{2ub}{L} + \frac{2ua}{L} \right]$ $M_{FB} = -\frac{QL}{d} \left[ \frac{2ua}{L} \cos 2u - 2u \cos \frac{2ua}{L} - \sin 2u \right. \\ \left. + \sin \frac{2ub}{L} + \sin \frac{2ua}{L} + \frac{2ub}{L} \right]$ <p>where</p> $d = 2u(2 - 2 \cos 2u - 2u \sin 2u)$
	$M_{FA} = \frac{wL^2}{8u^2 e} \left[ (2u \operatorname{cosec} 2u - 1) \left( \frac{2ub}{L} - \sin \frac{2ub}{L} \right) \right. \\ \left. + (\tan u) \left( 1 - \cos \frac{2ub}{L} - \frac{2u^2 b^2}{L^2} \right) \right]$ $M_{FB} = \frac{-wL^2}{8u^2 e} \left[ (2u \cot 2u - 1) \left( \frac{2ub}{L} - \sin \frac{2ub}{L} \right) \right. \\ \left. + (\tan u) \left( 1 - \cos \frac{2ub}{L} + \frac{2u^2 b^2}{L^2} \right) \right. \\ \left. - 2u \left( 1 - \cos \frac{2ub}{L} \right) \right]$ <p>where</p> $e = \tan u - u$
	$M_{FA} = \frac{M_0}{2e} \left[ (2u \operatorname{cosec} 2u - 1) \sin \frac{2ub}{L} \right. \\ \left. - (\tan u) \left( 1 - \cos \frac{2ub}{L} \right) \right]$ $M_{FB} = \frac{M_0}{2e} \left[ (1 - 2u \cot 2u) \sin \frac{2ub}{L} \right. \\ \left. - (\tan u) \left( 1 + \cos \frac{2ub}{L} \right) \right. \\ \left. + 2u \cos \frac{2ub}{L} \right]$ <p>where</p> $e = \tan u - u$

For either of these approaches, the linearized element stiffness equations may be expressed in either incremental or total force and displacement forms as

$$[K]\{d\} + \{r_f\} = \{r\} \quad (2.343)$$

where  $[K]$  is the element stiffness matrix,  $\{d\} = \{d_1, d_2, \dots, d_6\}^T$  is the element nodal displacement

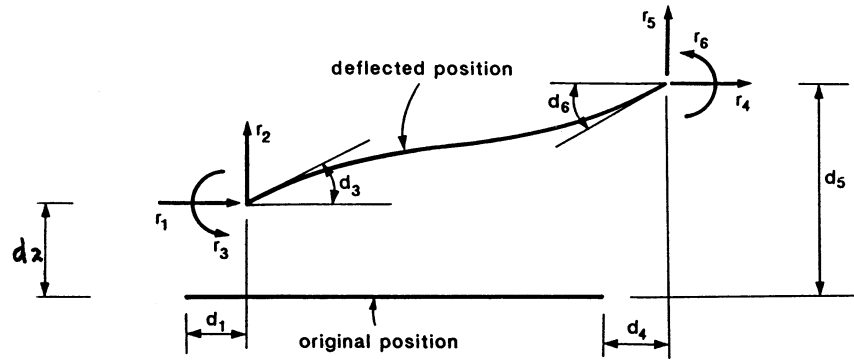


FIGURE 2.125: Nodal displacements and forces of a beam-column element.

vector,  $\{r_f\} = \{r_{f1}, r_{f2}, \dots, r_{f6}\}^T$  is the element fixed-end force vector due to the presence of in-span loading, and  $\{r\} = \{r_1, r_2, \dots, r_6\}^T$  is the nodal force vector as shown in Figure 2.125. If the stability function approach is employed, the stiffness matrix of a two-dimensional beam-column element may be written as

$$[K] = \frac{EI}{L} \begin{bmatrix} \frac{A}{T} & 0 & 0 & -\frac{A}{T} & 0 & 0 \\ \frac{2(S_{ii}+S_{ij})-(kL)^2}{L^2} & \frac{S_{ii}+S_{ij}}{L} & 0 & -\frac{2(S_{ii}+S_{ij})+(kL)^2}{L} & \frac{S_{ii}+S_{ij}}{L} & 0 \\ 0 & S_{ii} & 0 & \frac{-(S_{ii}+S_{ij})}{L} & S_{ij} & 0 \\ 0 & 0 & \frac{A}{T} & \frac{2(S_{ii}+S_{ij})-(kL)^2}{L^2} & 0 & -\frac{2(S_{ii}+S_{ij})}{L} \\ \text{sym.} & & & & & \frac{S_{ii}+S_{ij}}{L} \end{bmatrix} \quad (2.344)$$

where  $S_{ii}$  and  $S_{ij}$  are the member stiffness coefficients obtained from the elastic beam-column stability functions [14]. These coefficient may be expressed as

$$S_{ii} = \begin{cases} \frac{kL \sin(kL) - (kL)^2 \cos(kL)}{2 - 2 \cos(kL) - kL \sin(kL)} & \text{for } P < 0 \\ \frac{(kL)^2 \cosh(kL) - kL \sinh(kL)}{2 - 2 \cosh(kL) + kL \sinh(kL)} & \text{for } P > 0 \end{cases} \quad (2.345)$$

$$S_{ij} = \begin{cases} \frac{(kL)^2 - kL \sin(kL)}{2 - 2 \cos(kL) - \rho \sin(kL)} & \text{for } P < 0 \\ \frac{kL \sinh(kL) - (kL)^2}{2 - 2 \cosh(kL) + \rho \sinh(kL)} & \text{for } P > 0 \end{cases} \quad (2.346)$$

where  $kL = L\sqrt{\frac{P}{EI}}$ , and  $P$  is positive in compression and negative in tension.

The fixed-end force vector  $r_f$  is a  $6 \times 1$  matrix which can be computed from the in-span loading in the beam-column. If curvature shortening is ignored,  $r_{f1} = r_{f4} = 0$ ,  $r_{f3} = M_{FA}$ , and  $r_{f6} = M_{FB}$ .  $M_{FA}$  and  $M_{FB}$  can be obtained from Table 2.5 for different in-span loading conditions.  $r_{f2}$  and  $r_{f5}$  can be obtained from equilibrium of forces.

If the axial force in the member is small, Equation 2.344 can be simplified by ignoring the higher order terms of the power series expansion of the trigonometric functions. The resulting element stiffness matrix becomes:

$$[K] = \frac{EI}{L} \begin{bmatrix} \frac{A}{I} & 0 & 0 & -\frac{A}{I} & 0 & 0 \\ & \frac{12}{L^2} & \frac{6}{L} & 0 & \frac{-12}{L^2} & \frac{6}{L} \\ & & 4 & 0 & \frac{-6}{L} & 2 \\ & & & \frac{A}{I} & 0 & 0 \\ & & & & \frac{12}{L^2} & \frac{-6}{L} \\ & \text{sym.} & & & & 4 \end{bmatrix} + P \begin{bmatrix} 0 & 0 & 0 & 0 & 0 & 0 \\ & \frac{6}{5L} & \frac{1}{10} & 0 & \frac{-6}{5L} & \frac{1}{10} \\ & & \frac{2L}{15} & 0 & \frac{-1}{10} & \frac{-L}{30} \\ & & & 0 & 0 & 0 \\ & & & & \frac{6}{5L} & \frac{-1}{10} \\ & \text{sym.} & & & & \frac{2L}{15} \end{bmatrix} \quad (2.347)$$

The first term on the right is the first-order elastic stiffness matrix, and the second term is the geometric stiffness matrix, which accounts for the effect of axial force on the bending stiffness of the member. Detailed discussions on the limitation of the geometric stiffness approach vs. the stability function approach are given in White et al. [66].

### 2.12.6 Modifications to Account for Plastic Hinge Effects

There are two commonly used approaches for representing plastic hinge behavior in a second-order elastic-plastic hinge formulation [19]. The most basic approach is to model the plastic hinge behavior as a “real hinge” for the purpose of calculating the element stiffness. The change in moment capacity due to the change in axial force can be accommodated directly in the numerical formulation. The change in moment is determined in the force recovery at each solution step such that, for continued plastic loading, the new force point is positioned at the strength surface at the current value of the axial force. A detailed description of these procedures is given by Chen and Lui [15], Chen et al. [19], and Lee and Basu [35], among others.

Alternatively, the elastic-plastic hinge model may be formulated based on the “extending and contracting” plastic hinge model. The plastic hinge can rotate and extend/contract for plastic loading and axial force. The formulation can follow the force-space plasticity concept using the normality flow rule relative to the cross-section surface strength [13]. Formal derivations of the beam-column element based on this approach have been presented by Porter and Powell [46] and Orbison et al. [45], among others.

### 2.12.7 Modification for End Connections

The moment rotation relationship of the beam-column with end connections at both ends can be expressed as (Equations 2.332 and 2.333):

$$M_A = \frac{EI}{L} [s_{ii}^* \theta_A + s_{ij}^* \theta_B] \quad (2.348)$$

$$M_B = \frac{EI}{L} [s_{ij}^* \theta_A + s_{jj}^* \theta_B] \quad (2.349)$$

where

$$s_{ii}^* = \frac{S_{ii} + \frac{EIS_{ii}^2}{LR_{kB}} - \frac{EIS_{ij}^2}{LR_{kB}}}{\left[1 + \frac{EIS_{ii}}{LR_{kA}}\right] \left[1 + \frac{EIS_{jj}}{LR_{kB}}\right] - \left[\frac{EI}{L}\right]^2 \frac{S_{ij}^2}{R_{kA}R_{kB}}} \quad (2.350)$$

$$S_{jj}^* = \frac{S_{ii} + \frac{EIS_{ii}^2}{LR_{kA}} - \frac{EIS_{ij}^2}{LR_{kA}}}{\left[1 + \frac{EIS_{ii}}{LR_{kA}}\right] \left[1 + \frac{EIS_{jj}}{LR_{kB}}\right] - \left[\frac{EI}{L}\right]^2 \frac{S_{ij}^2}{R_{kA}R_{kB}}} \quad (2.351)$$

and

$$S_{ij}^* = \frac{S_{ij}}{\left[1 + \frac{EIS_{ii}}{LR_{kA}}\right] \left[1 + \frac{EIS_{jj}}{LR_{kB}}\right] - \left[\frac{EI}{L}\right]^2 \frac{S_{ij}^2}{R_{kA}R_{kB}}} \quad (2.352)$$

The member stiffness relationship can be written in terms of six degrees of freedom beam-column element shown in Figure 2.126 as

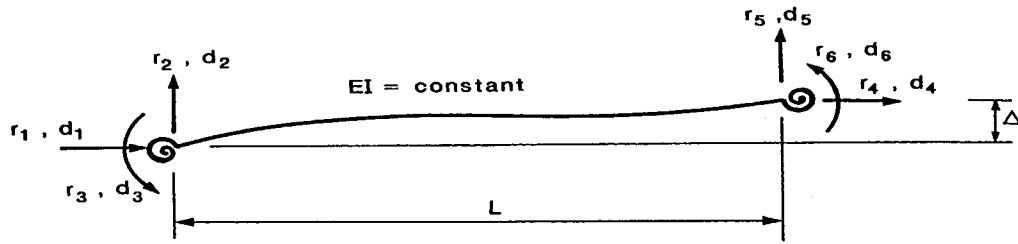


FIGURE 2.126: Nodal displacements and forces of a beam-column with end connections.

$$\begin{pmatrix} r_1 \\ r_2 \\ r_3 \\ r_4 \\ r_5 \\ r_6 \end{pmatrix} = \frac{EI}{L} \begin{bmatrix} \frac{A}{I} & 0 & 0 & -\frac{A}{I} & 0 & 0 \\ 0 & \frac{S_{ii}^* + 2S_{ij}^* + S_{jj}^* - (kL)^2}{L^2} & \frac{S_{ii}^* + S_{ij}^*}{L} & 0 & \frac{-(S_{ii}^* + 2S_{ij}^* + S_{jj}^*) + (kL)^2}{L^2} & \frac{S_{ij}^* + S_{jj}^*}{L} \\ 0 & \frac{S_{ii}^* + S_{ij}^*}{L} & S_{ii}^* & 0 & \frac{-(S_{ii}^* + S_{ij}^*)}{L} & S_{ij}^* \\ -\frac{A}{I} & 0 & 0 & \frac{A}{I} & 0 & 0 \\ 0 & 0 & 0 & 0 & \frac{S_{ii}^* + 2S_{ij}^* + S_{jj}^* - (kL)^2}{L^2} & \frac{-(S_{ij}^* + S_{jj}^*)}{L} \\ 0 & 0 & 0 & 0 & \frac{-(S_{ii}^* + S_{ij}^*)}{L} & S_{jj}^* \end{bmatrix} \begin{pmatrix} d_1 \\ d_2 \\ d_3 \\ d_4 \\ d_5 \\ d_6 \end{pmatrix} \quad (2.353)$$

### 2.12.8 Second-Order Refined Plastic Hinge Analysis

The main limitation of the conventional elastic-plastic hinge approach is that it over-predicts the strength of columns that fail by inelastic flexural buckling. The key reason for this limitation is the modeling of a member by a perfect elastic element between the plastic hinge locations. Furthermore, the elastic-plastic hinge model assumes that material behavior changes abruptly from the elastic state to the fully yielded state. The element under consideration exhibits a sudden stiffness reduction upon

the formation of a plastic hinge. This approach, therefore, overestimates the stiffness of a member loaded into the inelastic range [42, 64, 65, 66]. This leads to further research and development of an alternative method called the *refined plastic hinge approach*. This approach is based on the following improvements to the elastic-plastic hinge model:

1. A column tangent-modulus model  $E_t$  is used in place of the elastic modulus  $E$  to represent the distributed plasticity along the length of a member due to axial force effects. The member inelastic stiffness, represented by the member axial and bending rigidities  $E_t A$  and  $E_t I$ , is assumed to be the function of axial load only. In other words,  $E_t A$  and  $E_t I$  can be thought of as the properties of an effective core of the section, considering column action only. The tangent modulus captures the effect of early yielding in the cross-section due to residual stresses, which was believed to be the cause of the low strength of inelastic column buckling. The tangent modulus approach also has been utilized in previous work by Orbison et al. [45], Liew [38], and White et al. [66] to improve the accuracy of the elastic-plastic hinge approach for structures in which members are subjected to large axial forces.
2. Distributed plasticity effects associated with flexure are captured by gradually degrading the member stiffness at the plastic hinge locations as yielding progresses under increasing load as the cross-section strength is approached. Several models of this type have been proposed in recent literature based on extensions to the elastic-plastic hinge approach [47] as well as the tangent modulus inelastic hinge approach [41, 42, 66]. The rationale of modeling stiffness degradation associated with both axial and flexural actions is that the tangent modulus model represents the column strength behavior in the limit of pure axial compression, and the plastic hinge stiffness degradation model represents the beam behavior in pure bending, thus the combined effects of these two approaches should also satisfy the cases in which the member is subjected to combined axial compression and bending.

It has been shown that with the above two improvements, the refined plastic hinge model can be used with sufficient accuracy to provide a quantitative assessment of a member's performance up to failure. Detailed descriptions of the method and discussion of results generated by the method are given in White et al. [66] and Chen et al. [19].

### 2.12.9 Second-Order Plastic Zone Analysis

Plastic-zone analyses can be classified into two main types, namely 3-D shell element and 2-D beam-column approaches. In the 3-D plastic-zone analysis, the structure is modeled using a large number of finite 3-D shell elements, and the elastic constitutive matrix, in the usual incremental stress-strain relations, is replaced by an elastic-plastic constitutive matrix once yielding is detected. This analysis approach typically requires numerical integration for the evaluation of the stiffness matrix. Based on a deformation theory of plasticity, the combined effects of normal and shear stresses may be accounted for. The 3-D spread-of-plasticity analysis is computational intensive and best suited for analyzing small-scale structures.

The second-approach for plastic-zone analysis is based on the use of beam-column theory, in which the member is discretized into many beam-column segments, and the cross-section of each segment is further subdivided into a number of fibers. Inelasticity is typically modeled by the consideration of normal stress only. When the computed stresses at the centroid of any fibers reach the uniaxial normal strength of the material, the fiber is considered yielded. Compatibility is treated by assuming that full continuity is retained throughout the volume of the structure in the same manner as for elastic range calculations. Most of the plastic-zone analysis methods developed are meant for planar (2-D)

analysis [18, 59, 62]. Three-dimensional plastic-zone techniques are also available involving various degrees of refinements [60, 63].

A plastic-zone analysis, which includes the spread of plasticity, residual stresses, initial geometric imperfections, and any other significant second-order behavioral effects, is often considered to be an exact analysis method. Therefore, when this type of analysis is employed, the checking of member interaction equations is not required. However, in reality, some significant behavioral effects such as joint and connection performances tend to defy precise numerical and analytical modeling. In such cases, a simpler method of analysis that adequately captures the inelastic behavior would be sufficient for engineering application. Second-order plastic hinge based analysis is still the preferred method for advanced analysis of large-scale steel frames.

### 2.12.10 Three-Dimensional Frame Element

The two-dimensional beam-column formulation can be extended to a three-dimensional space frame element by including additional terms due to shear force, bending moment, and torsion. The following stiffness equation for a space frame element has been derived by Yang and Kuo [67] by referring to Figure 2.127:

$$[k_e]\{d\} + [k_g]\{d\} = \{^2f\} - \{^1f\} \quad (2.354)$$

where

$$\{d\}^T = \{d_1, d_2, \dots, d_{12}\} \quad (2.355)$$

is the displacement vector which consists of three translations and three rotations at each node, and

$$\{^i f\}^T = \{^i f_1, ^i f_2, \dots, ^i f_{12}\} \quad i = 1, 2 \quad (2.356)$$

are the force vectors which consist of the corresponding nodal forces at configurations  $i = 1$  and  $i = 2$ , respectively.

The physical interpretation of Equation 2.356 is as follows: By increasing the nodal forces acting on the element from  $\{^1f\}$  to  $\{^2f\}$ , further deformations  $\{d\}$  may occur with the element, resulting in the motion of the element from configuration associated with the forces  $\{^1f\}$  to the new configuration associated with  $\{^2f\}$ . During this process of deformation, the increments in the nodal forces, i.e.,  $\{^2f\} - \{^1f\}$ , will be resisted not only by the elastic actions generated by the elastic stiffness matrix  $[k_e]$  but also by the forces induced by the change in geometry as represented by the geometric stiffness matrix  $[k_g]$ .

The only assumption with the incremental stiffness equation is that the strains occurring with each incremental step should be small so that the approximations implied by the incremental constitutive law are not violated.

The elastic stiffness matrix  $[K_e]$  for the space frame element, which has a 12 x 12 dimension, can be derived as follows:

$$[k] = \begin{bmatrix} [k_1] & [k_2] \\ [k_2]^T & [k_3] \end{bmatrix} \quad (2.357)$$

where the submatrices are

$$[k_1] = \begin{bmatrix} \frac{EA}{L} & 0 & 0 & 0 & 0 & 0 \\ 0 & \frac{12EI_z}{L^3} & 0 & 0 & 0 & \frac{6EI_z}{L^2} \\ 0 & 0 & \frac{12EI_y}{L^3} & 0 & -\frac{6EI_y}{L^2} & 0 \\ 0 & 0 & 0 & \frac{GJ}{L} & 0 & 0 \\ 0 & 0 & 0 & 0 & \frac{4EI_y}{L} & 0 \\ 0 & 0 & 0 & 0 & 0 & \frac{4EI_z}{L} \end{bmatrix} \quad (2.358)$$

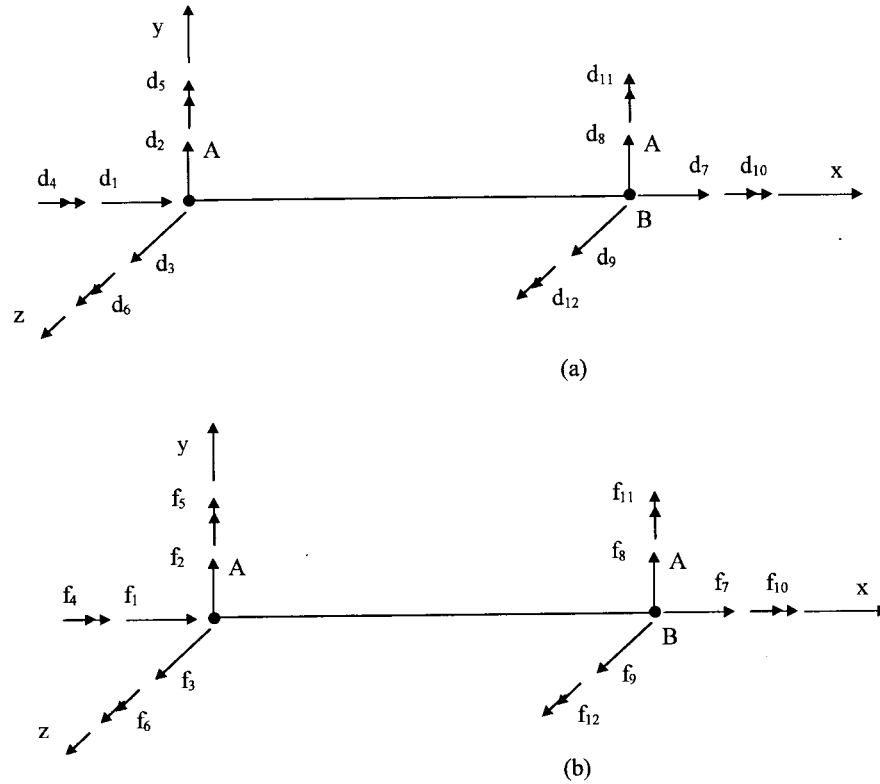


FIGURE 2.127: Three-dimensional frame element: (a) nodal degrees of freedom and (b) nodal forces.

$$[k_2] = \begin{bmatrix} -\frac{EA}{L} & 0 & 0 & 0 & 0 & 0 \\ 0 & -\frac{12EI_z}{L^3} & 0 & 0 & 0 & \frac{6EI_z}{L^2} \\ 0 & 0 & -\frac{12EI_y}{L^3} & 0 & -\frac{6EI_y}{L^2} & 0 \\ 0 & 0 & 0 & -\frac{GJ}{L} & 0 & 0 \\ 0 & 0 & \frac{6EI_y}{L^2} & 0 & \frac{2EI_y}{L} & 0 \\ 0 & -\frac{6EI_z}{L^2} & 0 & 0 & 0 & \frac{2EI_z}{L} \end{bmatrix} \quad (2.359)$$

$$[k_3] = \begin{bmatrix} \frac{EA}{L} & 0 & 0 & 0 & 0 & 0 \\ 0 & \frac{12EI_z}{L^3} & 0 & 0 & 0 & -\frac{6EI_z}{L^2} \\ 0 & 0 & \frac{12EI_y}{L^3} & 0 & \frac{6EI_y}{L^2} & 0 \\ 0 & 0 & 0 & \frac{GJ}{L} & 0 & 0 \\ 0 & 0 & 0 & 0 & \frac{4EI_y}{L} & 0 \\ 0 & 0 & 0 & 0 & 0 & \frac{4EI_z}{L} \end{bmatrix} \quad (2.360)$$

where  $I_x$ ,  $I_y$ , and  $I_z$  are the moment of inertia about  $x$ -,  $y$ -, and  $z$ -axes;  $L$  = member length,  $E$  = modulus of elasticity,  $A$  = cross-sectional area,  $G$  = shear modulus, and  $J$  = torsional stiffness.

The geometric stiffness matrix for a three-dimensional space frame element can be given as follows:

$$[k_g] = \begin{bmatrix} a & 0 & 0 & 0 & -d & -e & -a & 0 & 0 & 0 & -n & -o \\ & b & 0 & d & g & k & 0 & -b & 0 & n & -g & k \\ & & c & e & h & g & 0 & 0 & -c & o & -h & -g \\ & & & f & i & l & 0 & -d & -e & -f & -i & -l \\ & & & & j & 0 & d & -g & h & -i & p & -q \\ & & & & & m & e & -k & -g & -l & q & r \\ & & & & & & a & 0 & 0 & 0 & n & o \\ & & & & & & & b & 0 & -n & g & -k \\ & & & & & & & & c & -o & h & g \\ & & & & & & & & & f & i & l \\ \text{sym.} & & & & & & & & & & j & o \\ & & & & & & & & & & & m \end{bmatrix} \quad (2.361)$$

where

$$\begin{aligned} a &= -\frac{f_6+f_{12}}{L^2}, & b &= \frac{6f_7}{5L}, & c &= -\frac{f_5+f_{11}}{L^2}, & d &= \frac{f_5}{L}, & e &= \frac{f_6}{L}, & f &= \frac{f_7J}{AL}, \\ g &= \frac{f_{10}}{L}, & h &= -\frac{f_7}{10}, & i &= \frac{f_6+f_{12}}{6}, & j &= \frac{2f_7L}{15}, & k &= -\frac{f_5+f_{11}}{6}, & l &= \frac{f_{11}}{L}, \\ m &= \frac{f_{12}}{L}, & n &= -\frac{f_7L}{30}, & o &= -\frac{f_{10}}{2}. \end{aligned}$$

Further details can be obtained from [67].

## 2.13 Structural Dynamic

### 2.13.1 Equation of Motion

The essential physical properties of a linearly elastic structural system subjected to external dynamic loading are its mass, stiffness properties, and energy absorption capability or damping. The principle of dynamic analysis may be illustrated by considering a simple single-story structure as shown in Figure 2.128. The structure is subjected to a time-varying force  $f(t)$ .  $k$  is the spring constant that relates the lateral story deflection  $x$  to the story shear force, and the dash pot relates the damping force to the velocity by a damping coefficient  $c$ . If the mass,  $m$ , is assumed to concentrate at the beam,

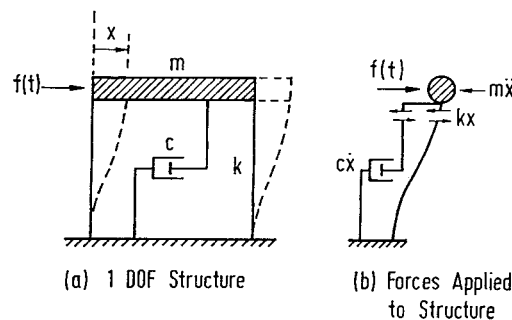


FIGURE 2.128: (a) One DOF structure; (b) forces applied to structures.

the structure becomes a single-degree-of-freedom (SDOF) system. The equation of motion of the

system may be written as:

$$m\ddot{x} + c\dot{x} + kx = f(t) \quad (2.362)$$

Various solutions to Equation 2.362 can give an insight into the behavior of the structure under dynamic situation.

### 2.13.2 Free Vibration

In this case the system is set to motion and allowed to vibrate in the absence of applied force  $f(t)$ . Letting  $f(t) = 0$ , Equation 2.362 becomes

$$m\ddot{x} + c\dot{x} + kx = 0 \quad (2.363)$$

Dividing Equation 2.363 by the mass  $m$ , we have

$$\ddot{x} + 2\xi\omega x + \omega^2 x = 0 \quad (2.364)$$

where

$$2\xi\omega = \frac{c}{m} \quad \text{and} \quad \omega^2 = \frac{k}{m} \quad (2.365)$$

The solution to Equation 2.364 depends on whether the vibration is damped or undamped.

#### Case 1: Undamped Free Vibration

In this case,  $c = 0$ , and the solution to the equation of motion may be written as:

$$x = A \sin \omega t + B \cos \omega t \quad (2.366)$$

where  $\omega = \sqrt{k/m}$  is the circular frequency.  $A$  and  $B$  are constants that can be determined by the initial boundary conditions. In the absence of external forces and damping the system will vibrate indefinitely in a repeated cycle of vibration with an amplitude of

$$X = \sqrt{A^2 + B^2} \quad (2.367)$$

and a natural frequency of

$$f = \frac{\omega}{2\pi} \quad (2.368)$$

The corresponding natural period is

$$T = \frac{2\pi}{\omega} = \frac{1}{f} \quad (2.369)$$

The undamped free vibration motion as described by Equation 2.366 is shown in Figure 2.129.

#### Case 2: Damped Free Vibration

If the system is not subjected to applied force and damping is presented, the corresponding solution becomes

$$x = A \exp(\lambda_1 t) + B \exp(\lambda_2 t) \quad (2.370)$$

where

$$\lambda_1 = \omega \left[ -\xi + \sqrt{\xi^2 - 1} \right] \quad (2.371)$$

and

$$\lambda_2 = \omega \left[ -\xi - \sqrt{\xi^2 - 1} \right] \quad (2.372)$$

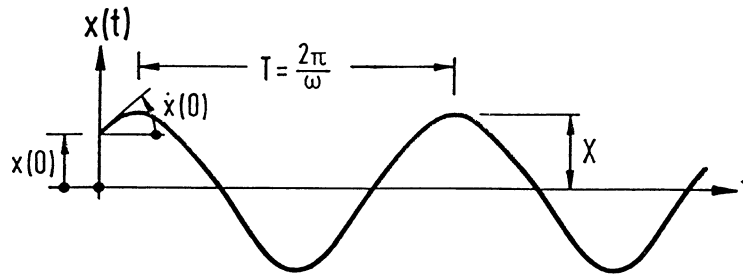


FIGURE 2.129: Response of undamped free vibration.

The solution of Equation 2.370 changes its form with the value of  $\xi$  defined as

$$\xi = \frac{c}{2\sqrt{mk}} \quad (2.373)$$

If  $\xi^2 < 1$  the equation of motion becomes

$$x = \exp(-\xi\omega t)(A \cos \omega_d t + B \sin \omega_d t) \quad (2.374)$$

where  $\omega_d$  is the damped angular frequency defined as

$$\omega_d = \sqrt{(1 - \xi^2)}\omega \quad (2.375)$$

For most building structures  $\xi$  is very small (about 0.01) and therefore  $\omega_d \approx \omega$ . The system oscillates about the neutral position as the amplitude decays with time  $t$ . Figure 2.130 illustrates an example of such motion. The rate of decay is governed by the amount of damping present.

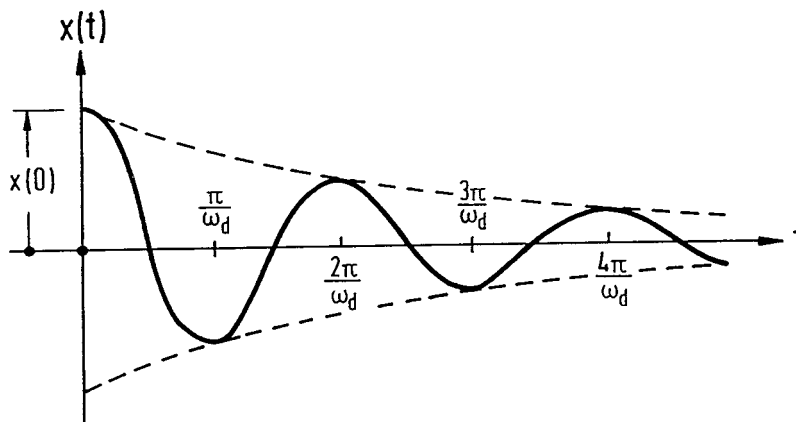


FIGURE 2.130: Response of damped free vibration.

If the damping is large, then oscillation will be prevented. This happens when  $\xi^2 > 1$  and the behavior is referred to as *overdamped*. The motion of such behavior is shown in Figure 2.131.

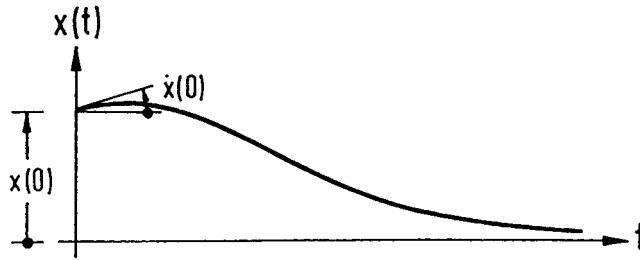


FIGURE 2.131: Response of free vibration with critical damping.

Damping with  $\xi^2 = 1$  is called critical damping. This is the case where minimum damping is required to prevent oscillation and the critical damping coefficient is given as

$$c_{cr} = 2\sqrt{km} \quad (2.376)$$

where  $k$  and  $m$  are the stiffness and mass of the system.

The degree of damping in the structure is often expressed as a proportion of the critical damping value. Referring to Equations 2.373 and 2.376, we have

$$\xi = \frac{c}{c_{cr}} \quad (2.377)$$

$\xi$  is called the critical damping ratio.

### 2.13.3 Forced Vibration

If a structure is subjected to a sinusoidal motion such as a ground acceleration of  $\ddot{x} = F \sin \omega_f t$ , it will oscillate and after some time the motion of the structure will reach a steady state. For example, the equation of motion due to the ground acceleration (from Equation 2.364) is

$$\ddot{x} + 2\xi\omega\dot{x} + \omega^2x = -F \sin \omega_f t \quad (2.378)$$

The solution to the above equation consists of two parts; the complimentary solution given by Equation 2.366 and the particular solution. If the system is damped, oscillation corresponding to the complementary solution will decay with time. After some time, the motion will reach a steady state and the system will vibrate at a constant amplitude and frequency. This motion, which is called force vibration, is described by the particular solution expressed as

$$x = C_1 \sin \omega_f t + C_2 \cos \omega_f t \quad (2.379)$$

It can be observed that the steady force vibration occurs at the frequency of the excited force,  $\omega_f$ , not the natural frequency of the structure,  $\omega$ .

Substituting Equation 2.379 into Equation 2.378, the displacement amplitude can be shown to be

$$X = -\frac{F}{\omega^2} \frac{1}{\sqrt{\left[1 - \left(\frac{\omega_f}{\omega}\right)^2\right]^2 + \left(\frac{2\xi\omega_f}{\omega}\right)^2}} \quad (2.380)$$

The term  $-F/\omega^2$  is the static displacement caused by the force due to the inertia force. The ratio of the response amplitude relative to the static displacement  $-F/\omega^2$  is called the dynamic displacement

amplification factor,  $D$ , given as

$$D = \frac{1}{\sqrt{\left[ \left\{ 1 - \left( \frac{\omega_f}{\omega} \right)^2 \right\}^2 + \left( \frac{2\xi\omega_f}{\omega} \right)^2 \right]}} \quad (2.381)$$

The variation of the magnification factor with the frequency ratio  $\omega_f/\omega$  and damping ratio  $\xi$  is shown in Figure 2.132.

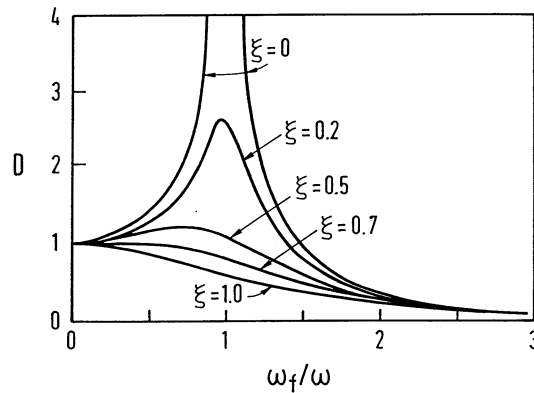


FIGURE 2.132: Variation of dynamic amplification factor with frequency ratio.

When the dynamic force is applied at a frequency much lower than the natural frequency of the system ( $\omega_f/\omega \ll 1$ ), the response is quasi-static. The response is proportional to the stiffness of the structure, and the displacement amplitude is close to the static deflection.

When the force is applied at a frequency much higher than the natural frequency ( $\omega_f/\omega \gg 1$ ), the response is proportional to the mass of the structure. The displacement amplitude is less than the static deflection ( $D < 1$ ).

When the force is applied at a frequency close to the natural frequency, the displacement amplitude increases significantly. The condition at which  $\omega_f/\omega = 1$  is known as resonance.

Similarly, the ratio of the acceleration response relative to the ground acceleration may be expressed as

$$D_a = \left| \frac{\ddot{x} + \ddot{x}_g}{\ddot{x}_g} \right| = \sqrt{\frac{1 + \left( \frac{2\xi\omega_f}{\omega} \right)^2}{\left[ \left\{ 1 - \left( \frac{\omega_f}{\omega} \right)^2 \right\}^2 + \left( \frac{2\xi\omega_f}{\omega} \right)^2 \right]}} \quad (2.382)$$

$D_a$  is called the dynamic acceleration magnification factor.

### 2.13.4 Response to Suddenly Applied Load

Consider the spring-mass damper system of which a load  $P_o$  is applied suddenly. The differential equation is given by

$$M\ddot{x} + c\dot{x} + kx = P_o \quad (2.383)$$

If the system is started at rest, the equation of motion is

$$x = \frac{P_o}{k} \left[ 1 - \exp(-\xi\omega t) \left\{ \cos \omega_d t + \frac{\xi\omega}{\omega_d} \sin \omega_d t \right\} \right] \quad (2.384)$$

If the system is undamped, then  $\xi = 0$  and  $\omega_d = \omega$ , and we have

$$x = \frac{P_o}{k} [1 - \cos \omega t] \quad (2.385)$$

The maximum displacement is  $2(P_o/k)$  corresponding to  $\cos \omega t = -1$ . Since  $P_o/k$  is the maximum static displacement, the dynamic amplification factor is equal to 2. The presence of damping would naturally reduce the dynamic amplification factor and the force in the system.

### 2.13.5 Response to Time-Varying Loads

Some forces and ground motions that are encountered in practice are rather complex in nature. In general, numerical analysis is required to predict the response of such effects, and the finite element method is one of the most common techniques to be employed in solving such problems.

The evaluation of responses due to time-varying loads can be carried out using the Piecewise Exact Method. In using this method, the loading history is divided into small time intervals. Between these points, it is assumed that the slope of the load curve remains constant. The entire load history is represented by a piecewise linear curve, and the error of this approach can be minimized by reducing the length of the time steps. Description of this procedure is given in [21].

Other techniques employed include Fourier analysis of the forcing function followed by solution for Fourier components in the frequency domain. For random forces, random vibration theory and spectrum analysis may be used [25, 61].

### 2.13.6 Multiple Degree Systems

In multiple degree systems, an independent differential equation of motion can be written for each degree of freedom. The nodal equations of a multiple degree system consisting of  $n$  degrees of freedom may be written as

$$[m]\{\ddot{x}\} + [c]\{\dot{x}\} + [k]\{x\} = \{F(t)\} \quad (2.386)$$

where  $[m]$  is a symmetrical  $n \times n$  matrix of mass,  $[c]$  is a symmetrical  $n \times n$  matrix of damping coefficient, and  $\{F(t)\}$  is the force vector which is zero in the case of free vibration.

Consider a system under free vibration without damping. The general solution of Equation 2.386 is assumed in the form of

$$\begin{Bmatrix} x_1 \\ x_2 \\ \vdots \\ x_n \end{Bmatrix} = \begin{bmatrix} \cos(\omega t - \phi) & 0 & 0 & 0 \\ 0 & \cos(\omega t - \phi) & 0 & 0 \\ \vdots & \vdots & \vdots & \vdots \\ 0 & 0 & 0 & \cos(\omega t - \phi) \end{bmatrix} \begin{Bmatrix} C_1 \\ C_2 \\ \vdots \\ C_n \end{Bmatrix} \quad (2.387)$$

where angular frequency  $\omega$  and phase angle  $\phi$  are common to all  $x$ 's. In this assumed solution,  $\phi$  and  $C_1, C_2, C_n$  are the constants to be determined from the initial boundary conditions of the motion and  $\omega$  is a characteristic value (eigenvalue) of the system.

Substituting Equation 2.387 into Equation 2.386 yields

$$\begin{bmatrix} k_{11} - m_{11}\omega^2 & k_{12} - m_{12}\omega^2 & \cdots & k_{1n} - m_{1n}\omega^2 \\ k_{21} - m_{21}\omega^2 & k_{22} - m_{22}\omega^2 & \cdots & k_{2n} - m_{2n}\omega^2 \\ \vdots & \vdots & \ddots & \vdots \\ k_{n1} - m_{n1}\omega^2 & k_{n2} - m_{n2}\omega^2 & \cdots & k_{nn} - m_{nn}\omega^2 \end{bmatrix} \begin{Bmatrix} C_1 \\ C_2 \\ \vdots \\ C_n \end{Bmatrix} \cos(\omega t - \phi) = \begin{Bmatrix} 0 \\ 0 \\ \vdots \\ 0 \end{Bmatrix} \quad (2.388)$$

or

$$[k] - \omega^2[m] \{C\} = \{0\} \quad (2.389)$$

where  $[k]$  and  $[m]$  are the  $n \times n$  matrices,  $\omega^2$  and  $\cos(\omega t - \phi)$  are scalars, and  $\{C\}$  is the amplitude vector. For non-trivial solutions,  $\cos(\omega t - \phi) \neq 0$ ; thus, solution to Equation 2.389 requires the determinant of  $[k] - \omega^2[m] = 0$ . The expansion of the determinant yields a polynomial of  $n$  degree as a function of  $\omega^2$ , the  $n$  roots of which are the eigenvalues  $\omega_1, \omega_2, \omega_n$ .

If the eigenvalue  $\omega$  for a normal mode is substituted in Equation 2.389, the amplitude vector  $\{C\}$  for that mode can be obtained.  $\{C_1\}, \{C_2\}, \{C_3\}, \{C_n\}$  are therefore called the *eigenvectors*, the absolute values of which must be determined through initial boundary conditions. The resulting motion is a sum of  $n$  harmonic motions, each governed by the respective natural frequency  $\omega$ , written as

$$\{x\} = \sum_{i=1}^n \{C_i\} \cos(\omega_i t - \phi) \quad (2.390)$$

### 2.13.7 Distributed Mass Systems

Although many structures may be approximated by lumped mass systems, in practice all structures are distributed mass systems consisting of an infinite number of particles. Consequently, if the motion is repetitive, the structure has an infinite number of natural frequencies and mode shapes. The analysis of a distributed-parameter system is entirely equivalent to that of a discrete system once the mode shapes and frequencies have been determined because in both cases the amplitudes of the modal response components are used as generalized coordinates in defining the response of the structure.

In principle an infinite number of these coordinates is available for a distributed-parameter system, but in practice only a few modes, usually those of lower frequencies, will provide a significant contribution to the overall response. Thus, the problem of a distributed-parameter system can be converted to a discrete system form in which only a limited number of modal coordinates is used to describe the response.

#### Flexural Vibration of Beams

The motion of the distributed mass system is best illustrated by a classical example of a uniform beam with a span length  $L$  and flexural rigidity  $EI$  and a self-weight of  $m$  per unit length, as shown in Figure 2.133a. The beam is free to vibrate under its self-weight. From Figure 2.133b, dynamic equilibrium of a small beam segment of length  $dx$  requires:

$$\frac{\partial V}{\partial x} dx = m dx \frac{\partial^2 y}{\partial t^2} \quad (2.391)$$

in which

$$\frac{\partial^2 y}{\partial x^2} = \frac{M}{EI} \quad (2.392)$$

and

$$V = -\frac{\partial M}{\partial x}, \quad \frac{\partial V}{\partial x} = -\frac{\partial^2 M}{\partial x^2} \quad (2.393)$$

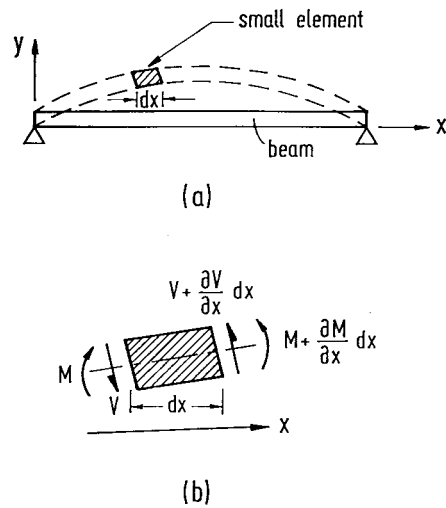


FIGURE 2.133: (a) Beam in flexural vibration; (b) equilibrium of beam segment in vibration.

Substituting these equations into Equation 2.391 leads to the equation of motion of the flexural beam:

$$\frac{\partial^4 y}{\partial x^4} + \frac{m}{EI} \frac{\partial^2 y}{\partial t^2} = 0 \quad (2.394)$$

Equation 2.394 can be solved for beams with given sets of boundary conditions. The solution consists of a family of vibration modes with corresponding natural frequencies. Standard results are available in Table 2.6 to compute the natural frequencies of uniform flexural beams of different supporting conditions. Methods are also available for dynamic analysis of continuous beams [21].

### Shear Vibration of Beams

Beams can deform by flexure or shear. Flexural deformation normally dominates the deformation of slender beams. Shear deformation is important for short beams or in higher modes of slender beams. Table 2.7 gives the natural frequencies of uniform beams in shear, neglecting flexural deformation. The natural frequencies of these beams are inversely proportional to the beam length  $L$  rather than  $L^2$ , and the frequencies increase linearly with the mode number.

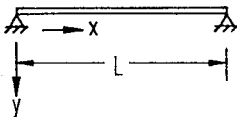
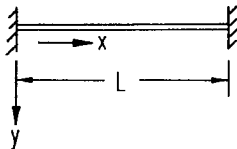
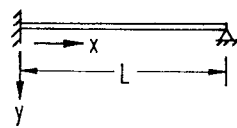
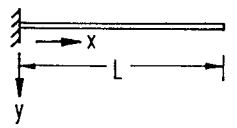
### Combined Shear and Flexure

The transverse deformation of real beams is the sum of flexure and shear deformations. In general, numerical solutions are required to incorporate both the shear and flexural deformation in the prediction of natural frequency of beams. For beams with comparable shear and flexural deformations, the following simplified formula may be used to estimate the beam's frequency:

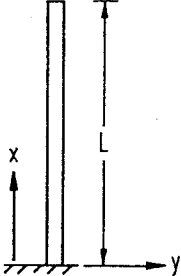
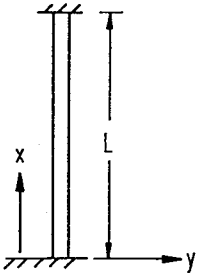
$$\frac{1}{f^2} = \frac{1}{f_f^2} + \frac{1}{f_s^2} \quad (2.395)$$

where  $f$  is the fundamental frequency of the beam, and  $f_f$  and  $f_s$  are the fundamental frequencies predicted by the flexure and shear beam theory [50].

**TABLE 2.6** Frequencies and Mode Shapes of Beams in Flexural Vibration

$f_n = \frac{k_n}{2\pi} \sqrt{\frac{EI}{mL^4}} \text{ HZ}$ $n = 1, 2, 3, \dots$			
		$L = \text{Length (m)}$ $EI = \text{Flexural Rigidity (Nm}^2\text{)}$ $M = \text{Mass per unit length (kg/m)}$	
Boundary Conditions	$K_n$ ; $n = 1, 2, 3$	Mode Shape $y_n\left(\frac{x}{L}\right)$	$A_n$ ; $n = 1, 2, 3, \dots$
Pinned - Pinned 	$(n\pi)^2$	$\sin \frac{n\pi x}{L}$	-
Fixed - Fixed 	22.37 61.67 120.90 199.86 298.55 $(2n+1)^2 \frac{\pi^2}{4}$ ; $n > 5$	$\cosh \frac{\sqrt{K_n} x}{L} - \cos \frac{\sqrt{K_n} x}{L}$ $- A_n \left( \sinh \frac{\sqrt{K_n} x}{L} - \sin \frac{\sqrt{K_n} x}{L} \right)$	0.98250 1.00078 0.99997 1.00000 0.99999 1.0; $n > 5$
Fixed - Pinned 	15.42 49.96 104.25 178.27 272.03 $(4n+1)^2 \frac{\pi^2}{4}$ ; $n > 5$	$\cosh \frac{\sqrt{K_n} x}{L} - \cos \frac{\sqrt{K_n} x}{L}$ $- A_n \left( \sinh \frac{\sqrt{K_n} x}{L} - \sin \frac{\sqrt{K_n} x}{L} \right)$	1.00078 1.00000 1.0; $n > 3$
Cantilever 	3.52 22.03 61.69 120.90 199.86 $(2n-1)^2 \frac{\pi^2}{4}$ ; $n > 5$	$\cosh \frac{\sqrt{K_n} x}{L} - \cos \frac{\sqrt{K_n} x}{L}$ $- A_n \left( \sinh \frac{\sqrt{K_n} x}{L} - \sin \frac{\sqrt{K_n} x}{L} \right)$	0.73410 1.01847 0.99922 1.00003 1.0; $n > 4$

**TABLE 2.7** Frequencies and Mode Shapes of Beams in Shear Vibration

$f_n = \frac{K_n}{2\pi} \sqrt{\frac{KG}{\rho L^2}} \text{ HZ}$ <p> <math>L</math> = Length  <math>K</math> = Shear Coefficient (Cowper, 1966)  <math>G</math> = Shear Modulus = <math>E/[2(1+\nu)]</math>  <math>\rho</math> = Mass Density                 </p>		
Boundary Condition	$K_n; n = 1,2,3\dots$	Mode Shape $y_n\left(\frac{x}{L}\right)$
Fixed - Free 	$n\pi; n = 1,2,3\dots$	$\cos \frac{n\pi x}{L}; n = 1,2,3\dots$
Fixed - Fixed 	$n\pi; n = 1,2,3\dots$	$\sin \frac{n\pi x}{L}; n = 1,2,3\dots$

### Natural Frequency of Multistory Building Frames

Tall building frames often deform more in the shear mode than in flexure. The fundamental frequencies of many multistory building frameworks can be approximated by [32, 48]

$$f = \alpha \frac{\sqrt{B}}{H} \quad (2.396)$$

where  $\alpha$  is approximately equal to  $11\sqrt{m}/s$ ,  $B$  is the building width in the direction of vibration, and  $H$  is the building height. This empirical formula suggests that a shear beam model with  $f$  inversely proportional to  $H$  is more appropriate than a flexural beam for predicting natural frequencies of buildings.

#### 2.13.8 Portal Frames

A portal frame consists of a cap beam rigidly connected to two vertical columns. The natural frequencies of portal frames vibrating in the fundamental symmetric and asymmetric modes are shown in Tables 2.8 and 2.9, respectively.

The beams in these frames are assumed to be uniform and sufficiently slender so that shear, axial, and torsional deformations can be neglected. The method of analysis of these frames is given in [68]. The vibration is assumed to be in the plane of the frame, and the results are presented for portal frames with pinned and fixed bases.

If the beam is rigid and the columns are slender and uniform, but not necessarily identical, then the natural fundamental frequency of the frame can be approximated using the following formula [49]:

$$f = \frac{1}{2\pi} \left[ \frac{12 \sum E_i I_i}{L^3 (M + 0.37 \sum M_i)} \right]^{1/2} \text{ Hz} \quad (2.397)$$

where  $M$  is the mass of the beam,  $M_i$  is the mass of the  $i$ -th column, and  $E_i I_i$  are the flexural rigidity of the  $i$ -th column. The summation refers to the sum of all columns, and  $i$  must be greater or equal to 2. Additional results for frames with inclined members are discussed in [11].

#### 2.13.9 Damping

Damping is found to increase with the increasing amplitude of vibration. It arises from the dissipation of energy during vibration. The mechanisms contributing to energy dissipation are material damping, friction at interfaces between components, and energy dissipation due to foundation interacting with soil, among others. Material damping arises from the friction at bolted connections and frictional interaction between structural and non-structural elements such as partitions and cladding.

The amount of damping in a building can never be predicted precisely, and design values are generally derived based on dynamic measurements of structures of a corresponding type. Damping can be measured based on the rate of decay of free vibration following an impact; by spectral methods based on analysis of response to wind loading; or by force excitation by mechanical vibrator at varying frequency to establish the shape of the steady state resonance curve. However, these methods may not be easily carried out if several modes of vibration close in frequency are presented.

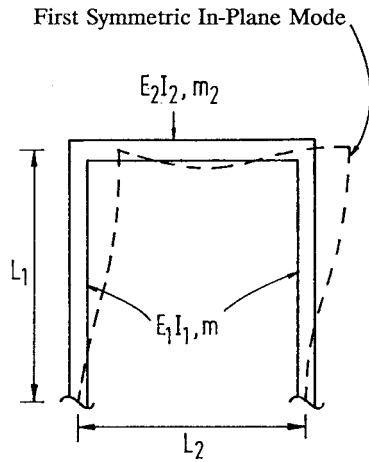
Table 2.10 gives values of modal damping that are appropriate for use when amplitudes are low. Higher values are appropriate at larger amplitudes where local yielding may develop, e.g., in seismic analysis.

**TABLE 2.8** Fundamental Frequencies of Portal Frames in Asymmetrical Mode of Vibration

							$f = \frac{\lambda^2}{2\pi L_1^2} \left( \frac{E_1 I_1}{m_1} \right)^{1/2} \text{ HZ}$ <p>E = Modulus of elasticity I = Area moment of inertia m = mass per unit length</p>				
$\frac{m_1}{m_2}$	$\frac{E_1 I_1}{E_2 I_2}$	$\lambda$ value									
		Pinned Bases					Clamped Bases				
		$L_1/L_2$					$L_1/L_2$				
		0.25	0.75	1.5	3.0	6.0	0.25	0.75	1.5	3.0	6.0
0.25	0.25	0.6964	0.9520	1.1124	1.2583	1.3759	0.9953	1.3617	1.6003	1.8270	2.0193
	0.75	0.6108	0.8961	1.0764	1.2375	1.3649	0.9030	1.2948	1.5544	1.7999	2.0051
	1.5	0.5414	0.8355	1.0315	1.2093	1.3491	0.8448	1.2323	1.5023	1.7649	1.9853
	3.0	0.4695	0.7562	0.9635	1.1610	1.3201	0.7968	1.1648	1.4329	1.7096	1.9504
	6.0	0.4014	0.6663	0.8737	1.0870	1.2702	0.7547	1.1056	1.3573	1.6350	1.8946
0.75	0.25	0.8947	1.1740	1.3168	1.4210	1.4882	1.2873	1.7014	1.9262	2.0994	2.2156
	0.75	0.7867	1.1088	1.2776	1.3998	1.4773	1.1715	1.6242	1.8779	2.0733	2.2026
	1.5	0.6983	1.0368	1.2281	1.3707	1.4617	1.0979	1.5507	1.8218	2.0390	2.1843
	3.0	0.6061	0.9413	1.1516	1.3203	1.4327	1.0373	1.4698	1.7454	1.9838	2.1516
	6.0	0.5186	0.8314	1.0485	1.2414	1.3822	0.9851	1.3981	1.6601	1.9072	2.0983
1.5	0.25	1.0300	1.2964	1.4103	1.4826	1.5243	1.4941	1.9006	2.0860	2.2090	2.2819
	0.75	0.9085	1.2280	1.3707	1.4616	1.5136	1.3652	1.8214	2.0390	2.1842	2.2695
	1.5	0.8079	1.1514	1.3203	1.4326	1.4982	1.2823	1.7444	1.9837	2.1515	2.2521
	3.0	0.7021	1.0482	1.2414	1.3821	1.4694	1.2141	1.6583	1.9070	2.0983	2.2206
	6.0	0.6011	0.9279	1.1335	1.3024	1.4191	1.1570	1.5808	1.8198	2.0234	2.1693
3.0	0.25	1.1597	1.3898	1.4719	1.5189	1.5442	1.7022	2.0612	2.1963	2.2756	2.3190
	0.75	1.0275	1.3202	1.4326	1.4981	1.5336	1.5649	1.9834	2.1515	2.2520	2.3070
	1.5	0.9161	1.2412	1.3821	1.4694	1.5182	1.4752	1.9063	2.0982	2.2206	2.2899
	3.0	0.7977	1.1333	1.3024	1.4191	1.4896	1.4015	1.8185	2.0233	2.1693	2.2595
	6.0	0.6838	1.0058	1.1921	1.3391	1.4395	1.3425	1.7382	1.9366	2.0964	2.2094
6.0	0.25	1.2691	1.4516	1.5083	1.5388	1.5545	1.8889	2.1727	2.2635	2.3228	2.3385
	0.75	1.1304	1.3821	1.4694	1.5181	1.5440	1.7501	2.0980	2.2206	2.2899	2.3268
	1.5	1.0112	1.3023	1.4191	1.4896	1.5287	1.6576	2.0228	2.1693	2.2595	2.3101
	3.0	0.8827	1.1919	1.3391	1.4395	1.5002	1.5817	1.9358	2.0963	2.2095	2.2802
	6.0	0.7578	1.0601	1.2277	1.3595	1.4502	1.5244	1.8550	2.0110	2.1380	2.2309

**TABLE 2.9** Fundamental Frequencies of Portal Frames in Asymmetrical Mode of Vibration.

$\left(\frac{m_2}{m_1}\right)^{1/4} \left(\frac{E_2 I_2}{E_1 I_1}\right)^{3/4}$		λ value						
		$\left(\frac{E_1 I_1}{E_2 I_2} \frac{m_2}{m_1}\right)^{1/4} \frac{L_2}{L_1}$						
		8.0	4.0	2.0	1.0	0.8	0.4	0.2
Pinned Bases	8.0	0.4637	0.8735	1.6676	3.1416	3.5954	3.8355	3.8802
	4.0	0.4958	0.9270	1.7394	3.1416	3.4997	3.7637	3.8390
	2.0	0.5273	0.9911	1.8411	3.1416	3.4003	3.6578	3.7690
	1.0	0.5525	1.0540	1.9633	3.1416	3.3110	3.5275	3.6642
	0.8	0.5589	1.0720	2.0037	3.1416	3.2864	3.4845	3.6240
	0.4	0.5735	1.1173	2.1214	3.1416	3.2259	3.3622	3.4903
	0.2	0.5819	1.1466	2.2150	3.1416	3.1877	3.2706	3.3663
	0.2	0.5842	1.1551	2.2575	3.8052	3.9266	4.0361	4.1276
Clamped Bases	8.0	0.4767	0.8941	1.6973	3.2408	3.9269	4.6167	4.6745
	4.0	0.5093	0.9532	1.7847	3.3166	3.9268	4.5321	4.6260
	2.0	0.5388	1.0185	1.9008	3.4258	3.9268	4.4138	4.5454
	1.0	0.5606	1.0773	2.0295	3.5564	3.9267	4.2779	4.4293
	0.8	0.5659	1.0932	2.0696	3.5988	3.9267	4.2351	4.3861
	0.4	0.5776	1.1316	2.1790	3.7176	3.9267	4.1186	4.2481
	0.2	0.5842	1.1551	2.2575	3.8052	3.9266	4.0361	4.1276



$$f = \frac{\lambda^2}{2\pi L_1^2} \left( \frac{E_1 I_1}{m_1} \right)^{1/2} \text{ HZ}$$

E = Modulus of elasticity

I = Area moment of inertia

m = mass per unit length

**TABLE 2.10** Typical Structural Damping Values

Structural type	Damping value, $\xi$ (%)
Unclad welded steel structures	0.3
Unclad bolted steel structures	0.5
Floor, composite and non-composite	1.5-3.0
Clad buildings subjected to sidesway	1

### 2.13.10 Numerical Analysis

Many less complex dynamic problems can be solved without much difficulty by hand methods. For more complex problems, such as determination of natural frequencies of complex structures, calculation of response due to time-varying loads, and response spectrum analysis to determine seismic forces, may require numerical analysis. The finite element method has been shown to be a versatile technique for this purpose.

The global equations of an undamped force-vibration motion, in matrix form, may be written as

$$[M]\{\ddot{x}\} + [K]\{\dot{x}\} = \{F(t)\} \quad (2.398)$$

where

$$[K] = \sum_{i=1}^n [k_i] \quad [M] = \sum_{i=1}^n [m_i] \quad [F] = \sum_{i=1}^n [f_i] \quad (2.399)$$

are the global stiffness, mass, and force matrices, respectively.  $[k_i]$ ,  $[m_i]$ , and  $\{f_i\}$  are the stiffness, mass, and force of the  $i^{\text{th}}$  element, respectively. The elements are assembled using the direct stiffness method to obtain the global equations such that intermediate continuity of displacements is satisfied at common nodes and, in addition, interelement continuity of acceleration is also satisfied.

Equation 2.398 is the matrix equation discretized in space. To obtain solution of the equation, discretization in time is also necessary. The general method used is called direct integration. There are two methods for direct integration: *implicit* or *explicit*. The first, and simplest, is an explicit method known as the central difference method [9]. The second, more sophisticated but more versatile, is an implicit method known as the Newmark method [44]. Other integration methods are also available in [7].

The natural frequencies are determined by solving Equation 2.398 in the absence of force  $F(t)$  as

$$[M]\{\ddot{x}\} + [K]\{x\} = 0 \quad (2.400)$$

The standard solution for  $x(t)$  is given by the harmonic equation in time

$$\{x(t)\} = \{X\}e^{i\omega t} \quad (2.401)$$

where  $\{X\}$  is the part of the nodal displacement matrix called natural modes, which are assumed to be independent of time,  $i$  is the imaginary number, and  $\omega$  is the natural frequency.

Differentiating Equation 2.401 twice with respect to time, we have

$$\ddot{x}(t) = \{X\}(-\omega^2)e^{i\omega t} \quad (2.402)$$

Substituting of Equations 2.401 and 2.402 into Equation 2.400 yields

$$e^{i\omega t}([K] - \omega^2[M])\{X\} = 0 \quad (2.403)$$

Since  $e^{i\omega t}$  is not zero, we obtain

$$([K] - \omega^2[M])\{X\} = 0 \quad (2.404)$$

Equation 2.404 is a set of linear homogeneous equations in terms of displacement mode  $\{X\}$ . It has a non-trivial solution if the determinant of the coefficient matrix  $\{X\}$  is non-zero; that is

$$[K] - \omega^2[M] = 0 \quad (2.405)$$

In general, Equation 2.405 is a set of  $n$  algebraic equations, where  $n$  is the number of degrees of freedom associated with the problem.

## 2.14 Defining Terms

---

**Arch:** Principal load-carrying member curved in elevation; resistance to applied loading developed by axial thrust and bending.

**Beam:** A straight or curved structural member, primarily supporting loads applied at right angles to the longitudinal axis.

**Bending moment:** Bending moment due to a force or a system of forces at a cross-section is computed as the algebraic sum of all moments to one side of the section.

**Built-in beam:** A beam restrained at its ends against vertical movement and rotation.

**Cables:** Flexible structures with no moment-carrying capacity.

**Cantilever:** A beam restrained against movement and rotation at one end and free to deflect at the other end.

**Continuous beam:** A beam that extends over several supports.

**Deflection:** Movement of a structure or parts of a structure under applied loads.

**Element:** Part of a cross-section forming a distinct part of the whole.

**Grillage:** Structures in which the members all lie in one plane with loads being applied in the direction normal to this plane.

**Hogging moment:** Bending moment causing upward deflection in a beam.

**Influence line:** An influence line indicates the effect at a given section of a unit load placed at any point on the structure.

**Member:** Any individual component of a structural frame.

**Moment of inertia:** The second moment of area of a section about the elastic neutral axis.

**Plastic analysis:** Analysis assuming redistribution of moments within the structure in a continuous construction.

**Plastic hinge:** Position at which a member has developed its plastic moment of resistance.

**Plastic moment:** Moment capacity allowing for redistribution of stress within a cross-section.

**Plastic section:** A cross-section that can develop a plastic hinge with sufficient rotational capacity to allow redistribution of bending moments within the section.

**Portal frame:** A single-story continuous plane frame deriving its strength from bending resistance and arch action.

**Reaction:** The load carried by each support.

**Rigid frame:** An indeterminate plane frame consisting of members with fixed end connections.

**Sagging moment:** An applied bending moment causing a sagging deflection in the beam.

**Second-order analysis:** Analysis considering the equilibrium formulated based on deformed structural geometry.

**Semi-rigid connection:** A connection that possesses a moment capacity intermediate between the simple and rigid connection.

**Shear force:** An internal force acting normal to the longitudinal axis; given by the algebraic sum

of all forces to one side of the section chosen.

Simple beam: A beam restrained at its end only against vertical movement.

Space frame: A three-dimensional structure.

Span: The distance between the supports of a beam or a truss.

Static load: A noncyclic load that produces no dynamic effects.

Statically determinate structure: A structure in which support reactions may be found from the equations of equilibrium.

Statically indeterminate structure: A structure in which equations of equilibrium are not sufficient to determine the reactions.

Thin plate: A flat surface structure in which the thickness is small compared to the other dimensions.

Thin shell: A curved surface structure with a thickness relatively small compared to its other dimensions.

Truss: A coplanar system of structural members joined at their ends to form a stable framework.

## References

---

- [1] Ackroyd, M. H. 1985. *Design of Flexibly Connected Steel Frames*, Final Research Report to the American Iron and Steel Institute for Project No. 333, Rensselaer Polytechnic Institute, Troy, NY.
- [2] AISC. 1989. *Allowable Stress Design Specification for Structural Steel Buildings*, American Institute of Steel Construction, Chicago, IL.
- [3] AISC. 1993. *Load and Resistance Factor Design Specification for Structural Steel Buildings*, American Institute of Steel Construction, 2nd ed., Chicago, IL.
- [4] Argyris, J. H. 1960. *Energy Theorems and Structural Analysis*, London, Butterworth. (Reprinted from *Aircraft Engineering*, Oct. 1954 - May 1955).
- [5] ASCE. 1971. *Plastic Design in Steel—A Guide and Commentary, Manual 41*, American Society of Civil Engineers.
- [6] Baker, L. and Heyman, J. 1969. *Plastic Design of Frames: 1. Fundamentals*, Cambridge University Press, 228 pp.
- [7] Bathe, K. J. 1982. *Finite Element Procedures for Engineering Analysis*, Prentice Hall, Englewood Cliffs, NJ, 735 pp.
- [8] Beedle, L. S. 1958. *Plastic Design of Steel Frames*, John Wiley & Sons, New York.
- [9] Biggs, J. M. 1964. *Introduction to Structural Dynamics*, McGraw-Hill, New York.
- [10] Borg, S. F. and Gennaro, J. J. 1959. *Advanced Structural Analysis*, D. Van Nostrand Company, Princeton, NJ.
- [11] Chang, C. H. 1978. Vibration of frames with inclined members, *J. Sound Vib.*, 56, 201-214.
- [12] Chen, W. F. and Atsuta, T. 1977. *Theory of Beam-Column, Vol. 2, Space Behavior and Design*, MacGraw-Hill, New York, 732 pp.
- [13] Chen, W. F. and Han, D. J. 1988. *Plasticity for Structural Engineers*, Springer-Verlag, New York.
- [14] Chen, W. F. and Lui, E. M. 1987. *Structural Stability—Theory and Implementation*, Prentice Hall, Englewood Cliffs, NJ, 490 pp.
- [15] Chen W. F. and Lui, E. M. 1991. *Stability Design of Steel Frames*, CRC Press, Boca Raton, FL, 380 pp.
- [16] Chen, W. F. and Sohal, I. S. 1995. *Plastic Design and Advanced Analysis of Steel Frames*, Springer-Verlag, New York.
- [17] Chen, W. F. and Kim, S. E. 1997. *LRFD Steel Design Using Advanced Analysis*, CRC Press, Boca Raton, FL.

- [18] Chen, W. F. and Toma, S. 1994. *Advanced Analysis in Steel Frames: Theory, Software and Applications*, CRC Press, Boca Raton, FL, 384 pp.
- [19] Chen, W. F., Goto, Y., and Liew, J. Y. R. 1996. *Stability Design of Semi-Rigid Frames*, John Wiley & Sons, New York, 468 pp.
- [20] Clark, M. J. 1994. Plastic-zone analysis of frames, in *Advanced Analysis of Steel Frames, Theory, Software, and Applications*, W.F. Chen and S. Toma, Eds., CRC Press, 195-319, chapt. 6.
- [21] Clough, R. W. and Penzien, J. 1993. *Dynamics of Structures*, 2nd ed., McGraw-Hill, New York, 738 pp.
- [22] Cowper, G. R. 1966. The shear coefficient in Timoshenko's beam theory, *J. Applied Mech.*, 33, 335-340.
- [23] Desai, C. S. and Abel, J. F. 1972. *Introduction to the Finite Element Method*, Van Nostrand Reinhold and Company, New York.
- [24] Dhillon, B. S. and Abdel-Majid, S. 1990. Interactive analysis and design of flexibly connected frames, *Computer & Structures*, 36(2), 189-202.
- [25] Dowrick D. J. 1988. *Earthquake Resistant Design for Engineers and Architects*, 2nd ed., John Wiley & Sons, New York.
- [26] Frye, M.J. and Morris, G. A. 1976. Analysis of flexibly connected steel frames, *Can. J. Civ. Eng.*, 2(3), 280-291.
- [27] Ghali, A. and Neville, A. M. 1978. *Structural Analysis*, Chapman and Hall, London.
- [28] Goto, Y. and Chen, W. F. 1987. On the computer-based design analysis for the flexibly jointed frames, *J. Construct. Steel Res.*, Special Issue on Joint Flexibility in Steel Frames, (W. F. Chen, Ed.), 8, 203-231.
- [29] Heyman, J. 1971. *Plastic Design of Frames: 2. Applications*, Cambridge University Press, 292 pp.
- [30] Heish, S. H. 1990. *Analysis of Three-Dimensional Steel Frames with Semi-Rigid Connections*, Structural Engineering Report 90-1, School of Civil and Environmental Engineering, Cornell University, Ithaca, NY, 211 pp.
- [31] Horne, M. R. 1964. *The Plastic Design of Columns*, BCSA Publication No. 23.
- [32] Housner, G. W. and Brody, A. G. 1963. Natural periods of vibration of buildings, *J. Eng. Mech. Div.*, ASCE, 89, 31-65.
- [33] Kardestuncer, H. and Norrie, D. H. 1988. *Finite Element Handbook*, McGraw-Hill, New York.
- [34] Knudsen, K. E., Yang, C. H., Johnson, B. G., and Beedle, L. S. 1953. Plastic strength and deflections of continuous beams, *Welding J.*, 32(5), 240 pp.
- [35] Lee, S. L. and Ballesteros, P. 1960. Uniformly loaded rectangular plate supported at the corners, *Int. J. Mech. Sci.*, 2, 206-211.
- [36] Lee, S. L. and Basu, P. K. 1989. Secant method for nonlinear semi-rigid frames, *J. Construct. Steel Res.*, 14(2), 49-67.
- [37] Lee, S. L., Karasudhi, P., Zakeria, M., and Chan, K. S. 1971. Uniformly loaded orthotropic rectangular plate supported at the corners, *Civil Eng. Trans.*, pp. 101-106.
- [38] Liew J. Y. R. 1992. *Advanced Analysis for Frame Design*, Ph.D dissertation, School of Civil Engineering, Purdue University, West Lafayette, IN, May, 393 pp.
- [39] Liew, J. Y. R. and Chen, W. F. 1994. Trends toward advanced analysis, in *Advanced Analysis in Steel Frames: Theory, Software and Applications*, Chen, W. F. and Toma, S., Eds., CRC Press, Boca Raton, FL, 1-45, chapt. 1.
- [40] Liew, J. Y. R., White, D. W., and Chen, W. F. 1991. Beam-column design in steel frameworks—Insight on current methods and trends, *J. Construct. Steel Res.*, 18, 259-308.
- [41] Liew, J. Y. R., White, D. W., and Chen, W. F. 1993a. Limit-states design of semi-rigid frames using advanced analysis, Part 1: Connection modelling and classification, Part 2: Analysis and design, *J. Construct. Steel Res.*, Elsevier Science Publishers, London, 26(1), 1-57.

- [42] Liew, J. Y. R., White, D. W., and Chen, W. F. 1993b. Second-order refined plastic hinge analysis for frame design: Parts 1 & 2, *J. Structural Eng.*, ASCE, Nov., 119(11), 3196-3237.
- [43] Mrazik, A., Skaloud, M., and Tochacek, M. 1987. *Plastic Design of Steel Structures*, Ellis Horwood Limited, 637 pp.
- [44] Newmark, N. M. 1959. A method of computation for structural dynamic, *J. Eng. Mech.*, ASCE, 85(EM3), 67-94.
- [45] Orbison, J. G. 1982. *Nonlinear Static Analysis of Three-Dimensional Steel Frames*, Department of Structural Engineering, Report No. 82-6, Cornell University, Ithaca, NY, 243 pp.
- [46] Porter, F. L. and Powell, G. M. 1971. Static and dynamic analysis of inelastic frame structures, Report No. EERC 71-3, Earthquake Engineering Research Center, University of California, Berkeley.
- [47] Powell, G. H. and Chen, P. F.-S. 1986. 3D beam column element with generalized plastic hinges, *J. Eng. Mech.*, ASCE, 112(7), 627-641.
- [48] Rinne, J. E. 1952. Building code provisions for aseismic design, in *Proc. Symp. Earthquake and Blast Effects on Structures*, Los Angeles, CA, 291-305.
- [49] Robert, D. B. 1979. *Formulas for Natural Frequency and Mode Shapes*, Van Nostrand Reinhold and Company, New York, 491 pp.
- [50] Rutenberg, A. 1975. Approximate natural frequencies for coupled shear walls, *Earthquake Eng. Struct. Dynam.*, 4, 95-100.
- [51] Seely, F. B. and Smith, J. O. 1952. *Advanced Mechanics of Materials*, John Wiley & Sons, New York, 137-187.
- [52] Shanmugam, N. E., Rose, H., Yu, C. H., Lee, S. L. 1988. Uniformly loaded rhombic orthotropic plates supported at corners, *Computers Struct.*, 30(5), 1037-1045.
- [53] Shanmugam, N. E., Rose, H., Yu, C. H., Lee, S. L. 1989. Corner supported isosceles triangular orthotropic plates, *Computers Struct.*, 32(5), 963-972.
- [54] Structural Stability Research Council. 1988. *Guide to Stability Design Criteria for Metal Structures*, Galambos, T. V., Ed., Fourth ed., John Wiley & Sons, New York, 786 pp.
- [55] Timoshenko, S. P. and Gere, J. M. 1961. *Theory of Elastic Stability*, McGraw-Hill, New York.
- [56] Timoshenko, S. P. and Krieger, S. W. 1959. *Theory of Plates and Shells*, McGraw-Hill, New York.
- [57] Tsai, S. W. and Cheron, T. 1968. *Anisotropic Plates* (translated from the Russian edition by S. G. Lekhnitskii), Gordon and Breach Science Publishers, New York, 1968.
- [58] Vijakhna, P., Karasudhi, P., and Lee, S. L. 1973. Corner supported equilateral triangular plates, *Int. J. Mech. Sci.*, 15, 123-128.
- [59] Vogel, U. 1985. *Calibrating Frames*, *Stahlbau*, 10, Oct., 295-301.
- [60] Wang, Y. C. 1988. Ultimate Strength Analysis of 3-D Beam Columns and Column Subassemblages with Flexible Connections, Ph.D thesis, University of Sheffield, England.
- [61] Warburton, G. B. 1976. *The Dynamical Behavior of Structures*, 2nd ed., Pergamon Press, New York.
- [62] White, D. W. 1985. Material and Geometric Nonlinear Analysis of Local Planar Behavior in Steel Frames Using Iterative Computer Graphics, M.S. thesis., Cornell University, Ithaca, NY, 281 pp.
- [63] White, D. W. 1988. Analysis of Monotonic and Cyclic Stability of Steel Frame Subassemblages, Ph.D. dissertation, Cornell University, Ithaca, NY.
- [64] White, D. W. and Hajjar, J. F. 1991. Application of second-order elastic analysis in LRFD: research to practice, *Engineering J., AISC*, 28(4), 133-148.
- [65] White, D. W., Liew, J. Y. R., and Chen, W. F. 1991. *Second-order Inelastic Analysis for Frame Design: A Report to SSRC Task Group 29 on Recent Research and the Perceived State-of-the-Art*, Structural Engineering Report, CE-STR-91-12, Purdue University, 116 pp.

- [66] White, D. W., Liew, J. Y. R., and Chen, W. F. 1993. Toward advanced analysis in LRFD, in *Plastic Hinge Based Methods for Advanced Analysis and Design of Steel Frames—An Assessment of The State-Of-The-Art*, Structural Stability Research Council, Lehigh University, Bethlehem, PA, 95-173.
- [67] Yang, Y. B. and Kuo, S. R. 1994. *Theory and Analysis of Nonlinear Framed Structures*, Prentice Hall, Singapore, 539-545.
- [68] Yang, Y. T. and Sun C. T. 1973. Axial-flexural vibration of frameworks using finite element approach, *J. Acoust. Soc. Am.*, 53, 137-146.
- [69] Ziemian, R. D., McGuire, W., and Deierlien, G. G. 1992. Inelastic Limit States Design: Part I - Planar Frame Studies, *J. Struct. Eng.*, ASCE, 118(9).
- [70] Ziemian, R. D., McGuire, W., and Deierlien, G.G. 1992. Inelastic Limit States Design: Part II - Three-Dimensional Frame Study, *J. Struct. Eng.*, ASCE, 118(9).

## Further Reading

---

The *Structural Engineering Handbook* by E. H. Gaylord and C. N. Gaylord provides a reference work on structural engineering and deals with planning, design, and construction of a variety of engineering structures.

The *Finite Element Handbook* by H. Kardestuncer and D. H. Norrie presents the underlying mathematical principles, the fundamental formulations, and both commonly used and specialized applications of the finite element method.